THE PLEOMORPHIC ROLE OF STROMAL CELLS IN THE FORMATION AND MAINTENANCE OF TERTIARY LYMPHOID ORGANS

by

JOANA DIAS DE CAMPOS

A thesis submitted to the University of Birmingham
for the degree of DOCTOR OF PHILOSOPHY

Institute of Inflammation and Ageing

School of Medical and Dental Sciences

University of Birmingham

April 2016

UNIVERSITY OF BIRMINGHAM

University of Birmingham Research Archive

e-theses repository

Abstract

A large body of evidence supports the role of activated stromal cells in the persistence of inflammation. The switch from resting to pathogenic stroma appears to be associated with the development of tertiary lymphoid organs (TLOs) within sites of chronic inflammation. However little is known about the immunological function of the stromal component.

We utilised a murine model of inducible TLO formation in inflamed salivary glands to investigate the role of activated stromal cells characterised by the expression of gp38 and FAP during TLO development.

We demonstrated that during inflammation, stroma-derived ICOSL engages ICOS on T cells, necessary for the release of lymphotoxin α and consequent TLO formation. Whilst dissecting the role of stromal cells in this context, we demonstrate that gp38 expression is required for the upregulation of adhesion molecules involved in cell clustering. Depletion of gp38+FAP+ stromal cells led to a significant reduction in lymphoid chemokine production, a decreased number of infiltrating lymphocytes and severely compromised TLO formation.

Collectively, we provide evidence that activated stromal cells express FAP, provide co-stimulatory signals, and are necessary for the establishment of viral-induced TLOs, highlighting a potential novel therapeutic target in TLO-associated autoimmune diseases.

Acknowledgments

insisted in not working. Last but not least, Manuela and I have spent a fortune at Costa, which made me feel closer to my Portuguese home.

I suspect that Tess and Kadri do not realise how much they have helped me whilst living with me; these two ladies made me feel at home in Birmingham.

Aos meus pais, Ana e Vitor, o meu maior obrigada por me deixarem voar e aventurar por novos caminhos sem nunca deixarem de me apoiar. Mesmo a 2404km de distância, são o meu maior apoio e eu sei que estão (e estarão) sempre ao meu lado. Ao meu irmão Henrique tenho que agradecer ser o meu melhor amigo e confidente, e para isso não há palavras suficientes. Mais uma vez, e sem surpresas, vocês foram o meu maior pilar nesta etapa.

O meu muito obrigada a todos vós!
Thank you very much to you all!

List of abbreviations

- – negative

+ – positive

-/- – knockout

AID – activation-induced cytidine deaminase

APCs – antigen presenting cells

ANA – antinuclear antibodies

BAFF – B-cell activating factor

BEC – blood endothelial cells

BM – bone marrow

CCL – chemokine (C-C motif) ligand

CCR – C-C chemokine receptor type

CD – cluster of differentiation

CIA – collagen-induced arthritis

CTLA-4 – cytotoxic T lymphocyte antigen 4

CXCL – chemokine (C-X-C motif) ligand

CXCR – C-X-C chemokine receptor type

DCs – dendritic cells

DN – double negative

DPPIV – dipeptidyl-peptidase IV

DTR – diphtheria toxin receptor

DTx – diphtheria toxin

E – embryonic day

EAE – experimental autoimmune encephalomyelitis

ECM – extracellular matrix

ELSs – ectopic lymphoid structures

FAP – fibroblast activation protein α

FDCs – follicular dendritic cells

FLSs – fibroblast-like synoviocytes

FRCs – fibroblastic reticular cells

GC – germinal centre

GM-CSF – granulocyte-macrophage colony-stimulating factor

Gp38 – glycoprotein 38

HEVs – high endothelial venules

iBALT – inducible bronchus-associated lymphoid tissue

ICAM-1 – intercellular adhesion molecule 1

ICOS – inducible co-stimulator

ICOSL – inducible co-stimulator ligand

IFN-γ – interferon gamma

Ig – immunoglobulin

IL – interleukin

ILCs – innate lymphoid cells

ILFs – isolated lymphoid follicles

KO – knockout

LEC – lymphatic endothelial cells

LESA – lymphoepithelial lesions

LLSc – lymphoid-like stromal cells

LPS – lypopolyssacharide

LT – lymphotoxin

$LT\alpha$ – lymphotoxin alpha

$LT\alpha_1\beta_2$ – lymphotoxin alpha beta

$LT\beta$ – lymphotoxin beta

$LT\beta R$ – lymphotoxin beta receptor

LTi – lymphoid tissue inducer cells

LTo – lymphoid tissue organizer cells

MAdCAM-1 – mucosal addressin cell adhesion molecule 1

MALT - mucosa-associated lymphoid tissues

MHC – major histocompatibility complex

MMP – metalloproteinases

NK – natural killer cells

NOD – non-obese diabetic

p.c. – post cannulation

PD-1 – programmed death 1

PD-L1 – programmed death-ligand 1

PDGFRβ – beta-type platelet-derived growth factor receptor

PDPN – podoplanin

PI3K – phosphatidylinositol-4,5-bisphosphate 3-kinase

PIP_3 – phosphatidylinositol (3,4,5)-trisphosphate

PNA – peanut agglutinin binding

PNAd – peripheral node addressins

PP – Peyer's Patches

pSS – primary Sjögren's syndrome

RA – rheumatoid arthritis

RANKL – receptor activator of NF-κB ligand

RIP – rat insulin promoter

RORC – retinoic acid-related orphan nuclear hormone receptor

RORγt – retinoic acid receptor-related orphan receptor-γt

SLE – systemic lupus erythematosus

SLOs – secondary lymphoid organs

SS – Sjögren's syndrome

TCR – T cell receptor

T_{FH} – T follicular helper cells

Tg – transgenic

TGF-β - transforming growth factor beta

T_H – T helper cells

TLOs – tertiary lymphoid organs

TLTs – tertiary lymphoid tissues

TNFα – tumor necrosis factor alpha

TNFR – tumour necrosis factor receptor

Tregs – regulatory T cells

VCAM-1 – vascular adhesion molecule 1

wt – wild-type

List of figures

List of tables

Table of contents

Chapter 1

INTRODUCTION

1.1. Tertiary Lymphoid Organs and their association with inflammation

Chronic inflammation is defined by two major features: persistence of the inflammatory process and specificity for certain anatomical sites (Buckley, 2011). Stromal cells (non-hematopoetic, non-epitelial and non-endothelial cells), namely fibroblasts, have been suggested as key effector cells involved in the switch to persistence of inflammation (Buckley et al., 2004, Barone et al., 2012). An important feature of inflammation is the communication between stromal and immune cells. In chronically inflamed tissue, activated tissue resident fibroblasts are essential in the homing of immune cells and maintaining inflammatory infiltrates through the inappropriate secretion of survival and retentive factors, therefore controlling recruitment, activation and survival of leukocytes (Pitzalis et al., 2014, Naylor et al., 2013).

Under specific conditions, infiltrating immune cells can cluster in chronically inflamed tissue and form structures histologically similar to secondary lymphoid organs (SLOs) (Pitzalis et al., 2014). Whilst the "specific conditions" required are still largely unknown, it has been shown that such structures are also functionally active and have been termed tertiary lymphoid organs (TLOs), ectopic lymphoid structures (ELSs) or tertiary lymphoid tissues (TLTs) (Pitzalis et al., 2014).

The transient formation of TLOs has been shown in physiological settings, for example, the development of gut isolated lymphoid follicles (ILFs), in response to intestinal flora, characterised by single B cell follicles surrounded by dendritic cells (DCs) (Buckley et al., 2015, Eberl and Lochner, 2009, Lochner et al., 2011, Constantinovits et al., 2012). ILFs seem to be critical for immune homeostasis and normal colonic mucosal regeneration (Buckley et al., 2015, Eberl and Lochner, 2009, Lochner et al., 2011, Constantinovits et al., 2012). Nevertheless, TLO formation is more classically associated with chronic inflammation, autoimmunity and cancer (Buckley et al., 2015). Within the target tissues of human autoimmune diseases, TLO formation is associated with the persistence of the inflammatory process and associated with a poor prognosis (Theander et al., 2011, Weyand and Goronzy, 2003). The events that generate highly specialized SLOs and transient hubs for autoreactive cell proliferation in TLOs are different. Still, in both settings the resident mesenchyme undergoes critical changes, in SLOs during embryonic life and postnatally in TLOs (Buckley et al., 2015).

1.1.1. Development of TLOs

Numerous signals have been implicated in the formation of TLO structures and these have been extensively investigated. Lymphotoxin (LT) signals are directly associated with increased expression of chemokine (C-X-C motif) ligand 13 (CXCL13), chemokine (C-C motif) ligand 19 (CCL19) and ligand 21 (CCL21), leading for example to recruitment of cluster of differentiation (CD) 62L+ T cells (Pitzalis et al., 2014). Lymphotoxin-alpha (LTα)-deficiency results in a complete absence of peripheral lymphoid organs (De Togni et al., 1994)

and combined overexpression of *Lta* and *Ltb* results in more prominent TLO formation compared with *Lta* overexpression on its own (Drayton et al., 2003).

Even though there is still ongoing research on this aspect, some cell subsets have been implicated in TLO formation, including: lymphoid tissue inducer cells (LTi cells), lymphoid tissue organizer cells (LTo cells), interleukin (IL)-17 secreting CD4+ T cells and T follicular helper cells (T_{FH} cells) (Pitzalis et al., 2014).

CD4+CD3-CD45+ LTi cells accumulate in the early stages of lymph node development, and their recruitment, activation and survival is controlled by expression of CXCL13, receptor activator of NF-κB ligand (RANKL) and (IL-7) (Pitzalis et al., 2014). These cells also express C-X-C chemokine receptor type 5 (CXCR5) and IL-7 receptor and interact with LTo cells, characterised by expression of vascular adhesion molecule 1 (VCAM-1), intercellular adhesion molecule 1 (ICAM-1) and the mucosal addressin cell adhesion molecule 1 (MAdCAM-1) (Mebius et al., 1997, Yoshida et al., 1999, Honda et al., 2001, Finke et al., 2002). Such cascade of events leads to homeostatic chemokine release and vascularization by high endothelial venules (HEVs) (Pitzalis et al., 2014). In the context of chronic inflammation-associated ectopic lymphoid structures, it has been hypothesized that stromal cells found in close relationship with TLOs may acquire lymphoid tissue organizer-like properties (Sato et al., 2011, Rangel-Moreno et al., 2007).

The hypothesis that, in chronic inflammation, stromal cells acquire lymphoid tissue organizer-like properties is consistent with the observation that adoptive transfer of adult LTi cells into *Cxcr5-/-* mice induces the formation of intestinal

lymphoid tissues and suggests that innate adult cells also play a role in TLO formation (Schmutz et al., 2009). Ectopic tissues that develop in response to transgenic overexpression of the *Il7* gene also require LTi cells (Meier et al., 2007). Adult LTi cells express the transcriptional regulator retinoic acid receptor-related orphan receptor-γt (RORγt) and can produce IL-17, a cytokine that is characteristic of group 3 innate lymphoid cells (ILCs) (Artis and Spits, 2015, Pitt et al., 2012, Powell et al., 2012). IL-17 and T helper (T$_H$) 17 cells have now been linked with ectopic lymphoid neogenesis, where they have a role in chronic allograft rejection, experimental autoimmune encephalomyelitis (EAE) and the development of inducible bronchus-associated lymphoid tissue (iBALT) (Deteix et al., 2010, Peters et al., 2011, Rangel-Moreno et al., 2011).

1.1.2. Cell organization within TLOs

In human pathology, TLOs are mainly characterised by the presence of organised B cell follicles, which can develop into germinal centres (GC) in the presence of activation-induced cytidine deaminase (AID) enzyme, B cell class switching and follicular dendritic cells network (FDCs) (Buckley et al., 2015, Neyt et al., 2012). In some pathologies, such as Sjögren's syndrome (SS) and primary biliary cirrhosis, T cell areas and stromal cell networks can also be identified (Buckley et al., 2015, Link et al., 2011).

Within TLOs, vessels resembling HEVs can also be found in the T cell zones and their expression of peripheral node addressins (PNAd) or MECA79 allows the recruitment of C-C chemokine receptor type (CCR)7+L-selectin+ T cells (Buckley et al., 2015, Neyt et al., 2012).

1.1.3. Function of TLOs

TLOs share a number of structural and functional features with SLOs, including: lymphocyte segregation into distinct areas (T and B cell area), local differentiation of FDCs and modification of the endothelium with acquisition of a plump morphology and expression of lymphoid associated addressins (PNAD or MAdCAM). Ectopic expression of lymphoid or homeostatic chemokines, known to regulate naïve and central memory T margination, CCL21 and CCL19, and B cell organization in follicles and germinal centres, CXCL13 and CXCL12, are also found in TLOs (Manzo et al., 2007, Amft et al., 2001).

During chronic inflammation, TLOs with different degrees of organization have been identified in the target tissues of human autoimmune disease, such as pancreas (Type I diabetes), thyroid tissue (during both Hashimoto's thyroiditis and, to a lesser extent, Grave's disease), in the thymus (during myasthenia gravis) and in the salivary glands (during SS) (Pitzalis et al., 2014).

The preferential formation of TLOs in association with epithelial tissue has been noted, with the exception of the formation in the synovial membrane (a non-epithelial organ) of patients affected by rheumatoid arthritis (RA). TLOs formation has been reported less frequently in the inflamed synovial membrane, being observed in only 25% of patients with RA (Klimiuk et al., 1997). Despite the observation that these structures have an inferior degree of organization as compared to the thyroid or the salivary glands they are

functional and capable of producing pathogenic disease specific autoantibodies (Klimiuk et al., 1997).

Allograft rejection and response to foreign bodies (metal hip implants) can also give rise to the formation of local TLOs and is believed to be involved in the pathogenic process of rejection (Mittal et al., 2013).

TLOs have also been reported to transiently form at sites of localized infections, influenza and microbacterial infections (Moyron-Quiroz et al., 2004, GeurtsvanKessel et al., 2009, Neyt et al., 2012, Carragher et al., 2008). During infection, TLOs are believed to represent an attempt to favour lymphocyte interaction at the site of antigen presentation without the need to spread the response to the SLOs (Buckley et al., 2015). Formal proof of this latter functional aspect has not yet been provided (Maglione et al., 2007, Buckley et al., 2015).

TLO formation during inflammation is associated with a higher degree of humoral immune response and in some cases systemic involvement, suggesting that TLOs might provide an additional hub (as compared to SLOs) for the production of autoantibodies. The direct correlation between TLO detection and certain clinical features, such as levels of immunoglobulins, systemic detection of autoantibodies, diffuse disease manifestations and tissue damage has been largely supported (Klimiuk et al., 1997, Weyand et al., 1998, Takemura et al., 2001, Weyand and Goronzy, 2003, Bugatti et al., 2005).

The products of TLO organization such as elevated serum levels of CXCL13 in the blood of patients with RA have also been associated with increased

disease severity and persistence of subclinical synovitis (Bugatti et al., 2012). TLO detection has been more recently considered a prognostic biomarker, for example in SS TLO detection (that occurs in up to 25% of the patients) has been associated with an increased risk of non-Hodgkin B cell lymphoma of the salivary glands (Theander et al., 2011).

1.1.4. Cytokines and chemokines in TLO formation

In chronic inflammatory settings, the pathways involved in TLO formation overlap with some of the pathways necessary for lymphoid organogenesis (Neyt et al., 2012).

Persistent antigenic stimulation and the presence of pro-inflammatory cytokines enable the conversion of stromal cells into a lymphoid tissue-like cell phenotype (Peduto et al., 2009). This lymphoid-like stroma is one of the key drivers of TLO organization (Barone et al., 2015b) and expression of cytokines (LTα, LTβ) and lymphoid chemokines (CXCL13, CCL21, CCL19, CXCL12) are linked to organisation of lymphoid aggregates and TLO size, with high expression of LTα, CXCL13 and CCL19 associated with highly organized follicles (Aloisi and Pujol-Borrell, 2006, Amft et al., 2001, Barone et al., 2005, Manzo et al., 2005).

While, CXCL13 and CCL21 control the segregation of B and T cells (Luther et al., 2002, Luther et al., 2000), CCL19 and CXCL12 promote lymphocyte infiltration and the positioning of DCs, B cells and plasma cells within these aggregates (Luther et al., 2002). Overexpression of CXCL13 led to TLO formation characterised by highly organised T and B cell zones, presence of

DCs and a BP3+ stromal cell network (Luther et al., 2000, Link et al., 2011). Similarly, rat insulin promoter (RIP)-CCL21 Tg mice and ectopic expression of CCL21 in thyroid presented similar organised lymphoid structures to that observed in RIP-CXCL13 Tg mice (Chen et al., 2002, Fan et al., 2000, Lira, 2005), however overexpression of CCL21 under the RIP promoter alone does not seem sufficient to induce full lymphoid neogenesis since no formation of CD35+ FDCs or CXCL13+ cells were observed (Chen et al., 2002, Fan et al., 2000). Indeed, there is some evidence that CXCL13 and LTβ expression might predict the development of ectopic GCs in patients with RA and SS (Barone et al., 2005, Carragher et al., 2008, Weyand and Goronzy, 2003, Salomonsson et al., 2002).

On the other hand, in the absence or blockade of CXCL13, CXCR5, CCR7 or LTα TLO formation is critically impaired (Furtado et al., 2007, Gatumu et al., 2009, Grabner et al., 2009, Rangel-Moreno et al., 2007, Wengner et al., 2007, Winter et al., 2010).

Ruddle's work has elucidated the importance of LTα in TLO formation (Sacca et al., 1995, Kratz et al., 1996). Overexpression of LTα under the control of RIP resulted in TLO formation in both pancreas and kidney with segregated T and B cell areas, FDCs, stromal cell networks and HEVs (Sacca et al., 1995, Kratz et al., 1996). Moreover, LTα signalling through tumour necrosis factor receptor I (TNFRI) seemed to trigger TLO formation by inducing the secretion of CXCL13 and CCL21 (Sacca et al., 1995, Kratz et al., 1996). LTα seems to be crucial for the development of stromal cells into FDCs and HEVs (Drayton et al., 2003).

Mice deficient in IL-7, a homeostatic cytokine, completely lack lymph nodes and Peyer's Patches (PP), since it seems to be directly involved in T cell survival and activation of LTi cells (von Freeden-Jeffry et al., 1995).

1.1.5. Stromal cells in TLO formation and function

The function of the Immune system relies on numerous interactions between various cell populations. Stroma is an important tissue that consists of extracellular matrix (ECM) and mesenchymal cells, known for providing a structural scaffold and conduit for blood and lymphatic vessels, nerves and leukocytes (Barone et al., 2012). Non-hematopoietic stromal cells are recognized as essential counterparts to leucocytes in pathogenicity, as they have been shown to be actively involved in migration, activation and survival of immune cells in persistent inflammatory conditions (Barone et al., 2012, Chang et al., 2002).

Fibroblasts, traditionally described by their spindle shaped morphology and their ability to adhere to tissue culture plastic *in vitro*, are the most abundant cells of the stroma. Fibroblasts comprise a heterogeneous population of distinctly differentiated cell types involved in the synthesis of ECM and form the structural framework characteristic of stromal tissue (Chang et al., 2002, Tarin and Croft, 1969, Filer et al., 2007). Fibroblasts are thought to differentiate from at least three sources: primary mesenchyme, local epithelial-mesenchymal transition, and bone marrow-derived precursors (Bucala et al., 1994, Chesney and Bucala, 1997, Iwano et al., 2002, Kalluri and Neilson, 2003, Parsonage et al., 2005). Fibroblasts are responsible for the synthesis of

ECM components, type I, III and V collagen and fibronectin, and also proteins involved in the formation (type IV collagen and laminin) and degradation of basement membrane (metalloproteinases) (Marinkovich et al., 1993, Sabatelli et al., 2001, Tomita et al., 2002).

A particular type of stromal cells termed FDCs represents a critical cell type in SLOs and provides antigen presentation and survival factors to the expanding B cell population leading to affinity maturation (Aguzzi et al., 2014). The maturation of FDCs is dependent on the expression of tumour necrosis factor alpha (TNFα) and LT by GC B cells. Mice deficient in the expression of TNFα and LT or of their downstream signalling pathways are unable to develop FDCs and GCs within their SLOs (Allen and Cyster, 2008, Tumanov et al., 2004). In the periphery, FDC networks form only within large TLOs, when a critical number of B cells are clustered in the tissue (Barone et al., 2005). Interestingly, not all tissues, and only a minority of TLOs form mature FDC networks (Pitzalis et al., 2014), suggesting that while the stimulus for FDC differentiation might be the same as that observed in SLO (TNFα and LTα), it is possible that the threshold required for FDC formation in peripheral tissue is higher than in SLOs. Whether the phenotype, origin and function of FDCs in peripheral TLOs are different from FDCs in SLO is not known, neither is their dependency on LT or LT-inducing pathways.

The biology of stromal cells is still to be fully understood but it appears that activated fibroblasts are intimately involved in the switch from resolving to persistent inflammation, for example providing retention and survival factors to infiltrating immune cells within non-lymphoid organs (Buckley, 2011, Filer et al., 2007, Naylor et al., 2013).

Pathogenic stromal cells have also been associated with the formation of TLOs and their persistence is thought to be mainly related to an inappropriate expression by activated stromal cells of adhesion molecules, survival factors, such as B-cell activating factor (BAFF) and IL-7, inflammatory and homeostatic chemokines and their receptors, CXCL8, CCL5, CXCL1, CXCL12, CXCL13, CCL19, CCL21 and CCL17 (Mueller and Germain, 2009, Buckley, 2011). Consistent with these observations, under appropriate conditions, tissue resident fibroblasts can mature into glycoprotein 38 (gp38)+ lymphoid-like stromal cells both in cancer and inflammation (Peduto et al., 2009).

A model of stromal cell differentiation is illustrated in **Figure 1.1**.
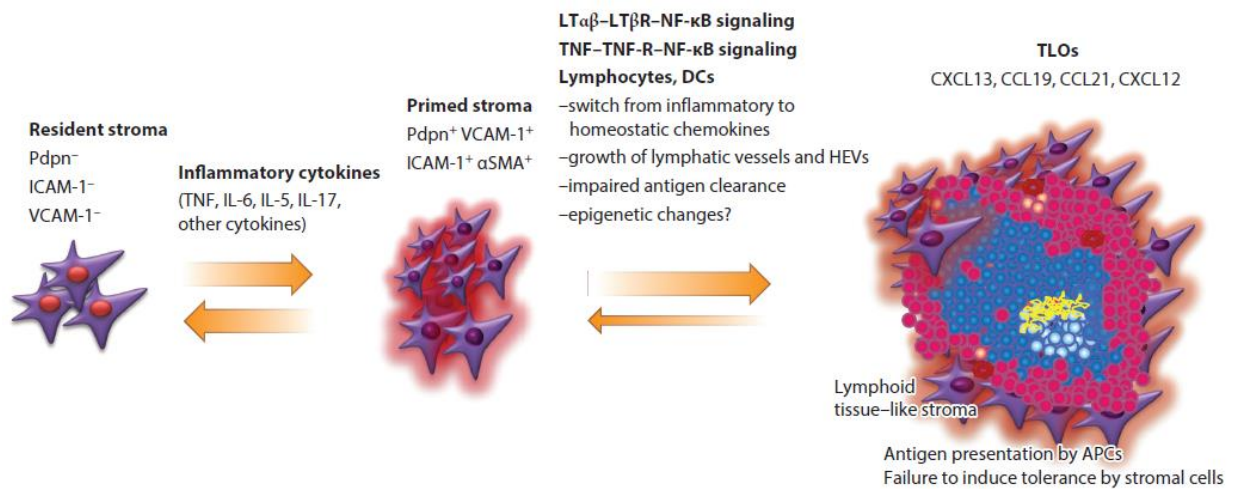
Figure 1.1. Model of stromal cell differentiation during the switch to chronic inflammation. In response to inflammatory cytokines, resident stromal cells produce inflammatory chemokines upon stimuli. In cases of chronic inflammation stromal cells acquire a lymphoid-like phenotype and taking part in the formation of TLOs (Buckley et al., 2015).

Cupedo et al. have shown that intradermal injections of new-born lymph node-derived cells into adult mice induce the ectopic formation of lymph node-like

structures and highly organised TLOs, in which lymphoid-like stromal cells recruit host lymphocytes (Cupedo et al., 2004). In the absence of additional stimuli, injections of adult lymph node-derived cells did not result in formation of such structures (Cupedo et al., 2004). Similarly, Suematsu and Watanabe demonstrated that transplantation of stromal cells under the kidney capsule of adult mice was sufficient to trigger the development of lymphoid-like tissue (Suematsu and Watanabe, 2004).

Recently, Pikor and colleagues have demonstrated that a cytokine- and chemokine-producing stromal cell network forms in the meninges of mice during EAE and that LTαβ-expressing T_H17 cells and LTβR expressed by local resident cells, cooperate in the development of TLOs (Pikor et al., 2015).

In summary, there is compelling evidence that the cross talk between both the stromal and hematopoietic compartments is necessary for the development of TLOs (Nishikawa et al., 2000, Mebius, 2007, Buckley et al., 2015, Peters et al., 2011, Pikor et al., 2015).

The following sections will describe a co-stimulatory pathway in the context of inflammation and autoimmunity and two distinct proteins discretely expressed by stromal cells in resting conditions but overexpressed during inflammation. These proteins, namely gp38/podoplanin (PDPN) and fibroblast activation protein α (FAP) can not only be used to identify subtypes of stromal cells but are also believed to play a functional role in chronic inflammation.

1.2. Co-stimulatory molecules

Antigens processed by antigen-presenting cells (APCs) are presented to the T cell receptor (TCR) via major histocompatibility complex (MHC); consequently this interaction induces T cell activation. However, T cell activation, tolerance and secretion of most lymphokines only occur upon the engagement of signals in addition to TCR stimulation. Indeed, other co-stimulatory molecules, often described as 'signal 2', expressed by both T cells and APCs are necessary to further enhance T cell activation and proliferation (Stuart and Racke, 2002, Sharpe and Freeman, 2002). Some of the most studied and better understood co-stimulatory molecules include CD80 (B7-1), CD86 (B7-2), CD28, cytotoxic T lymphocyte antigen 4 (CTLA-4), inducible co-stimulator (ICOS), programmed death 1 (PD-1), OX40 and CD40 ligand (CD40L) (Stuart and Racke, 2002). CD28, ICOS, OX40 and CD40L promote T cell activation; from these molecules, CD28, which binds to CD80 and CD86, targets naïve T cells and leads to IL-2 secretion (Hara and Fu, 1985, Lucas et al., 1995, Lenschow et al., 1996, Thompson et al., 1989). On the other hand, CTLA-4 and PD-1 are considered inhibitory co-stimulatory molecules (Stuart and Racke, 2002).

It is now believed that such co-stimulatory pathways have a critical role in regulating and shaping the character and magnitude of T cell responses (Ford et al., 2014). Therefore, co-stimulatory pathways have become a very appealing therapeutic target in cancer and in autoimmune diseases since its manipulation can determine the fate of immune responses (Stuart and Racke, 2002).

1.2.1. ICOS and ICOSL

1.2.1.1 Structure

ICOS was firstly described by Hutloff *et al.* as a member of the CD28 family (Hutloff et al., 1999). Immunoprecipitation of ICOS revealed a disulphide-linked homodimer in which each chain has a molecular weight that can vary between 27K and 29K, depending on post-translational modifications (Hutloff et al., 1999). ICOS is a type-I transmembrane molecule, containing an immunoglobulin V-like domain, a transmembrane region of 23 amino acids and a cytoplasmic tail of 35 amino acids. It also comprises a Src-homology SH2 and SH3 domains that can be found in intracellular signal-transducing proteins (Stuart and Racke, 2002). This predicted structure unveiled an obvious structural resemblance with CD28 and CTLA-4 (Hutloff et al., 1999). The amino acid sequence shows 39% similarity with CD28 and CTLA-4 in which the residue allegedly responsible for the disulphide bridge formed between the two dimers in CD28 and CTLA-4 is also conserved in the ICOS molecule (Hutloff et al., 1999, Brunet et al., 1987). However, the motif MYPPPY that is critically involved in binding of CD28 and CTLA-4 to their receptors B7-1 and B7-2 is not present in ICOS, suggesting that ICOS binds to a different receptor (Hutloff et al., 1999, Peach et al., 1994, Truneh et al., 1996). Human and murine ICOS amino acid sequences have 69% homology (Yoshinaga et al., 1999).

ICOS ligand (ICOSL or B7RP-1), a member of the B7 family, is the only known ligand to ICOS and it does not bind proteins in the CD28 or CTLA-4 co-stimulatory pathways (Swallow et al., 1999, Yoshinaga et al., 2000). There is

41% amino acid identity between the human and murine ICOSL (Yoshinaga et al., 2000). The protein consists of 302 amino acids and structurally resembles CD80 and CD86, being a type I transmembrane protein with a main domain, two extracellular immunoglobulin-like domains, a transmembrane region and a short cytoplasmic tail (Yoshinaga et al., 2000, Swallow et al., 1999).

1.2.1.2. Expression

ICOS was firstly identified in activated CD4+ and CD8+ T cells (post TCR stimulation) and proliferation induced by ICOS signalling was equally as potent to that observed after CD28 co-stimulation (Hutloff et al., 1999). ICOS is also expressed by T_H1, T_H2, T_H17, T_{FH} and regulatory T cells (Treg) (Tan et al., 2008, Nakae et al., 2007, Burmeister et al., 2008, Akiba et al., 2005).

In contrast to CD28 co-stimulation, ICOS signalling does not induce secretion of IL-2 but rather promotes upregulation of IL-4, IL-5, interferon gamma (IFN-γ), TNFα and granulocyte-macrophage colony-stimulating factor (GM-CSF) and greatly induces IL-10 secretion, a cytokine implicated in the generation of B cell memory and plasma cells (Hutloff et al., 1999, van Berkel and Oosterwegel, 2006). But similarly to CD28 signalling, ICOS also induces expression of CD69, CD25, CD71 and CD40L (CD154 or TRAP), the latter being a key ligand for CD40 on B cells and a prerequisite for isotype switching and synthesis of immunoglobulin (Ig) G, IgA and IgE by B cells (Hutloff et al., 1999, Kroczek et al., 1994).

Indeed, with monoclonal antibodies F44 (anti-ICOS) and 9.3 (anti-CD28), it was shown that co-stimulation via either ICOS or CD28 enhances Ig

production by B cells (Hutloff et al., 1999). High levels of ICOS expression were found in 50 to 70% of tonsillar T cells which were mostly all also positive for CD28 and CD45RO, an established marker for memory T cells (Hutloff et al., 1999, Merkenschlager and Beverley, 1989). ICOS upregulation was also described in most T cells post stimulation with PMA and ionomycin (Yoshinaga et al., 2000). Interestingly, nearly all T_{FH} cells in GC, a subset of T cells that has been appointed as the main T cell help towards Ig production by GC B cells via induction of AID synthesis and class switch recombination, are also ICOS+ (Hutloff et al., 1999, Dong et al., 2001a, Kim et al., 2005, Liang et al., 2002).

Accordingly, in tonsil, ICOS+ T cells are mainly confined to GCs, particularly in the apical light zone where T_{FH} cells can be found and where the differentiation from B cells into antibody-secreting plasma cells takes place (Hutloff et al., 1999, Vinuesa et al., 2005). Studies in ICOS deficient mice have unveiled a key role for T_{FH} cells in B cell differentiation and generation of autoantibodies in autoimmune disease (Hu et al., 2009).

In mice, ICOS expression was first described in T cells, isolated from the inguinal lymph nodes of mice with inflammatory colitis, however only low levels of ICOS are detectable in the lymph nodes of resting mice (Yoshinaga et al., 1999, Boirivant et al., 1998). ICOS is also expressed *de novo* in activated CD4+ and CD8+ T cells (Yoshinaga et al., 1999). In aged mice, a significant number of splenic ICOS+ T cells also express high levels of CD44 and low levels of expression of CD45RB, consistent with the observation of ICOS expression in human memory T cells (Yoshinaga et al., 1999).

ICOSL was first found in B cells in murine lymph nodes, both in resting conditions and experimental colitis, in the splenic marginal zone, PP follicles and thymus medulla (Yoshinaga et al., 1999).

ICOSL is also expressed by other murine APCs such as macrophages, DCs and also by their human counterparts (Yoshinaga et al., 1999, Yoshinaga et al., 2000). *In vitro* treatment with TNFα efficiently induced ICOSL upregulation in B cells and monocytes but it had the opposite effect on DCs (Yoshinaga et al., 2000).

An *in vitro* study has shown that ICOSL expression in fibroblasts can be induced by TNFα stimulation via activation of the NF-κB/Rel family of transcription factors, known to control immune and inflammatory responses and to be persistently activated in chronic inflammatory conditions (Swallow et al., 1999, Pena and Penate, 2002, Satoh et al., 2007, Oikonomidou et al., 2006, Greetham et al., 2007). Accordingly, in mice challenged with lypopolyssacharide (LPS), non-lymphoid tissues upregulated ICOSL (Swallow et al., 1999). However to date, there is no *in vivo* evidence of ICOSL expression in non-hematopoietic cells. In the absence of ICOS or ICOSL, T cell development is not affected and GC structure was normal in resting mice. However, due to abrogated levels of IL-2 secreted by ICOS$^{-/-}$ CD4+ T cells, T cell activation and proliferation are defective in ICOS knockout mice (KO) (Dong et al., 2001a, Wong et al., 2003, Dong et al., 2001b).

In PP, part of the mucosa-associated lymphoid tissues (MALT), the ICOS pathway has been implicated in their development, but not organogenesis. ICOS deficiency does not affect the number of GC in PP nor their cellular composition; however, ICOS$^{-/-}$ PP are significantly smaller and lack peanut

agglutinin binding (PNA)+ B cells (Iiyama et al., 2003). Similar findings were observed in the ICOS-YF mice, a knock-in strain with a modified cytoplasmatic tail that prevents ICOS binding to phosphatidylinositol-4,5-bisphosphate 3-kinase (PI3K) (Gigoux et al., 2009). Consistent with previous findings, the proportion of IgA- and IgG-producing cells, but not IgM, was significantly reduced in ICOS^{-/-} (Iiyama et al., 2003). In summary, ICOS signalling seems to be necessary for the complete establishment of GC within PP.

1.2.1.3. Regulation

At a transcriptional level, ICOS is regulated by molecules downstream of TCR engagement, such as Src kinase Fyn and MAP kinase ERK (Zamoyska et al., 2003, Tan et al., 2006). Src kinase Fyn seems to be directly involved in NFATc2 dephosphorylation and nuclear translocation, which can as well as ERK bind to the ICOS promoter (Simpson et al., 2010). Accordingly, *in vitro* upregulation of ICOS by mouse T cells is regulated by NFATc2 and ERK (Tan et al., 2006, Simpson et al., 2010).

Post-transcriptionally, ICOS expression can also be suppressed by Roquin, a member of the RING-type ubiquitin ligase family, which induces degradation of *Icos* mRNA when micro RNA-101 binds to the 3' UTR region (Vinuesa et al., 2005, Yu et al., 2007). In fact, Yu and colleagues have described the development of a lupus-like autoimmune condition in *sanroque* mice. This transgenic strain contains a mutation of one amino acid substitution of the Roquin ROQ domain leading to ICOS overexpression by T cells, increased

development of GC, uncontrolled differentiation of T_{FH} cells and IL-21 production (Yu et al., 2007, Vinuesa et al., 2005, Bertossi et al., 2011). Roquin knockout mice are lethal shortly after birth (Bertossi et al., 2011).

In T_H1 cells, ICOS upregulation is dependent on the interaction of NFATc2 and T-bet to its promoter; furthermore, IRF4 has also been shown to bind to the ICOS promoter in Tregs (Tan et al., 2008, Zheng et al., 2009). On the other hand, ICOS expression levels in Th2 cells rely on the binding of NFATc2 and GATA-3 to the untranslated 3' UTR region of *Icos* mRNA (Tan et al., 2008, Simpson et al., 2010).

ICOS signalling occurs through PI3K, which contains a catalytic p85 and regulatory p50α subunits (Fos et al., 2008). This particular form of PI3K shows greater lipid kinase activity leading to increased production of phosphatidylinositol (3,4,5)-trisphosphate (PIP_3) and consequently elevated levels of the kinase Akt (Fos et al., 2008, Parry et al., 2003). Akt is one of the most important signalling molecules downstream of PIP_3 and has been described as a key modulator of T cell survival and proliferation factors (Fruman, 2004, Song et al., 2005). Indeed, in a study from 2009, PP of ICOS-YF mice were challenged, resulting in decreased secretion of Th2- and T_{FH}-derived cytokines (IL-4, IL-10, IL-21), compromised generation and development of T_{FH} and impaired GC formation and Ab class switching (Gigoux et al., 2009)

1.2.1.4. Role in T cell responses

The ICOS-ICOSL interaction provides a further co-stimulatory signal to previously activated T cells (Swallow et al., 1999, Yoshinaga et al., 1999).

When ICOS$^{-/-}$ mice are immunized with an adjuvant known to induce a T_H2 response the draining lymph nodes from the knockout mouse are smaller, total cell number is reduced to half of what is observed in the controls and IL-4 production is completely abrogated in ICOS$^{-/-}$ T cells, suggesting defective T_H2 function and cytokine production (Dong et al., 2001b).

Accordingly, immunization with sheep red blood cells, which induces splenic T cell dependent immune response, leads to the formation of smaller GC in an ICOS$^{-/-}$ spleen and reduced numbers of IgG1+ GC, a process dependent on T_H2 cytokines (Dong et al., 2001a, Dong et al., 2001b). However, ICOS was absolutely necessary to mount a secondary immune response post re-challenge (Dong et al., 2001b). Using the same immunization model in ICOS deficient or in anti-ICOSL treated mice, Akiba *et al.* reported defective development of CXCR5+ T_{FH} cells in both spleen and lymph nodes in the absence of ICOS (Akiba et al., 2005).

Similarly, ICOSL$^{-/-}$ showed defective T cell-dependent but not T cell-independent immune responses, and Ag-specific B cells were absent from the follicles of immunized spleens (Wong et al., 2003). Such impairment in GC formation has been hypothesized to be due to the lack of communication between T and B cells in the T cell areas of SLOs via ICOS-ICOSL signalling, which prevents B cell migration to form GCs (Wong et al., 2003). More recently, Hamel and colleagues have shown that in the spleen of ICOSL$^{-/-}$ mice post immunization the percentage of GC is drastically reduced and so

are the numbers of CD4+CXCR5+CD62L^{low}PD-1+ICOS+ cells (Hamel et al., 2014).

ICOS is now considered a key player in T$_{FH}$ development in both mice and humans and in fact ICOS$^{-/-}$ mice have fewer T$_{FH}$ cells and these secrete reduced levels of IL-21, IL-23R and transcription factor c-Maf; all of which are involved in T$_{FH}$ development (Warnatz et al., 2006, Akiba et al., 2005, Bossaller et al., 2006, Bauquet et al., 2009, Simpson et al., 2010).

In a mouse model of airway hyper-responsiveness, ICOS deficient lungs are infiltrated by similar numbers of leukocytes and re-challenged cells from draining lymph nodes secreted reduced levels of two relevant T$_H$2 cytokines, IL-13 and IL-4 (Dong et al., 2001a).

1.2.1.5. Role in autoimmunity

ICOS$^{-/-}$ mice are significantly more susceptible to EAE, with greater infiltrates found in the brain and higher numbers of CD4+ T cells in general and increased proportion of interferon gamma (IFNγ)-producing T cells (Dong et al., 2001a, Sporici et al., 2001). It has been suggested that the deficient production of IL-13 by ICOS$^{-/-}$ T cells could explain the increased severity of murine EAE model as disease was ameliorated by administration of IL-13 in rats (Dong et al., 2001a, Cash et al., 1994). In this particular study, ICOS seems to act as a negative regulator of inflammation. In contrast, Sporici and colleagues described an improvement in clinical score when EAE mice with ongoing disease were treated with ICOS-Fc (Sporici et al., 2001). ICOSL expression was detected in B cells and macrophages from the brain of EAE

mice (Sporici et al., 2001). ICOS-Ig treatment decreased production of IL-10 and IFN-γ and increased T cell apoptosis (Sporici et al., 2001).

Iwai *et al.* first explored the potential role of ICOS-ICOSL interaction in the pathogenesis of autoimmune arthritis by using an anti-ICOSL monoclonal Ab in a model of collagen-induced arthritis (CIA) (Iwai et al., 2002). ICOS was found in T cells and ICOSL in B cells, macrophages and DCs of inflamed synovium (Iwai et al., 2002). Both therapeutic and prophylactic blockade resulted in significant improvement in disease clinical score, lymphocytic infiltration, hyperplasia of the synovium and bone erosion (Iwai et al., 2002). Furthermore, blockade of this interaction significantly reduced the expression of pro-inflammatory cytokines TNF-α, IL-1β and IL-6 (Iwai et al., 2002). Another study investigated the role of ICOS in the pathogenesis of arthritis and found that ICOS deficient mice are protected against CIA, with normal histological appearance and greatly reduced anti-collagen IgM and IgG2a levels (Nurieva, 2005). Hu *et al.* used the same approach of ICOS-ICOSL blockade and reported reduced numbers of T_{FH} and GC B cells in CIA and mouse model of systemic lupus erythematosus (SLE) (Hu et al., 2009). Moreover, recently Hamel *et al.* described that ICOSL deficient mice are fully protected when challenged with the cartilage proteoglycan-induced arthritis model and confirmed other reported results such as suppression of pro-inflammatory cytokines IL-17, IL-10, IL-4, IL-21 and IFN-γ (Hamel et al., 2014). Furthermore, a similar degree of protection towards the development of arthritis was found when the same group generated B-cell specific ICOSL^{-/-} chimeric mice (Hamel et al., 2014). In patients with RA, analysis of both peripheral blood and synovial fibroblasts revealed increased expression of

ICOS by T cells from patients when compared to controls (Okamoto et al., 2003). SLE patients with active disease also have higher numbers of ICOS+ T cells and following *in vitro* ICOS co-stimulation T cells from SLE patients produced elevated amounts of IFN-γ (Kawamoto et al., 2006).

Anti-ICOS treatment was reported to suppress the development of autoimmune diabetes in non-obese diabetic (NOD) mice, following treatment administered to 1 and 10 weeks old mice (Nanji et al., 2006, Ansari et al., 2008). NOD mice spontaneously develop type 1 (insulin dependent) diabetes, an autoimmune T cell mediated response that characterized by leukocyte infiltration around the insulin-producing islet β cells ultimately leading to its destruction (Atkinson and Leiter, 1999, Delovitch and Singh, 1997). T cell accumulation can also be found in the salivary glands of NOD mice, in lesions that resemble SS lesions (Bach, 1994), but the effect of ICOS blockade in NOD salivary glands has not yet been reported.

In the context of TLO formation, this pathway has not been extensively explored but a recent study has reported that blockade of ICOS/ICOSL interaction suppresses the formation of ectopic lymphoid structures in a mouse model of atherosclerotic plaque development (Clement et al., 2015). The observed impairment was associated with a disrupted T_{FH} - GC B cell axis as T_{FH} cells are known to express ICOS and were shown to take an active part in GC reaction within TLOs in diseased arteries (Clement et al., 2015).

ICOS null patients showed similar phenotypes of defective class switch recombination and GC formation as these patients fail to generate and maintain memory B cells and Ig levels (McAdam et al., 2001, Mak et al., 2003,

Grimbacher et al., 2003). Takahashi *et al.* reported the case of two ICOS deficient siblings with reduced numbers of CD4+ central and effector memory T cells, the latter one associated with deficient upregulation of T-bet, GATA3 and MAF and retinoic acid-related orphan nuclear hormone receptor (RORC) (Takahashi et al., 2009). Confirming what was reported in ICOS deficient mice, CD4+ T cells from these patients also secrete poor levels of T_H1, T_H2 and T_H17 cytokines (Takahashi et al., 2009).

1.3. Stromal cell markers

1.3.1. Podoplanin

Gp38 or PDPN was first identified by Farr et al. (1992) in stromal cells of peripheral lymphoid tissues (Farr et al., 1992), including in lymph node fibroblastic reticular cells (FRCs). More than 2 decades later, despite the fact that gp38 expression has been extensively characterised in tissues under both physiological and pathological conditions little is known regarding its functional role under these conditions.

1.3.1.1. Structure

Gp38 is a 43 kDa protein and its cloning revealed a 172 amino acid sequence. Gp38 is a mucin-like type I integral membrane protein with an extracellular domain rich in both Serine and Threonine residues, containing one potential N-linked glycosylation site, six O-glycosylation sites, a hydrophobic transmembrane domain, and a short cytoplasmic domain with two potential phosphorylation sites (Farr et al., 1992, Breiteneder-Geleff et al., 1997).

1.3.1.2. Regulation

Gp38 is expressed by lymphatic endothelial cells (LEC), where it is regulated by the gene Prox1 (Hong et al., 2002). IL-3 stimulation has been shown to control expression of both Prox-1 and gp38 in LEC (Groger et al., 2004, Schacht et al., 2003). Moreover, IL-3 presence in culture medium induces differentiation of blood endothelial cells (BEC) into LEC (Groger et al., 2004).

The authors further demonstrated that TNFα/IFN-γ stimulation also induces gp38 expression by LEC via IL-3 (Groger et al., 2004).

Splenic expression of gp38 is dependent on the secretion of LTα by B cells (Ngo et al., 2001). Also in spleen, lack of gp38 expression has been linked to impaired B and T cell segregation (Bekiaris et al., 2007).

The only known endogenous ligand/receptor for gp38 is CLEC-2, a C-type lectin receptor mainly expressed on platelets and DCs (Acton et al., 2014, Astarita et al., 2015), and its expression is linked to thrombosis, tumour metastasis and lymphangiogenesis (Suzuki-Inoue et al., 2010).

1.3.1.3.   Expression during embryogenesis and post natal

During embryonic development the expression of gp38 is both temporally and spatially regulated. At embryonic day 9 (E9) gp38 is expressed in the central nervous system and foregut (Rishi et al., 1995, Ramirez et al., 2003). At embryonic day 11 (E11.0) its expression becomes restricted to lymphatic progenitor cells (Schacht et al., 2003) and by E11.5 and E12.5, gp38 can be found in all endothelial cells of the cardinal vein (Schacht et al., 2003). Moreover, gp38 expression has also been reported in the developing mammalian kidney, choroid plexus, intestine and oesophagus (Williams et al., 1996).

After birth, gp38 expression is mostly confined to lymphatic endothelial cells and FRCs in lymphoid organs, mature osteoblasts, alveolar type I cells and a subset of F4/80+ macrophages induced following zymosan peritonitis

(Wetterwald et al., 1996, Williams et al., 1996, Hou et al., 2010, Schacht et al., 2003).

Both in the lymph node and spleen, gp38+ cells are found in close association with T cell areas (Farr et al., 1992). Kidney glomerular epithelial cells, also called podocytes, express gp38 on their cell membranes and epithelial cells of Bowman's capsule express gp38 at the luminal surfaces in resting conditions but not in a model of rat nephropathy (Breiteneder-Geleff et al., 1997).

Gp38 is also expressed by LEC, myoepithelial cells, subsets of lymphocytes and DCs (Yazisiz et al., 2013, Jones et al., 2015).

1.3.1.4. *Expression in pathology*

Gp38 expression is induced in epidermal carcinogenesis and in skin remodelling processes (Scholl et al., 1999).

In the salivary glands of patients with SS, both gp38 expression in myoepithelial cells and the number of lymphatic vessels are increased (Yazisiz et al., 2013). In healthy synovium gp38 seems to be absent but it is significantly upregulated in the inflamed synovium of patients with RA (Ekwall et al., 2011). Concordantly, cultured synoviocytes upregulate gp38 after stimulation with IL-1β, TNF-α and transforming growth factor beta (TGF-β) (Ekwall et al., 2011).

In EAE, T_H17 cells that express gp38 were directly involved in the formation of ectopic lymphoid aggregates in the central nervous system, particularly with

27

the microarchitecture of T cell zones (Peters et al., 2011, Link et al., 2011, Pitzalis et al., 2014, Pikor et al., 2015).

1.3.1.5. Function of gp38

$PDPN^{-/-}$ mice die at birth due to respiratory failure and exhibit critical defects in lymphatic structure and organization, but not in blood vessel formation. Such defects include impaired lymphatic transport, lymphedema and dilation of lymphatic vessels (Bertozzi et al., 2010, Finney et al., 2012, Herzog et al., 2013, Suzuki-Inoue et al., 2010, Watson et al., 2010, Schacht et al., 2003). In contrast to what happens in $Prox1^{-/-}$ mice in which lymphatic vasculature is completely absent, the fact that lymphatic vessels still develop in $PDPN^{-/-}$ mice suggests that gp38 might play a role at later stages of lymphatic development (Schacht et al., 2003).

Similarly, CLEC-2 deficient mice are also lethal at neonatal stages with blood-filled lymphatic vessels and edema, both features also observed in $PDPN^{-/-}$ mice (Suzuki-Inoue et al., 2010). Interaction between gp38+ lymphatic endothelial cells with circulating platelets during development has been shown to be critical for the separation of the lymphatic from the blood system (Uhrin et al., 2010). In lymph nodes, gp38+ FRCs engage with CLEC-2+ DCs inducing cytoskeleton rearrangement and consequent cell migration across stromal cell areas (Acton et al., 2012). Indeed, gp38-CLEC-2 interaction plays a role in lymph node elasticity and the absence of CLEC-2 in DCs significantly affects lymph node expansion (Acton et al., 2014).

Interaction between gp38 and CLEC-2 is also crucial for HEVs integrity where lack of gp38 leads to bleeding in draining lymph nodes post immunization (Herzog et al., 2013).

Gp38 has been identified in actin-rich microvilli and plasma membrane projections and its overexpression in keratinocyte cell lines leads to the acquisition of a fibroblast-like shape with augmented membrane projections, reorganization of the cytoskeleton and increased motility (Scholl et al., 1999, Schacht et al., 2003). In lymphatic endothelial cells, gp38 expression is associated with increased cell adhesion and migration (Schacht et al., 2003).

Peduto *et al.* have demonstrated that, during inflammation, resting stromal cells can upregulate the expression of gp38 and acquire a lymphoid-like phenotype similar to that observed in secondary lymphoid organs (Peduto et al., 2009). Gp38+ cells also upregulate the expression of adhesion molecules, chemokines and cytokines known to be involved in the development of lymphoid tissues (Mebius, 2003, Kratz et al., 1996).

1.3.2. Fibroblast Activation Protein α

FAP, also designated as seprase, was first described as a cell surface antigen identified with a monoclonal antibody F19 on human astrocytoma and sarcoma cell lines *in vitro* (Garin-Chesa et al., 1990a). *Fap* gene expression is significantly upregulated in activated fibroblasts in pathological sites, including cancer, wound healing and chronic inflammation (Dolznig et al., 2005, Bauer et al., 2006, Garin-Chesa et al., 1990b, Levy et al., 1999). Evidence of FAP

expression in these tissues may indicate possible roles in promoting cell invasion.

1.3.2.1. *Structure*

FAP is a 170kDa type II cell surface glycoprotein and a member of the serine prolyl oligopeptidase family, a type-II transmembrane serine protease (Ayoama and Chen, 1990, Niedermeyer et al., 1997, Garin-Chesa et al., 1990b, Scanlan et al., 1994). Homodimerisation is essential for its catalytic function and the active FAP enzyme is constituted of two 97kDa subunits on the cell surface (Pineiro-Sanchez et al., 1997). It comprises of a large COOH-terminal extracellular domain, a hydrophobic transmembrane segment of approximately 20 amino acids and a short cytoplasmic domain only 6 amino acids long. The extra cellular domain contains six potential N-glycosylation sites, 13 cysteine residues and three highly conserved catalytic domains (Scanlan et al., 1994). FAP belongs to the family of post prolyl amino peptidases that are capable of cleaving the –NH2-terminal dipeptides from polypeptides with penultimate L-prolines or L-alanines (Niedermeyer et al., 1998).

In both human and mouse, the *Fap* gene is located on chromosome 2 and 89% of the amino acid sequence is shared between the two species, including a perfectly conserved catalytic domain (Niedermeyer et al., 1998). FAP shares 61% nucleotide sequence and 48% amino acid sequence identity with its closest family member dipeptidyl-peptidase IV (DPPIV), a T cell activation antigen, also known as CD26 (Mathew et al., 1995, Park et al., 1999, Scanlan

et al., 1994). FAP and DPPIV have an identical domain structure and 70% identity in the catalytic domain (Goldstein et al., 1997, Pineiro-Sanchez et al., 1997, Scanlan et al., 1994). Under physiological conditions, DPPIV is ubiquitously expressed and has been shown to play a role in various processes such as T cell co-stimulation, chemokine biology, glucose metabolism and cancer (Van Damme et al., 1999, Drucker, 2003).

1.3.2.2. Regulation

The active FAP protein is a 170 kDa homodimer of two N-glycosylated 97 kDa subunits (Pineiro-Sanchez et al., 1997). Dimerization and post-translation glycosylation of FAP subunits are required for its catalytic function (Park et al., 1999, Sun et al., 2002). Interestingly, FAP can also form an active heterodimer with DPPIV and other proteases on the surface of migratory connective tissue cells, promoting cell migration during connective tissue repair (Ghersi et al., 2002, Scanlan et al., 1994). The assembly of the FAP homo and heterodimers is reported to occur in endoplasmic reticulum and the golgi apparatus (Kelly et al., 1994).

Milner *et al.* described upregulation of *Fap* gene expression when cultured chondrocytes were stimulated with IL-1 and oncostatin, both pro-inflammatory molecules known to promote cartilage resorption (Milner et al., 2006). Also, Chen *et al.* demonstrated that cancer cells activate stromal fibroblasts through IL-1β and TGF-β by inducing FAP expression (Chen et al., 2009).

A role for transcription factor EGR1 in regulating FAP expression has been proposed (Zhang et al., 2010). EGR1 is known to control a variety of genes,

including growth factors (TGFβ, PDGFβ), cytokines (IL-2), cell cycle regulators (cyclinD1) and matrix proteins (collagen and fibronectin) (Baron et al., 2006, Khachigian, 2006). Similar to FAP, EGR1 is also involved in wound healing and tumorigenesis (Abdulkadir, 2005, Baron et al., 2006).

1.3.2.3. Expression during embryogenesis

In wild-type mouse embryos, FAP was found to be expressed in the primitive mesenchymal tissue adjacent to the eye and to the cartilaginous primordial of bones (Niedermeyer et al., 2000). In a FAP$^{-/-}$ mouse model generated to also express β-galactosidase under the control of the endogenous *Fap* promoter, β-galactosidase was firstly detected at embryonic day 10.5 (E10.5) within the somites with a similar expression pattern at E11.5 and E12.5 (Niedermeyer et al., 2001). The protein was also identified in developing myotubes (11.5 d.p.c.), paravertebral regions (12.5 d.p.c.), and in peri-chondral mesenchymal cells from the primitive cartilage of the ribs and intercostal muscle fibers and also in dermal fibroblasts (Niedermeyer et al., 2001). The physiological role of FAP during embryogenesis appears to be mainly related to tissue remodelling and angiogenesis activity.

1.3.2.4. Expression in resting tissues

In adult tissues, FAP is considered to be selectively expressed by activated fibroblasts in areas undergoing tissue remodelling, such as embryonic mesenchyme, wound healing, gravid uterus and reactive stroma of epithelial cancers (Niedermeyer et al., 2000). A more recent analysis, carried out by

Dolznig *et al.* showed that normal tissues generally present low FAP expression, with the exception of transient expression in uterus and cervix (Dolznig et al., 2005).

1.3.2.5. *Expression in pathology*

FAP was first identified as an inducible antigen by the F19 monoclonal antibody expressed on reactive mesenchyme of various tumours and transformed cell lines and granulation tissue of wound healing (Rettig et al., 1986, Rettig et al., 1988, Garin-Chesa et al., 1990b, Aoyama and Chen, 1990, Kelly et al., 1994, Monsky et al., 1994).

Activated fibroblasts present in tumour associated stroma, granulation tissue of healing wounds and chronic inflammatory conditions differ from resting fibroblasts by a characteristic gene expression, which includes *fap* upregulation (Scanlan et al., 1994).

Epithelial cancers induce the formation of new blood vessels to secure an efficient blood supply to the malignant tissue, and allow the recruitment of activated fibroblasts, lymphoid and phagocytic infiltrates, as well as facilitating the release of peptide mediators and proteases (Scanlan et al., 1994). These events lead to the production of a transformed ECM. FAP-expressing activated fibroblasts, as well as FAP positive pericytes, can be found closely associated with tumour capillaries, forming a separate compartment between the tumour capillary endothelium and the basal portion of malignant epithelial cell clusters (Welt et al., 1994, Scanlan et al., 1994, Rettig et al., 1993).

Benign and premalignant epithelial cancers generally consist of very low or moderate FAP-expressing stromal cells. However, FAP positive cells are a common feature of reactive tumour mesenchyme of several types of epithelial cancers, including more than 90% of breast, lung, colorectal and pancreatic carcinomas (Garin-Chesa et al., 1990b). Furthermore, high FAP expression has also been shown in a large proportion of bone and soft tissue sarcomas (Rettig et al., 1986, Dohi et al., 2009, Aoyama and Chen, 1990, Monsky et al., 1994). Particularly, in pancreatic ductal adenocarcinoma an association between FAP expression and tumour size, fibrotic focus, perineural invasion and worse prognosis has been established (Shi et al., 2012). Similarly, in colon cancers increased stromal FAP staining is positively correlated with disease prognosis and development of metastases (Henry et al., 2007). Despite these studies, the role of FAP in the tumour microenvironment is unclear. However, the most compelling evidence suggests a key role for FAP+ cells in cancer invasion, tumour angiogenesis and subsequent growth and metastases (Mori et al., 2004, Iwasa et al., 2005, Kelly et al., 1998, Kraman et al., 2010).

Apart from cancer associated fibroblasts, FAP expression is also reported in activated fibroblasts at the tissue remodelling interface of healing wounds, cirrhotic liver and in the fibrotic interstitial space in lungs from patients suffering from idiopathic pulmonary fibrosis (Garin-Chesa et al., 1990a, Levy et al., 1999, Acharya et al., 2006).

In synovial biopsy samples from patients with RA, FAP is highly expressed throughout the synovium but also in synovial fibroblasts (Waldele et al., 2015). FAP-expressing fibroblast-like synoviocytes (FLSs) were predominantly found

in the lining layer of the synovium, co-localised with metalloproteinases (MMP-1 and MMP-13) as well as CD44, molecules known to be involved in ECM degradation in the synovial membranes of diseased joints (Bauer et al., 2006). In mouse models of arthritis, gene expression profiles displayed a seven-fold increase in *Fap* and *DPPIV* transcripts in inflamed paws when compared to non-inflamed counterparts (McIndoe et al., 1999) and, based on FAP$^{-/-}$ mice, it has been suggested that in the context of chronic inflammation in arthritic joints FAP might be involved in cartilage and bone damage (Waldele et al., 2015).

FAP expression, induced by macrophage-derived TNFα, was also detected in human aortic atherosclerotic plaques, in smooth muscle cells, where it contributes to type I collagen degradation (Brokopp et al., 2011).

1.3.2.6. *Function*

FAP exhibits both prolyl dipeptidyl peptidase, which overlaps with that of DPPIV, and collagenolytic activity capable of degrading gelatin and type 1 collagen, which distinguishes FAP from DPPIV (Levy et al., 1999). Both functions utilise the common active serine 624 in FAP (Park et al., 1999). However, not much is known about its natural substrate and the significance of its peptidase activity *in vivo* (Park et al., 1999). *In* vitro exposure of a metastatic ovarian cancer cell line to different FAP doses demonstrated increased invasion, migration and proliferation ability in a dose-dependent manner (Chen et al., 2009). Due to its enzymatic activity FAP is known to denature collagen, playing a role in the degradation of ECM; thus, acting in

physiological tissue repair and remodelling (Milner et al., 2006, Niedermeyer et al., 2001). This is particularly evident during tadpole metamorphosis in *Xenopus laevis* in which FAP activity has been reported (Brown et al., 1996). Interestingly, according to Niedermeyer *et al.*, FAP$^{-/-}$ mice are viable, fertile and show no development effects or structural abnormalities when compared to wildtype mice (Niedermeyer et al., 2000).

When overexpressed in epithelial and fibroblastic cell lines, FAP significantly affects cell adhesion, migration, proliferation and apoptosis and also tumour invasion (Wang et al., 2005, Lee et al., 2011). Inhibition of FAP proteolytic activity with blocking antibodies or antisense strategies suppress its function, reducing tumour growth (Cheng et al., 2002, Santos et al., 2009, Goodman et al., 2003). Furthermore, overexpression of FAP upregulates MMP2 and CD44 and downregulates integrin-β1, the latter known to connect the cytoskeleton to the ECM thereby facilitating tumour cell migration (Wang et al., 2005).

Recently, Waldele *et al.* showed that FAP$^{-/-}$ crossed with hTNFtg mice were less affected by cartilage degradation and their synovial fibroblasts exhibited reduced capability to adhere to cartilage (Waldele et al., 2015). Therefore, in the context of chronic inflammatory arthritis FAP seems to be involved in the loss of proteoglycans and consequent cartilage degradation (Waldele et al., 2015).

1.3.2.7. Inducible depletion of FAP+ cells: the FAP-DTR transgenic mouse

In this project, a FAP-DTR Tg mouse model, a kind gift from Prof Douglas Fearon, was used to clarify the role of FAP in the context of TLO formation. In

this model the *Fap* gene has been modified by insertion of a cassette encoding the primate diphtheria toxin receptor (DTR), not expressed in mice. Administration of Diphtheria Toxin (DTx) to mice via injection induces specific deletion of the FAP-expressing cells. This model has been previously used by our collaborators to address the role of FAP+ cell in cancer biology, where deletion of the FAP+ cell caused growth arrest of immunogenic tumours through hypoxic necrosis of both cancer and stromal cells (Kraman et al., 2010).

According to Schreiber and Rowley, the ablation of FAP-expressing fibroblasts and pericytes damages the blood supply to the tumour causing death to some cancer cells. The resulting signals released by cancer cells undergoing cell death activate circulating T cells, which in turn, secrete the pro-inflammatory cytokines IFNγ and TNFα, leading to an immune response against the remaining tumour (Schreiber and Rowley, 2010). This model has therefore suggested an immunosuppressive role for FAP+ cells in cancer biology raising the intriguing possibility that a similar role might be played by FAP in physiological conditions and linked to immunosuppression during autoimmunity and inflammation.

More recently, the same model has been used to deplete lymph node FRCs (which express FAP) leading to loss of T, B and dendritic cells, disrupting normal lymph node homeostasis (Denton et al., 2014). Furthermore, in a mouse model of influenza infection mice lacking FAP+ cells mounted diminished immune responses characterised by reduced numbers of GC B cells, plasma B cells and T$_{FH}$ cells (Denton et al., 2014). This work has

established FAP expressing FRCs in the lymph node as a key cell type in the

retention of naïve lymphocytes and initiation of immune responses.

1.4. Sjögren's syndrome

1.4.1. Clinical features

SS is an inflammatory disease of autoimmune aetiology characterised by chronic focal lymphocytic infiltration of exocrine glands, predominately the lachrymal and salivary glands. Chronic sialadenitis results in progressive tissue damage with loss of secretory gland function leading to the primary clinical features of keratoconjunctivitis sicca (dry eyes) and xerostomia (dry mouth). The inflammatory process can progress to involve almost any organ system resulting in systemic manifestations of disease (Fox, 2005, Ramos-Casals et al., 2008). In addition, patients with primary disease are at increased risk of B cell lymphomas compared to the general population (Theander et al., 2006).

The disorder was first described both clinically and histologically in 1933 by the Swedish ophthalmologist Henry Sjögren. The organ specific pathology is caused by local inflammation and progressive loss of the glandular parenchyma (Chisholm and Mason, 1968). In 50-60% of cases this disorder is associated with other systemic autoimmune diseases, such as RA or SLE where it is considered to be a secondary, rather than primary disease process (Chisholm and Mason, 1968, Moutsopoulos, 1994).

Primary SS (pSS), which occurs in the absence of other conditions, has a higher frequency in female patients (9:1) and a prevalence of 0.5% in the general population, making SS one of the three most frequent autoimmune diseases (Bowman et al., 2004, Chisholm and Mason, 1968, Fox et al., 1999, Pillemer et al., 2001).

Compelling evidence now suggests that several biological processes are involved in pSS and contribute to the establishment of salivary gland pathology. Those encompass pathways of activation belonging to both the innate and acquired immune systems, such as IFN activation (Brkic et al., 2013), defective regulatory T cell activity (Christodoulou et al., 2008), an increased number and function of T_H17 cells (Katsifis et al., 2009) and excessive co-stimulation (Dimitriou et al., 2002, Gong, 2012). Lymphoneogenesis with GC formation and clonal expansion of malignant B cells is ascribed to the aberrant B cell activation that characterises a subset of patients with high serum titres of autoantibodies and systemic manifestations of the disease. These patients also have an increased risk of the development of lymphoma (Theander et al., 2011).

PSS is characterized by, but not limited to, secretory dysfunction. One third of patients exhibit systemic extra-glandular manifestations, whose development and onset varies during the disease progression (Moutsopoulos, 1994, Shiboski et al., 2012). As a result, clinical management of the disease requires a multi-disciplinary approach including input from rheumatologists, ophthalmologists and oral medicine specialists.

The extra-glandular manifestations include cutaneous vasculitis (leucocytoclastic vasculitis), peripheral neuropathy, polyarthralgia and synovitis, fatigue, renal tubular acidosis, interstitial lung disease, lymphoproliferative disease and immunological abnormalities, such as lymphopenia, anaemia or thrombocytopenia (Anaya et al., 2006, Ramos-Casals et al., 2008). Immunological findings are also observed in pSS, such as the presence of anti-Sjögren's-syndrome-related antigen A and B

autoantibodies (antiSSA/Ro and SSB/La), hyper-gammaglobulinaemia and low complement levels (C4) (Malladi et al., 2012).

Approximately 5% patients with pSS develop lymphoma, conferring a higher mortality risk in pSS as compared to the normal population (Moutsopoulos and Manoussakis, 1998). Patients with pSS have a 16 to 44 times increased risk of developing lymphoma. Histologically, the malignancy is predominantly a MALT non-Hodgkin's lymphoma that forms in extra-nodal sites, mainly within the acquired MALT present in affected major salivary glands (Theander et al., 2006, Voulgarelis et al., 1999). However other forms of B cell lymphoma, such as diffuse large B cell lymphoma, are also observed.

1.4.2. Histological findings in the salivary glands from Sjögren's syndrome patients

Salivary glands are classified as exocrine glands, which secrete saliva through a duct system from a secretory structure called the salivary acinus (Holsinger and Bui, 2007). There are three main types of acini: serous, mucous and mixed (Holsinger and Bui, 2007). Between the epithelial cells and basal lamina of the acinus, flat myoepithelial cells form a latticework and possess cytoplasmic filaments on their basal side to aid in contraction, and thus forced secretion, of the acini. Spindle shaped myoepithelial cells are also observed around the intercalated ducts (Holsinger and Bui, 2007, Dawes et al., 2012).

The formation of small lymphocytic foci around the intra-lobular and inter-lobular ducts represents the typical histological lesion in pSS (Chisholm and

Mason, 1968, Greenspan et al., 1974, Christodoulou et al., 2010). PSS is characterized by the formation of peri-epithelial mononuclear cell infiltrates, which preferentially form in the exocrine glands: salivary glands, lachrymal glands and exocrine pancreas. The histological lesions characteristic of SS occurs both in major and in minor salivary glands. Nonetheless, it has to be acknowledged the predominance of lympho-epithelial lesions (LESA, areas of lymphocytic infiltration of the duct that result in atrophy of the columnar ductal epithelium and proliferation of the basal epithelial cells) and the detection of better-organized GCs in major but not minor salivary glands (Carbone et al., 2000, Barone et al., 2005, Bombardieri et al., 2007).

In the early stages of the disease, CD4+ T cells and DCs mainly inhabit initial aggregates and progressive B cell infiltration is often observed during the disease course. The large diffuse infiltrate then spreads into the parenchyma, resulting in the loss of tissue architecture and atrophic involution of the acini (Gonzalez et al., 2011). Parenchymal and ductal alterations can be observed in the affected glands including atrophic involution of the acini and hyperplasia of the lining cells of the intra-glandular ducts (Chisholm and Mason, 1968, Greenspan et al., 1974, Christodoulou et al., 2010, Gonzalez et al., 2011). Accumulation of hyaline material is also found in the lumen of altered ducts and around blood vessels (Gonzalez et al., 2011, Greenspan et al., 1974). Small foci consist predominantly of plasma cells with a smaller lymphocytic component that is distributed throughout the foci. Larger foci are mainly composed of lymphocytes with fewer macrophages and plasma cells. A discrete plasma cell component can be observed at the periphery of the larger foci (Greenspan et al., 1974).

Activated CD4+ T cells predominate in small aggregates and decrease in severe lesions; on the other hand, B cell infiltration predominates in the larger foci (Christodoulou et al., 2008, Christodoulou et al., 2010). Accordingly, the T/B cell ratio is negatively associated with the degree of inflammation (Christodoulou et al., 2010). Instead, the percentage of CD8+ T cells and natural killer (NK) cells does not significantly change with lesion severity (Christodoulou et al., 2010). Higher numbers of Tregs have been found in patients with pSS as compared to patients with secondary SS or connective tissue disease patients without SS (Furuzawa-Carballeda et al., 2014). Sarigul et al. also described a higher percentage of FoxP3-expressing CD4+ T cells in the salivary glands of pSS patients, even though similar numbers were found in peripheral blood of patients with either pSS or RA and healthy controls (Sarigul et al., 2010). The frequency of regulatory T cell detection appears to correlate with lesion severity (Sarigul et al., 2010). Plasmacytoid DCs, CD123+BDCA-2+ cells are the main source of IFN-α, and have also been identified in all pSS salivary gland biopsies analysed by Gottenberg et al. (Gottenberg et al., 2006, Fitzgerald-Bocarsly et al., 2008). Circulatory plasmacytoid DCs are more activated in pSS patients with a higher expression of CD40 (Wildenberg et al., 2008).

Infiltrating lymphocytes in the ducts can give rise to the formation of LESA, such areas of lymphocytic infiltration (mainly B cells) can lead to atrophy of the columnar ductal epithelium and proliferation of the basal epithelial cells (Carbone et al., 2000). B cells represent the predominant infiltrating cell type, often acquiring monocytoid features or centrocyte-like morphology frequently accompanied by immunoblasts, plasmacytoid lymphocytes and plasma cell

43

differentiation (Greaves and Wang, 2011). In up to 50 % of cases clonal intra epithelial B cell infiltration is present (Carbone et al., 2000) and, in some cases it is possible to observe, either by *in situ* hybridization or immunohistochemistry, kappa or lambda light chain excess production in the infiltrating cells (Harris, 1999).

1.4.3. Germinal centre detection in biopsies from Sjögren's syndrome

In approximately 20-25% of patients with SS salivary gland aggregates are organized into segregated T and B cell areas, and are characterised by the formation of areas of active B cell proliferation and FDC networks within defined GC-like structures (**Figure 1.2**) (Salomonsson et al., 2003).

In GCs within SLOs the process of antigen selection is tightly regulated; in contrast, it is believed that in ectopic GCs, chronic antigen stimulation may contribute to persistent activation of innate and adaptive immune cells (Berg et al., 1986, Vinuesa et al., 2009, Aloisi and Pujol-Borrell, 2006). Indeed, the chronic antigenic stimulation together with the local ectopic expression of B and T cell survival factors are likely to provide the ideal microenvironment for the development of hyperactive B cell clones (Pitzalis et al., 2014).

A large body of literature has highlighted the potential role for the GC-like structures present in the salivary glands in sustaining the process of B cell affinity maturation of autoreactive clones. GCs are mainly composed of B lymphocytes but also macrophages, DCs, FDCs and T cells. DCs play a key role in ectopic GC formation and persistence supporting antigen presentation

and producing key cytokines for B cell maturation and proliferation (Aguzzi et al., 2014). Structurally, a dark zone that is inhabited by highly proliferating centroblasts and a light zone, populated by FDCs and centrocytes, form GCs (MacLennan, 1994). While the dark zone represents the area where the B cell clones undergo expansion; the light zone is the site of antigen presentation and affinity maturation of the B cell compartment (MacLennan, 1994).

Indeed, the local expression of AID, the enzyme instrumental for B cell affinity maturation, is associated with the presence of inflammatory aggregates (Barone et al., 2005, Bombardieri et al., 2007). Moreover a positive correlation between the persistence of the GC-like structures and the development of B cell lymphoma has been suggested (Barone et al., 2008).

Salivary gland lymphoid organization and GC formation is accompanied by the ectopic production of lymphoid chemokines CXCL13, CCL21 and CXCL12, that localize, within the aggregates, in discrete areas resembling the lymphoid organization observed in secondary lymphoid organs (Barone et al., 2005, Bombardieri et al., 2007, Ansel et al., 2000, Luther et al., 2000, Luther et al., 2002, Mebius, 2003). Increased local and systemic (serum and saliva) levels of CXCL13 correlates with xerostomia and it has been previously demonstrated that in lymphoid aggregates the level of CXCL13 or CCL21 correlates with the degree of organization of the foci (Kramer et al., 2013, Barone et al., 2005, Bombardieri et al., 2007).

During the disease course the detection of GCs in salivary gland biopsy has been associated with more aggressive disease development both serologically and clinically (Risselada et al., 2013b). The presence of histologically detectable GCs in approximately 25% of pSS patients has been

found to correlate with the presence of a higher focus score (1.25 points higher) (Risselada et al., 2013b). Specifically, the presence of a positive RF or anti-Ro/SSA and anti-La/SSB antibodies is much higher in patients with GCs than in patients without, suggesting a possible contribution of these structures in the local production of autoantibodies (Risselada et al., 2013b). In terms of autoantibody production and inflammatory cytokine release, no significant differences have been observed between SS patients with positive or negative biopsies for presence of GC (Szodoray et al., 2005, Jonsson et al., 2005).

Figure 1.2
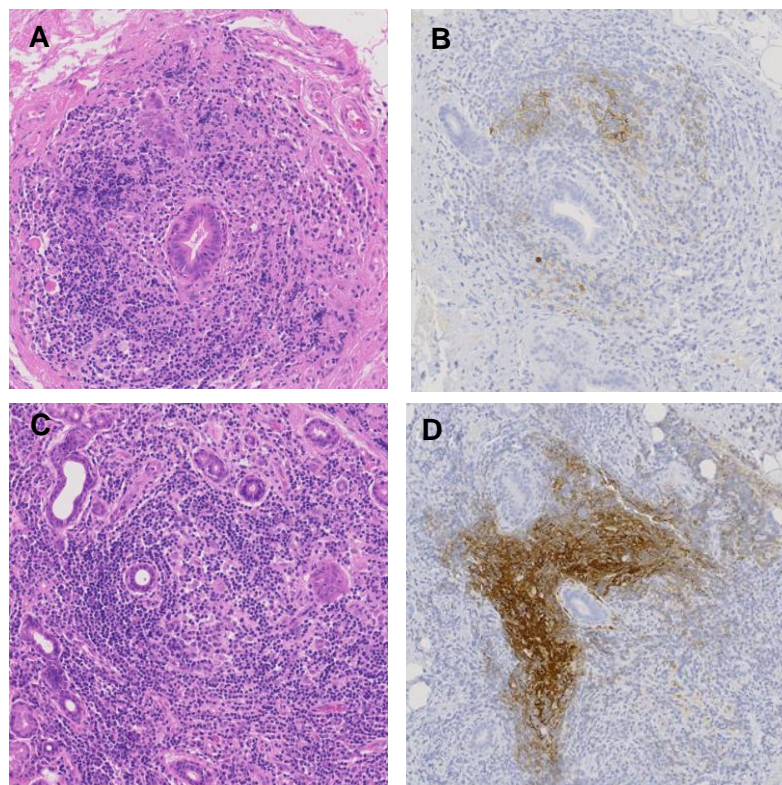
Figure 1.2. Germinal centres in TLOs in Sjögren's syndrome salivary gland biopsies. Hematoxylin and eosin staining of SS salivary gland (A and C) and immunohistological staining anti-CD21 in germinal centre B cell area. (Barone et al., 2015a)

1.4.4. Classification criteria

The large spectrum of manifestations typical of SS has provided a major challenge for the definition and validation of unifying classification criteria (Shiboski et al., 2012). In 1993 the European Study Group On Diagnostic Criteria for SS proposed a set of 6 items including 2 subjective and 4 objective criteria (Vitali et al., 1996). These items included: ocular symptoms; oral symptoms; ocular signs; presence of focal lymphocytic sialoadenitis; instrumental evidence of salivary gland involvement; and presence of autoantibodies (anti-SSA/Ro and/or anti-SSB/La). According to these guidelines, the presence of any four of the above mentioned criteria were indicative of pSS, in the absence of any other associated autoimmune disease (Vitali et al., 1996). The main criticism raised to these criteria was the potential inclusion of patients with no evidence of sialoadenitis or presence of autoantibodies as long as they fulfilled the remaining four criteria (Vitali et al., 2002). In 2002 Vitali et al. revised these criteria, making the presence of a histological diagnosis of SS or the presence in the serum of anti-SSA/Ro and/or anti-SSB/La antibodies mandatory for the diagnosis of pSS (Vitali et al., 2002).

More recently, in 2012 the Sjögren's International Collaborative Clinical Alliance (SICCA) published the first set of criteria approved by the American College of Rheumatology. According to these guidelines, the classification of an individual as having pSS is based exclusively on the presence of objective criteria which include the detection of serum anti-Ro/SSA and/or anti-La/SSB antibodies, or positive rheumatoid factor and antinuclear antibody (ANA); a positive salivary gland biopsy exhibiting a focal lymphocytic sialoadenitis with

a focus score ≥ 1 or the presence of keratoconjuctivitis sicca (Shiboski et al., 2012). Two out of three of those criteria are required for disease diagnosis. Several criticisms of these proposed new criteria have been made (Bowman and Fox, 2014); however, Rasmussen *et al*. have recently demonstrated concordance between the AECG and ACR sets of classification criteria when applied to the same cohort (Rasmussen et al., 2014).

Whilst the classification criteria have been designed for clinical studies and trials, they are often used in the clinical practice to support the diagnostic process. In this context, the performance of a salivary gland biopsy and the relative histological examination is critical for a number of patients that present with negative ANA antibodies (Giovelli et al., 2015). In those cases the positivity of the histological assessment is required to substantiate the clinical diagnosis of pSS (Vitali et al., 2002).

1.4.5. Histological evaluation of the salivary gland biopsy

The classical method to score SS biopsy relies on the Chisholm and Mason criteria (1968). This grading system (4 grades) relies on the detection in the gland of focal lymphocytic and/or diffuse lymphocytic infiltration. The presence of more than 50 periductal lymphocytes (histiocytes and plasma cells) in $4mm^2$ square of salivary gland tissue is used as criteria for the definition of a focus (Chisholm and Mason, 1968).

Greenspan elaborated the focus score in 1974 as an extension of the Chisholm and Mason classification. According to its definition the identification of focal lymphocytic sialoadenitis is followed by the quantification of the

number of foci per 4mm^2 of tissue section adjacent to normal parenchyma (Greenspan et al., 1974).

The focus score has been validated as a histologic index of severity of the salivary gland involvement in pSS. A series of manuscripts have correlated the presence of high focus scores with indices of local or systemic disease activity. The presence of a higher focus score has been found to correlate with acinar damage (Greenspan et al., 1974), presence of anti-SSA/B serology (12 times higher among those with focus score ≥ 1 than among those with focus score < 1 or without focal lymphocytic sialoadenitis (95% CI: 9.3; 15.5) and the presence of specific extraglandular features, such as Raynaud's phenomenon (reduced blood flow), vasculitis, lymph node or spleen enlargement and leucopenia (Gerli et al., 1997). A focus score ≥ 1 has also been found to correlate with positive RF serology, high ANA titres and IgG concentrations, the presence of keratoconjunctivitis sicca and low unstimulated salivary flow rates (Daniels et al., 2011, Haldorsen et al., 2008). More recently, Risselada *et al.* (2013) established that a high focus score (≥ 3) has a significant predictive value for the development of non-Hodgkin B cell lymphoma (Risselada et al., 2013a).

The focus score, whilst giving an idea of the extent of the cellular infiltrate, fails to provide discrete data on the foci size and its organization (Greenspan et al., 1974). The focus score does not require quantification of the presence of GC-like structures or the evaluation of the aggregation of lymphocytes in segregated T and B cells areas. The introduction of additional measurements such as average of focus area, area of lymphocytic infiltration and evaluation

of the degree of organization is currently debated in the SS community to integrate the information provided by the simple focus score.

1.5. A murine model of viral-induced TLO formation

Salivary gland inflammation can be induced by the delivery of a replication-deficient adenovirus-5 in submandibular glands of wild type mice through retrograde excretory duct cannulation (Bombardieri et al., 2012).

This inflammatory process leads to the formation of viral-induced lymphoid aggregates that organise into TLOs resembling the histological lesions that can be found in approximately 20-40% of SS salivary glands (Barone et al., 2005). TLOs form progressively over 2 weeks in the infected gland and are characterised by organized B and T cell zones, ectopic expression of lymphoid chemokines (CXCL13, CCL19, CCL21), lymphoid associated cytokines (such as LTβ), FDC network formation and expression of PNAd on HEVs (Bombardieri et al., 2012).

The model is a useful tool to study the molecular and cellular mechanisms involved in TLO formation (Bombardieri et al., 2012).

Indeed, our group has previously shown that expansion of a gp38+ stromal population occurs in this model, starting at 3 hours post cannulation (p.c.) with replication-deficient adenovirus. This population secretes CXCL13 and CCL19 and expresses lymphoid-associated stromal markers VCAM-1 and ICAM-1, RANKL and MadCAM (Saba Nayar, unpublished data). Therefore, we believe that gp38+ stromal cells (CD45-EpCAM-CD31-gp38+), termed lymphoid-like stromal cells (LLSc), actively participate in the formation of TLOs in inflamed SG.

1.6. Project hypothesis

We have previously demonstrated that critical changes occur to tissue resident stromal cells during the establishment of TLOs, including: the upregulation of adhesion molecules, expression of lymphoid chemokines and upregulation of gp38 and FAP, two stromal cell markers associated with lymphoid stromal cells in secondary lymphoid organs and in target tissues of inflammation.

We hypothesize that those markers and the stromal cells identified by their expression play a functional role in the establishment and homeostasis of TLOs. To test this hypothesis we aim to delete *Pdpn* and FAP+ cells and evaluate the downstream effects on TLO formation.

1.7. Project aims

- Identify the potential signals provided by lymphoid-like stromal cells in the phase of recruitment, activation and retention of leukocytes in inflamed salivary glands.

- Dissect the role of gp38+ activated lymphoid-like stromal cells in the development of TLOs in murine salivary glands.

- Evaluate the consequences of depleting salivary gland activated stromal cells in the formation of TLOs, taking advantage of the expression of FAP on activated gp38+ lymphoid-like stromal cells.

Chapter 2

MATERIALS AND METHODS

2.1. Mice

Conditional KO of the *Pdpn* gene, C57BL/6-*Pdpn*^{tm2418Arte} (PDPN^{fl/fl}) was generated by Taconic Biosciences (NY, USA) for Prof Christopher Buckley and Prof Steve Watson (University of Birmingham), in which the *Pdpn* exon 3 was flanked by loxP sites. B6.129-*Gt(ROSA)26Sor*^{tm1(cre/ERT2)Tyj}/J (Rosa26^{+/CreER}), were purchased from The Jackson Laboratory (ME, USA) (Stock Number: 008463). To generate this strain, a conditional Cre-ER^{T2} (Cre recombinase – estrogen receptor T2) cassette was introduced to the gene. The ER^{T2} retains the Cre recombinase in the cytoplasm until tamoxifen administration releases this inhibition, thus permitting the recombination of genomic *loxP* sites. Rosa26^{CreER} mice were bred with the PDPN^{fl/fl} mice in order to enable temporal control of Pdpn *gene* expression by tamoxifen induction *in vivo*. Cre-mediated recombination leads to deletion of the *Pdpn* exon 3 and consequent loss of function of the *Pdpn* gene by generating a frameshift from exon 2 to all downstream exons (premature Stop codon in exon 5). Homozygous mice for both the floxed Pdpn gene and the Cre allele were used for experiments.

FAP-DTR transgenic (Tg) embryos were a kind gift from Prof Douglas Fearon (University of Cambridge). FAP-DTR mice were generated to express the DTR, luciferase reporter (Luc2) and mCherry under the murine *fap* promoter, by insertion of a 206kb BAC clone (RP23-16A15) (Roberts, 2013). FAP-DTR+

mice were bred with albino C57BL/6 females (C57BL/6J-Tyr^{c-2J}) and heterozygous animals were used for experiments.

Colony of ICOSL$^{-/-}$ mice was established by Dr Francesca Barone (University of Birmingham) with homozygous breeding pairs donated by Dr David Withers (University of Birmingham).

Lta-/- and tnfr-/- (p55/75) mice were provided by Dr J. Caamaño (University of Birmingham) and CD3ε-/- mice by Prof Peter Lane (University of Birmingham).

C57BL/6 and C57BL/6J-Tyr^{c-2J} were purchased from Harlan or Charles River.

All mice were bred at the Biomedical Services Unit (BMSU), University of Birmingham, and kept under pathogen-free conditions according to Home Office regulations.

Experiments were carried out at the University of Birmingham, UK (project licence number 30/2796) following strict guidelines governed by the UK Animal (Scientific Procedures) Act 1986 and approved by the local ethics committee (BERSC: Birmingham Ethical Review Subcommittee). Mice used in this study were housed in individually ventilated cages in groups of 3-6 individuals on a 12-hour light-dark cycle.

2.1.1. Tamoxifen-mediated conditional KO of *Pdpn* gene

Pdpn$^{fl/fl}$Rosa26$^{+/CreER}$ female mice, between 26 and 30 days old, were treated with 2mg of tamoxifen (Sigma Aldrich) or vehicle control, corn oil, for 5 consecutive days via intraperitoneal (i.p.) injections. Animals were then left for a tamoxifen washout period of 35 days prior to any further experimental

procedures, to rule out previously reported anti-inflammatory properties of tamoxifen (Wu et al., 2000, Dayan et al., 1997).

2.1.2. Diphtheria Toxin-mediated deletion of FAP+ cells

DTx (List Biological Laboratories, USA) was administered by i.p. injection to 8 week old FAP-DTR female mice at a dose of 25ng/g at day 0 and day 2, twice a day. Further experimental procedures were performed at day 7 after the first DTx i.p. injection.

2.1.3. Generation of Bone Marrow Chimeric Mice

ICOSLKO and C57BL/6 females, 8-10 weeks old, were given Baytril for 7 days in drinking water prior to two doses of irradiation of 475rad, with an interval of 3 hours. One hour after the second dose of irradiation, ICOSLKO mice were intravenously (i.v.) injected with 1×10^7 bone marrow cells from C57BL/6 animals to reconstitute their immune system and C57BL/6 mice were transplanted with 1×10^7 ICOSLKO bone marrow cells. Mice were kept on Baytril after irradiation and, 6 weeks later, the salivary glands were cannulated with replication-deficient adenovirus.

2.1.4. Anti-ICOS treatment

C57BL/6 female mice were injected i.p. with 10mg/kg with an anti-mouse ICOS blocking antibody (J51HG1-TM) or isotype control (R347-TM) (Yusuf et al., 2014) every 4 days starting from day 0 post cannulation.

2.2. Salivary Gland Cannulation

Submandibular salivary glands of anaesthetised mice were cannulated through the excretory duct with 1×10^8 – 1×10^9 plaque-forming units of replication-deficient adenovirus type 5, encoding the luciferase gene (Bombardieri et al., 2012).

2.2.1. Adenovirus Preparation

HEK 293 cells were cultured in 150x25mm tissue culture petri dishes and, when 80% confluency was reached, these cells were infected with 2ml of adenovirus supernatant and incubated for 2 to 3 days until massive detachment was observed. Cells were then harvested, centrifuged and resuspended in 100mM Tris pH8 and put through three cycles of freeze-thaw to ensure lysis of infected cells and release of virus particles in the supernantant. After centrifugation, the supernatant containing the viral particles was purified using a discontinuous CsCl gradient, 1.4g/ml and 1.25g/ml. The resulting band formed of appropriately packaged viral particles was collected and purified further with 1.3g/ml CsCl. Once again, the resulting band was collected, inserted into a 3500MWCO dialysis cassette (Thermo Scientific) and dialysed against 2L of a 1mM $MgCl_2$, 10mM Tris (pH7.4) and 150mM NaCl with 10% glycerol solution for 24h.

After dialysis, the AdV particles were titrated using an Adeno-X Rapid Titer Kit (Clontech), according to manufacturer's instructions in which serial dilutions of the resulting AdV solution was prepared and seeded with HEK 293 cells in a

12 well plate, incubated for 48 hours at 37°C. Infected cells were then fixed with ice cold 100% methanol for 10min at -20°C and incubated with an anti-hexon antibody, followed by a HRP-conjugated antibody. Chromogenic staining was revealed with DAB, the substrate for HRP. Positive infected cells were counted and infectious units were calculated according to manufacturer's instructions.

2.2.2. Intrasalivary gland delivery of Adenovirus

Animals to be cannulated were administered buprenorphine (0.03mg/kg) subcutaneously, at least 30 minutes before the start of the procedure. Mice were anaesthetised with ketamine (76mg/kg) and domitor (1mg/kg) (i.p.) and using a heat-drawn glass gas chromatography tubing (0.1mm internal diameter; Sigma Aldrich) $1x10^8$ – $1x10^9$ plaque forming units of replication-deficient adenovirus which carries Luciferase gene was delivered to the submandibular salivary glands via the excretory duct. After delivery of virus, cannula was removed and mice were given antipamezole (0.075mg/mouse) to reverse anaesthesia.

2.2.3. Luciferase Assay

Luciferase assay was used to assess the efficiency of the salivary gland cannulation. After gland dissection, a piece of each salivary gland was kept in RNAlater (Qiagen) at -20°C. Samples were thawed at room temperature, transferred into bijoux containing 350µl of Glo Lysis Buffer (Promega) and homogenised with a tissue homogeniser. Lysates were then centrifuged at

13000rpm for 5 minutes and 25µl of supernatant was added to a flat-bottomed 96 well plate and incubated with 25µl of Luciferase Assay Substrate (Promega, UK) for 5 minutes at room temperature. Plates were run in a Berthold Technologies CentroLB 960 using MikroWin software.

2.3. Human salivary gland biopsies from Sjögren's Syndrome patients

Minor salivary gland samples were obtained from Human Biomaterials Resource Centre at the University of Birmingham under ethics number 10-018. Specimens were selected among samples presenting the histological criteria for the diagnosis of SS.

2.4. Flow Cytometry

2.4.1. Stromal tissue digestion

For flow cytometric analysis, salivary glands and lymph nodes were dissected and collected in 2ml of RPMI-1640 (+2% FCS) on ice. Tissues were transferred into 1.5ml of Digestion Buffer 1 – RPMI-1640 (Sigma Aldrich) (+2% FCS) containing 0.1g/ml Collagenase D (Roche) and 0.01g/ml of DNase I (Sigma Aldrich) – and gently pierced with fine forceps. Samples were incubated at 37°C in a water bath for 40 minutes with stirring and centrifuged at 1800rpm for 4 minutes. Fresh Digestion Buffer 2, 1.5ml RPMI-1640 (Sigma Aldrich) (+2% FCS) containing 0.1g/ml Collagenase Dispase (Roche) and 0.01g/ml DNase I (Sigma Aldrich), was added to the samples and contents

were gently mixed and incubated at 37°C for 20 minutes with magnetic stirring. Finally, 15µl of 0.5M EDTA (Sigma Aldrich) was added to the samples followed by incubation at 37°C for 5 minutes. Cell suspensions were filtered through 70µm cell strainers into a 50ml falcon tube containing RPMI-1640 (Sigma Aldrich) (+2% FCS) and resulting contents centrifuged at 1800rpm for 4 minutes at 4°C. Cell pellets were resuspended in MACS Buffer, 0.25g BSA (Sigma Aldrich) and 0.5M EDTA in PBS (Thermo Fisher Scientific), for subsequent staining.

2.4.2. Leukocyte digestion

For flow cytometric analysis salivary glands were transferred into 2ml of Digestion Buffer, comprised of 0.1g/ml Collagenase Dispase and 0.01g/ml of DNase I, and pierced with fine forceps. Samples in digestion buffer were transferred into 5ml falcon tubes (BD biosciences) and incubated for 20 minutes at 37°C with stirring. 40µl of 0.5M EDTA (Sigma Aldrich) was added to the solution and incubated at 37°C for another 5 minutes. Cell suspensions were filtered through a 70µm cell strainer into a 50ml falcon tube containing 2ml of RPMI-1640 (Sigma Aldrich) (+2% FCS) and resulting contents centrifuged at 1800rpm for 4 minutes at 4°C. Cell pellet was resuspended in MACS Buffer for staining.

2.4.3. Collagenase P Digestion

Collagenase P digestion protocol was an alternative protocol optimised in order to enable staining for both stromal and leukocyte markers in samples

that have undergone the same digestion protocol. Since this is a milder technique most of the leukocyte markers are not cleaved by the enzymes.

Salivary glands were transferred into 5ml falcon tubes (BD biosciences) with 2ml of Digestion Buffer, containing RPMI-1640 (Sigma Aldrich) (+2% FCS), 0.8mg/ml Dispase (Roche), 0.2mg/ml Collagenase P (Roche) and 0.1mg/ml DNase I (Sigma Aldrich), cut with scissors and incubated at 37°C with magnetic stirrers. After 20 minutes, samples were taken out of the water bath and left for 30 seconds for large fragments to settle. Enzyme mix was collected and added to 15ml of ice-cold MACS Buffer in a 50ml falcon tube. 2ml of new Digestion Buffer was added to the samples, mixed by pipetting and incubated for a further 10min. All enzyme mix was collected, transferred once again into the 50ml falcon tubes, strained through a 70µm cell strainer (BD biosciences) and centrifuged at 300g for 4 minutes at 4°C. Cell pellet was resuspended in MACS Buffer for staining.

2.4.4. Staining

Cells were incubated with 100µl (50µl for lymph node stromal cells) of diluted primary antibodies for 30 minutes in MACS Buffer. Cells were washed with MACS Buffer followed by fixation with Fixing solution (eBioscience) and further washing with Fixation/Permeabilization Wash Buffer (eBioscience).

For FAP staining, cells were incubated with Fc block for 15 minutes prior to incubation with sheep anti-FAP and biotinylated mouse anti-sheep/goat antibodies.

Intracellular staining for cytokine production was performed (BD Cytofix/Cytoperm) according to the manufactures protocol. In brief, following surface staining with cocktails of desired antibodies, cells were washed in PBS (with 0.5% BSA and 2mM EDTA), re-suspended in 150 µl Cytofix/Cytoperm (BD Pharmingen) and incubated overnight at 4°C. Cells were washed twice with the BD Perm/Wash Buffer and subsequently intracellular LTα (Geneway) antibody was added and incubated at 4°C for 30–40 minutes, the LTα was detected by secondary antibody. Afterwards cells were washed twice, resuspended and then analyzed using a CyAn™ ADP Analyzer (Beckman Coulter) with forward/side scatter gates set to exclude non-viable cells. Data were analyzed with FlowJo software (Tree Star). For cell sorting, stained cells were sorted using MoFlo-XDP (Beckman Coulter Inc). The purity of sorted stromal populations routinely exceeded 96%.

A list of antibodies used for flow cytometry can be found in Table 2.1.

Antibody specificity	Isotype	Clone	Format	Supplier	Dilution used
CD45	Rat IgG2b	30-F11	PERCPCy5.5 PECy7 APC-Cy7	ebiosciences	1:300 1:500 1:800
Podoplanin (gp38)	Hamster IgG	ebio8.1.1	PE	ebiosciences	1:200
CD31 (PECAM-1)	Rat IgG2a	390	FITC/PECy7	ebiosciences	1:200
CD326 (EpCAM)	Rat IgG2b	G8.8	PECy7	ebiosciences	1:500
CD54 (ICAM-1)	Rat IgG2b	YN1/1.7.4	PE	ebiosciences	1:200
CD106 (VCAM-1)	Rat IgG2a	429 (MVCAM.A)	PERCPCy5.5	Biolegend	1:50
Ki67	Mouse IgG1	B56	Alexa-Fluor647	BD biosciences	1:50
CD3e	Hamster IgG	145-2C11	PECy7	BD biosciences	1:100
B220 (CD45R)	Rat IgG2a	RA3-6B2	APCCy7	BD biosciences	1:100
CD4	Rat IgG2a	RM4-5	efluor 450	ebiosciences	1:50
CD8α	Rat IgG2a	53-6.7	PE-TexasRed	BD biosciences	1:200
CD19	Rat IgG2a	eBio1D3 (1D3)	APC	ebiosciences	1:100
LTα	Mouse IgG2b	AT15 A3	unconjugated	GenWay	1:50
CD278 (ICOS)	Hamster IgG	C398.4A	PE	ebiosciences	1:100
CD275 (ICOSL)	Rat IgG2a	HK5.3	biotin	ebiosciences	1:50
FAP	Polyclonal Sheep IgG	-	unconjugated	R&D Systems	1:50
Anti-goat/sheep	Mouse IgG1	GT-34	biotin	Sigma	1:1000
Streptavidin	-	-	APC	ebiosciences	1:600

Table 2.1. Antibodies for flow cytometry staining.

2.4.5. In vitro LTα cytokine stimulation assay

Isolated stromal cells or dendritic cells were re-suspended at the same cell density in 500µl of DMEM (with 10% FCS, 1%GPS, 1% NEAA, 1%HEPES and 50µM β-mercaptoethanol) for in vitro LTα cytokine stimulation assay in 48 well plates. T cells isolated from spleen of wt mice were incubated with

50ng/ml PMA (Phorbol-12-Myristate-13-Acetate), 750ng/ml Ionomycin and 10ul of 10^8-10^9 p.f.u. of adenovirus for 4 h at 37°C. Stimulated cells T cells were then added at 1:4 ratios to 48 well plates with stromal cells and dendritic cells (DCs) with or without virus. DCs were FACS sorted from inflamed salivary glands (day 5 p.c.). Cells were harvested after 24 hours and taken for quantitative PCR analysis.

2.5. Histology

2.5.1. Tissue Harvesting

After dissection, a portion of the cannulated salivary gland was saved for histology analysis. Freshly dissected tissue was placed in a cryomold (Sakura Finetek), embedded in OCT compound (Sakura Finetek) and frozen in dry ice and stored at -80°C.

2.5.2. Cryosectioning

Tissues were sectioned (5-7μm) using a Leica cryostat at -20°C. Slides were left to dry overnight; on the following day, were covered in foil and kept at -80°C until use.

Sectioning for mRNA isolation was carried out in the same cryostat, however extra care was taken to keep surfaces as clean as possible. Five to seven thick sections of 15μm were collected in an RNase-free eppendorf tubes (StarLab), using a sterile needle. Tubes were kept at -80°C until further use.

2.5.3. Immunofluorescence

Stored slides were defrosted and fixed for 20 minutes in acetone (Sigma Aldrich). PFA fixed slides were incubated with Dako Target Antigen Retrieval Solution in a water bath at 95°C for 10 minutes. Slides were left to cool in the Target Antigen Retrieval Solution followed by wash in PBS. In order to block endogenous biotin, sections were incubated with avidin (1:20, Sigma Aldrich) and biotin (1:4, Sigma Aldrich) both for 15 minutes and with 5 minute washes with PBS in between. Finally, sections were blocked with 10% horse serum (Sigma Aldrich) for 10 minutes and incubated for 1 hour with primary antibodies diluted in PBS (1% BSA); followed by 10 minutes washing in PBS and incubation with secondary antibodies for 30 minutes. Secondary antibodies had been previously cross-adsorbed with 10% mouse serum (Sigma Aldrich) in a total volume of 100μl of PBS (1% BSA). Slides were washed again and stained with tertiary antibodies with nuclear yellow Hoechst (Invitrogen) for further 30 minutes. Slides were washed in PBS for 10 minutes and mounted using ProLong® Gold Antifade Reagent (Invitrogen) and stored at -20°C. Images were acquired using a Zeiss LSM 780 confocal microscope and processed using ZEN software.

A list of primary and secondary antibodies used for immunofluorescence can be found in Tables 2.2 and 2.3, respectively.

Antibody	Clone	Format	Supplier	Dilution Used
Hamster anti-mouse gp38	8.1.1	unconjugated	ebiosciences	1:100
Goat anti-mouse CCL21	AF457	unconjugated	R&D Systems	1:100
Hamster anti-mouse CD3ε	eBio500A2 (500A2)	biotin	ebiosciences	1:50
Hamster anti-mouse CD3ε	eBio500A2 (500A2)	FITC	ebiosciences	1:100
Rat anti-mouse CD19	eBio1D3 (1D3)	eFluor660	ebiosciences	1:50
Rat anti-mouse CD45	30-F11	APC	ebiosciences	1:50
Rat anti-mouse CD4	GK1.5	eFluor660	ebiosciences	1:50
Rabbit anti-mouse Lyve-1	polyclonal	unconjugated	Abcam	1:400
Rabbit anti-mouse FAP	polyclonal	unconjugated	Abcam	1:50

Table 2.2. Primary antibodies for immunofluorescence staining.

Antibody	Format	Supplier	Dilution Used
Goat anti-hamster	biotin	Biolegend	1:100
Goat anti-rabbit	Alexa-Fluor488	Invitrogen	1:100
Rabbit anti-FITC	unconjugated	Invitrogen	1:200
Donkey anti-goat	FITC	Jackson Immunoresearch Laboratoies Inc.	1:100
Donkey anti-rabbit	Alexa-Fluor647	Invitrogen	1:100
Streptavidin	555	Invitrogen	1:500
Streptavidin	647	Invitrogen	1:300

Table 2.3. Secondary antibodies for immunofluorescence staining.

2.5.4. Image analysis of immunofluorescence staining

In order to quantify the size of the lymphocytic infiltrates in cannulated murine salivary glands, frozen salivary gland sections were stained with anti-CD3 and anti-CD19 and tile scans were acquired on a Zeiss LSM 780 confocal microscope. Using the ZEN software, a region of interest was drawn around the aggregates and total area of salivary gland tissue. Volume fraction of lymphoid follicles and average follicle area were calculated according to the formulas below.

$$Volume\ fraction\ (\mu m^2) = \frac{Total\ area\ of\ lymphoid\ follicles}{Total\ tissue\ area}$$

$$Average\ lymphoid\ follicle\ area\ (\mu m^2) = \frac{Total\ follicle\ area}{Number\ of\ follicles}$$

2.5.5. Immunohistochemistry

Formalin-fixed paraffin-embedded labial salivary gland biopsies from Sjögren's syndrome patients were dewaxed in xylene three times (10 minutes, 10minutes, 5minutes) and hydrated through decreasing ethanol concentrations (100%, 95%, 80%, 75%, 50%) for 2 minutes each. Slides were then washed in distilled water three times for 2 minutes each and incubated with Dako Target Antigen Retrieval Solution (Dako) for 35 minutes at 96°C. When finished, the slides were left to cool in the plastic jar at room temperature or at 4°C. Once the Target Antigen Retrieval Solution became

clear, slides were washed in TBS and sections were bordered with hydrophobic PAP pen for immunostaining (Sigma Aldrich).

For incubation of primary antibodies, amplification methods and chromogens, the EnVision™ G|2 Doublestain System, Rabbit/Mouse (DAB+/Permanent Red) (Dako) was used according to manufacturer's instructions. This system allows the simultaneous detection of two different antigens in one section; the first antigen is identified with peroxidase (HRP) and DAB as the chromogen, and the second with alkaline phosphatase (AP) and Permanent Red. In brief, sections were blocked with Dual Endogenous Enzyme Block for 5 minutes, washed in TBS and the first primary antibody, diluted in TBS (+ 1% BSA) was incubated for 1 hour at room temperature. The secondary antibody with Polymer/HRP was incubated for 10 minutes and slides washed twice with TBS. Incubation with DAB took place under the light microscope and the reaction was stopped with distilled water when optimal brown staining was achieved. Followed by a blocking step with Doublestain Block reagent (3 minutes), the sections were incubated with the second diluted primary antibody for 1 hour. The following step was the Rabbit/Mouse (LINK) for 10 minutes and then another 10 minutes with Polymer/AP. The second reaction was then developed with Permanent Red and once again it took place under the light microscope until optimal red staining was achieved.

Sections were dehydrated in increasing concentrations of ethanol (80%, 95% and 100%) and placed in xylene for five minutes, twice. Finally, slides were mounted with Mouting Medium DPX (Sigma Aldrich) and scanned using a Zeiss AxioScan.Z1 slide scanner.

A list of primary antibodies used for immunohistochemistry can be found in Tables 2.4.

Antibody	Clone	Format	Supplier	Dilution Used
CD3	Polyclonal	unconjugated	Dako	1:80
CD20	L26	unconjugated	Dako	1:20
CD11c	5D11	unconjugated	Leica	1:10
Gp38	D2-40	unconjugated	AbD serotec	1:10
ICOS	SP98	unconjugated	Novus Biologicals	1:10
ICOSL	N/A	unconjugated	LSBio	1:10

Table 2.4. Primary antibodies for immunohistochemistry staining.

2.6. Relative Quantification of Gene Expression

2.6.1. RNA extraction

Total RNA was extracted using the RNeasy Mini Kit (Qiagen) as appropriate and following the manufacturer's instructions. Salivary gland specimens were sectioned in the cryostat as mentioned above and, once thawed, lysed in 200µl RLT Buffer (Qiagen) with 10% of β-mercaptoethanol (Sigma Aldrich). Samples were vortexed and centrifuged for 1 minute at 13000rpm, followed by 200µl of ice-cold 70% ethanol (ratio 1:1 to RLT Buffer). After mixing by pipetting, samples were transferred to RNeasy mini spin columns and centrifuged for 2 minutes at 13000rpm. Solution in collection tube was discarded and 350µl of Buffer RW1 was added and centrifuged once again. 80µl of DNase I (previously prepared with 10µl of DNase I to 70µl of Buffer RDD) was added directly to the column membrane and incubated for 15

minutes at room temperature. After DNase I incubation, centrifugation with 350µl of Buffer RW1 was repeated, followed by 500µl of Wash Buffer RPE and a 1 minute spin, twice. The collection tube was discarded; pink columns were placed in new 2ml collection tubes and centrifuged for 5 minutes at 13000rpm in order to dry the membrane. Columns were then placed in new 1.5ml collection tubes and 12.5µl of RNase-free water was directly added to the membrane, twice, in order to elute the extracted RNA.

To isolate total RNA from sorted cells the RNeasy Micro Kit (Qiagen) was used according to manufacturer's instructions. In brief, there were three key differences to the protocol of RNA extraction from tissues. After adding 200µl of RLT Buffer to each sample, a 19G needle and a 2ml syringe was used to break up the cells further. Secondly, instead of a second wash with Wash Buffer RPE, 500µl of ice-cold 80% ethanol was added and centrifuged at 13000rpm for 2 minutes. Lastly, at first RNA was eluted with 12.5µl of RNase-free water and after centrifugation the eluted 12.5µl of RNA were put through the membrane again to ensure a higher concentration of RNA.

2.6.2. cDNA Reverse Transcription

cDNA was synthesized from total RNA on the same day as the RNA isolation, using High Capacity cDNA Reverse Transcription Kit (Applied Biosystems) in a 96 well plate (Applied Biosystems). A mix comprising 10X RT Buffer (5µl), 10X Random Primers (5µl), 100nM dNTPs Mix (2µl), reverse transcriptase enzyme (2.5µl) and RNase-free water (10.5µl) was added to the RNA sample in a ratio 1:1. The plate was sealed with a MicroAmp™ Clear Adhesive Film

(Applied Biosystems) and spun for 2 minutes at 1200rpm. Reaction was carried out on a Techne TC-Plus thermal cycler with the following protocol: 25°C for 10 minutes, 37°C for 2 hours and 85°C for 5 minutes. Once the reaction was completed, cDNA was diluted with 50µl of RNase-free whather (ratio 1:1) and kept at -20°C.

2.6.3. Quantitative Real-Time PCR

Following cDNA synthesis, quantitative real-time PCR (qRT-PCR) was performed on a 7900HT Real-Time PCR System (Applied Biosystems), using TaqMan® Gene Expression Master Mix (Applied Biosystems). Primers/probes (Applied Biosystems) were diluted in Master Mix at their reported optimal concentration and pre-labelled with 6-FAM™. Master Mix with primers/probes (2.6µl) and cDNA (2.3µl) were loaded into a 384-well plate (Applied Biosystems) in duplicate in a final volume 5.1µl. The plate was sealed with a MicroAmp™ Clear Adhesive Film (Applied Biosystems) and spun for 2 minutes at 1200rpm. As mentioned above, the reaction took place on a 7900HT Real-Time PCR System with standard thermal cycling conditions, 40 cycles of: 2 minutes at 50°C for UNG activation; 10 minutes at 95°C for Taq polymerase enzyme activation; denaturation for 15 seconds at 95°C; and 1 minute at 60°C for annealing. Results were analysed with RQ Manager 1.2 software and Ct values were determined within the logarithmic phase of the PCR reaction, which correspond to the cycle number at which the amplification plot crosses the defined fluorescence threshold. The mean of the two technical replicates of the Ct values was calculated for each sample and gene, for both endogenous controls (β-actin and PDGFRβ) and targets. ΔCt

was determined by subtracting the endogenous control Ct value to the gene of interest Ct value and the relative amount was calculated as $2^{-\Delta Ct}$. All target genes were normalised to β-actin, except for stromal cell dependent genes that were normalised to PDGFRβ to account for possible differences in percentage of infiltrating cells.

Relative quantity expression (RQ) of the target gene as compared to the endogenous control was calculated as $2^{-\Delta\Delta Ct}$, in which ΔΔCt corresponds to the difference between Ct values of genes in cannulated salivary glands (or sorted cells for cannulated glands) and Ct values from resting non-cannulated salivary glands (or from sorted cells from day 0 salivary glands).

A list of primers used for qRT-PCR can be found in Table 2.5.

Gene	mRNA Accession number	Assay ID	Source
Mouse β-actin	NM_007393.3	Mm01205647_g1	Applied Biosystems
Mouse Pdgfrβ	NM_001146268.1 NM_008809.2	Mm00435546_m1	Applied Biosystems
Mouse CXCL13	NM_018866	Mm00444533_m1	Applied Biosystems
Mouse CXCR5	NM_007551	Mm00432086_m1	Applied Biosystems
Mouse CCL19	NM_011888	Mm00839967_g1	Applied Biosystems
Mouse CCR7	NM_007719	Mm01301785_m1	Applied Biosystems
Mouse FAP	NM_007986.3	Mm01329175_m1	Applied Biosystems
Mouse ICOS	NM_017480.2	Mm00497600_m1	Applied Biosystems
Mouse ICOSL	NM_015790.3	Mm00497237_m1	Applied Biosystems
Mouse LTβ	NM_007986	Mm00484254_m1	Applied Biosystems
Mouse LTα	NM_007986	Mm00484254_m1	Applied Biosystems
Mouse Pdpn	NM_001290822.1 NM_010329.3	Mm01348912_g1	Applied Biosystems
Mouse TNFα	NM_013693	Mm00443258_m1	Applied Biosystems
Mouse TNFR	NM_011609.4	Mm00441883_g1	Applied Biosystems

Table 2.5. Primers used for qRT-PCR.

2.7. Statistical Analysis

Statistical analysis was performed using GraphPad Prism and difference between groups assessed by student's t test or, where appropriate and as indicated in relevant sections, one-way ANOVA. Significance was accepted at $p \leq 0.05$. All graphs are presented as mean (SD).

Chapter 3

ICOSL EXPRESSION BY LYMPHOID-LIKE STROMAL CELLS CONTRIBUTES TO T CELL ACTIVATION AND RELEASE OF LYMPHOTOXIN ALPHA THAT ENABLE CHEMOKINE PRODUCTION AND TLO ESTABLISHMENT

3.1. Introduction

Complex aggregates of lymphocytes are often found at sites of chronic inflammation (Pitzalis et al., 2014). These structures, namely TLOs, recapitulate in form and function the lymphoid follicles found in spleen and lymph nodes (Buckley et al., 2015). The stromal cell component of TLOs largely overlaps with that of SLOs and gp38+ICAM+VCAM+ stromal cell network (Link et al., 2011), FDCs and high endothelial cell formation have been described in TLOs (Barone et al., 2005).

While SLOs are known to house mainly naïve lymphocytes, TLOs are prevalently inhabited by activated, memory T and B cells (Pitzalis et al., 2014). Formation of GCs with polyclonal B cell proliferation, class-switching recombination and somatic hypermutation has been observed in TLOs and believed to contribute to local expansion of auto-reactive B cell clones (Buckley et al., 2015). TLO assembly and GC formation are dependent on the expression of lymphoid chemokines that regulates lymphocyte organization in discrete areas (Allen et al., 2004, Ansel et al., 2000, Luther et al., 2002, Barone et al., 2005, Manzo et al., 2007). While in SLOs this phenomenon is

strictly dependent on LT (Cupedo and Mebius, 2005), several evidence suggests that in the periphery, lymphoid chemokine expression by resident stromal cells can be, at least in part, regulated by pro-inflammatory cytokines (Barone et al., 2015b, Fleige et al., 2014).

Co-stimulatory signals provided by CD4+/bcl-6+/CXCR5+ T_{FH} cells are also required for the establishment of GC, cytokine production, B cell differentiation and expansion (Schaerli et al., 2000, Haynes et al., 2007, Fazilleau et al., 2009). Among those, ICOS (inducible co-stimulatory molecule), a member of the CD28 family, expressed on activated T cells (Hutloff et al., 1999) is critical for T_{FH} differentiation and generation of the GC reaction (Dong et al., 2001a, Dong et al., 2001b, Wong et al., 2003). ICOSL is expressed on APCs, B cells and other non-hematopoietic cells, its expression can be enhanced in inflammatory conditions by exposure to IFN-γ and TNFα (Swallow et al., 1999).

ICOS/ICOSL interaction enhances basic T-cell responses to a foreign antigen support B cells antibody secretion (Hutloff et al., 1999), memory B cells and plasma cell differentiation (Hutloff et al., 1999, van Berkel and Oosterwegel, 2006). Pharmacological or genetic interference with the ICOS pathway prevents the development of spontaneous disease in pre-diabetic NOD mice (Ansari et al., 2008), ameliorates collagen-induced arthritis and systemic lupus erythematous (Hu et al., 2009, Iwai et al., 2002). Treatment with anti-ICOSL blocking antibodies is currently the subject of clinical trials in autoimmune diseases characterized by TLO formation (http://www.clinicaltrials.gov; NCT00774943); however the mechanism of action of these molecules in TLO assembly is not fully understood.

In this chapter we explored the role of ICOS/ICOSL interaction in the formation of tertiary lymphoid organs during inflammation. We have investigated the expression of both co-stimulatory molecules in salivary gland biopsies from SS patients, and further examined their role and pathways involved in our murine model of TLO formation.

3.2. Results

3.2.1. ICOS-ICOSL interaction influences chemokine expression on gp38+ stromal cells

In order to dissect the potential changes occurring to the lymphoid aggregates in mice treated prophylactically with an anti-ICOS blocking antibody, immunofluorescence staining for T and B cells was performed on salivary gland sections obtained from mice at day 5 and 8 p.c.. Consistent with our previous findings both untreated and isotype-treated wild-type (wt) animals developed a significant number of salivary gland lymphoid aggregates, characterized initially by predominant T cell infiltration followed by B cell aggregation leading to the development of segregated and organized ectopic lymphoid structures (**Figure 3.1A**). In anti-ICOS treated mice a defect in TLO formation was observed with fewer T cells and minimal B cell influx (**Figure 3.1A**). Accordingly, the transcript level of CCL19, the chemokine known to enable T cell recruitment in the early phases of TLO aggregation, was significantly reduced in anti-ICOS treated mice as compared to wt controls (**Figure 3.1B**). CXCL13 production, on the contrary, was not significantly affected by ICOS blockade (**Figure 3.1C**).

Percentage of LLSc, a population of gp38+ stromal cells, was assessed by flow cytometry staining (**Figure 3.1D**) and the results between untreated wt and anti-ICOS treated mice were matched at days 2 and 5 p.c. (**Figure 3.1E**). At day 8 p.c., anti-ICOS treated salivary glands presented a significantly higher percentage of activated stromal cells (**Figure 3.1E**).

Figure 3.1

CD3ε / CD19

A

	WT untreated	anti-ICOS	isotype
day5 p.c.	i	ii	iii
day8 p.c.	iv	v	vi

B

CCL19 mRNA

C

CXCL13 mRNA

D

Gated on CD45-EpCAM-

77

Figure 3.1 (cont.)

E
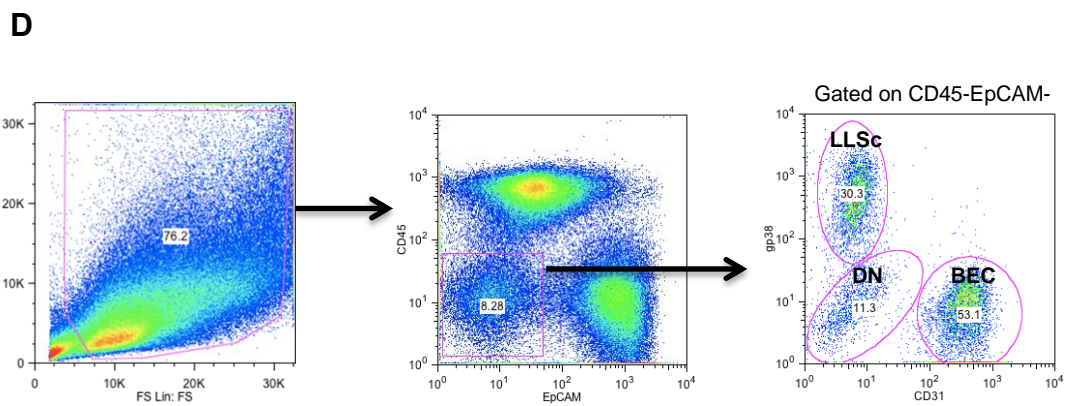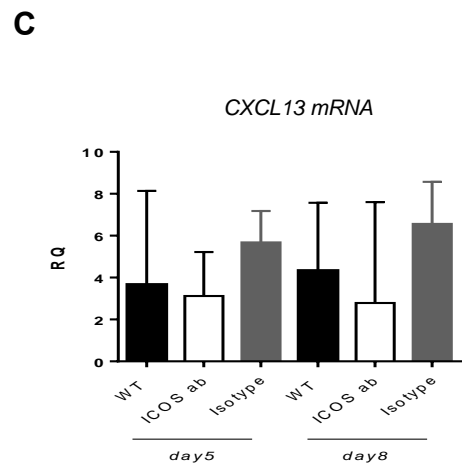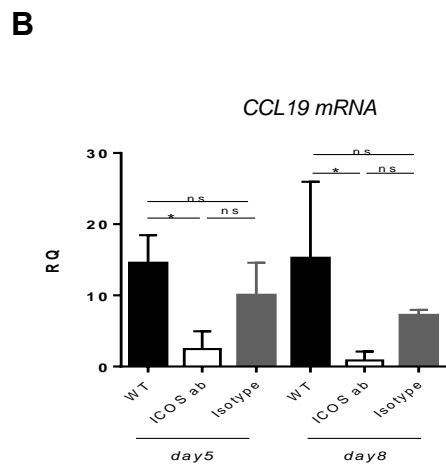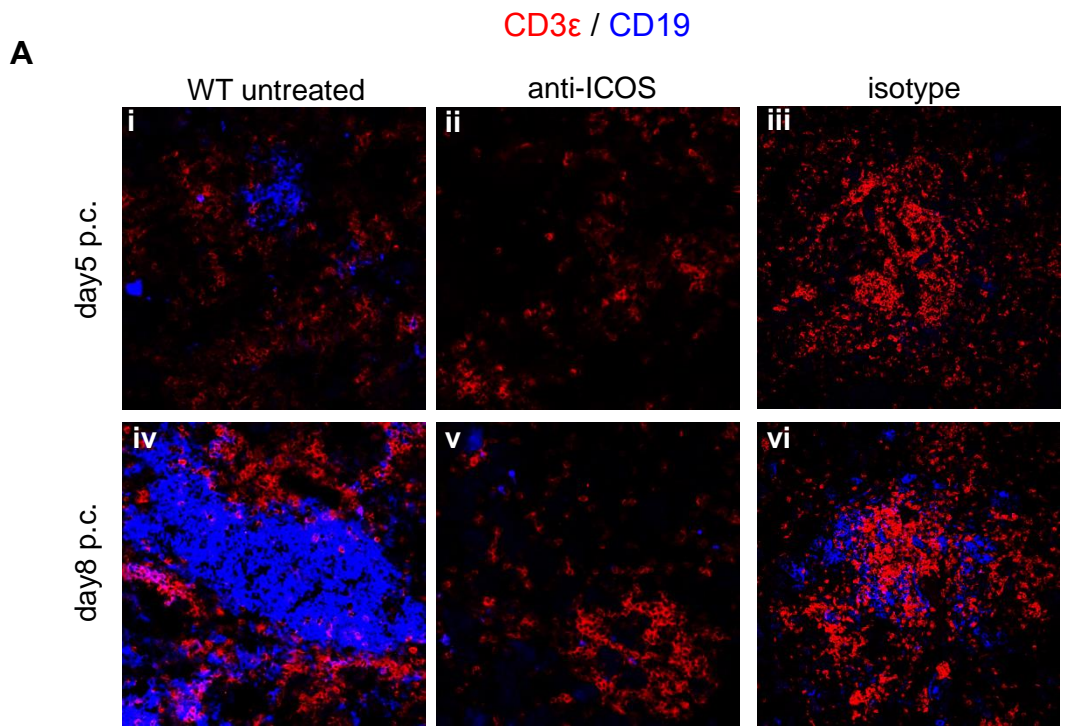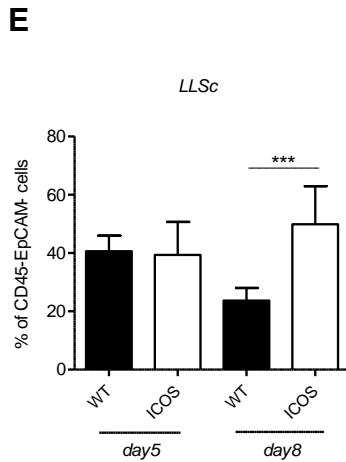
Figure 3.1. *In vivo* **blockade of ICOS results in an unexpected defect in TLO formation.** (A) Wt mice were left untreated (i, iv) or treated with anti-ICOS blocking antibody (ii, v), isotype control (iii, vi) from day 0 post salivary gland cannulation and sacrificed at days 5 and 8 p.c. (post cannulation). Representative microphotographs of salivary glands examined by immunofluorescence for CD3ε (red) and CD19 (blue) showing lymphocytic infiltration. Original magnification 25X. (B-C) Quantitative RT-PCR analysis of mRNA obtained from salivary glands at day 5 and 8 p.c. showing lymphoid chemokine *ccl19* (B) and *cxcl13* (C) in anti-ICOS treated wt mice (white bars) in comparison to their wt untreated (black bars) and isotype treated (grey bars) counterparts. *ccl19* and *cxcl13* mRNA transcripts were normalised to *pdgfrβ* mRNA and results are presented as relative quantitation (RQ). * $p < 0.05$; *** $p < 0.001$, unpaired *t* test. Data are representated as mean ± (SD) of two independent experiments with at least four glands analysed per group. (D) Representative gating strategy of flow cytometry identification of CD45-EpCAM-CD31-gp38+ lymphoid-like stromal cells (LLSc), double negative cells (DN) and blood endothelial cells (BEC) in enzymatically digested salivary glands. (E) Time course analysis, following enzymatic digestion of dissected salivary glands, of the percentage of CD45-EpCAM-CD31-gp38+ (LLSc) after cannulation assessed by flow cytometry in cannulated untreated (black bars) and anti-ICOS treated (white bars) wt mice. Data presented as mean (SD) of two independent experiments with two to six glands analysed per group. *** $p < 0.001$, unpaired *t* test.

3.2.2. ICOSL is expressed by salivary gland activated stromal cells upon inflammation

ICOSL is highly expressed on hematopoietic antigen presenting cells and ICOSL expression has been shown to be inducible in non-hematopoietic cells. In SLOs, gp38+ FRCs produce CCL19, in order to investigate whether the decrease in CCL19 was directly mediated due to a defect in the stromal cells or via interaction of other cell type, we sorted LLSc from inflamed murine salivary glands and in wt mice we demonstrated up-regulation of ICOSL on both gp38+ stromal cells and on hematopoietic cells (CD11c+ cells from inflamed salivary glands), both at mRNA and protein level post cannulation (**Figure 3.2A-B**).

Figure 3.2

A
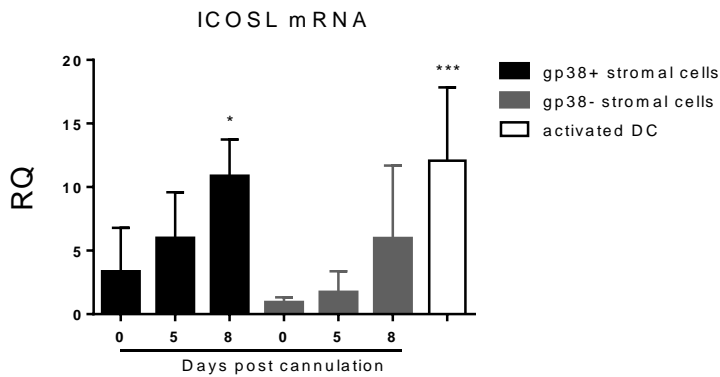
B
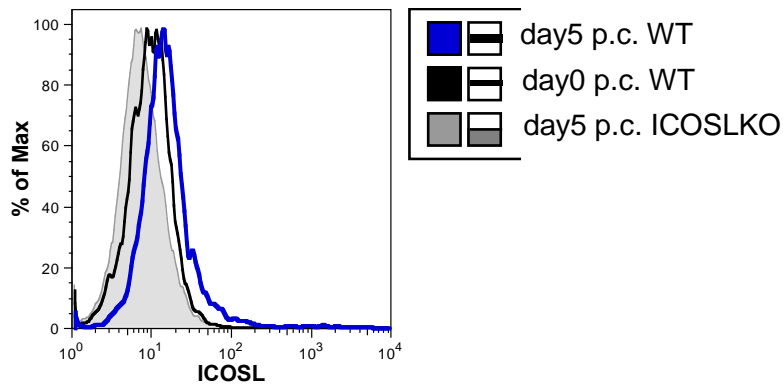
Figure 3.2. ICOSL is expressed by activated stromal cells upon salivary gland inflammation. (A) *Icosl* expression in FACS sorted CD45-EpCAM-CD31-gp38+ (LLSc) (black bars), CD45-EpCAM-CD31-gp38- (DN) (grey bars), activated CD11c+ dendritic cells (white bars). mRNA transcripts were assessed by qRT-PCR and normalised to housekeeping gene β-actin. RQ values calculated with calibrator day 0 DN cells. Data showed as mean (SD) of two independent experiments with at least two salivary glands per group. * $p < 0.001$; *** $p < 0.001$, one-way ANOVA. (B) Histogram showing flow cytometry staining for ICOSL expression in wt mice at day 0 p.c. (black line), wt mice at day 5 p.c. (blue line) and ICOSLKO mice at day 5 p.c. (grey line).

3.2.3. ICOSL$^{-/-}$ mice display impaired TLO formation, but normal numbers of LLSc upon salivary gland cannulation

Consistent with our observations in anti-ICOS treated animals, ICOSLKO mice showed aberrant T cell recruitment and aborted TLO formation when compared to wt control mice (**Figure 3.3A**). In SLOs, FRCs provide the largest source of CCL19 (Link et al., 2007) and we previously demonstrated that, in TLOs, gp38+ cells express CXCL13 but not CXCL12 (Barone et al., 2015b). Evaluation of (CD31-EpCAM-) gp38+ absolute cell number in ICOSLKO mice revealed similar levels to wt control (**Figure 3.3B**), thus suggesting that interfering with the ICOS/ICOSL pathways results in a functional rather than numerical impairment of the gp38+ stroma component. Sorted gp38+ cells from ICOSLKO mice showed significantly decreased CCL19 expression (**Figure 3.3Ci**); CXCL13 levels were not as affected as compared to their wt counterparts (**Figure 3.3Cii**).

Figure 3.3
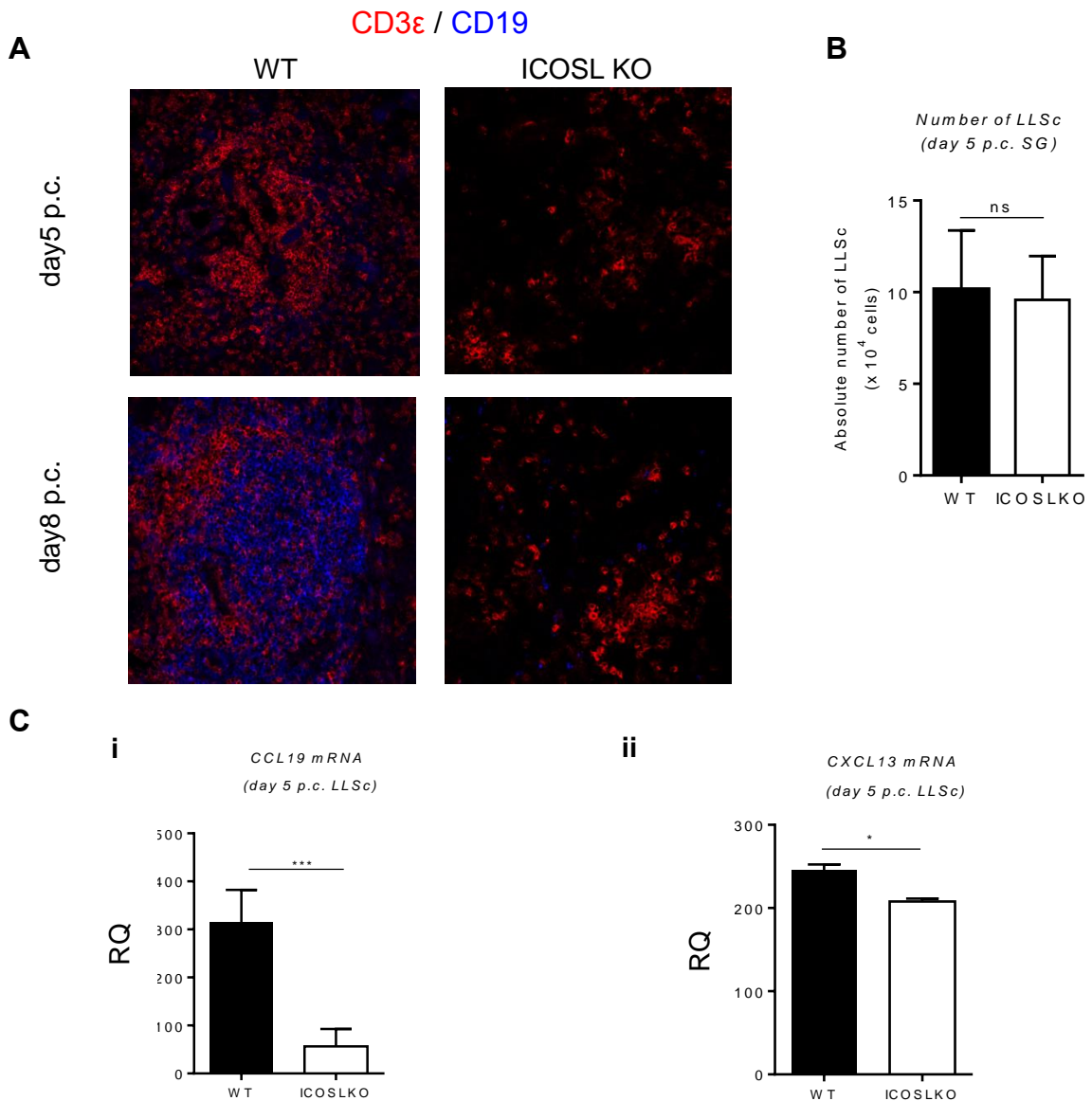
Figure 3.3. ICOSLKO mice display impaired TLO formation, but normal numbers of LLSc, upon salivary gland cannulation. (A) Salivary glands from WT and ICOSLKO mice were cannulated and mice were sacrificed at days 5 and 8 p.c.. Representative microphotographs of salivary glands examined by immunofluorescence for CD3ε (red) and CD19 (blue) showing lymphocytic infiltration. Original magnification 25X. (B) Absolute numbers of CD45-EpCAM-CD31-gp38+ cells (LLSc) were determined by flow cytometry in both wt and ICOSLKO salivary glands at day 5 p.c.. ns = non-sgnificant, unpaired *t* test. Data expressed as mean (SD) of one experiment with four glands analysed per group. qRT-PCR analysis of *ccl19* (i) and *cxcl13* (ii) mRNA transcripts in FACS sorted LLSc from wt (black bars) and ICOSLKO (white bars) mice at day 5 p.c. Transcripts levels were normalised to β-actin and expressed relative to day 0 LLSc results. * $p < 0.05$; *** $p < 0.001$, unpaired *t* test, data represented as mean (SD) from two independent experiments with three to seven glands analysed per group.

3.2.4. T cells are the main source of ICOS in inflamed salivary glands

T cells are known to express ICOS upon activation; accordingly, we detected ICOS expression on T cells and NK1.1+ cells infiltrating the cannulated salivary glands (**Figure 3.4A**). In ICOSLKO, ICOS transcript levels were not affected (**Figure 3.4Ci**). In order to investigate the role of T cells in the regulation of CCL19 expression we performed salivary gland cannulation of T cell deficient mice (cd3ε). Quantification of mRNA transcripts on infected salivary glands showed a significant defect in CCL19 expression at different time points post cannulation (**Figure 3.4Bi**) and both LTα and LTβ mRNA levels were significantly reduced (**Figure 3.4Bii-iii**). Interestingly, T cells isolated from ICOSL$^{-/-}$ salivary glands post inflammation produced lower levels of LTα than the wt controls but expressed normal levels of LTβ and TNFα (**Figure 3.4Cii-iv**).

Figure 3.4

A

B

C
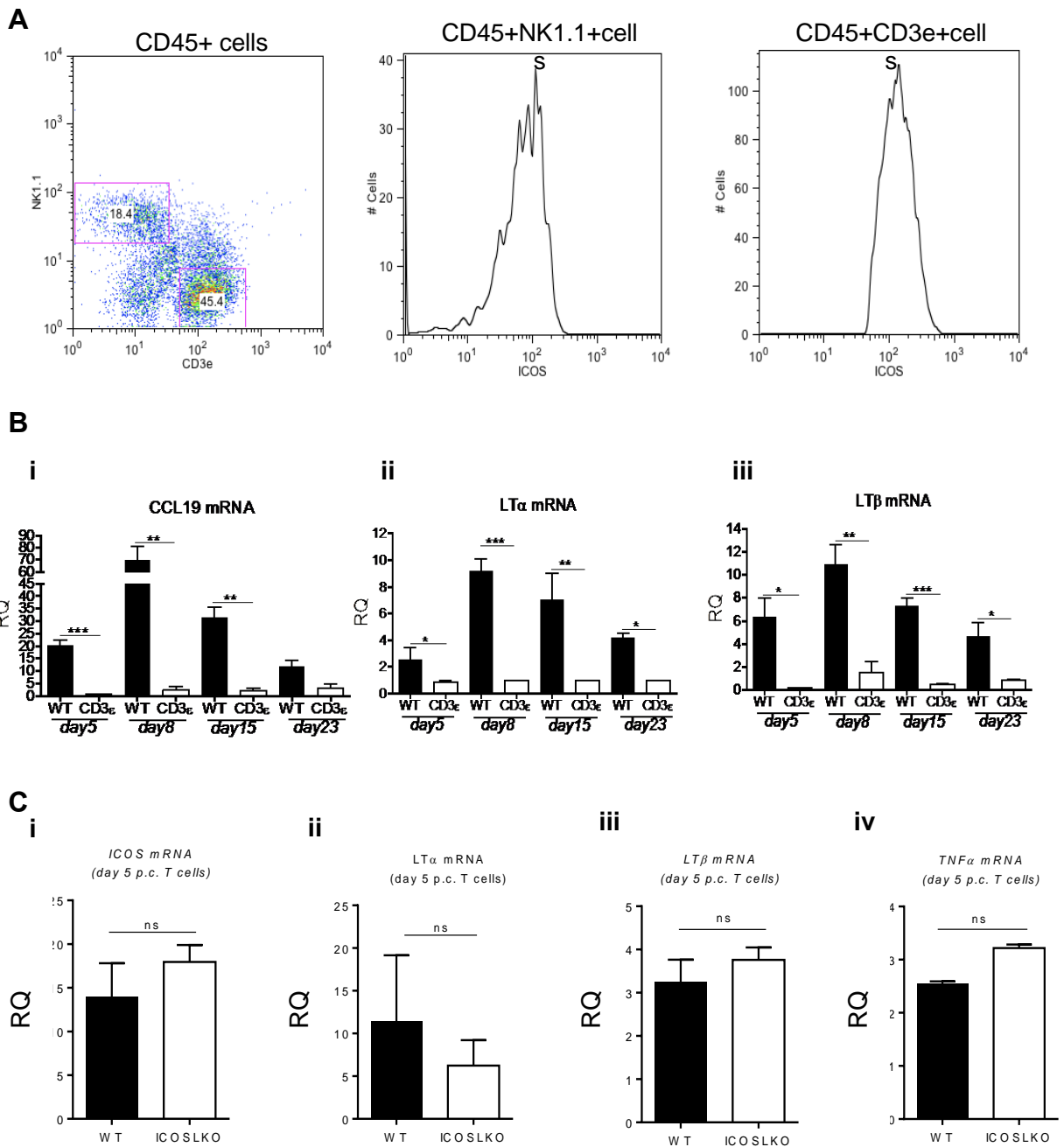
Figure 3.4. T cells are the main source of ICOS in inflamed salivary glands. (A) Representative dot plot showing flow cytometry staining for ICOS expression in wt salivary glands at day 5 p.c. by CD3ε+ T cells and NK1.1. (B) qRT-PCR analysis of c*cl19* (i), *lta* (ii) and *ltb* (iii) mRNA transcripts from wt (black bars) and CD3ε-/- (white bars) salivary glands at day 5, 8, 15 and 23 p.c.. *lta* and *ltb* were normalised to housekeeping gene β-actin, *ccl19* results to pdgfrb and expressed as RQ values relative to day 0 mRNA transcripts results.. * $p < 0.05$; ** $p < 0.01$; *** $p < 0.001$, unpaired *t* test, data represented as mean (SD) from two independent experiments with four to six glands analysed per group. (C) qRT-PCR analysis of *icos* (i), *lta* (ii), *ltb* (iii) and *tnfa* (iv) mRNA transcripts in FACS sorted CD3ε+ T cells from wt (black bars) and ICOSLKO (white bars) mice at day 5 p.c. Transcripts levels were normalised to β-actin and expressed relative to day 0 CD45+ cells results. ns = non significant, unpaired *t* test, data represented as mean (SD). from two independent experiments with three to four glands analysed per group.

3.2.5. ICOS activation on T cells induces release of LTα during inflammation

These findings suggest a potential role of ICOS/ICOSL interaction in LTα production by T cells during inflammation. In wt cannulated mice, T cells were found to represent the predominant source of LTα (**Figure 3.5A**). Indeed ICOSLKO infected salivary glands contain lower T cells number and decreased expression of LTα as compared to wt controls (**Figure 3.5B**), thus justifying our finding of reduced CCL19 expression in this strain. Salivary glands from LtαKO mice, exhibited, upon cannulation a similar profile of chemokine expression as observed in cd3ε mice, showing abrogated levels of both CCL19 and CXCL13 (**Figure 3.5Ci-ii)**.

These findings suggest a novel role for ICOS/ICOSL interaction in the regulation of LTα production by activated T cells during TLO formation and a stringent dependency of CCL19 expression on local levels of LTα.
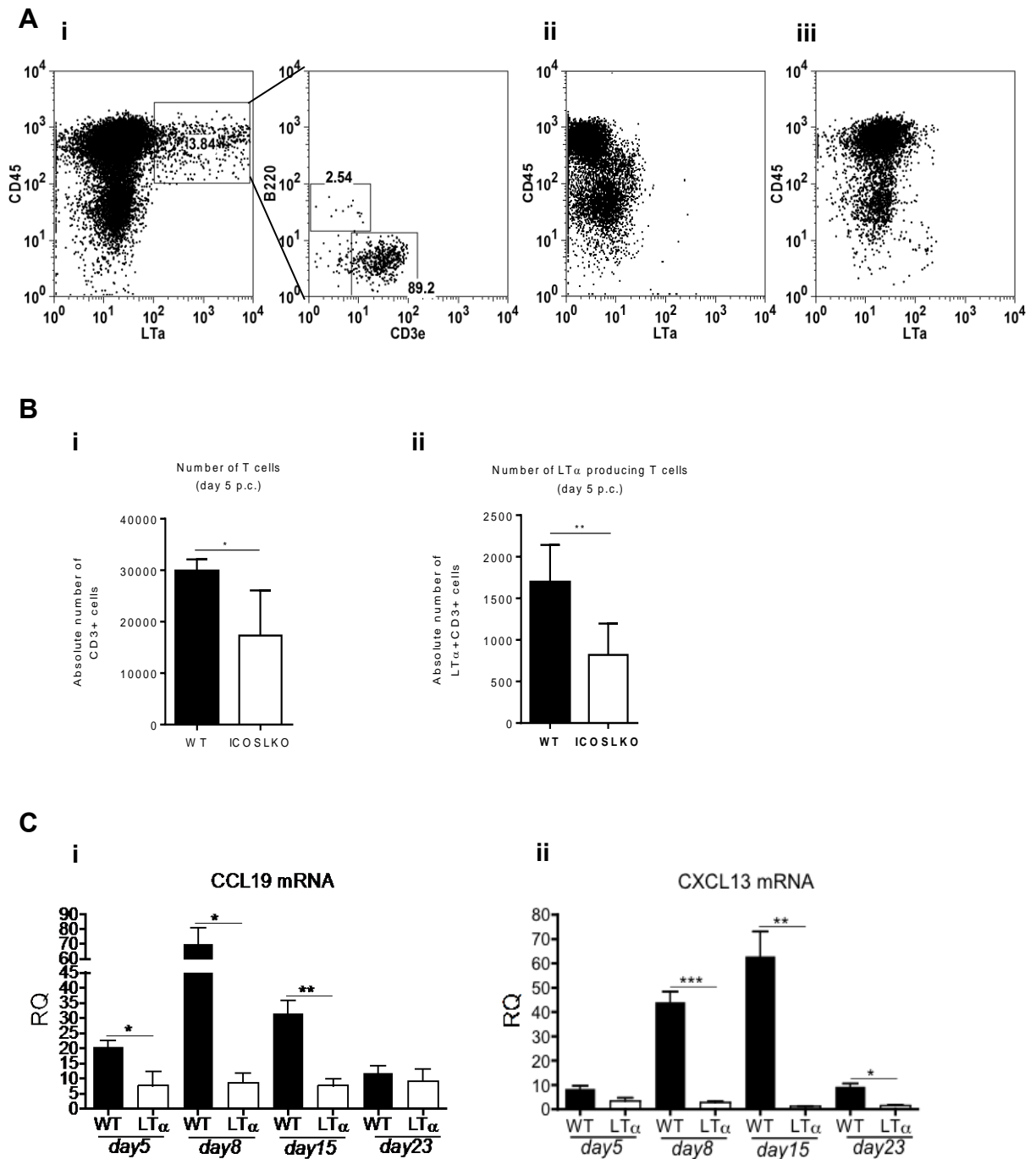
Figure 3.5

Figure 3.5. ICOS activation on T cells induces release of LTα during inflammation. (A) Representative dot plot of flow cytometry staining for LTα expression by T and B cells in wt (i) and LTαKO (iii) salivary glands at day 5 p.c.. Isotype control staining for LTα expression (ii). (B) Absolute numbers of T cells (i) and LTα-producing T cells (ii) in wt (black bars) and ICOSLKO (white bars) salivary glands at day 5p.c.. Results were determined by flow cytometry and presented as mean (SD) of two independent experiments with three to eight salivary glands per group. * p < 0.05; ** p < 0.01, unpaired *t* test. (C) qRT-PCR analysis of *ccl19* (i) and *cxcl13* (ii) mRNA transcripts from wt (black bars) and LTαKO (white bars) salivary glands at days 5, 8, 15 and 23 p.c.. Transcripts levels were normalised to *pdgfrβ* mRNA and results are presented as relative quantitation (RQ). * p < 0.05; ** p < 0.01; *** p < 0.001, unpaired *t* test. Data represented as mean (SD) from two independent experiments with three to four glands analysed per group.

3.2.6. TNFR mediates the effects of LTα in our model of TLO formation

Since LTα is known to signal through TNFRα to induce chemokine expression, we postulated that salivary gland cannulation in TNFRαKO mice would mimic the phenotype observed in LTαKO, CD3εKO and ICOSLKO mice. Indeed, FRC like (CD31-EpCAM-) gp38+stromal cells isolated from wt infected mice express TNFRI and increased this expression post cannulation (**Figure 3.6C**). In TNFRαKO mice, gene expression analysis of cannulated salivary glands unveiled a defect both in CCL19 and CXCL13 (**Figure 3.6A**) transcript levels. Accordingly, immunofluorescence staining revealed smaller lymphocytic aggregates with reduced T and B cell aggregation (**Figure 3.6B**).

These data suggest that early CCL19 expression is regulated by TNFR signalling on stromal cells by engagement of ICOS+ T cells with ICOSL.

Figure 3.6

A

i

CCL19 mRNA

ii

CXCL13 mRNA

B

C

tnfrα mRNA
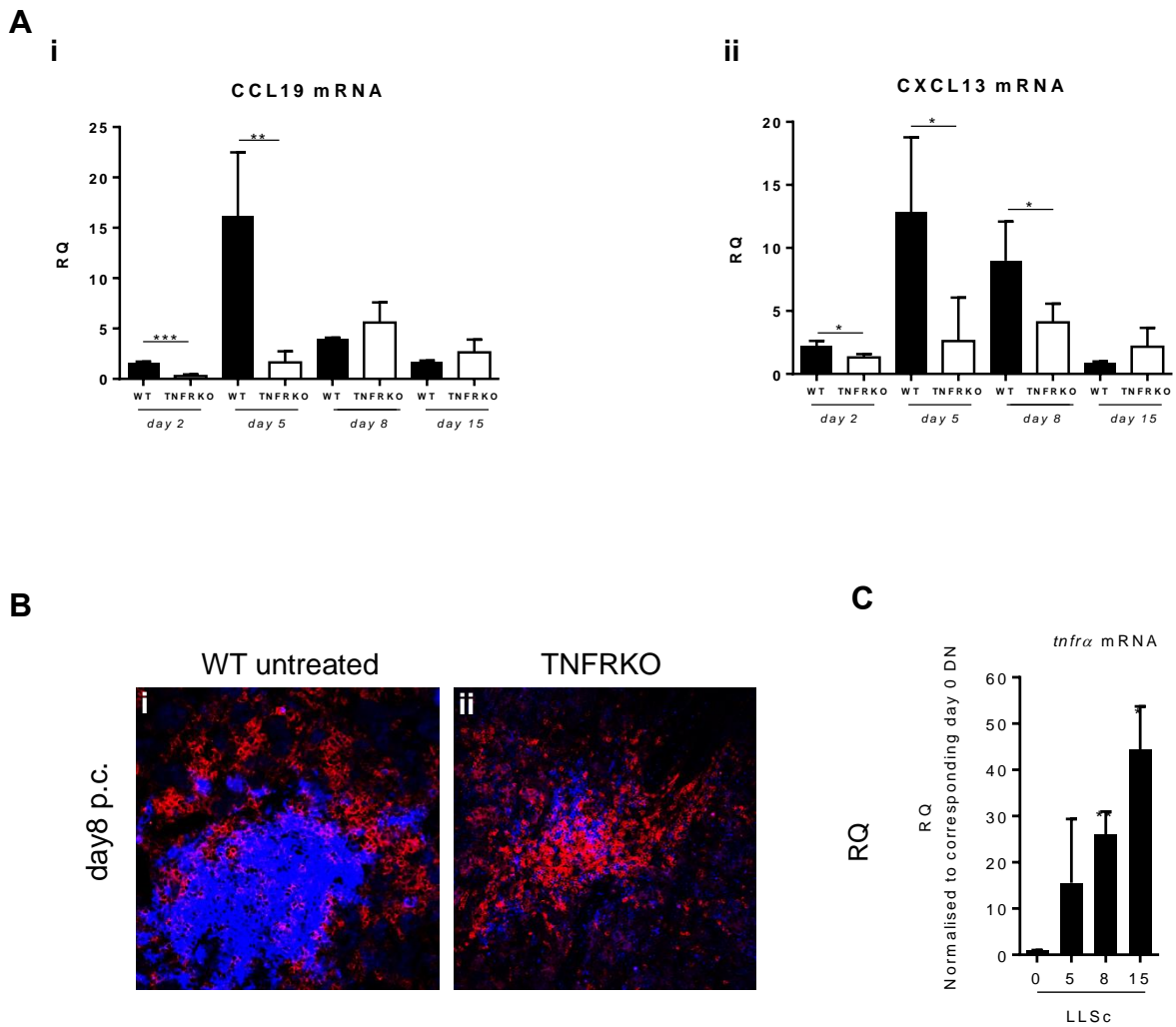
Figure 3.6. TNFR mediates the effects of LTα in our model of salivary gland inflammation. (A) qRT-PCR analysis of *ccl19* (i) and *cxcl13* (ii) mRNA transcripts from wt (black bars) and TNFRKO (white bars) salivary glands at day 2, 5, 8 and 15 p.c.. *ccl19* and *cxcl13* mRNA transcript results were normalised to pdgfrb. * p < 0.05; ** p < 0.01; *** p < 0.001, unpaired *t* test, data represented as mean (SD) from two independent experiments with at least two salivary glands analysed per group. (B) Immunofluorescence staining in salivary glands from wt and TNFRKO mice for CD3ε (red) and CD19 (blue) at day 8 p.c.. Original magnification 25X. (C) *tnfra* expression in FACS sorted CD45-EpCAM-CD31-gp38+ (LLSc) (black bars) at day 0, 5, 8 and 15 p.c.. mRNA transcripts were assessed by quantitative real time PCR and normalised to housekeeping gene β-actin. Relative quantitation (RQ) values were calculated with calibrator day 0 DN cells. Data showed as mean (SD) of two independent experiments with two to four salivary glands analysed per group. * p < 0.05; ** p < 0.01, one-way ANOVA.

3.2.7. Engagement of non-hematopoietic derived ICOSL contributes to the expression of LTα by T cells

ICOSL is highly expressed on hematopoietic APCs and ICOSL expression *in vitro* has been shown to be inducible in non-hematopoietic cells. In order to investigate the relevance of stromal cell derived ICOSL in the early establishment of TLOs, we generated bone marrow (BM) chimeras of both ICOSLKOmice reconstituted with wt BM and wt mice reconstituted with ICOSLKO BM and studied TLO development as well as the regulation of LTα on T cells isolated from these mice. Flow cytometry analysis showed reduced numbers of infiltrating T cells in both groups of chimeric mice compared to wt controls (**Figure 3.7Ai**). Similarly, the number of LTα-producing T cells was also compromised when mice lacked ICOSL in both the hematopoietic and non-hematopoietic compartments (**Figure 3.7Aii**). This defect seen by flow cytometry was also confirmed by qRT-PCR analysis, showing decreased levels of *lta* and *ccl19* mRNA in BM reconstituted animals (**Figure 3.7Bi, ii**).

These findings demonstrated that ICOSL expressed early post inflammation by both the hematopoietic and stromal cell compartment is necessary for the expression of LTα by T cells.

Figure 3.7

A

i

ii

B

i

ii
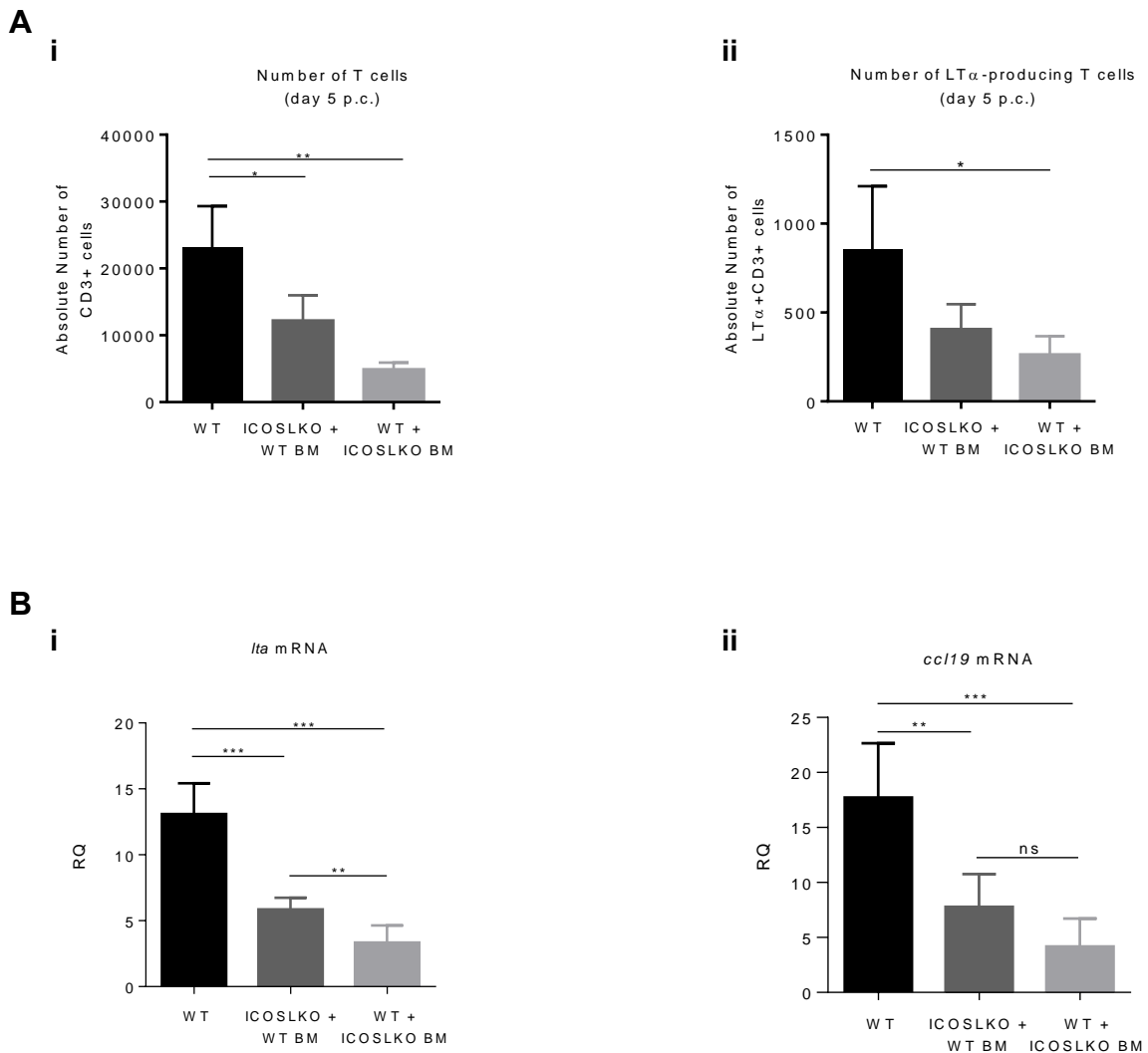
Figure 3.7. Engagement of stroma-derived ICOSL contributes to the expression of LTα by T cells. (A) Absolute numbers of T cells (i) and LTα-producing T cells (ii) in wt (black bars), ICOSLKO mice reconstituted with wt bone marrow (dark grey bars) and wt mice reconstituted with ICOSLKO bone marrow (light grey bars) at day 5 p.c.. Results were determined by flow cytometry and presented as mean (SD) of two independent experiments with at least four salivary glands per group. * $p < 0.05$; *** $p < 0.001$, one-way ANOVA. (B) Quantitative real time PCR analysis of mRNA transcripts of *lta* (i) and *ccl19* (ii) in wt (black bars), ICOSLKO mice reconstituted with wt bone marrow (dark grey bars) and wt mice reconstituted with ICOSLKO bone marrow (light grey bars). *lta* mRNA transcripts were normalised to housekeeping gene β-actin and *ccl19* results to pdgfrβ. ns = non-significant; ** $p < 0.01$; *** $p < 0.001$, one-way ANOVA, data presented as mean (SD) of two independent experiments with four to seven salivary glands analysed per group.

3.2.8. ICOSL expression by both activated stromal cells and dendritic cells supports the expression of LTα by T cells

In order to validate these results *in vitro*, T cells isolated from spleen were co-cultured with LLSc or DCs from either wt or ICOSLKO salivary glands. *Lta* mRNA signal was substantially decreased when T cells were cultured with lymphoid stroma as well as DCs from ICOSLKO, comparatively to when cultured with the correspondent wt control (**Figure 3.8A**).

Additionally, a trans-well assay in which T cells were cultured in the same well, but not in contact with the other cell population, showed no significant differences in the expression of LTα by T cells. Of note, in the trans-well setting the induction of LTα expression was between 3 to 15 fold lower as compared to the direct co-culture experiment (**Figure 3.8B**).

Those data suggest that cell-cell interaction is required by either professional APC or activated stromal cells to provide ICOSL required to activated newly recruited T cells and stimulate LTα production in early TLOs.

Figure 3.8

A

Itα mRNA
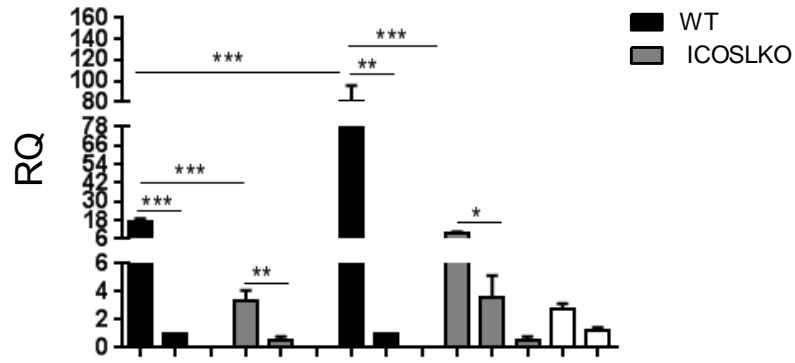
gp38+ stromal cells	+	+	+	+	+	+	-	-	-	-	-	-	-	-
DCs	-	-	-	-	-	-	+	+	+	+	+	+	-	-
T cells	+	+	-	+	+	-	+	+	-	+	+	-	+	+
Virus	+	-	-	+	-	-	+	-	-	+	-	-	+	-

B

Itα mRNA
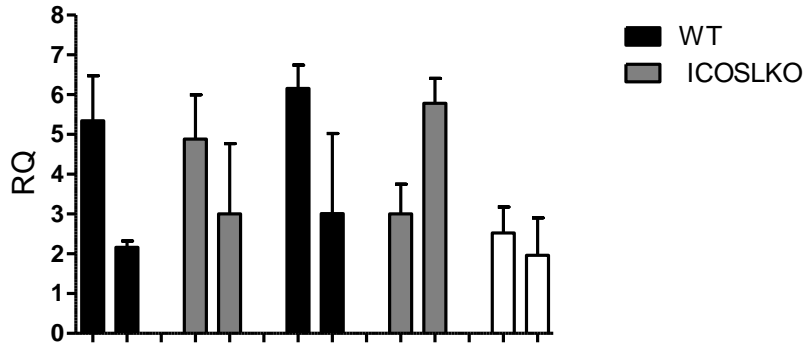
gp38+ stromal cells	+	+	+	+	+	+	-	-	-	-	-	-	-	-
DCs	-	-	-	-	-	+	+	+	+	+	+	-	-	
T cells	+	+	-	+	+	-	+	+	-	+	+	-	+	+
Virus	+	-	-	+	-	-	+	-	-	+	-	-	+	-

Figure 3.8 (cont.)

Figure 3.8. ICOSL expression by both activated stromal cells and dendritic cells supports the expression of LTα by T cells. (A) T cells were FACS sorted from wt mice and LLSc and DCs were isolated from both wt and ICOSLKO mice at day 0 p.c.. wt T cells were co-cultured with either wt or ICOSLKO LLsc or DCs, additionally stimulated with adenovirus. Graph presents quantitative real time PCR analysis that determined *lta* mRNA transcripts. qRT-PCR results were normalised to the housekeeping gene β-actin mRNA transcripts and results are presented as relative quantitation (RQ) values calibrated to unstimulated T cells cultured alone. * p < 0.05; ** p < 0.01; *** p < 0.001, one-way ANOVA, data are representative as mean (SD) of two independent experiments. (B) T cells were FACS sorted from wt mice and LLSc and DCs were isolated from both wt and ICOSLKO mice at day 0 p.c.. wt T cells were cultured in trans-wells with either wt or ICOSLKO LLsc or DCs, additionally stimulated with adenovirus. Graph presents quantitative real time PCR analysis that determined *lta* mRNA transcripts. qRT-PCR results were normalised to the housekeeping gene β-actin mRNA transcripts and results are presented as RQ values calibrated to unstimulated T cells cultured alone. ns = non-significant, one-way ANOVA, data are representative as mean (SD) of two independent experiments.

3.2.9. ICOS and ICOSL expression in salivary glands of Sjögren's syndrome patients

In order investigate the relevance of our findings in human disease we investigated the expression of ICOS and ICOSL by immunohistochemistry on labial salivary gland biopsies from SS patients. Immunohistochemistry staining showed significant expression of ICOS and ICOSL in SS samples, confirming engagement of the ICOS-ICOSL pathway in inflamed salivary glands. ICOS expression was mainly detected on CD3+ cells (**Figure 3.9A**). ICOSL expression was detected within but not limited to the lymphocyte rich area in co-localization with CD20+ cells (**Figure 3.9B**), CD11c+ cells (**Figure 3.9C**) and on gp38+ cells thus suggesting a similar role for this pathway in human disease (**Figure 3.9D**).

Figure 3.9

A

B

C

D
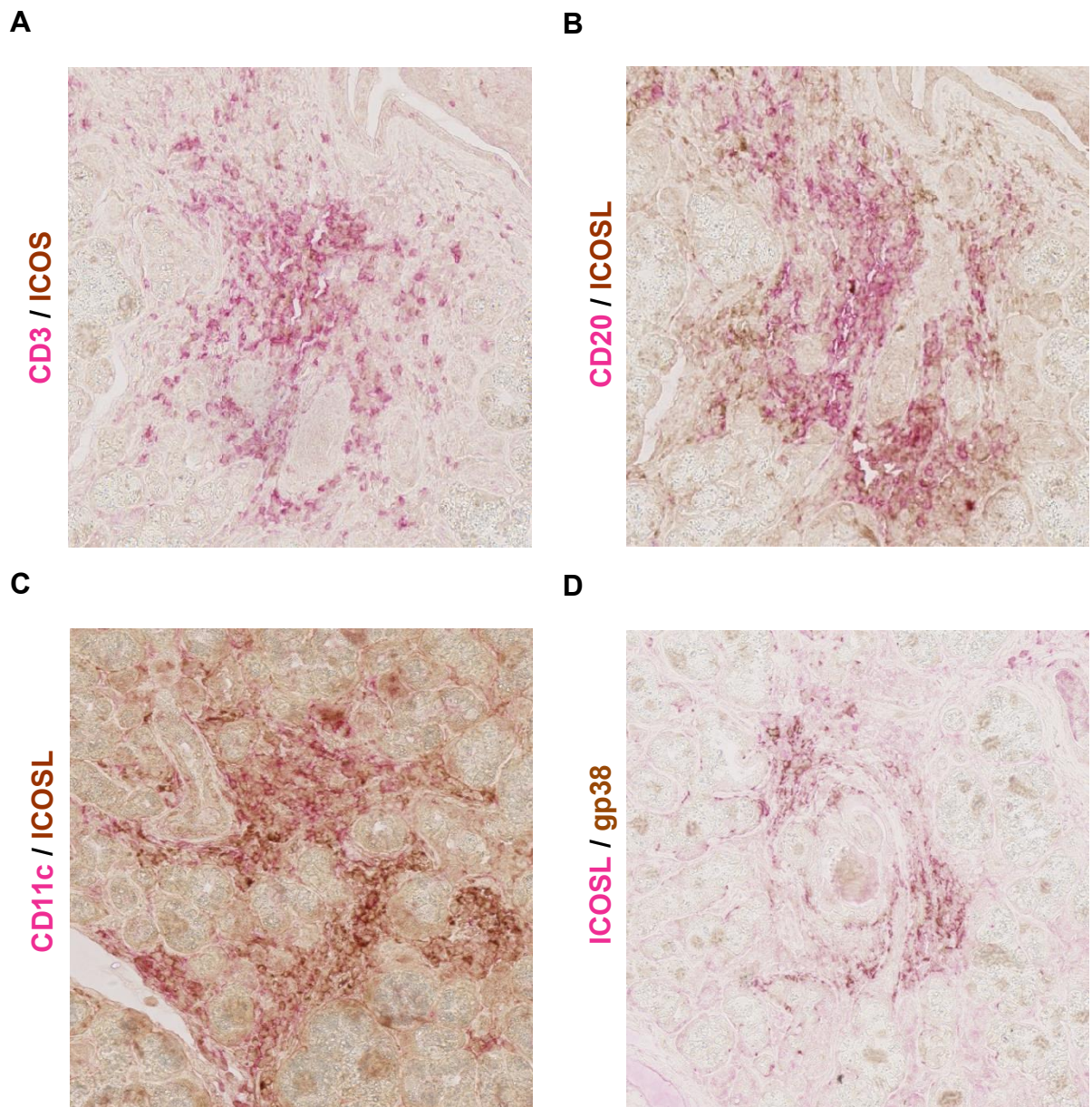
Figure 3.9. ICOS and ICOSL expression in salivary glands of Sjögren's syndrome patients. (A-D) Representative microphotographs of human salivary glands examined by immunohistochemistry for ICOS (brown, A), ICOSL (brown, B-C; pink, D) CD3 (red; A), CD20 (pink; B), CD11c (pink; C) and gp38 (brown, D). Original magnification 25X.

3.3. Discussion

In this chapter we describe a novel role of co-stimulatory molecules ICOS and ICOSL in TLO formation and, moreover, activated stromal cells as a previously unidentified source of ICOSL during inflammation.

Co-stimulation via ICOS-ICOSL interaction is critical for the generation of functional GCs, maturation of recruited T lymphocytes into cytokine-producing cells and production of antibodies. In autoimmunity this pathway is known to contribute to the development of autoreactive B cells and autoantibody production (Hondowicz et al., 2010). In autoimmune conditions such as SLE, RA and SS, higher frequencies of CD4+CXCR5+ICOS^{hi} T cells have been described (Hutloff et al., 2004, Ma et al., 2012, Simpson et al., 2010, Tangye et al., 2013). Furthermore, significantly increased levels of CD4+CXCR5+CCR6+ T cells, the T_H17-like 'circulating' T_{FH} were found in blood of SS patients and it was strongly correlated with increased detection of anti-Ro/SSA, anti-La/SSB (Jin et al., 2014, Li et al., 2012). Recently, Szabo et al. used immunohistochemistry to characterise the inflammatory infiltrates regarding their expression of T_{FH}-related markers and found them mostly present in biopsies with higher focus score (Szabo et al., 2014).

While those functions support ICOS-ICOSL targeting in TLO GCs this pathway has not been extensively explored but a recent study has reported that blockade of ICOS/ICOSL interaction suppresses the formation of ectopic lymphoid structures in a mouse model of artherosclerotic plaque development (Clement et al., 2015). The observed impairment was associated with a disrupted T_{FH} - GC B cell axis as T_{FH} cells are known to express ICOS and

were shown to take an active part in GC reaction within TLOs in diseased arteries (Clement et al., 2015).

We previously demonstrated that activated stromal cells at site of TLO formation are responsible for chemokine production and early aggregation of recruited lymphocytes (Barone et al., 2015b). Here we show that gp38+ LLSc are also involved in the functional activation of the locally recruited lymphocytes, by up regulating ICOSL on their surface and contributing to the production of LTα from locally recruited ICOS+T cells. Indeed, absence of ICOSL in genetically modified mice or interference with ICOS/ICOSL interaction induced abrogation of TLO formation with significantly decreased expression of lymphoid chemokines and defective lymphocyte recruitment. Using bone marrow chimeras and co-culture *in vitro* experiments we demonstrated that ICOSL expressed by both the hematopoietic and stromal cell compartment contributes to the expression of LTα by T cells. Of note, wt controls reconstituted with wt bone marrow are missing from this experiment. These would have accounted for possible secondary effects from from irradiation and Baytril administration.

Expression of co-stimulatory molecules on non-hematopoietic stromal cells has been previously reported and up regulation of ICOSL has been described on FRCs in the lymph node (ImmGen) and on TNFα stimulated fibroblasts (Swallow et al., 1999, Yoshinaga et al., 2000). However, to our knowledge this is the first report of functional stromal cell derived co-stimulation in the context of TLO establishment.

During lymph node organogenesis, stromal activation occurs prior and independently of lymphocytes. However, lymphocytes are critical in adult SLOs for maintenance of lymphoid structures. Evidence suggests that the maintenance of homeostatic lymphoid chemokine expression and FDCs in B cell follicles is dependent on LTαβ and TNFα expression on mature B cells (Endres et al., 1999, Fu et al., 1997b, Randall et al., 2008). It has been suggested that lymphocytes can substitute for the inductive function of LTi cells within SLOs, particularly when they are activated (Ware et al., 1992, Androlewicz et al., 1992, Tumanov et al., 2004, Tumanov et al., 2002, Fu et al., 1997a, Endres et al., 1999, Cupedo et al., 2004) and CD4+ T cells have been shown to be crucial for development of TLO in the thyroid (Marinkovic et al., 2006). TLO dependency on lymphotoxin signalling has been demonstrated in mice deficient in LT signaling or treated with anti-LTβR antibody (Columba-Cabezas et al., 2006, Gatumu et al., 2009, Gommerman et al., 2003, Lee et al., 2006, Rangel-Moreno et al., 2011, Boulianne et al., 2012, Grabner et al., 2009). Accordingly, LTα over-expression under the control of RIP, is able to induce TLO formation in a process that is dependent on TNFR1 but not LTβR, suggesting that signals through TNFR1, are sufficient to sustain TLO development (Sacca et al., 1995, Picarella et al., 1993, Kratz et al., 1996, Hjelmstrom, 2001).

LTα expression is increased in synovium and serum from RA patients (Robak et al., 1998, O'Rourke et al., 2008), and interestingly RA patients that did not respond to anti-TNFα treatment were additionally treated with anti-TNFR, leading to clinical remission (Buch et al., 2004, Calmon-Hamaty et al., 2011). An *in vitro* study has shown that LTα stimulates proliferation and induces

secretion of IL-6, IL-8 and MMP3 by RA fibroblast-like synoviocytes (Calmon-Hamaty et al., 2011). In SS patients, LTα is also increased in both the salivary glands and sera (Shen et al., 2010).

Indeed, in our model, LTα effect was mediated by the activation of TNFRI; nonetheless the phenotype observed in the TNFRKO is not as severe as that observed in the LTαKO mice, thus suggesting that LTβR signalling collaborates with TNFRI for chemokine production by stromal cells. Similarly, Frances et al., previously shown that GC B cells from ICOSKO mice express lower levels of LTαβ compared with wild-type GC B cells in vivo. Interestingly, in that setting administration of agonistic anti-LTβ receptor antibody was unable to restore the GC response suggesting that additional input from another pathway or engagement of a different receptor is required to accomplish GC generation (Vu et al., 2008).

Interestingly, in our system, CCL19 is more susceptible to the decrease in LTα as compared to CXCL13 and the production of the B cell recruiting chemokine is only partially dependent on ICOS-dependent T cells activation. We have previously shown that CXCL13 expression can be induced by cytokines other than lymphotoxin (Barone et al., 2015b). On the contrary, our data suggest that CCL19 expression requires the specific activation of a lymphoid axis that involves lymphotoxin. Indeed, while CXCL13 expression can be found in several infective conditions, not necessarily charaterised by lymphoneogenesis, the expression of both B and T cell chemokines in a regulated and organised manner is key to TLO formation. In this context, the early expression of LTα that regulates CCL19 production by local stromal might be critical to establish new TLOs.

Therefore, this work provides a relevant new insight to the role of co-stimulation in TLO formation by establishing a functional connection between ICOS/ICOSL interaction, activation of pathogenic stroma and T cell importance in TLO development (**Figure 3.10**), as well as introducing potential new therapeutic targets in the context of SS.

Figure 3.10
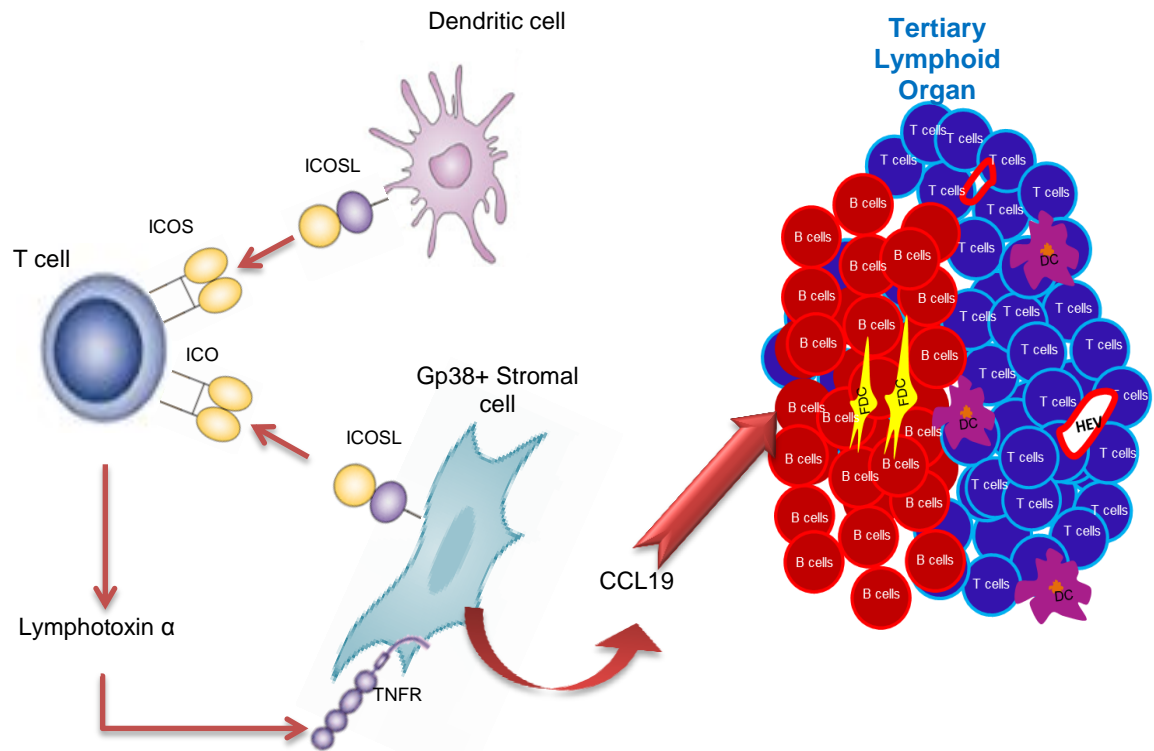
Figure 3.10. Model of stroma-T cell cross-talk via ICOSL-ICOS interaction that is critical for TLO formation. At sites of TLO formation, activated LLSc and DCs upregulate ICOSL that interacts with the locally recruited ICOS+T cell stimulating the secretion of LTα. Engagement of LTα with TNFR upregulated on the activated stromal cells induces chemokine production, in particular CCL19, that in turn contributes to the recruitment and organization of further T cells and establishing the feedback loop required for TLO formation.

Chapter 4

EARLY DELETION OF GP38 POST SALIVARY GLAND INFLAMMATION DOES NOT IMPAIR TLO FORMATION

4.1. Introduction

During inflammation expression of gp38 is induced on tissue resident fibroblasts (Peduto et al., 2009). Up-regulation of gp38 expression by these stromal cells is associated with the acquisition of a lymphoid-like cell phenotype similar to that observed in secondary lymphoid organs. These cells establish a network that supports lymphocyte recruitment and survival (Peduto et al., 2009). However, most studies regarding gp38 expression are descriptive and fail to establish a functional role for this molecule in pathology. Recently, Acton et al. have shown that engagement of gp38 with CLEC-2 on dendritic cells is necessary for cytoskeleton rearrangement and the consequent cell motility along stromal cell surfaces (Acton et al., 2012). On the other hand, interaction between gp38 and CLEC-2 allows relaxation of FRC cytoskeleton and cell stretching, allowing rapid lymph node expansion (Acton et al., 2014).

Previous data from our group has shown that a population of gp38+ stromal cells expands in the target organ of inflammation (salivary glands). This population is characterised by expression of ER-TR7, ICAM-1 and VCAM-1 (Saba Nayar, unpublished data).

During lymph node formation, mature LTo stromal cells express ICAM-1 and VCAM-1 and produce homeostatic chemokines. The maturation of resident mesenchyme from ICAM^{int}VCAM^{int} to ICAM^{hi}VCAM^{hi}MadCAM+ cells is dependent on LTβR signalling and crosstalk with LTi cells (Cupedo et al., 2004, White et al., 2007, Benezech et al., 2010).

Accordingly, the population of gp38+ stromal cells found in inflamed salivary glands acquire the capability to secrete lymphoid chemokines CXCL13 (Barone et al., 2015b), CCL19 and CCL21, survival factors BAFF and IL-7 and also LTβR and TNFR1 (Saba Nayar, unpublished data). On the basis of these features we named these cells lymphoid-like stromal cells (LLSc). In our published model of viral-induced TLO formation, this gp38+CD31- LLSc population expands from as early as 3 hours post cannulation (p.c.) and peaks at day 5, representing over 40% of the CD45-EpCAM- component. FACS analysis for Ki67 and BrdU suggested that the expansion of this population within the first few hours of virus delivery was most likely not due to proliferation but to upregulation of gp38 on CD45-EpCAM-CD31- cells, since active proliferation was observed between day 2 and day 5 (Saba Nayar, unpublished data). Resolution of the lymphoid aggregates occurs from day 23 p.c. and by day 26 the percentage of LLSc is comparable with what can be observed in resting salivary glands (about 7%) (Saba Nayar, unpublished data).

Histologically, gp38 expression is largely present in inflamed salivary glands on epithelial, lymphatic endothelial and stromal cells; while LLSc are detected in close proximity with lymphoid aggregates (**Figure 4.1**).

In order to investigate the role of g38 expression by resident stromal cells during inflammation we utilised a conditional *Pdpn* knockout mice to specifically dissect the role of gp38 in the formation of ectopic lymphoid structures. Since the genetic deletion of *Pdpn* is lethal (Schacht et al., 2003), we have induced TLO formation in a conditional *Pdpn* knockout strain (PDPN$^{fl/fl}$R26ERT2$^{Cre/Cre}$), where deletion of gp38+ cells will be obtained upon administration of tamoxifen.

Figure 4.1

A

DAPI / gp38
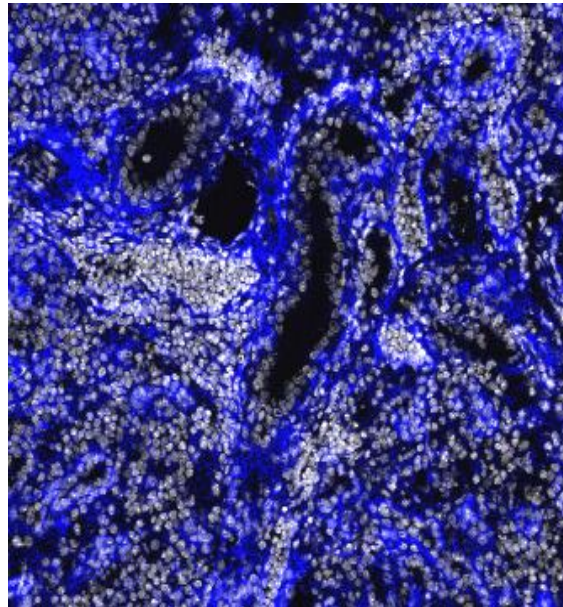
B

gp38 CD45
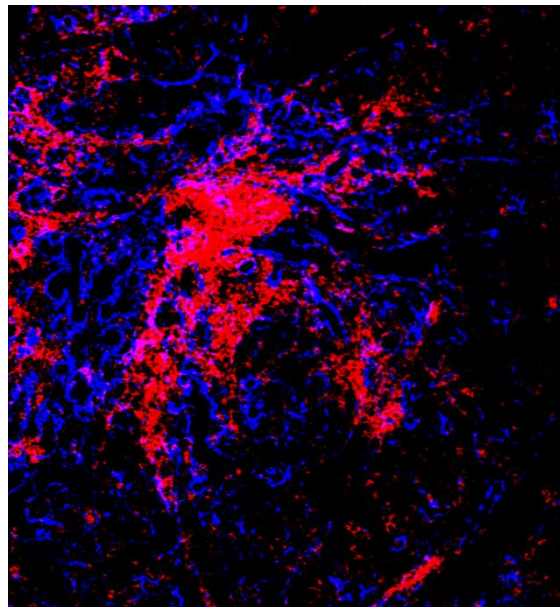
Figure 4.1. Gp38 expression in inflamed salivary glands. Wt mice were cannulated, virus administered and mice sacrificed at day 8 p.c. (post cannulation). (A) Representative microphotograph of salivary glands examined by immunofluorescence for gp38 (blue) and DAPI nuclear staining (grey). Original magnification 25X. (B) Confocal image of cannulated wt salivary gland stained for gp38 (blue) and CD45 (red). Original magnification 10X.

4.2. Results

4.2.1. Tamoxifen treatment efficiently downregulates gp38 expression in stromal cells from PDPN^{fl/fl}R26ERT2^{Cre/Cre} salivary glands

In order to study the role of gp38 expression we have used a conditional *Pdpn* knockout. Tamoxifen was administered for five consecutive days to 28 day old PDPN$^{fl/fl}$R26ERT2$^{Cre/Cre}$ mice; as described in section 2.1.1. Mice remained un-manipulated for a further period of 35 days to account for Tamoxifen wash out.

FACS analysis was performed to address level of gp38 deletion. Dissected salivary glands from wt untreated, non-cannulated mice (8 weeks old) revealed the presence of two stromal cells populations within the CD45-EpCAM-CD31- cell fraction. These two populations were defined by the presence or absence of gp38 expression; respectively named lymphoid-like stromal cells (LLSc) (gp38+CD31-) and double negative (DN) (gp38-CD31-) (**Figure 4.2A and Bi**). Similar stromal populations with distinct levels of gp38 expression were also observed in Tamoxifen treated control PDPN$^{+/+}$R26ERT2$^{Cre/Cre}$ mice (**Figure 4.2A and Bii**).

On the contrary salivary glands isolated from PDPN$^{fl/fl}$R26ERT2$^{Cre/Cre}$, at day 36 post Tamoxifen, showed a significant loss of gp38 expression within the CD45-EpCAM-CD31- compartment (**Figure 4.2A**). Enzymatically digested salivary glands from PDPN$^{fl/fl}$R26ERT2$^{Cre/Cre}$ mice not only presented a smaller percentage of LLSc (3.97%) but also this population expressed lower levels of gp38 (**Figure 4.2Biii**), showing that even though the strain did not

behave as a complete knockout, Tamoxifen treatment did result in a significant downregulation of gp38 expression by the CD45-EpCAM-CD31-compartment in the salivary glands.

Figure 4.2

A

CD45-EpCAM-CD31-

■□	Pdpn Fl Cre F3 SG1 day36 p.Tamox.fcs	20.4
■□	Pdpn + Cre F1 SG1 day36 p.Tamox.fcs	16.5
■□	WT SG2 un-manipulated.fcs	17.2

B
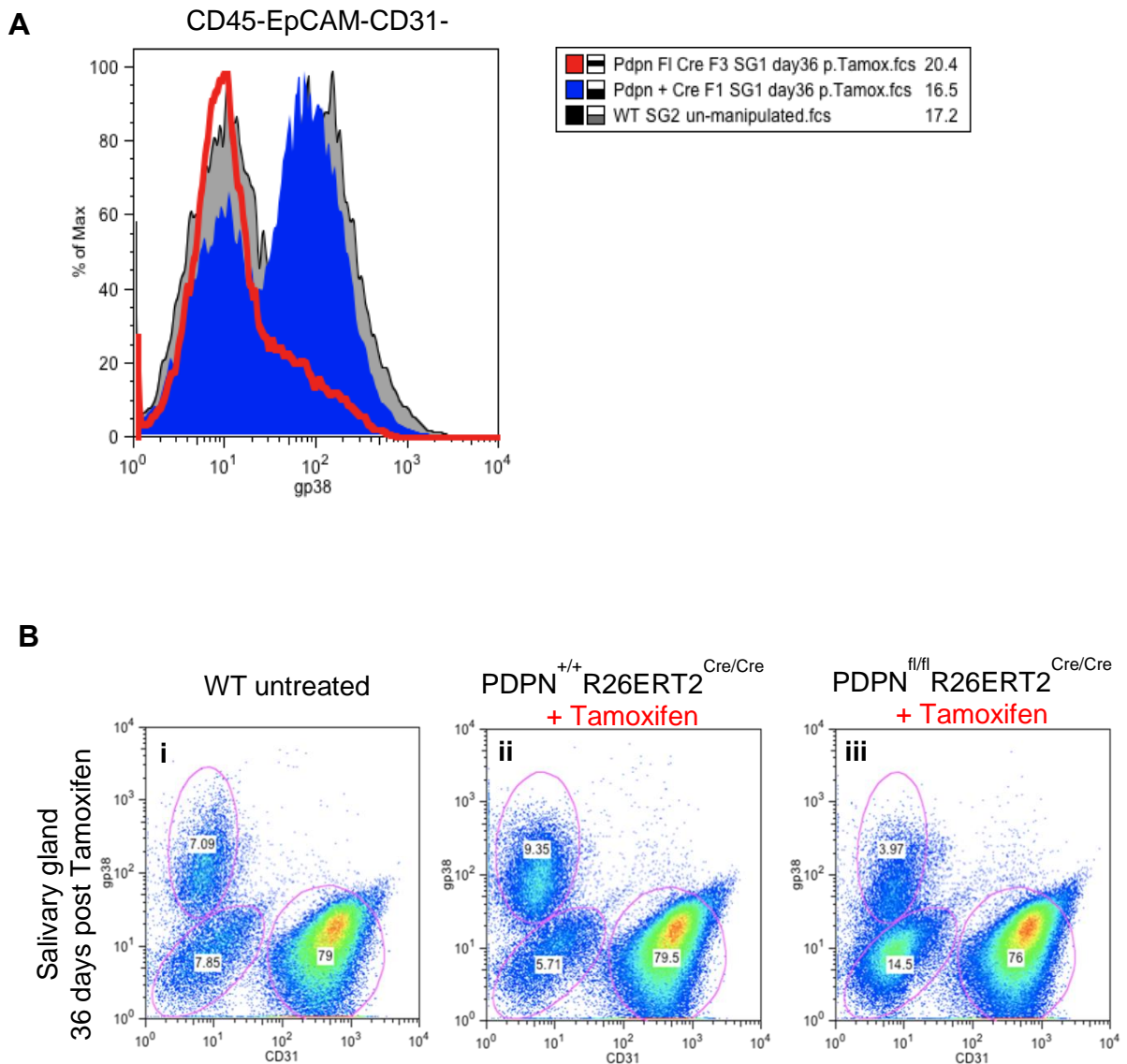
Figure 4.2. Tamoxifen treatment efficiently downregulates gp38 expression in stromal cells from Tamoxifen treated PDPN$^{Fl/Fl}$R26ERT2$^{Cre/Cre}$ salivary glands. (A) Histogram showing flow cytometry staining for gp38 expression in wt (grey), PDPN$^{+/+}$R26ERT2$^{Cre/Cre}$ (blue) and PDPN$^{Fl/Fl}$R26ERT2$^{Cre/Cre}$ (red) mice at day 36 post Tamoxifen administration. (B) Representative dot plot showing flow cytometry staining for gp38 expression in CD45-EpCAM- cells from wt (i), PDPN$^{+/+}$R26ERT2$^{Cre/Cre}$ (ii) and PDPN$^{fl/fl}$R26ERT2$^{Cre/Cre}$ (iii) salivary glands at day 36 post Tamoxifen.

4.2.2. Lower levels of gp38 expression by stromal cells is not maintained during inflammation in PDPN$^{fl/fl}$R26ERT2$^{Cre/Cre}$ mice

After verifying that tamoxifen treatment downregulates gp38 expression in CD45-EpCAM-CD31- cells from PDPN$^{fl/fl}$R26ERT2$^{Cre/Cre}$ salivary glands, we aimed to study the development and maintenance of TLOs in these mice post adenoviral delivery.

Post salivary gland cannulation and adenovirus infection, FACS analysis of gp38 expression in PDPN$^{+/+}$R26ERT2$^{Cre/Cre}$ cannulated glands revealed a similar dynamic to that observed in the wt mice (Saba Nayar unpublished). The LLSc population in the control mice expanded to about 40% (of CD45-EpCAM- cells) at days 5 and 8 p.c. (**Figure 4.3Ai and Bi**). On the contrary, in the salivary glands from PDPN$^{fl/fl}$R26ERT2$^{Cre/Cre}$ mice the percentage of LLSc was around 10%, thus showing a significant decrease as compared to controls (**Figure 4.3Aii and Bii**). At day 15 p.c., the percentage of gp38+ stromal cells in the PDPN$^{fl/fl}$R26ERT2$^{Cre/Cre}$ was closer to control mice, although still showing a difference in the expression of gp38 (**Figure 4.3Ci, ii**). A similar phenotype was observed at day 23 p.c. (**Figure 4.3Di, ii**).

The mean fluorescence intensity for gp38 expression from the flow cytometry data was significantly reduced at days 5 and 15 p.c. in PDPN$^{fl/fl}$R26ERT2$^{Cre/Cre}$ salivary glands (**Figure 4.3E**).

Figure 4.3
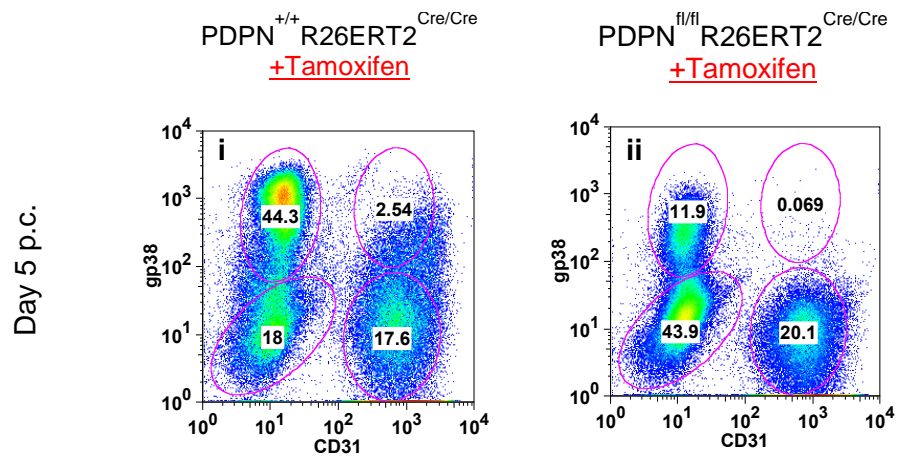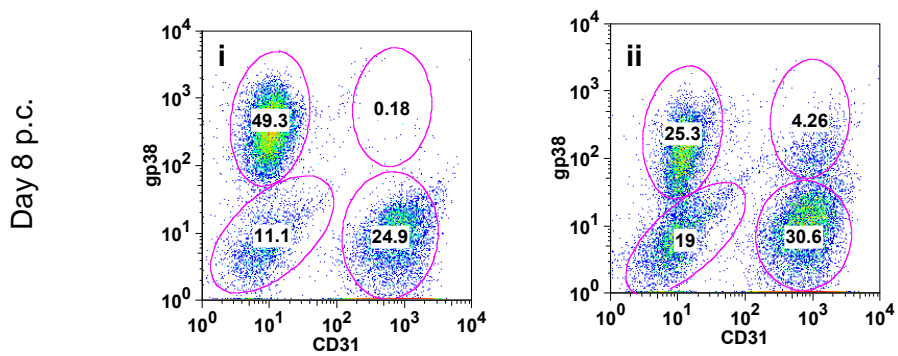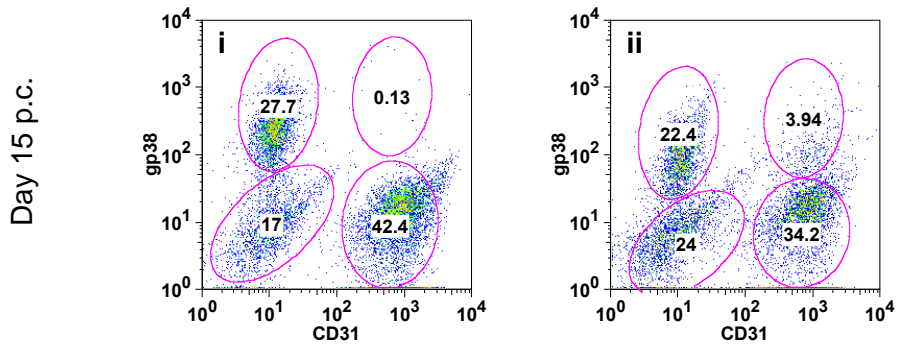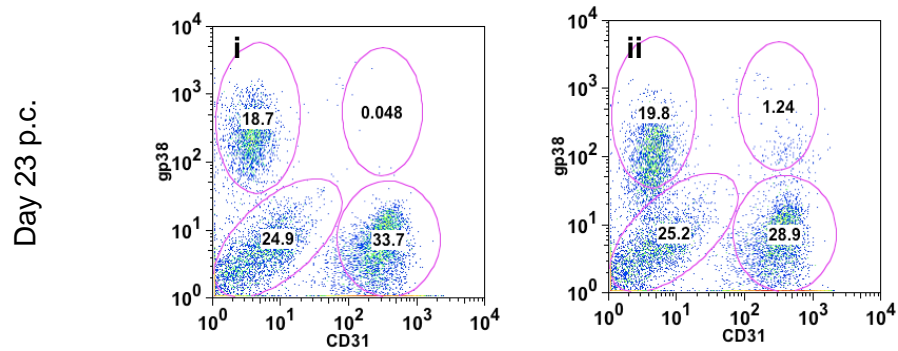
Figure 4.3 (cont.)

E
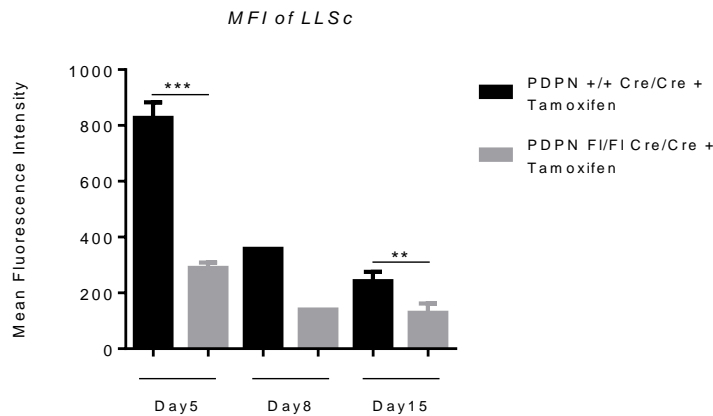
Figure 4.3. Stromal cells from cannulated PDPN$^{fl/fl}$R26ERT2$^{Cre/Cre}$ salivary glands post Tamoxifen treatment express reduced levels of gp38. PDPN$^{+/+}$R26ERT2$^{Cre/Cre}$ and PDPN$^{fl/fl}$R26ERT2$^{Cre/Cre}$ mice were treated with Tamoxifen and cannulated at day 35. Mice were sacrificed at days 5 (A), 8 (B), 15 (C) and 23 (D) p.c.. Representative dot plots showing flow cytometry staining for gp38 expression in CD45-EpCAM- cells from PDPN$^{+/+}$R26ERT2$^{Cre/Cre}$ (i) and PDPN$^{Fl/Fl}$R26ERT2$^{Cre/Cre}$ (ii) salivary glands. (E) Mean fluorescence intensity of gp38 in LLSc at days 5, 8 and 15 p.c. from PDPN$^{+/+}$R26ERT2$^{Cre/Cre}$ (i) and PDPN$^{Fl/Fl}$R26ERT2$^{Cre/Cre}$ (ii) salivary glands. Data presented as mean (SD) with three to four glands analysed per group. ** $p < 0.01$; *** $p < 0.001$, unpaired *t* test.

Absolute numbers of this population of activated stromal cells was also reduced between PDPN$^{fl/fl}$R26ERT2$^{Cre/Cre}$ and control mice, however no significant differences were found between the tamoxifen treated mice and the controls (**Figure 4.4B**).

Ki67 analysis showed a trend in increased proliferation in the tamoxifen treated mice that was found statistically significant at day 8 and 23 post cannulation and interpreted as mechanism of compensation of the stromal cell compartment for the loss of gp38 (**Figure 4.4C**).

Figure 4.4

A

% of LLSc

PDPN^{+/+}R26ERT2[Cre/Cre]
+ Tamoxifen

PDPN[Fl/Fl]R26ERT2[Cre/Cre]
+ Tamoxifen

B

Numbers of LLSc

PDPN^{+/+}R26ERT2[Cre/Cre] +
Tamoxifen

PDPN[Fl/Fl]R26ERT2[Cre/Cre]
+ Tamoxifen

C

% Ki67+ LLSc

PDPN^{+/+}R26ERT2[Cre/Cre]
+ Tamoxifen

PDPN[Fl/Fl]R26ERT2[Cre/Cre]
+ Tamoxifen
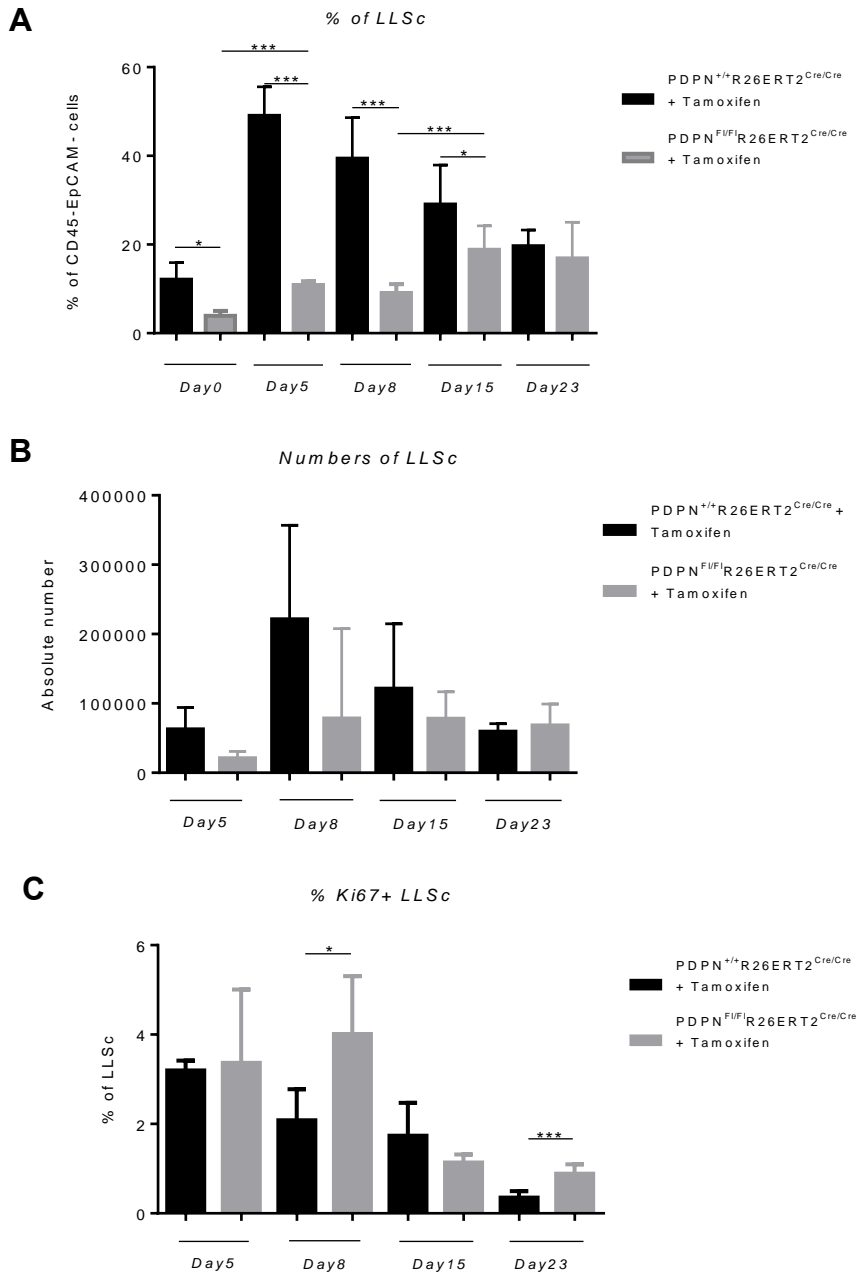
Figure 4.4. Tamoxifen treated PDPN[Fl/Fl]R26ERT2[Cre/Cre] salivary glands fail to expand LLSc population early post salivary gland cannulation. PDPN^{+/+}R26ERT2[Cre/Cre] and PDPN^{fl/fl}R26ERT2[Cre/Cre] mice were treated with Tamoxifen and cannulated at day 35. Mice were sacrificed at days 5 (A), 8 (B), 15 (C) and 23 (D) p.c.. Percentage (A) and absolute numbers (B) of LLSc as well as percentage of Ki67+LLSc (C) was assessed by flow cytometry staining for gp38+CD31- cells in a CD45-EpCAM- population from day 0 to day 23 p.c. in PDPN^{+/+}R26ERT2[Cre/Cre] treated with Tamoxifen (black) and PDPN^{fl/fl}R26ERT2[Cre/Cre] mice treated with Tamoxifen (grey). Data presented as mean (SD) with two to fifteen glands analysed per group. * p < 0.05; *** p < 0.001, unpaired *t* test.

4.2.3. Lymphoid chemokine expression is not affected by gp38 downregulation in PDPN$^{fl/fl}$R26ERT2$^{Cre/Cre}$ mice

Analysis of mRNA transcripts from whole frozen tissue sections has further confirmed gp38 downregulation in tamoxifen treated PDPN$^{fl/fl}$R26ERT2$^{Cre/Cre}$ salivary glands (**Figure 4.5A**). Nonetheless, consistent with what we had observed in single cell suspensions, low expression of gp38 expression was maintained in the early inflammatory phases, although significantly reduced as compared to control glands. mRNA transcripts for gp38 were significantly increased at day 15 and 23 p.c. in the salivary glands from PDPN$^{fl/fl}$R26ERT2$^{Cre/Cre}$, while maintaining significantly lower levels as compared to the wt and PDPN$^{+/+}$R26ERT2$^{Cre/Cre}$ controls (**Figure 4.5A**).

Within the lymph node environment, gp38+ lymphoid stromal cells have been shown to produce lymphoid chemokines responsible for lymphocyte recruitment and lymphoid aggregate organization (Peduto et al., 2009). Our group and others have described similar functions of the gp38+ LLSc in ectopic TLO structures and murine salivary glands upon cannulation (Peduto et al., 2009, Barone et al., 2015b).

In *Pdpn*-deficient salivary glands, levels of mRNA transcripts coding lymphoid chemokines CCL19 and CXCL13 were not affected, showing an analogous dynamic to experimental controls (**Figure 4.5B and C**).

Figure 4.5

A

gp38 mRNA

B

ccl19 mRNA

C

cxcl13 mRNA
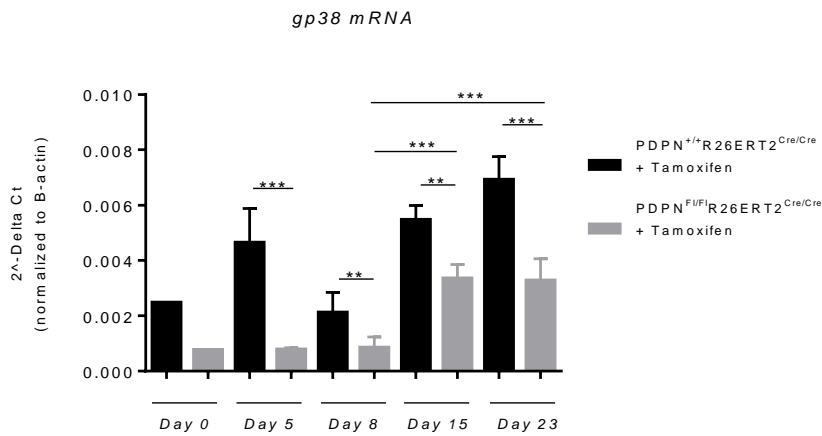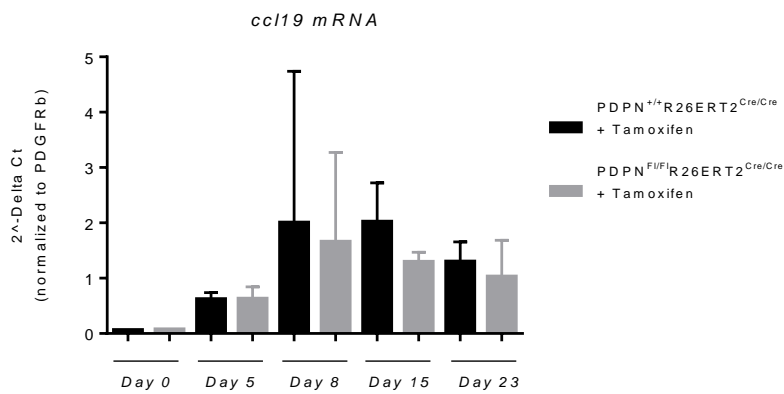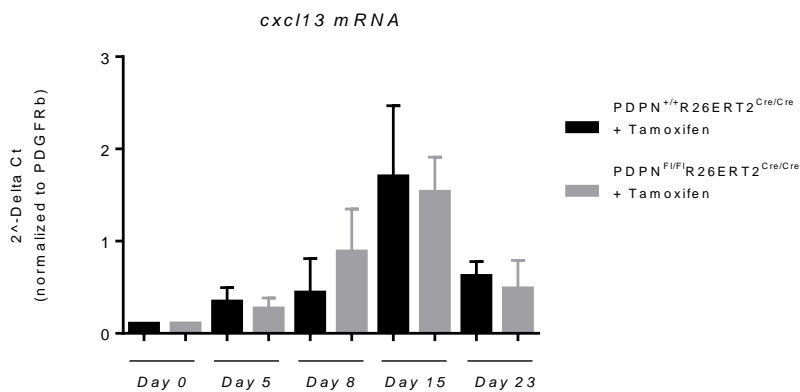
Figure 4.5. Tamoxifen treatment downregulates gp38 expression but does not affect expression levels of lymphoid chemokines. qRT-PCR analysis of *Pdpn* (A), *ccl19* (B) and *cxcl13* (C) mRNA transcripts from PDPN^{+/+}R26ERT2[Cre/Cre] treated with Tamoxifen (black) and PDPN^{fl/fl}R26ERT2[Cre/Cre] mice treated with Tamoxifen (grey). qRT-PCR results for *Pdpn* were normalised to housekeeping gene β-actin and *ccl19* and *cxcl13* results normalised to *Pdgfrb*. ** p < 0.01; *** p < 0.001, unpaired *t* test, data represented as mean (SD) with two to nine glands analysed per group.

4.2.4. TLO formation is not impaired in cannulated salivary glands of Tamoxifen treated PDPN$^{fl/fl}$R26ERT2$^{Cre/Cre}$ mice

Cannulated salivary glands from both tamoxifen treated PDPN$^{+/+}$R26ERT2$^{Cre/Cre}$ and PDPN$^{fl/fl}$R26ERT2$^{Cre/Cre}$ mice were sectioned and stained for identification and characterisation of lymphoid aggregates using immunofluorescence.

At day 8 p.c. aggregates comprising both CD3ε+ and CD19+ cells could be equally observed in both experimental groups (**Figure 4.6Ai, ii**). Also, as expected for this specific time point, scattered CD3+ cells were found and no striking differences were noted between salivary glands lacking gp38 and control glands (**Figure 4.6Ai, ii**).

Later, when full TLO formation was expected and indeed observed in control salivary glands at day 15 p.c., tamoxifen treated PDPN$^{fl/fl}$R26ERT2$^{Cre/Cre}$ glands presented fully developed, organised and segregated lymphoid aggregates (**Figure 4.6Aiii, iv**).

Image analysis of immunofluorescence staining on both groups unveiled a higher area of salivary gland tissue occupied by lymphoid aggregates in PDPN$^{fl/fl}$R26ERT2$^{Cre/Cre}$ mice (**Figure 4.6B**). The average follicle area was also increased in this group, however also for this parameter the difference observed was not statistically significant (**Figure 4.6B**).

Figure 4.6

A

B

116
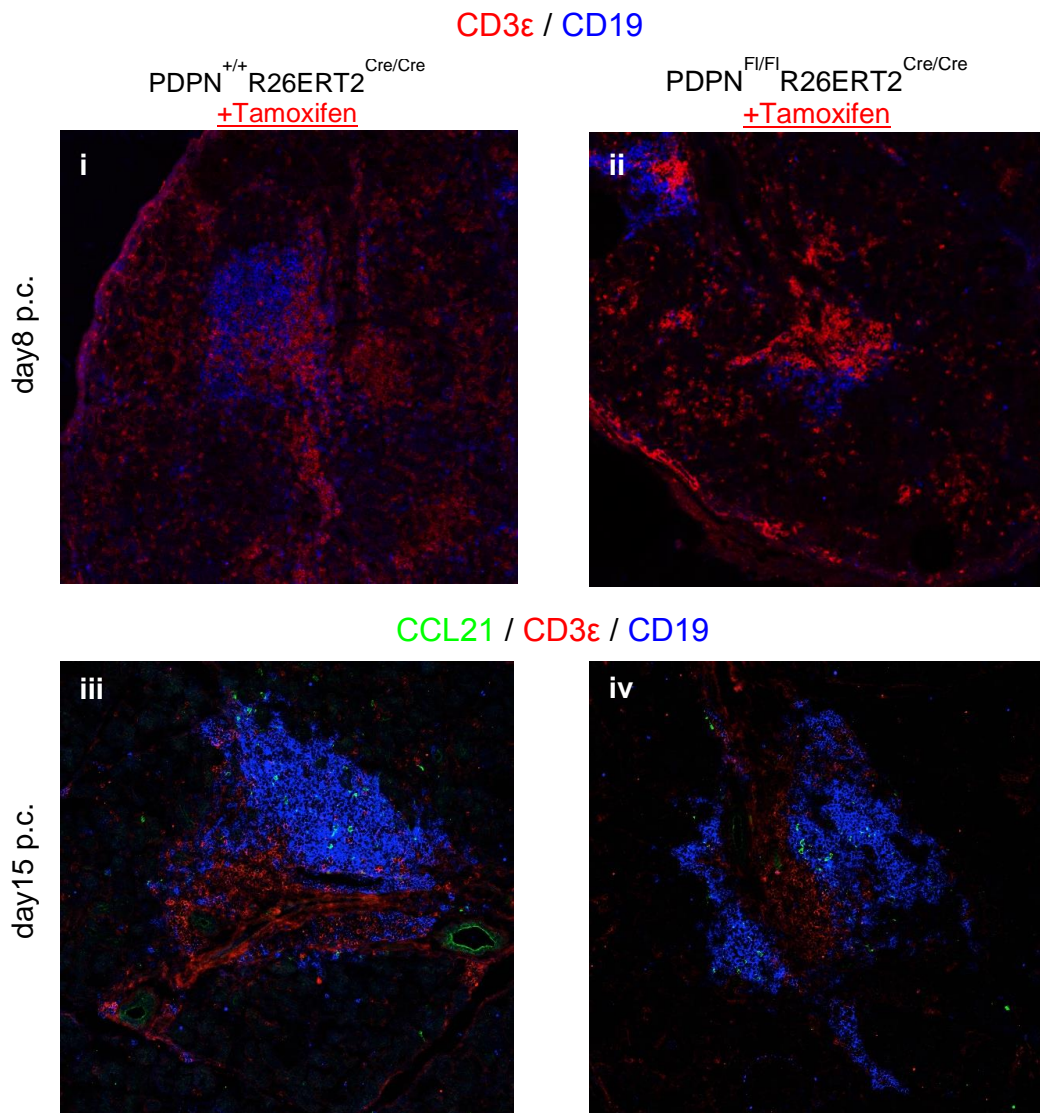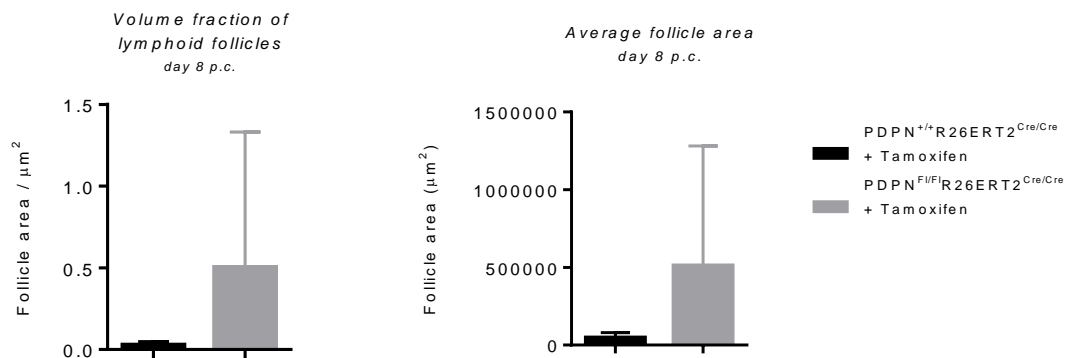
Figure 4.6 (cont.)

Figure 4.6. Diminished expression of gp38 do not impair TLO formation in inflamed salivary glands. PDPN$^{+/+}$R26ERT2$^{Cre/Cre}$ and PDPN$^{fl/fl}$R26ERT2$^{Cre/Cre}$ mice were treated with tamoxifen and cannulated at day 35. Mice were sacrificed at days 8 and 15 p.c.. (A) Representative microphotographs of salivary glands examined by immunofluorescence for CCL21 (green), CD3ε (red) and CD19 (blue) showing lymphocytic infiltration. Original magnification 25X. (B) Image analysis of immunofluorescence images for volume fraction of lymphoid follicles and average follicle area. Data presented as mean (SD) with three glands analysed per group, unpaired *t* test.

4.2.5. Decreased gp38 expression associates with failed upregulation of adhesion chemokines at day 8 p.c.

In the context of secondary lymphoid organ formation, upregulation of adhesion chemokines by gp38+ stromal cells has been described as one of the features of their maturation into lymphoid tissue organizer cells (Benezech et al., 2010)

Here we have investigated by flow cytometry analysis both percentage and absolute numbers of VCAM^{int}ICAM^{int} and VCAM^{hi}ICAM^{hi} cells within the CD45-EpCAM-CD31- compartment of PDPN$^{fl/fl}$R26ERT2$^{Cre/Cre}$ and control mice. In the VCAM^{int}ICAM^{int} population no significant changes were observed between the two groups, with the exception of an increase in percentage (but not absolute cell number) in the PDPN$^{fl/fl}$R26ERT2$^{Cre/Cre}$ salivary glands at day 15 p.c. (**Figure 4.7Ai, ii**). However, a reduction of about 50% in both absolute number and percentage of VCAM^{hi}ICAM^{hi} cells was observed in cannulated salivary glands of PDPN$^{fl/fl}$R26ERT2$^{Cre/Cre}$ mice at day 8 p.c. (**Figure 4.7Bi, ii**). No other time point showed any statistically significant changes in the proportion of VCAM^{hi}ICAM^{hi} stromal cells.

Figure 4.7

A

i
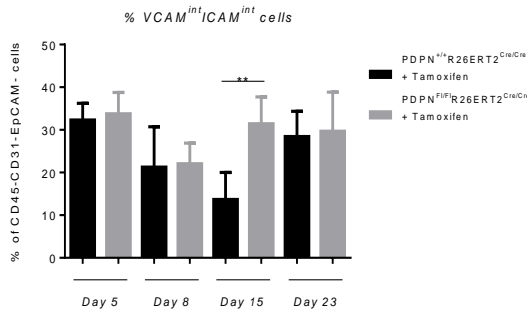
ii
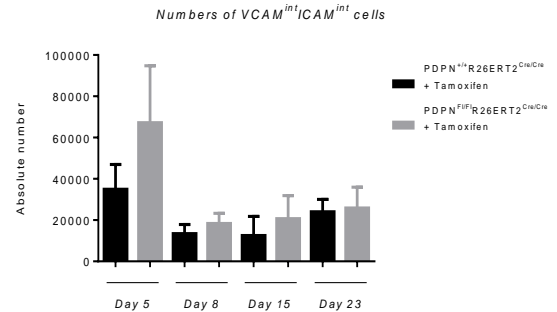
B

i
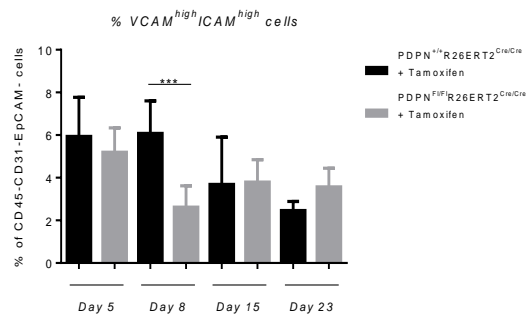
ii
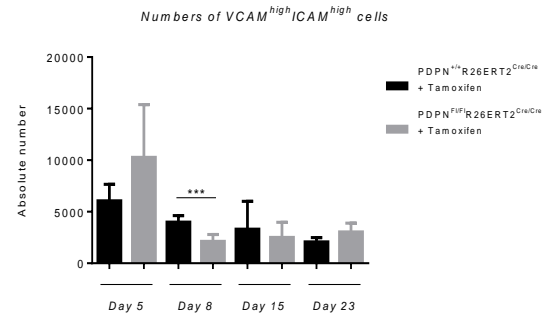
Figure 4.7. Gp38 expression do not affect upregulation of adhesion molecules by activated stromal cells. PDPN$^{+/+}$R26ERT2$^{Cre/Cre}$ (blue) and PDPN$^{fl/fl}$R26ERT2$^{Cre/Cre}$ (red) mice were treated with Tamoxifen and cannulated at day 35. Mice were sacrificed at days 5, 8, 15 and 23 p.c.. Percentage and absolute numbers of VCAM^{int}ICAM^{int} (A) VCAM^{hi}ICAM^{hi} (B) was assessed by flow cytometry staining of CD45-CD31-EpCAM- cells Data presented as mean (SD) with two to fifteen glands analysed per group. ** p < 0.01; *** p < 0.001, unpaired t test.

4.2.6. Resting and immunized PDPN^{fl/fl}R26ERT2^{Cre/Cre} lymph nodes exhibit no defects in architecture or organization

We then sought to explore the consequences of gp38 downregulation in SLOs, particularly in the capability to mount an immune response against a T cell dependent antigen by immunizing brachial lymph nodes of *Pdpn*-deficient mice.

Firstly we examined resting un-immunized brachial lymph nodes from Tamoxifen treated PDPN$^{+/+}$R26ERT2$^{Cre/Cre}$ mice and found normal lymph node architecture with well-defined CD3+ and CD19+ areas (**Figure 4.8A**). Gp38 positive staining was identified in both CD3+ and CD19+ areas as well as co-localization with Lyve-1+ lymphatic vessels (**Figure 4.8A**). Lymph nodes from PDPN$^{fl/fl}$R26ERT2$^{Cre/Cre}$ mice were, on the contrary almost completely negative for gp38 staining and only a few scattered gp38+ cells could be found in T cell areas and in close proximity with lymphatic vessels (**Figure 4.8B**). Nonetheless, in the absence of gp38, lymph node structure and organization was intact.

Post immunization, both the wt and PDPN$^{+/+}$R26ERT2$^{Cre/Cre}$ control mice exhibited highly expanded lymph nodes with dense networks of gp38+ cells and an enlarged lymphatic structure (**Figure 4.9A and B**). Immunized lymph nodes from gp38-deficient mice lacked the gp38+ networks observed in the control mice (**Figure 4.9C**).

Figure 4.8

Un-immunised bLN day 8

A

PDPN$^{+/+}$R26ERT2$^{Cre/Cre}$
+Tamoxifen

CD3 / gp38 / CD19   Lyve-1 / gp38 / CD4
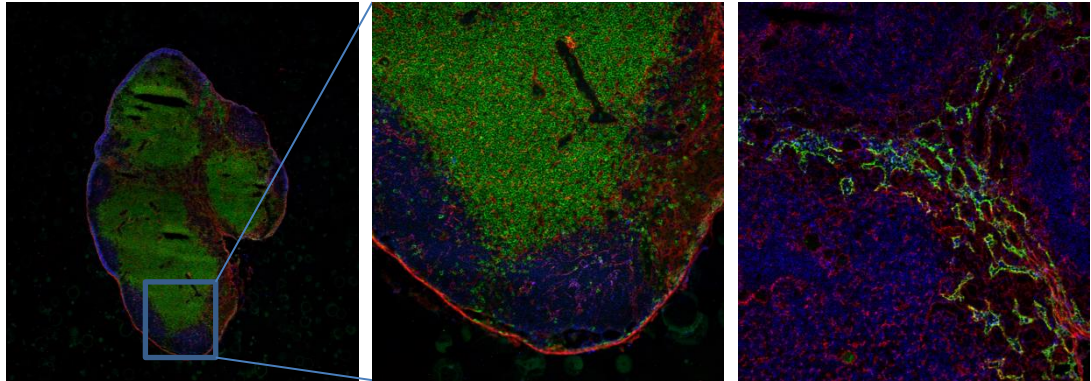
B

PDPN$^{fl/fl}$R26ERT2$^{Cre/Cre}$
+Tamoxifen

CD3ε / gp38 / CD19   Lyve-1 / gp38 / CD4
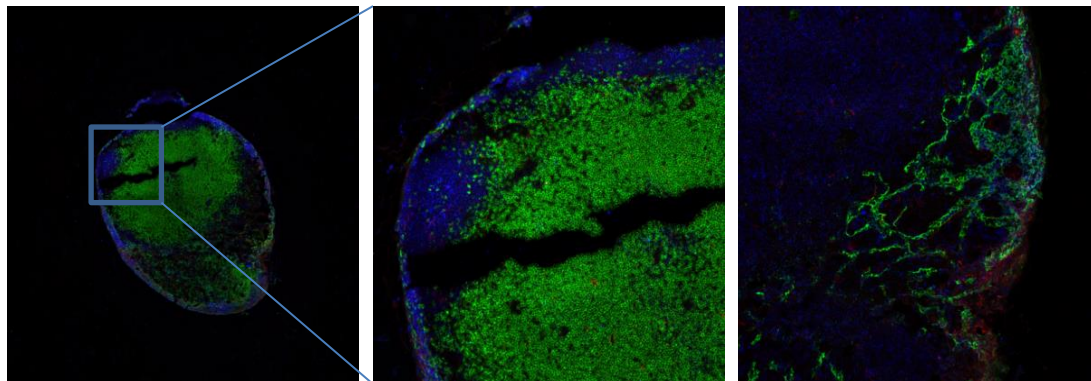
Figure 4.8. Lymph nodes from un-manipulated PDPN$^{fl/fl}$R26ERT2$^{Cre/Cre}$ mice show normal architecture and organization. Brachial lymph nodes from PDPN$^{+/+}$R26ERT2$^{Cre/Cre}$ (A) and PDPN$^{fl/fl}$R26ERT2$^{Cre/Cre}$ (B) mice post tamoxifen administration were dissected. Representative immunofluorescence staining of lymph nodes for CD3ε (green), gp38 (red) and CD19 (blue), and Lyve-1 (green), gp38 (red) and CD4 (blue). Original magnification 25X.

Figure 4.9

Immunised bLN day 8

A

wt untreated

CD3ε / gp38 / CD19   Lyve-1 / gp38 / CD4
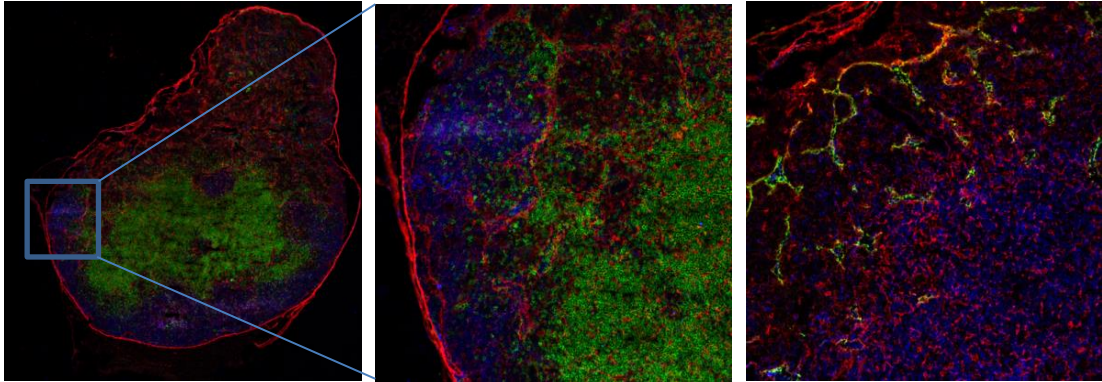
B

PDPN$^{+/+}$R26ERT2$^{Cre/Cre}$
+Tamoxifen

CD3ε / gp38 / CD19   Lyve-1 / gp38 / CD4

C

PDPN$^{fl/fl}$R26ERT2$^{Cre/Cre}$
+Tamoxifen

CD3ε / gp38 / CD19   Lyve-1 / gp38 / CD4

Figure 4.9 (cont.)

Figure 4.9. In the absence of gp38, immunized lymph nodes from PDPN^{fl/fl} R26ERT2^{Cre/Cre} mice show no apparent defect. Brachial lymph nodes from Tamoxifen-treated PDPN$^{+/+}$R26ERT2$^{Cre/Cre}$ (A) and PDPN$^{fl/fl}$R26ERT2$^{Cre/Cre}$ (B) mice were dissected at day 8 post immunization. Representative immunofluorescence staining of lymph nodes for CD3ε (green), gp38 (red) and CD19 (blue), and Lyve-1 (green), gp38 (red) and CD4 (blue). Original magnification 25X.

4.3. Discussion

It has been shown previously that during inflammation and cancer, activated tissue-resident stromal cells acquire features similar to those of lymphoid stromal cells and are able to sustain TLO formation (Peduto et al., 2009). Lymphoid stromal cells induced upon inflammation were characterized by upregulation of adhesion molecules and gp38 expression (Peduto et al., 2009).

Accordingly, our group has demonstrated the ability of gp38+ stromal cells to secrete lymphoid chemokines (CCL19, CCL21 and CXCL13) under inflammatory conditions at sites of TLO formation, in a model of viral induced salivary gland inflammation. While in resting salivary glands of wt mice gp38 expression is detected on epithelial cells and in a small percentage of stromal cells, this expression is significantly increased during inflammation.

In patients with RA, gp38 expression was found to be abundant in inflamed joints, but not detectable in normal synovial tissues (Del Rey et al., 2014). Interestingly, gp38 overexpression appeared to correlate with the presence of ectopic TLO in the synovium (Del Rey et al., 2014). Expansion of the gp38+ compartment has also been described in SS and primary biliary cirrhosis patients as well as in animal models of salivary gland, pancreas, kidney and liver injuries (Link et al., 2011, Buckley et al., 2015, Barone et al., 2015b, Eckert et al., 2016).

Genetic deletion of *Pdpn* is lethal and mice die shortly after birth due to respiratory complications and exhibit severe defects in lymphatic vessel formation (Schacht et al., 2003). In this chapter we aimed to investigate the

consequences of gp38 deletion in the context of TLO formation, using a Tamoxifen mediated conditional *Pdpn* knockout.

Here we demonstrate that we can achieve efficient downregulation of gp38 with tamoxifen administration, both in resting conditions and at the early time points after salivary gland cannulation. However, an apparent inflammation-induced upregulation of gp38 was observed, both at protein and at mRNA levels that was sufficient to re-establish the levels of gp38 observed in the wt mice and in the PDPN$^{fl/fl}$R26ERT2$^{Cre/Cre}$ mice. These results led us to conclude that the conditional knockout PDPN$^{fl/fl}$R26ERT2$^{Cre/Cre}$ strain might not represent the ideal model to dissect the role of gp38 in inflammation. We are aware of the limitation of our ablation technique, however we are confident that our results sustain the conclusion that gp38 is not an essential requirement in the initiation of the processes involved in TLO formation, however the cells that express this molecule may have a role.

As previously described, both by Yang et al. and our group (Saba Nayar, unpublished data), gp38 upregulation takes place as quickly as 3 hours post inflammatory insult, acting as an activation/danger signal for the neighbouring cells (Yang et al., 2014). Furthermore, unpublished data from our group shows that gp38+ stromal cells are significantly more proliferative than their gp38- counterparts. In line with these findings, and considering that tamoxifen administration does not induce a complete *Pdpn* knockout phenotype, increased gp38 expression upon inflammation in these mice can be explained by the expansion of resident cells that acquire the ability to express gp38, and are not deleted by our original treatment. Indeed, even though PDPN$^{fl/fl}$R26ERT2$^{Cre/Cre}$ salivary glands have reduced numbers of gp38+

stromal cells to start with, these cells exhibited a significantly higher proliferative ability, which we believe is acting as a compensatory mechanism in an attempt to repopulate the gp38+ compartment and sustain TLO formation in these mice.

On the other hand, even though an upregulation of gp38 was observed, the levels of gp38 mRNA were still significantly lower in PDPN$^{fl/fl}$R26ERT2$^{Cre/Cre}$ salivary glands as compared to control mice, and at all time points post salivary gland cannulation. Still, this defect did not affect lymphocyte aggregation within the TLO or the expression of lymphoid chemokines by stromal cells. This suggests that either gp38 might not be required for ectopic lymphoid tissue neogenesis or that the lower levels of gp38 maintained in our knockout were sufficient to provide and contribute to the initiation of the cascade of activation signals required in this model.

A significant decrease in both absolute numbers and percentage of VCAM^{hi}ICAM^{hi} cells was found in the CD45-EpCAM-CD31- compartment of PDPN$^{fl/fl}$R26ERT2$^{Cre/Cre}$ at day 8 p.c.. As already discussed above, this reduction was not maintained but the levels of gp38 mRNA significantly increased after day 8 p.c.. Benezech et al. demonstrated that VCAM^{int}ICAM^{int} cells give rise to VCAM^{hi}ICAM^{hi} MAdCAM-1+ stromal organizer cells (Benezech et al., 2010) and our results lead us to hypothesize that, if the strain maintained the knockout phenotype throughout inflammation, gp38 expression could potentially be required for the full maturation of stromal cells and acquisition of some of the LTo features such as expression of high levels of adhesion molecules.

In a murine model of sepsis, FRCs have been described as immunosuppressive since their administration significantly reduced mortality and secretion of pro-inflammatory cytokines (Fletcher et al., 2014). Furthermore, FRCs can suppress T cell proliferation via nitric oxide synthase 2 (NOS2); particularly, nitric oxide expression was associated with a reduction in the proportion of activated T cells in lymph nodes and the DC ability to prime T cells (Lukacs-Kornek et al., 2011, Siegert et al., 2011, Khan et al., 2011).

Chai et al. have reported that in the absence of gp38+ FRCs, following conditional ablation of LTβR, lymph nodes were not able to generate an appropriate immune response against a virus insult (Chai et al., 2013). Our preliminary work on lymph nodes from PDPN$^{fl/fl}$R26ERT2$^{Cre/Cre}$ following immunization with NP-CGG showed a general apparent normal structure and expansion of brachial lymph nodes. However, no functional analysis was performed during this preliminary experiment. Interestingly, at day 8 post immunization the gp38+ stromal cell network, usually easily identified in wt mice, was not present in PDPN$^{fl/fl}$R26ERT2$^{Cre/Cre}$ mice. The functional consequences of gp38 loss in lymph nodes and within the TLO have to be addressed.

Collectively, the results described in this chapter show that temporary deletion of gp38 does not affect the formation of ectopic lymphoid structure but significantly affects the number of VCAM^{hi}ICAM^{hi} cells. The mechanism by which this reflects a stronger ANA reactivity in the mice is not clear. Possibly our deletion protocol has not been appropriate and an improved one could be implemented, possibly by extending the original depletion with a tamoxifen

based diet. A persistent downregulation of gp38 would allow us to better dissect the role of this molecule not only in TLO establishment but also in maintenance of such structures. Similarly the role of gp38 in lymph node remodelling after insult could be addressed by maintaining gp38 suppression. These experiments are currently been undertaken in our laboratory.

In order to further dissect the role of LLSc we have taken advantage of co-expression of FAP by gp38+ stromal cells and utilised a murine model of conditional depletion of FAP-expressing cells (Kraman et al., 2010). Results illustrating the consequences of depleting LLSc, rather than downregulating gp38 expression, in our model of salivary gland inflammation are described in Chapter 5.

Chapter 5

DEPLETION OF FAP+GP38+ STROMAL CELLS IMPAIRS TLO FORMATION

5.1. Introduction

Postnatal TLO formation is seen in association with chronic inflammation, cancer and chronic antigen stimulation. The development of these structures is associated with the activation of tissue resident stromal fibroblasts, their up-regulation of the expression of gp38 and the acquisition by these stromal cells, of an FRC-like phenotype. Critically, the development of this lymphoid tissue like stroma derived from inflammatory stromal cells is a key determinant of TLO formation within chronically inflamed tissue (Buckley et al., 2015). Despite their importance, studies into the functional role of lymphoid-like stromal cells in the development of TLOs has been compounded by an inability to examine the functional consequence of experimental deletion of these cells.

The conditional deletion of *Pdpn* could not be used to address this question, since in the salivary gland we observed a significant up-regulation of gp38 post inflammatory insult. However, the co-expression of FAP by FRCs allowed us to use an alternative approach utilising a Tg mouse in which FAP expressing cells can be experimentally ablated (Denton et al., 2014, Kraman et al., 2010).

FAP was first described as a cell-surface antigen identified on human astrocytoma and sarcoma cell lines *in vitro* (Garin-Chesa et al., 1990a). *Fap* gene expression is significantly upregulated in activated fibroblasts under pathological conditions, including cancer, wound healing and chronic inflammation (Dolznig et al., 2005, Bauer et al., 2006, Garin-Chesa et al., 1990b, Levy et al., 1999). FAP is highly expressed in fibroblast-like synovial cells, resident in the synovial lining layer of inflamed joints of patients with RA (Bauer et al., 2006). Furthermore, it has been suggested that in the context of chronic synovial inflammation, FAP might be involved in both cartilage and bone damage (McIndoe et al., 1999, Waldele et al., 2015).

Fearon et al., have addressed the role of FAP+ fibroblasts in cancer biology using a FAP-DTR mouse strain that carries the DTR under the FAP promoter that allows for the selective deletion of FAP-expressing cells on administration of DTx. The researchers demonstrated that selective experimental deletion of FAP+ cells caused growth arrest of immunogenic tumours through hypoxic necrosis of both cancer and stromal cells (Kraman et al., 2010). These results implied an immunosuppressive role for FAP+ cells in neoplastic disease raising the intriguing possibility that these cells might play a relevant biological role in the context of autoimmunity, inflammation and TLO formation.

Denton et al. has recently reported that about 90% of CD45-FAP+ cells in the lymph node are CD31-gp38+, meaning that almost the totality of the CD45-FAP+ component in the lymph node is composed of FRCs (Denton et al., 2014). The group used the same FAP-DTR mouse model described above to deplete FRCs in the lymph node, leading to disrupted homeostatic numbers of DCs, T and B cells (Denton et al., 2014). Influenza A infection post depletion

of FAP+ cells resulted in diminished numbers of T_{FH} and plasma B cells (Denton et al., 2014).

Given the significant degree of overlap between gp38 and FAP expression in the lymph node we hypothesized that FRC-like cells forming in the salivary glands post cannulation with adenovirus would also upregulate FAP. If this were the case, the FAP-DTR mouse strain would allow us to experimentally deplete FRC-like gp38+ stromal cells during TLO formation, based on their co-expression of FAP, and dissect the role of this cell component in lymphoneogenesis and autoimmunity in our model of salivary gland inflammation.

In the studies described in this chapter we aimed to characterise the expression of FAP in wt salivary glands during inflammation and examine the functional consequences of experimental deletion of these cells in a murine model of inflammatory TLO formation.

5.2. Results

5.2.1. FAP is expressed in murine salivary glands during inflammation

In order to investigate the expression of FAP in murine salivary glands, immunofluorescence, flow cytometry and qRT-PCR were used in both resting and inflamed salivary glands (following cannulation and administration of virus).

Immunofluorescent staining showed that resting salivary glands do not express FAP (**Figure 5.1A**) but, upon inflammatory insult, at day 15 p.c., positive staining for FAP could be detected in cells surrounding the lymphoid infiltrates, areas known to be rich in gp38+ stromal cells (**Figure 5.1A**). Flow cytometry staining confirmed FAP expression by more than 50% of gp38+ stromal cells (CD45-EpCAM-CD31-) at day 8 p.c. (**Figure 5.1B**). Accordingly, upregulation of FAP expression in murine salivary glands post virus delivery was demonstrated by qRT-PCR in whole-tissue frozen sections (**Figure 5.1C**) and gene expression analysis in FACS sorted cells revealed increased FAP expression in gp38+LLSc upon salivary gland cannulation at days 5 and 8 p.c., which progressively decreases with resolution of inflammation (**Figure 5.1D**).

Figure 5.1

A

B FAP+ LLSc

C

FAP mRNA
(Total salivary gland)

D

FAP mRNA
(sorted cells)
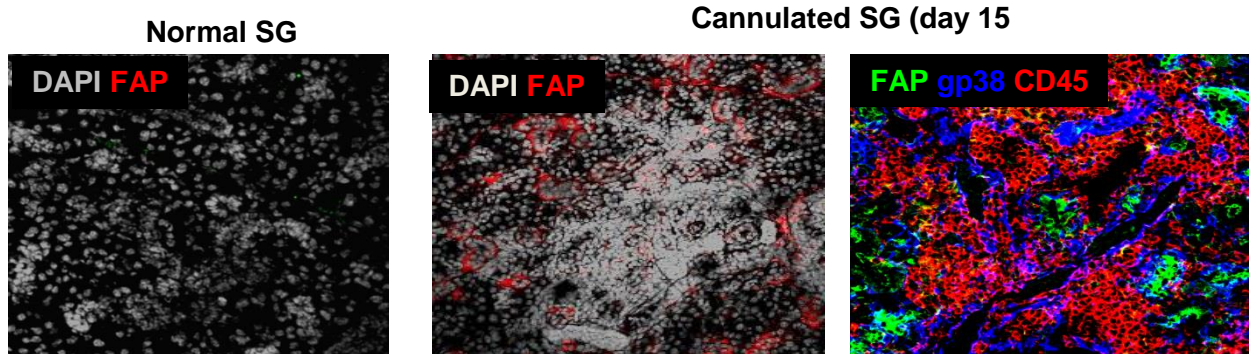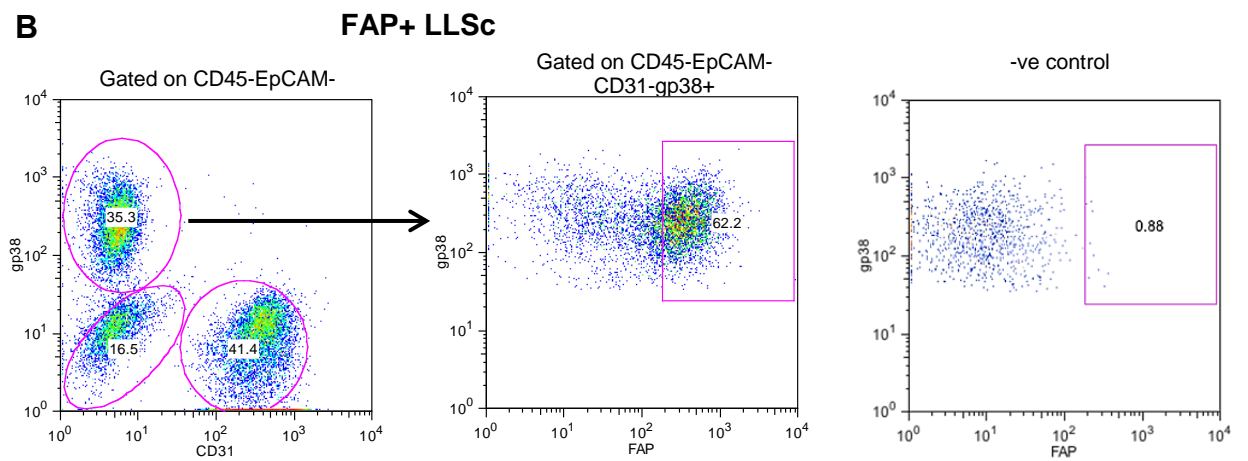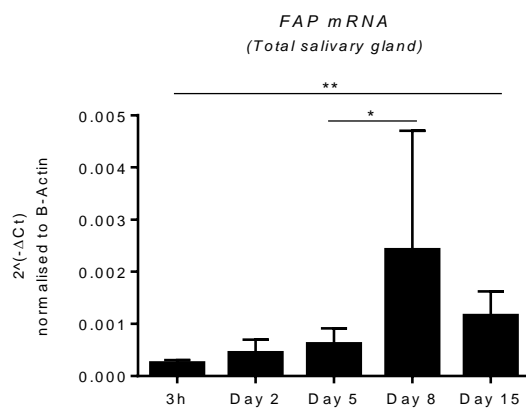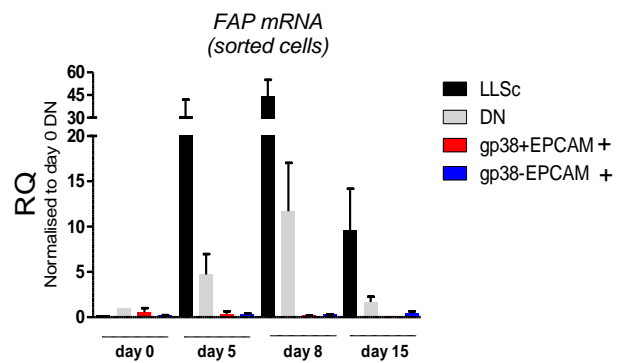
Figure 5.1 (cont.)

Figure 5.1. Expression of FAP in murine salivary glands post viral delivery. (A) Representative microphotographs of resting and inflamed salivary glands at 8 days p.c: examined by immunofluorescence for DAPI nuclear staining (grey), FAP (red or green), gp38 (blue) and CD45 (red). Original magnification 10X. (B) Representative FACS plot for FAP+ staining in CD45-EpCAM-CD31-gp38+ cells and respective isotype control. (C) qRT-PCR results for *Fap* mRNA in whole tissue sections from cannulated wt salivary glands from 3h to day 15 p.c.. Transcript levels were normalized to housekeeping gene *β-actin.* Data represented as mean (SD) with four to nine glands analysed per group. * p < 0.05; ** p < 0.01, unpaired *t* test. (D) *Fap* expression in FACS sorted CD45-EpCAM-CD31-gp38+ (LLSc) (black bars), CD45-EpCAM-CD31-gp38- (DN) (grey bars), gp38+EpCAM+ (red bars) and gp38-EpCAM+ (blue bars). mRNA transcripts were assessed by qRT-PCR and normalised to housekeeping gene *β-actin*. RQ values calculated with calibrator day 0 DN cells. Data showed as mean (SD) of two independent experiments with at least two salivary glands per group.

5.2.2. Deletion of FAP expressing cells using the FAP-DTR Tg mouse strain is an efficient model of gp38+ stromal cell depletion

The co-expression of FAP by gp38+ LLSc allowed us to consider a targeted and selective approach to depletion of gp38+ stromal cells using the FAP-DTR Tg mouse. To induce ablation of FAP-expressing cells, as described previously (Chapter 2.1.2.), FAP-DTR mice were treated with 4 doses of DTx or vehicle control, twice/day, at day 0 and day 2 (**Figure 5.2A**). Mice were cannulated and virus administrated 8 days after the first DTx/vehicle administration and sacrificed at days 8, 15 and 23 p.c. Findings from those time points will be described throughout the next section of this chapter.

Body weight of every animal was recorded for all experimental groups and FAP-DTR+ mice treated with DTx consistently exhibited a weight loss of approximately 10% as compared to wt mice injected with DTX and control mice injected with sterile water in the first week following DTx administration (**Figure 5.2B**). Weight loss occurred as a result of the loss of muscle mass and developed cachexia (Roberts et al., 2013).

In order to assess the efficiency of FAP+ cell deletion in the salivary glands of FAP-DTR+ mice administrated DTx, we investigated by flow cytometry the proportion of gp38+ stromal cells (as a surrogate marker of cell deletion) (**Figure 5.3A**). Un-manipulated mice (no salivary gland cannulation) and FAP-DTR+ mice treated with vehicle, or FAP-DTR- mice treated with DTx were used as experimental controls. All mice, apart from those in the un-manipulated group, were cannulated and sacrificed at day 8 p.c. (peak of FAP mRNA expression) (**Figure 5.1C, D**). Indeed, upon treatment with DTx, FAP-

DTR+ mice but not controls, exhibited a significant reduced percentage and absolute numbers of gp38+ stromal cells (**Figure 5.3A, B**). In the remaining gp38+ stromal cells that were still present post DTx, the percentage of FAP+LLSc was also reduced (**Figure 5.3Aiii**).

Figure 5.2

A
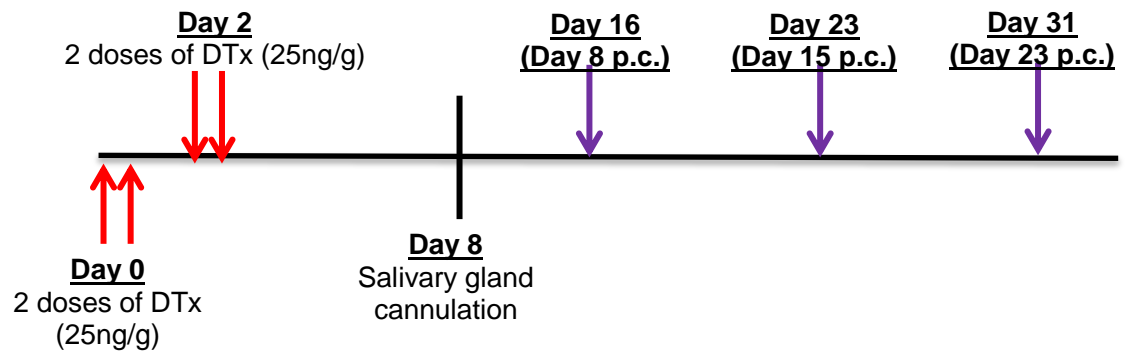
B
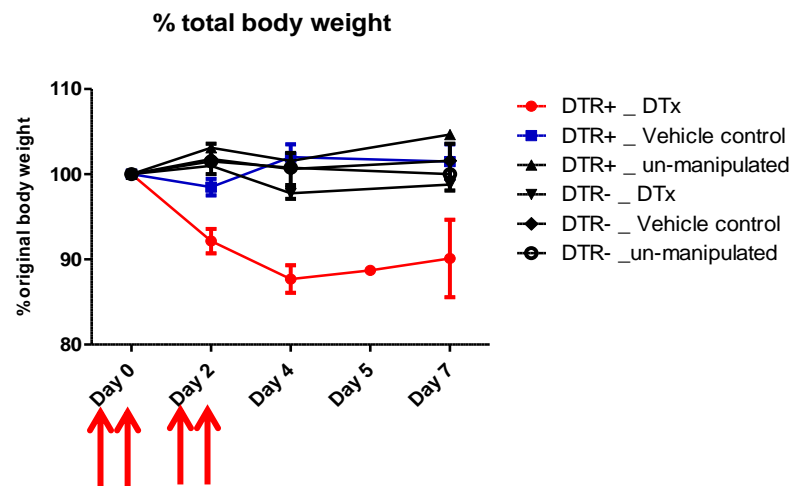
Figure 5.2. DTx treatment regime to FAP-DTR mice. (A) DTx or vehicle control administration to FAP-DTR mice (DTR+ or DTR-). (B) Percentage of total body weight of resting DTR+ and DTR-, DTR+ treated with DTx and vehicle, and DTR- treated with DTx and vehicle control. Red arrows indicate DTx/vehicle i.p. injections

Figure 5.3

A
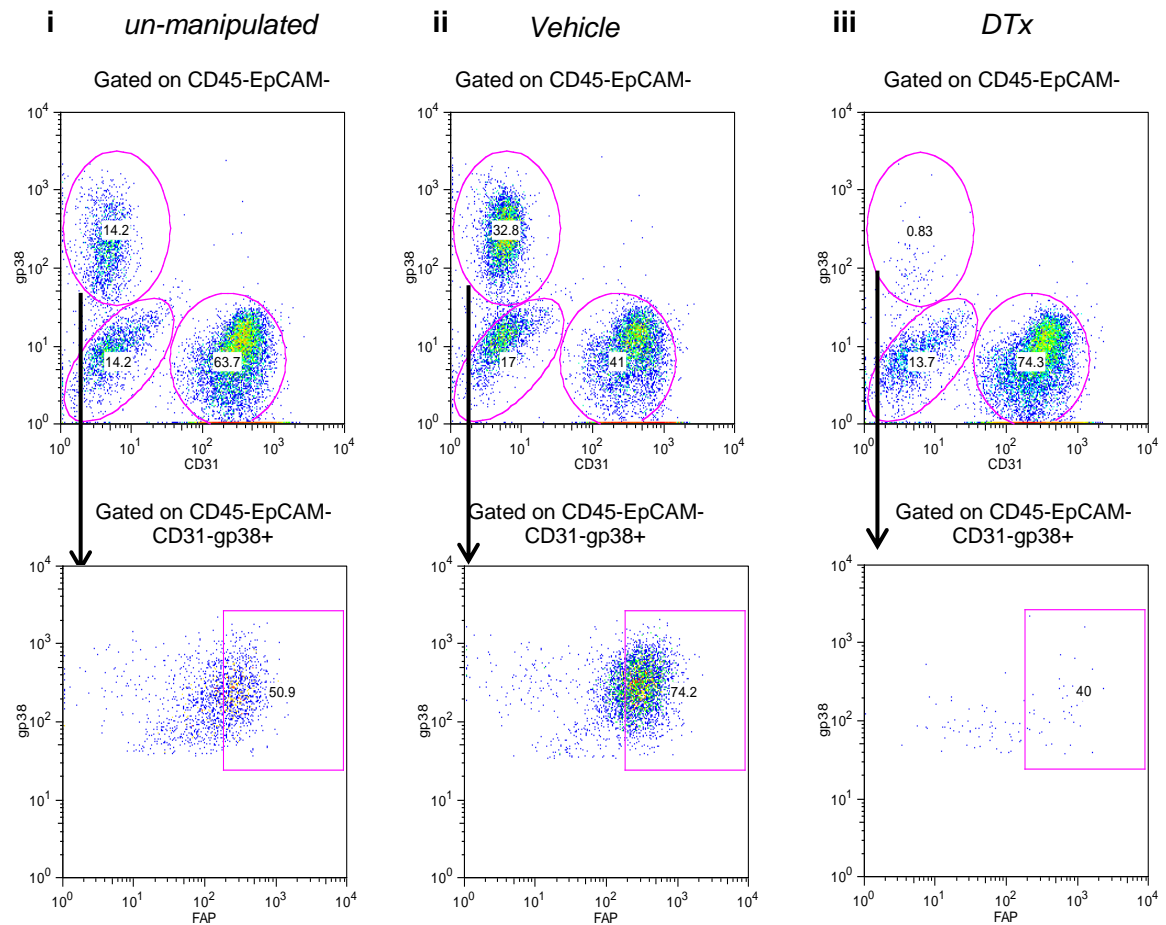
B
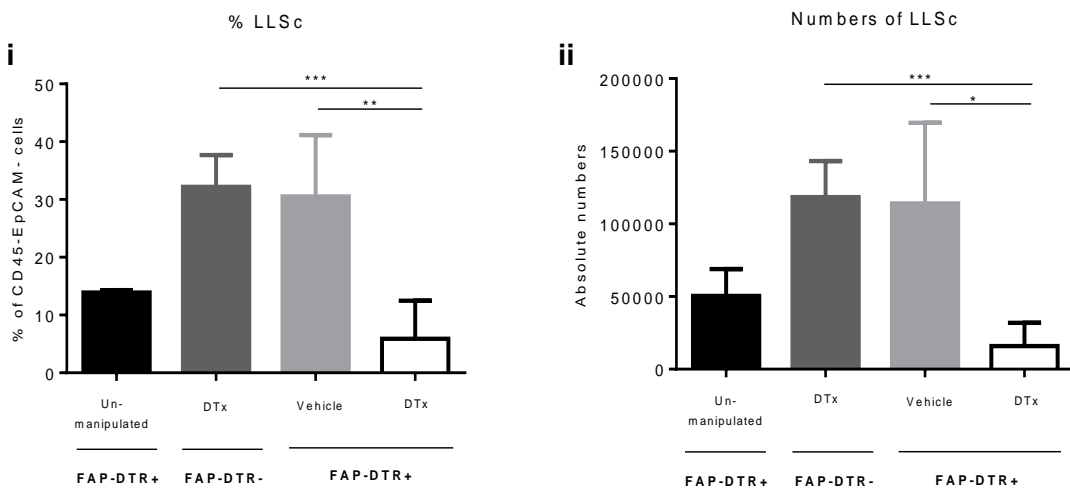
Figure 5.3. LLSc depletion in FAP-DTR salivary glands is achieved post DTx administration. (A) Representative dot plots showing flow cytometry staining for FAP expression in CD45-EpCAM-CD31-gp38+ cells (LLSc) in FAP-DTR un-manipulated (i), vehicle (ii) and DTx treated (iii) salivary glands at day 8 p.c.. (B) Percentage (i) and absolute numbers (ii) of LLsc in day 8 p.c. salivary glands of FAP-DTR+ un-manipulated (black), FAP-DTR- treated with DTx (dark grey), vehicle (light grey) and DTx treated (white). Results were determined by flow cytometry and presented as mean (SD) of two independent experiments with at least four salivary glands per group. * $p < 0.05$; ** $p < 0.01$; *** $p < 0.001$, unpaired t test.

5.2.3. Depletion of LLSc impairs full TLO development

After confirming that the FAP-DTR mouse strain can be used to efficiently delete gp38+ LLSc we aimed to investigate the impact of such depletion on TLO formation in inflamed salivary glands. A week after administration of the first DTx dose, mice were cannulated and sacrificed at days 8, 15 and 23 p.c. and their salivary glands were analysed by IF, flow cytometry and real time PCR. Due to unexpected results in FAP-DTR+ mice treated with vehicle (discussed in section 5.3.) each section of the following described results compares findings between FAP-DTR+ treated with either vehicle or DTx.

5.2.3.1.   Analysis of day 8 samples

At day 8 p.c., flow cytometric analysis revealed a significant loss of the gp38+ stromal cells in FAP-DTR+ mice treated with DTx, both in percentage and absolute numbers of cells. The LLSc compartment was reduced by ~2/3 compared to untreated and DTR- mice (**Figure 5.4Ai, ii**). Following DTx treatment, the numbers of LLSc FAP expressing cells were also significantly reduced, whilst in percentage no significant changes were detected (**Figure 5.4Bii**). The proliferative status of the remaining gp38+ stromal cells following deletion was assessed by Ki67 intracellular staining and showed increased percentage of Ki67+ LLSc but, unsurprisingly, reduced absolute numbers of Ki67+LLSc, confirming the proliferative status of LLSc prior to deletion of FAP+ cells (**Figure 5.4Ci, ii**).

Infiltrating leukocytes were also analysed by flow cytometry staining that show a reduction in the percentage of CD45+, CD3ε+, CD19+ and CD4+CD3ε+

cells (**Figure 5.5Ai, Bi, Ci, Cii, Di**). Absolute numbers of the populations above were also reduced but no significant differences were found (**Figure 5.5Aii, Bii, Dii**). Regarding infiltrating CD8+ T cells, the absolute numbers in DTx-treated FAP-DTR+ mice were significantly reduced and the percentage was also decreased, but this difference was found not statistically significant (**Figure 5.5Ei, ii**).

mRNA levels of *Fap, Pdpn, Ccl19* and *Cxcl13* were analysed in whole-tissue cryosections but only CCL19 expression was found to be significantly reduced in mice lacking FAP+ cells (**Figure 5.6A-D**).

Histologically, DTx treated FAP-DTR+ mice developed less and smaller lymphoid aggregates (**Figure 5.7A-C**) and a significantly smaller area of salivary gland tissue was occupied by infiltrating lymphocytes when compared to DTR- controls (**Figure 5.7B**). At this particular time point, salivary glands from FAP+ cell depleted mice were characterised by an obvious absence of infiltrating B cells (**Figure 5.7A**).

When the results from DTx treated FAP-DTR+ mice are compared only to DTR+ mice treated with vehicle, at day 8 p.c. only the percentage (**Figure 5.4Ai**) and numbers of LLSc (**Figure 5.4Aii**), number of FAP+LLSc (**Figure 5.7Bii**) and percentage of Ki67+ LLSc (**Figure 5.4C**) are significantly decreased in DTx treated mice.

Figure 5.4
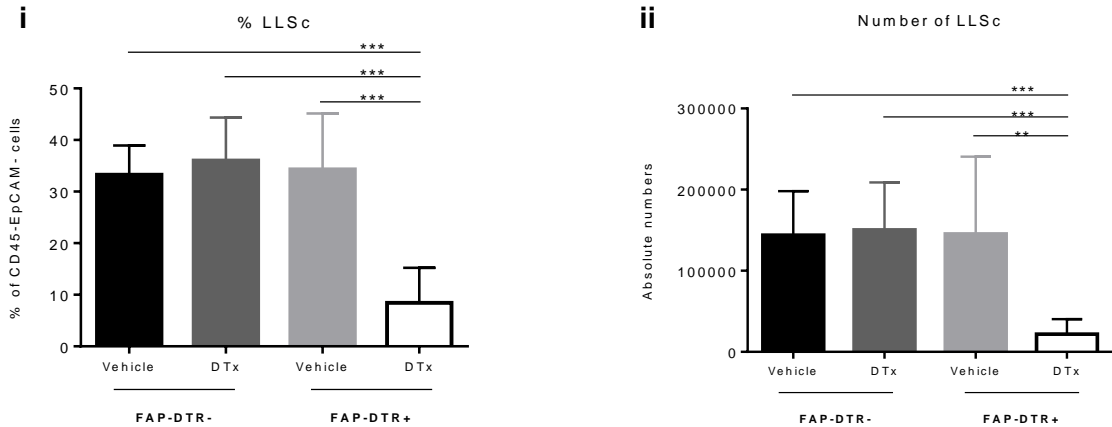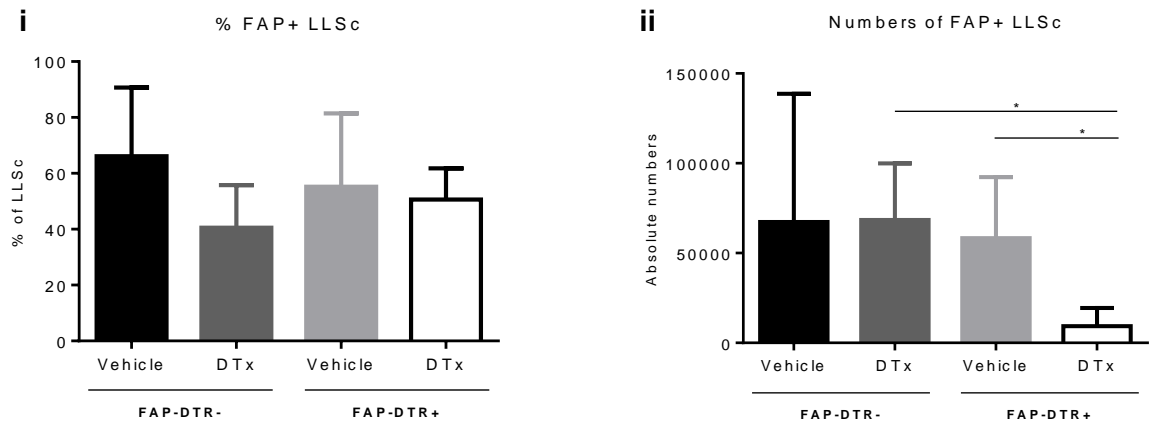
Day 8 p.c.
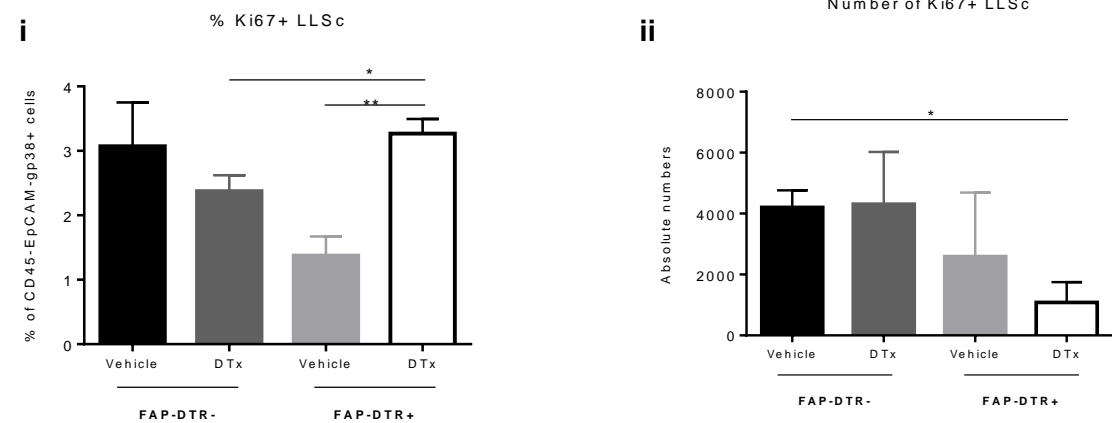
Figure 5.4. Flow cytometry analysis of the stroma compartment in FAP-DTR mice at day 8 p.c.. FAP-DTR- mice treated with vehicle (black) and DTx (dark grey) and FAP-DTR+ mice treated with vehicle (light grey) and DTx (white) were cannulated post DTx or vehicle administration and sacrificed at day 8 p.c.. Percentage (i) and absolute numbers (ii) of LLSc (A), FAP+LLSc (B) and Ki67+LLSc (C) were determined by flow cytometry staining and presented as mean (SD) of two independent experiments with at least four salivary glands per group. * p < 0.05; ** p < 0.01; *** p < 0.001, unpaired *t* test.

Figure 5.5

Day 8 p.c.

A

i

% CD45+ cells

ii

Number of CD45+ cells

B

i

% CD3e+ cells

ii

Number of CD3e+ cells

C

i

% CD19+ cells

ii

Number of CD19+ cells

Figure 5.5 (cont.)

Day 8 p.c.

D

i

% CD4+ T cells

ii

Number of CD4+ T cells

E

i

% CD8+ T cells

ii

Number of CD8+ T cells
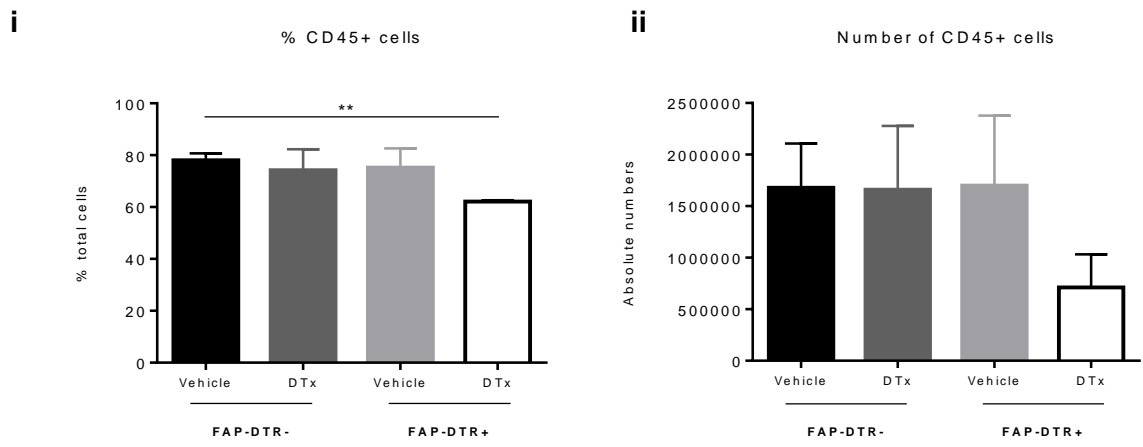
Figure 5.5. Flow cytometry analysis of the leukocyte compartment of inflamed salivary glands in FAP-DTR mice at day 8 p.c.. FAP-DTR- mice treated with vehicle (black) and DTx (dark grey) and FAP-DTR+ mice treated with vehicle (light grey) and DTx (white) were cannulated post DTx or vehicle administration and sacrificed at day 8 p.c.. Percentage (i) and absolute numbers (ii) of CD45+ cells (A), CD3ε+ T cells (B), CD19+ B cells (C), CD4+CD3ε+ T cells (D) and CD8+CD3ε+ T cells (E) were determined by flow cytometry staining and presented as mean (SD) of two independent experiments with at least four salivary glands per group. * $p < 0.05$; ** $p < 0.01$, unpaired *t* test.

Figure 5.6

A

B

C

D

Figure 5.6. DTx treatment affects expression levels of lymphoid chemokines. qRT-PCR analysis of *Fap* (A), *Pdpn* (B), ccl19 (C) and cxcl13 (D) mRNA transcripts from FAP-DTR- mice treated with vehicle (black) and DTx (dark grey) and FAP-DTR+ mice treated with vehicle (light grey) and DTx (white) at day 8 p.c.. qRT-PCR results for *Fap* and *Pdpn* were normalised to housekeeping gene *β-actin* and *ccl19* and *cxcl13* results normalised to *Pdgfrb*. * $p < 0.05$; ** $p < 0.01$, unpaired *t* test, data represented as mean ± s.e.m. with two to nine glands analysed per group.

Figure 5.7

A

Day 8 p.c. CD3/CD19

| **FAP-DTR+**
treated with DTx | **FAP-DTR+**
treated with vehicle | **FAP-DTR-**
treated with DTx | **FAP-DTR-**
treated with vehicle |

B

Volume fraction of lymphoid follicles
day 8 p.c.

C

Average follicle area
day 8 p.c.

Figure 5.7. TLO formation is impaired in DTx treated FAP-DTR+ mice at day 8 p.c.. FAP-DTR- mice treated with vehicle (black) and DTx (dark grey) and FAP-DTR+ mice treated with vehicle (light grey) and DTx (white) were cannulated post DTx or vehicle administration and sacrificed at day 8 p.c.. (A) Representative microphotographs of salivary glands examined by immunofluorescence for CD3ε (green) and CD19 (blue) showing lymphocytic infiltration. Original magnification 25X. Volume fraction of lymphoid follicles (B) and average follicle area (C) were determined in all experimental groups and data represented as mean (SD) of two independent experiments with at least four salivary glands per group. * $p < 0.05$, unpaired *t* test.

5.2.3.2. Analysis of day 15 samples

At day 15 p.c., DTx treated FAP-DTR+ mice showed a significant reduction in percentage and absolute numbers of LLSc (**Figure 5.8Ai, ii**) and also in absolute number of FAP+gp38+ stromal cells (**Figure 5.8Bii**). Similarly to what was observed at day 8 p.c., no differences were registered in the percentage of FAP+LLSc between any of the groups (**Figure 5.8Bi**).

At this time point, when the lymphocyte infiltrates are fully organized into TLOs in wt mice, in FAP-DTR+ mice lacking FAP+ stromal cells a significant decrease in the percentage of infiltrating CD45+ cells, percentage and absolute numbers of CD19+ cells was observed (**Figure 5.9Ai, Ci, Cii**). Total number of CD45+, CD3ε+, CD4+CD3ε+ and CD8+CD3ε+ cells was also affected in the absence of FAP+ cells, but did not reach significance (**Figure 5.9Aii, Bii, Dii, Eii**).

Once again, levels of *Fap* and *Pdpn* were not diminished in DTx treated FAP-DTR+ mice (**Figure 5.10A, B**). However, mRNA transcripts for lymphoid chemokines *Ccl19* and *Cxcl13* were found to be greatly reduced in our group of interest when compared to vehicle treated FAP-DTR- mice (**Figure 5.10C, D**). Accordingly, also *Ccr7* and *Cxcr5* levels were affected in FAP-DTR+ mice treated with DTx (**Figure 5.10E, F**).

Immunofluorescence staining revealed presence of smaller lymphocytic aggregates with a particular defect in the B cell component (**Figure 5.11A**). This was reflected in the decreased salivary gland area occupied by lymphoid aggregates in the DRT+ DTX treated mice as compared to their littermate controls FAP-DTR- (DTx and vehicle treated) (**Figure 5.11 B and C**).

When the results from DTx treated FAP-DTR+ mice are compared only to DTR+ mice treated with vehicle, at day 15 p.c. only the expression levels of *cxcl13* (**Figure 5.10D**) and *cxcr5* (**Figure 5.10F**) mRNA are significantly decreased in DTx treated mice.

Figure 5.8

Day 15 p.c.

A

i

% LLSc

ii

Number of LLSc

B

i

% FAP+ LLSc

ii

Numbers of FAP+ LLSc

Figure 5.8. Flow cytometry analysis of the stroma compartment in FAP-DTR mice at day 15 p.c.. FAP-DTR- mice treated with vehicle (black) and DTx (dark grey) and FAP-DTR+ mice treated with vehicle (light grey) and DTx (white) were cannulated post DTx or vehicle administration and sacrificed at day 15 p.c.. Percentage (i) and absolute numbers (ii) of LLsc (A) and FAP+LLSc (B) were determined by flow cytometry staining and presented as mean (SD) of two independent experiments with at least four salivary glands per group. * $p < 0.05$; ** $p < 0.01$, unpaired *t* test.
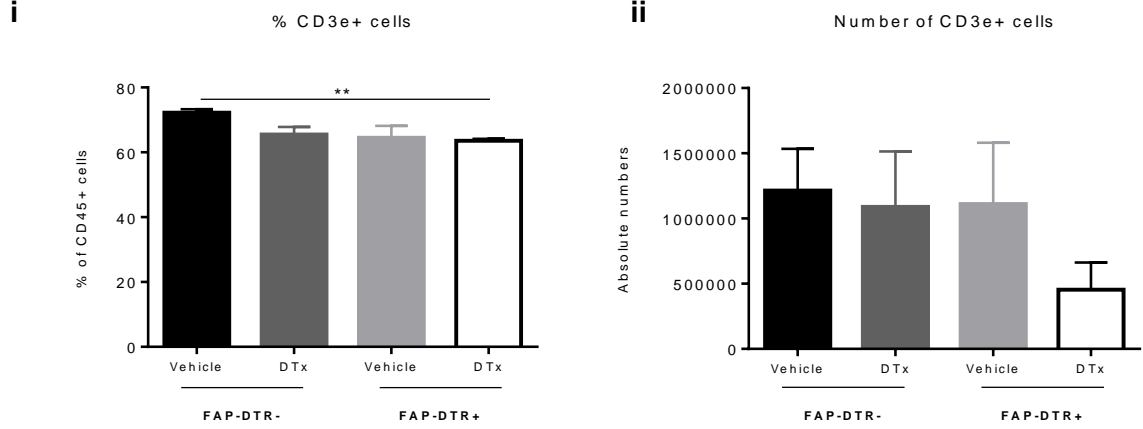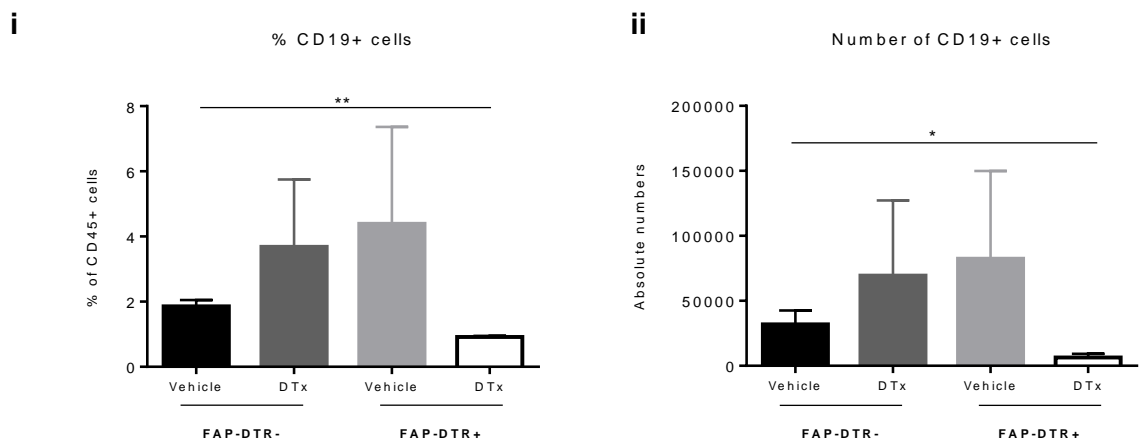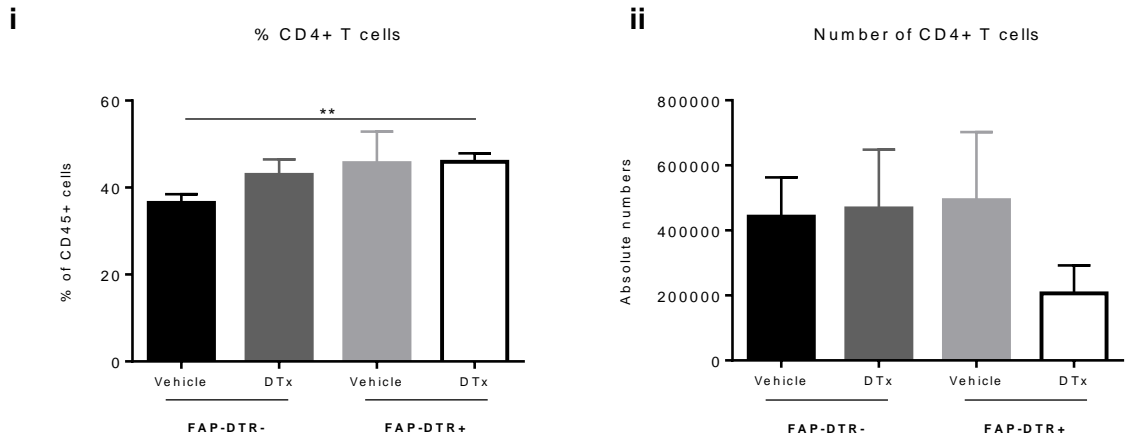
Figure 5.9

Day 15 p.c.

149

Figure 5.9 (cont.)

Day 15 p.c.

D

i

% CD4+ T cells

ii

Number of CD4+ T cells

E

i

% CD8+ T cells

ii

Number of CD8+ T cells
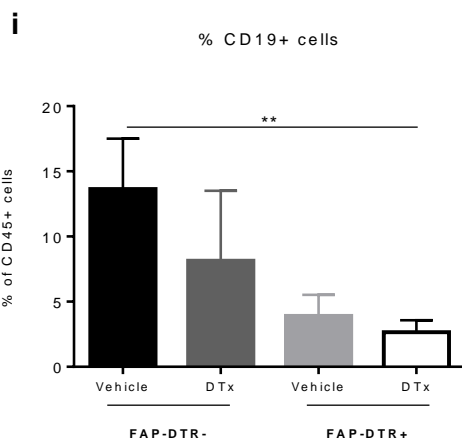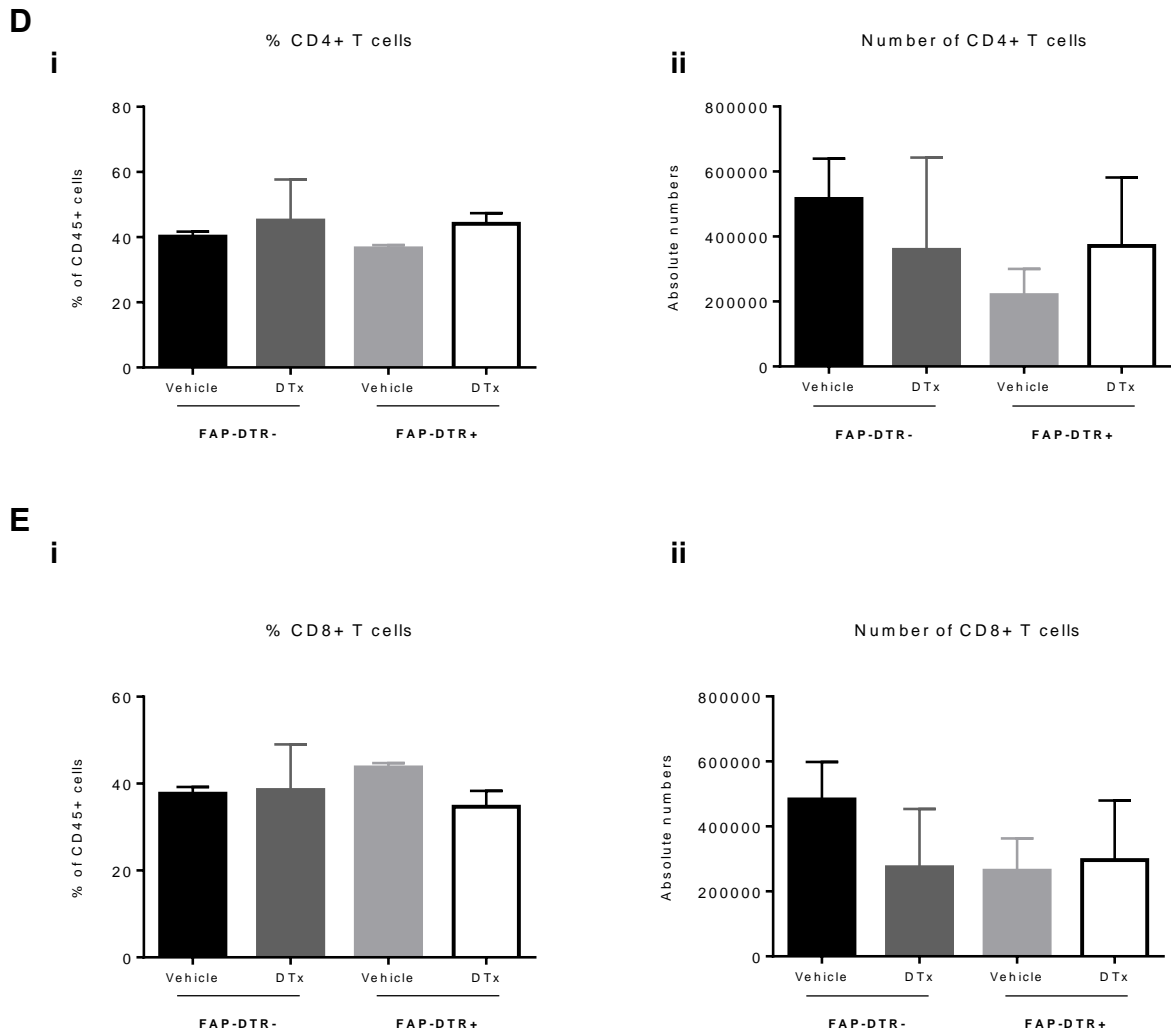
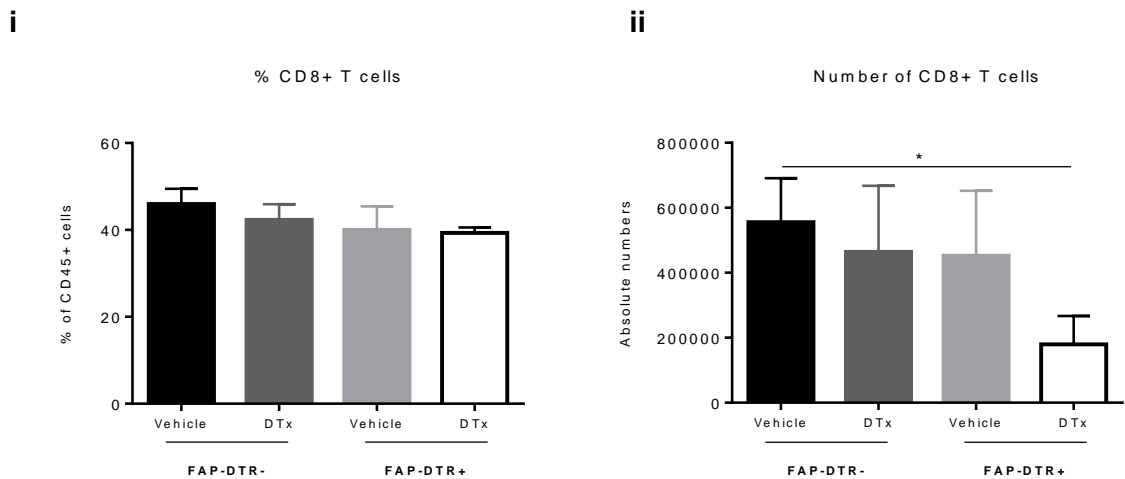**Figure 5.9. Flow cytometry analysis of the leukocyte compartment in FAP-DTR mice at day 15 p.c..** FAP-DTR- mice treated with vehicle (black) and DTx (dark grey) and FAP-DTR+ mice treated with vehicle (light grey) and DTx (white) were cannulated post DTx or vehicle administration and sacrificed at day 15 p.c.. Percentage (i) and absolute numbers (ii) of CD45+ cells (A), CD3ε+ T cells (B), CD19+ B cells (C), CD4+CD3ε+ T cells (D) and CD8+CD3ε+ T cells (E) were determined by flow cytometry staining and presented as mean (SD) of two independent experiments with at least four salivary glands per group. ** p < 0.01, unpaired *t* test.
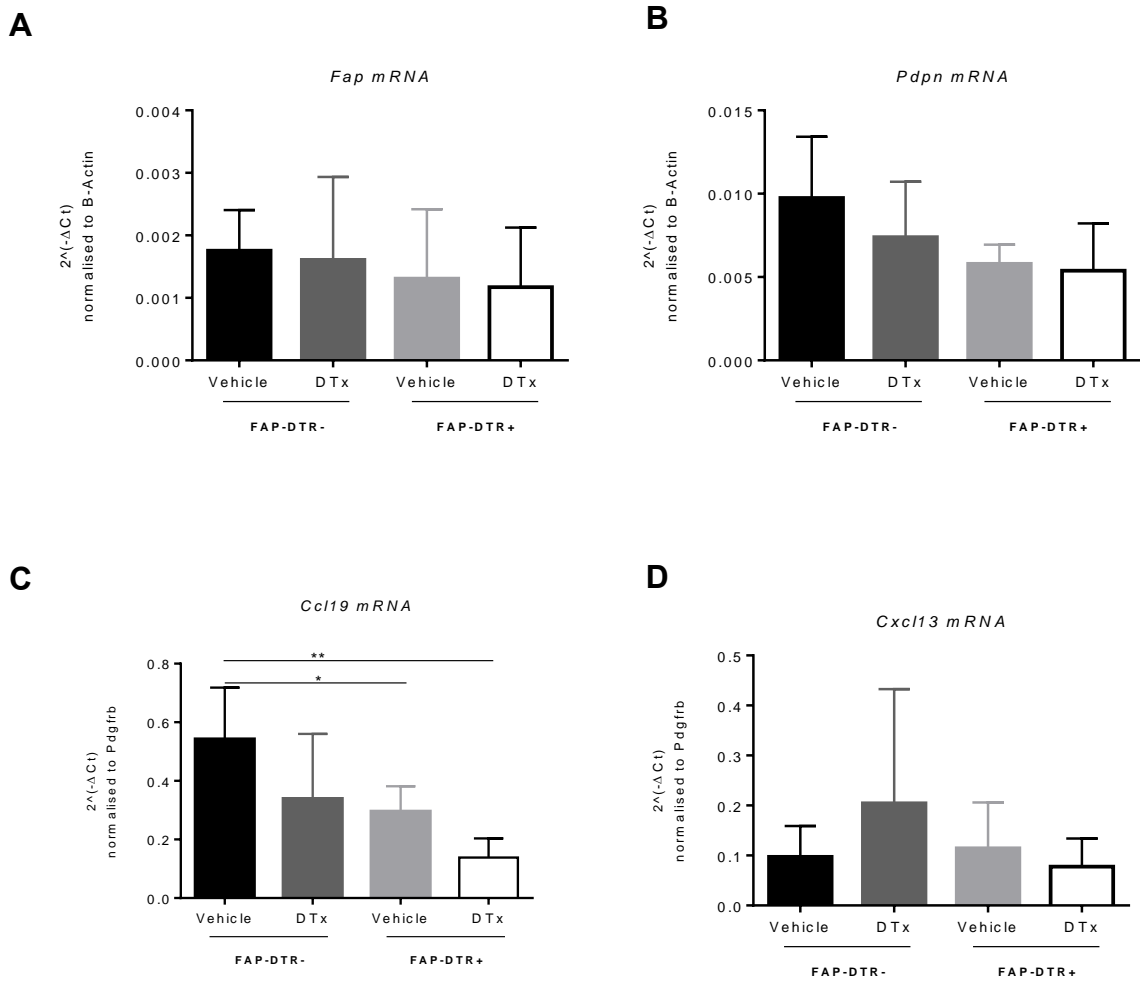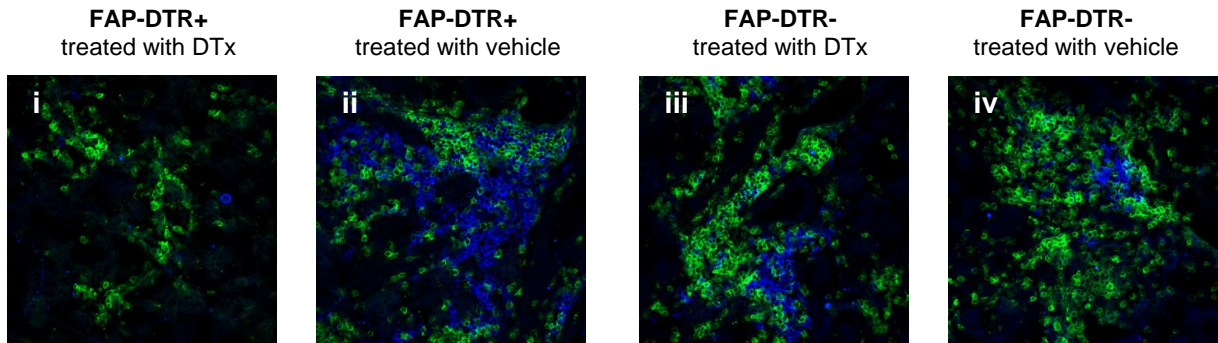
Figure 5.10

Day 15 p.c.

A

Fap mRNA

B

Pdpn mRNA

C

Ccl19 mRNA

D

Cxcl13 mRNA

E

Ccr7 mRNA

F

Cxcr5 mRNA
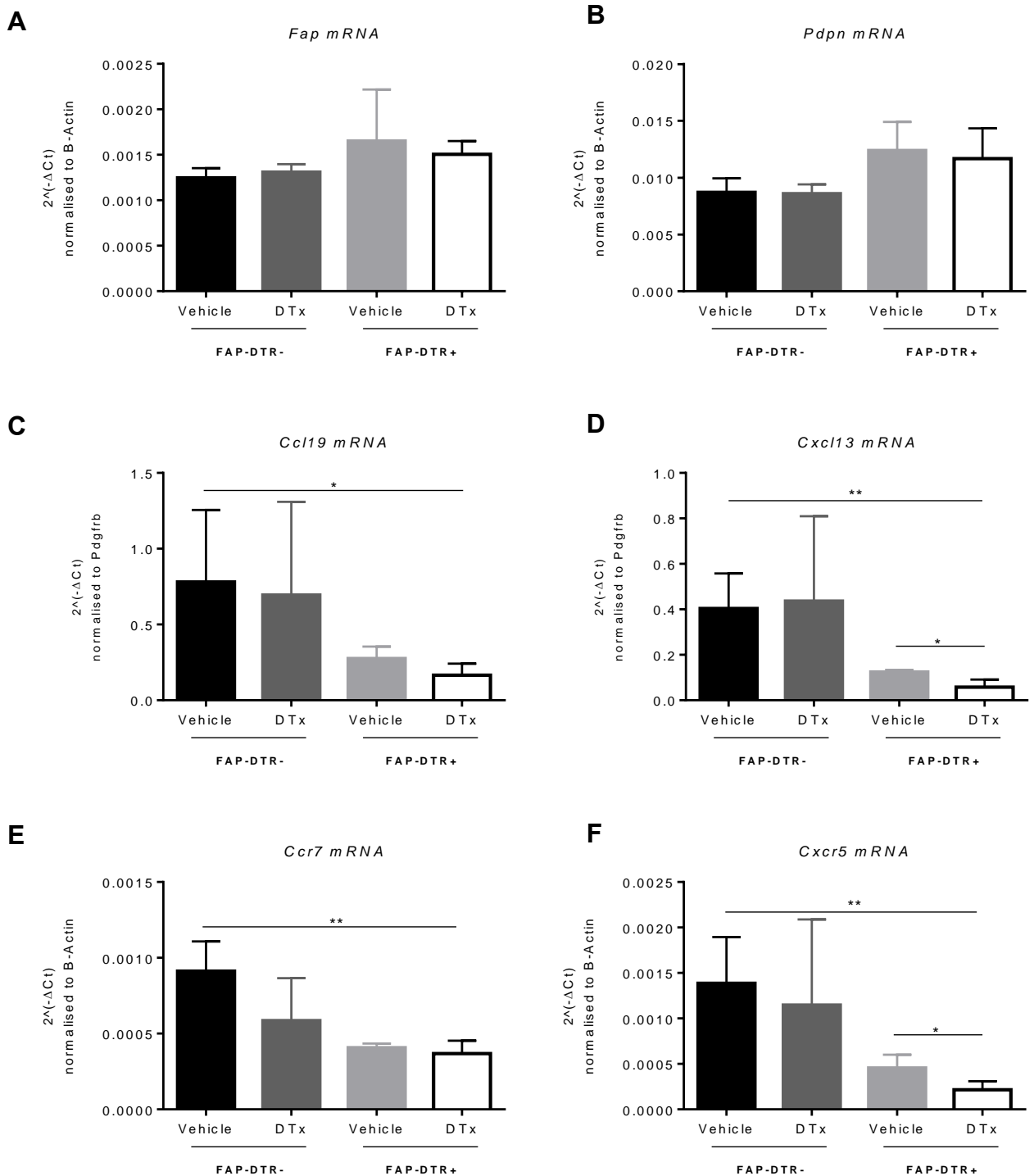
Figure 5.10. DTx treatment in FAP-DTR mice affects expression levels of lymphoid chemokines and recruitment of lymphocytes. qRT-PCR analysis of *Fap* (A), *Pdpn* (B), ccl19 (C), cxcl13 (D), *ccr7* (E) and *cxcr5* (F) mRNA transcripts from FAP-DTR- mice treated with vehicle (black) and DTx (dark grey) and FAP-DTR+ mice treated with vehicle (light grey) and DTx (white) at day 15 p.c.. qRT-PCR results for *Fap, Pdpn, ccr7* and *cxcr5* were normalised to housekeeping gene *β-actin* and *ccl19* and *cxcl13* results normalised to *Pdgfrb*. * p < 0.05; ** p < 0.01, unpaired *t* test, data represented as mean (SD) with two to nine glands analysed per group.
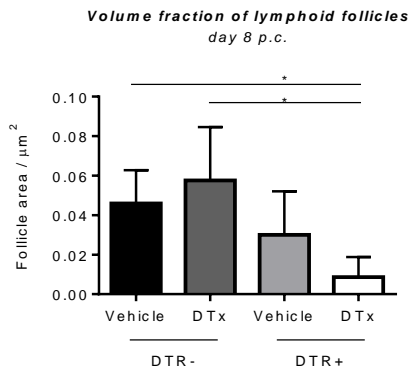
151

Figure 5.11

A

Day 15 p.c. CD3/CD19

FAP-DTR+ treated with DTx	**FAP-DTR+** treated with vehicle	**FAP-DTR-** treated with DTx	**FAP-DTR-** treated with vehicle

B

Volume fraction of lymphoid follicles
day 15 p.c.

C
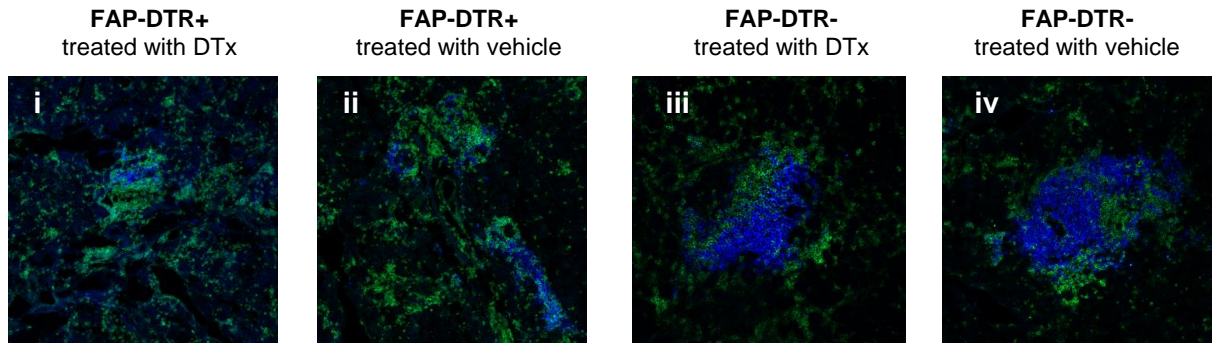
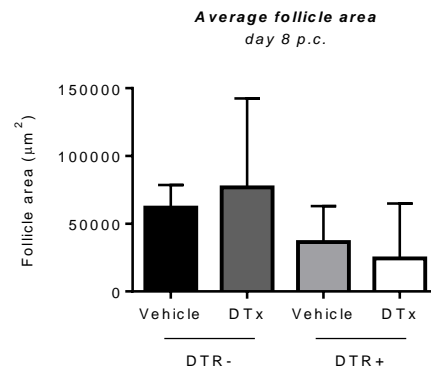
Average follicle area
day 15 p.c.

Figure 5.11. TLO formation is impaired in DTx treated FAP-DTR+ mice at day 15 p.c.. FAP-DTR- mice treated with vehicle (black) and DTx (dark grey) and FAP-DTR+ mice treated with vehicle (light grey) and DTx (white) were cannulated post DTx or vehicle administration and sacrificed at day 15 p.c.. (A) Representative microphotographs of salivary glands examined by immunofluorescence for CD3ε (green) and CD19 (blue) showing lymphocytic infiltration. Original magnification 25X. Volume fraction of lymphoid follicles (B) and average follicle area (C) were determined in all experimental groups and data represented as mean (SD) of two independent experiments with at least four salivary glands per group. * $p < 0.05$, unpaired *t* test.

5.2.3.3. Analysis of day 23 samples

At day 23 p.c., the salivary glands of cannulated FAP-DTR+ and FAP-DTR-mice treated with both DTx and vehicle control were analysed by flow cytometry and qRT-PCR. No significant differences were found in the percentage or absolute numbers of LLSc or FAP+LLSc between experimental groups (**Figure 5.12Ai, Aii, Bi, Bii**). On the other hand, a significant decreased in the numbers of CD45+, CD3ε+ and CD19+ cells was still registered in mice that display (non-significant) reduction of the FAP+ cells (**Figure 5.13 Aii, Bii, Cii**). We also observed a selective reduction in percentage of CD19+ cells but not in the total CD45 component or in the CD3+ cells (**Figure 5.13Ai, Bi, Ci**). Proportions of CD4+ and CD8+ T cells were unchanged in the different experimental groups (**Figure 5.13Di, Ei**); however, less CD3+ and CD8+ T cells we found in the DTR+ DTX treated mice (**Figure 5.13Aii**).

Analysis of mRNA transcripts in whole-tissue sections revealed a 3-fold increase in the levels of *Fap* mRNA in FAP-DTR+ treated with vehicle, when compared to the other 3 experimental groups (**Figure 5.14A**). *Pdpn* and *Ccr7* transcripts did not show any significant changes between groups but FAP-DTR+ mice treated with DTx presented slightly increased levels (**Figure 5.14B, E**). *Cxcl13, Ccl19* and *Cxcr5* transcripts showed a, non-significant, trend towards decreased levels in FAP-DTR+ treated with DTx (**Figure 5.14C, D, F**).

When the results from DTx treated FAP-DTR+ mice are compared only to DTR+ mice treated with vehicle, at day 23 p.c. only the percentage of

infiltrating CD19+ cells (**Figure 5.13Ci**) are significantly decreased in DTx treated mice.

Figure 5.12

Day 23 p.c.

A

i
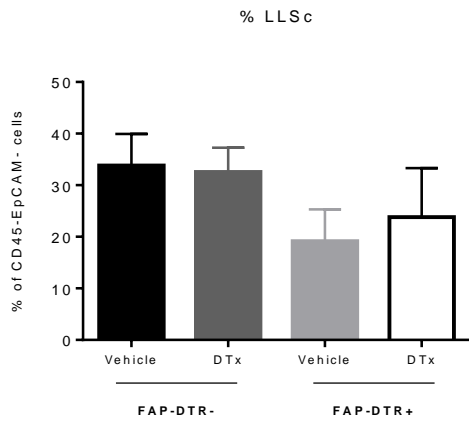
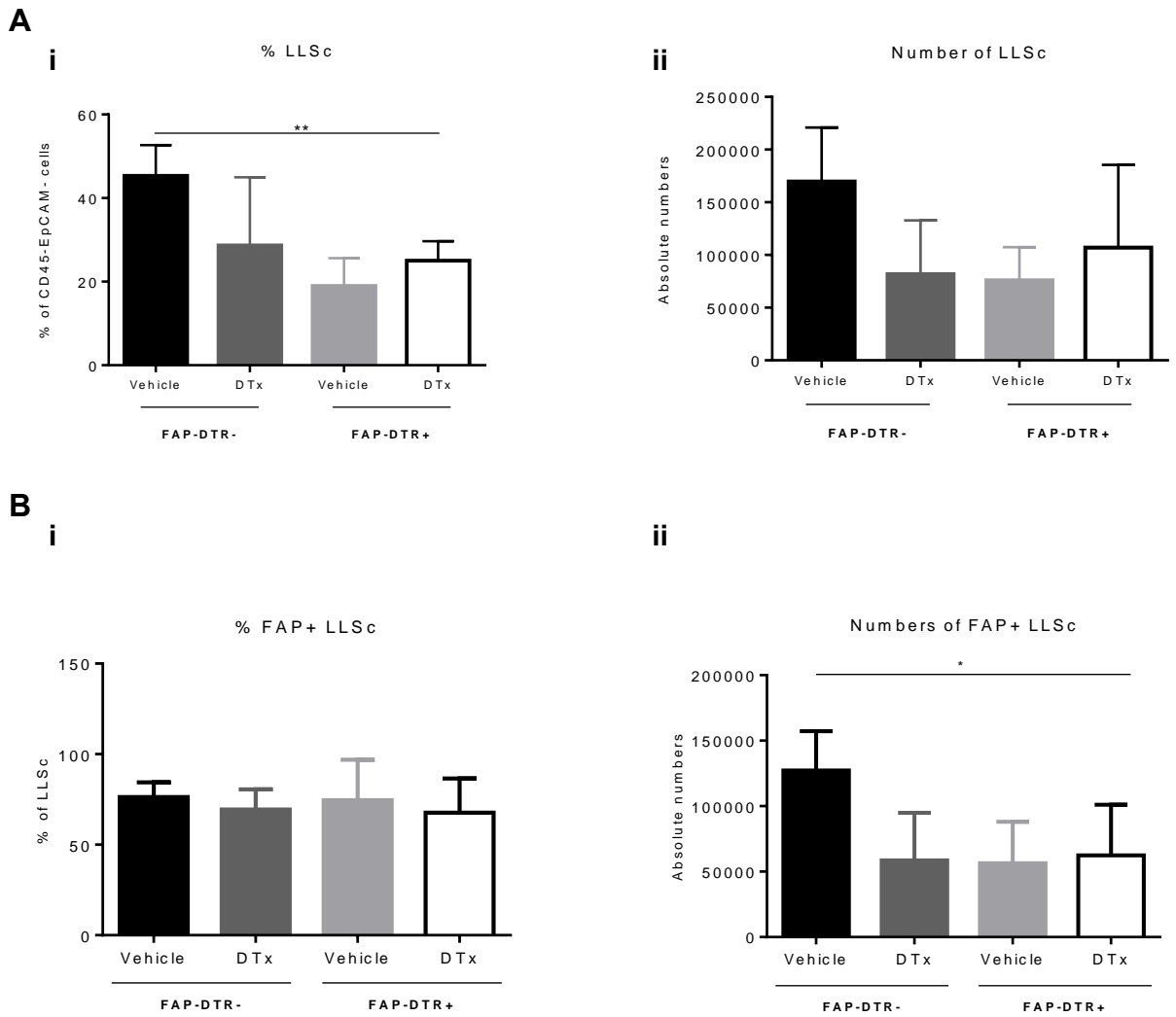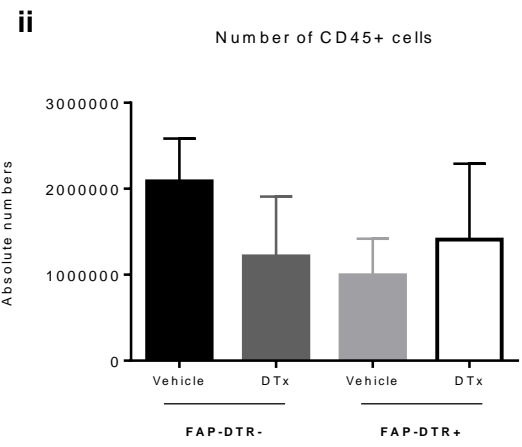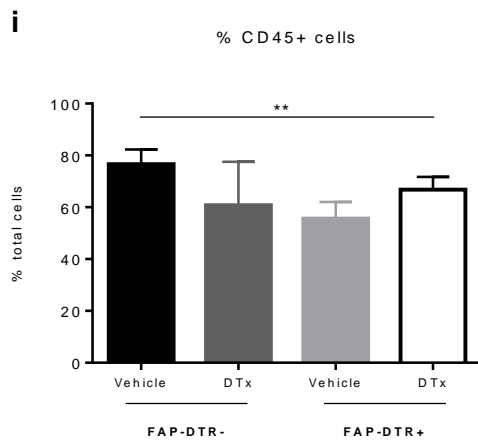**ii**
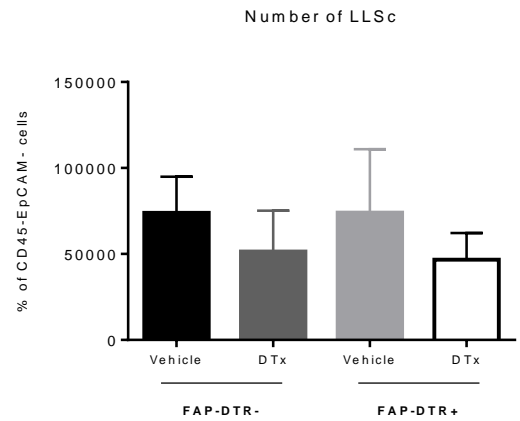
B

i
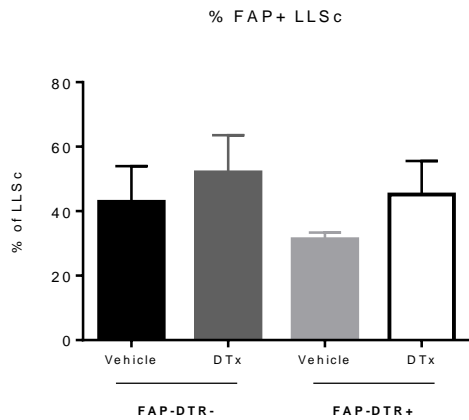
ii
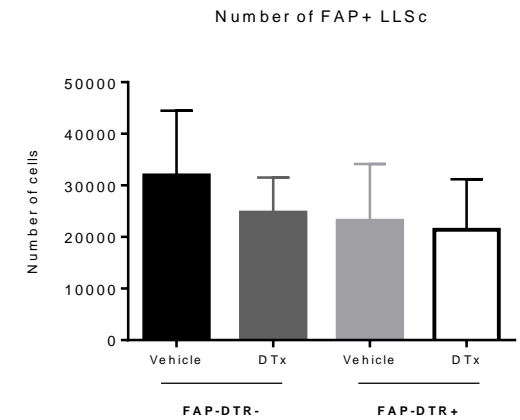
Figure 5.12. Flow cytometry analysis of the stroma compartment in FAP-DTR mice at day 23 p.c.. FAP-DTR- mice treated with vehicle (black) and DTx (dark grey) and FAP-DTR+ mice treated with vehicle (light grey) and DTx (white) were cannulated post DTx or vehicle administration and sacrificed at day 23 p.c.. Percentage (i) and absolute numbers (ii) of LLsc (A) and FAP+LLSc (B) were determined by flow cytometry staining and presented as mean (SD) of two independent experiments with at least four salivary glands per group.

Figure 5.13

Day 23 p.c.

A

i

% CD45+ cells

ii

Number of CD45+ cells

B

i

% CD3e+ cells

ii

Number of CD3e+ cells

C

i

% CD19+ cells

ii

Number of CD19+ cells
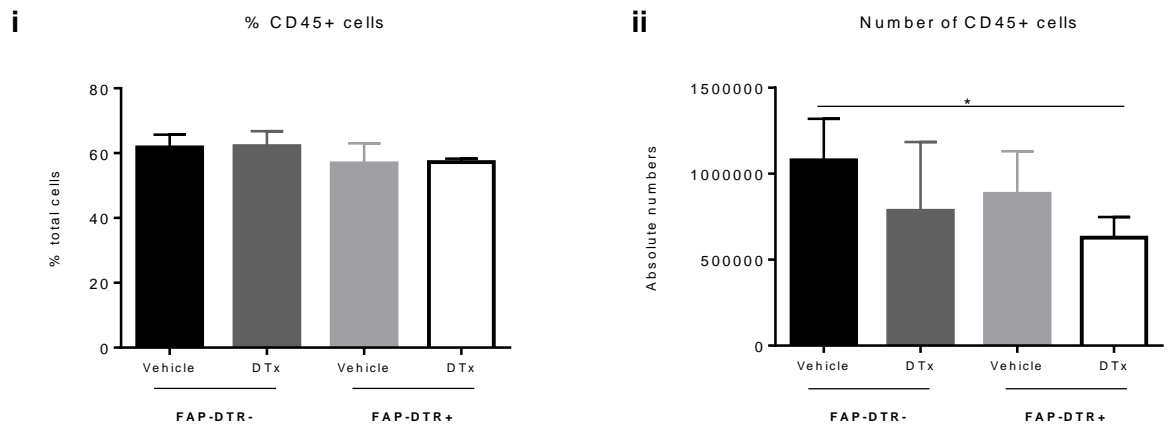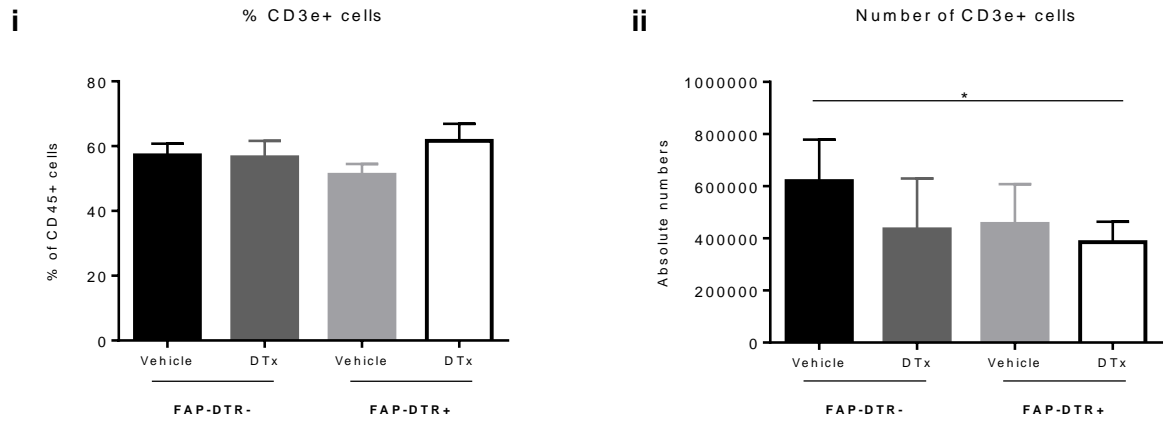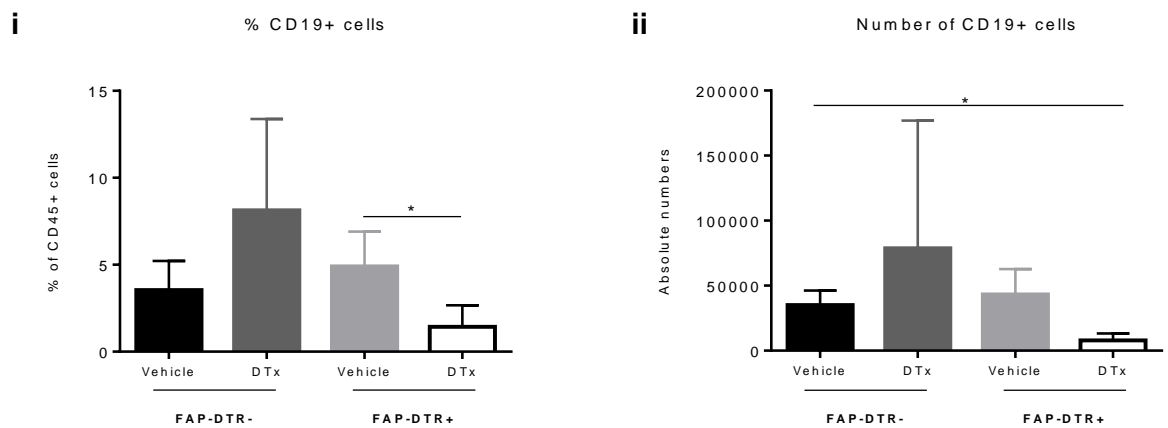
Figure 5.13 (cont.)

Day 23 p.c.

D

i

% C D 4+ T cells

ii

Number of C D 4+ T cells

E

i

% C D 8+ T cells

ii

Number of C D 8+ T cells
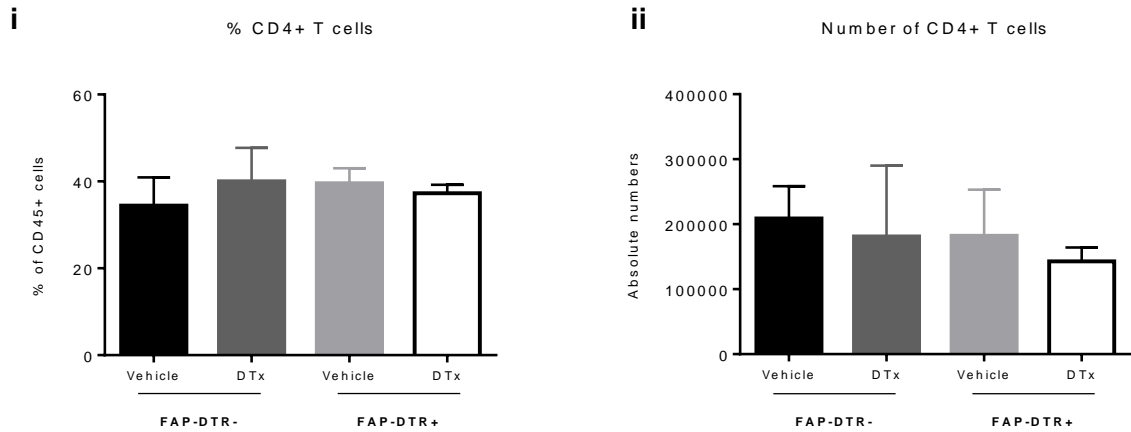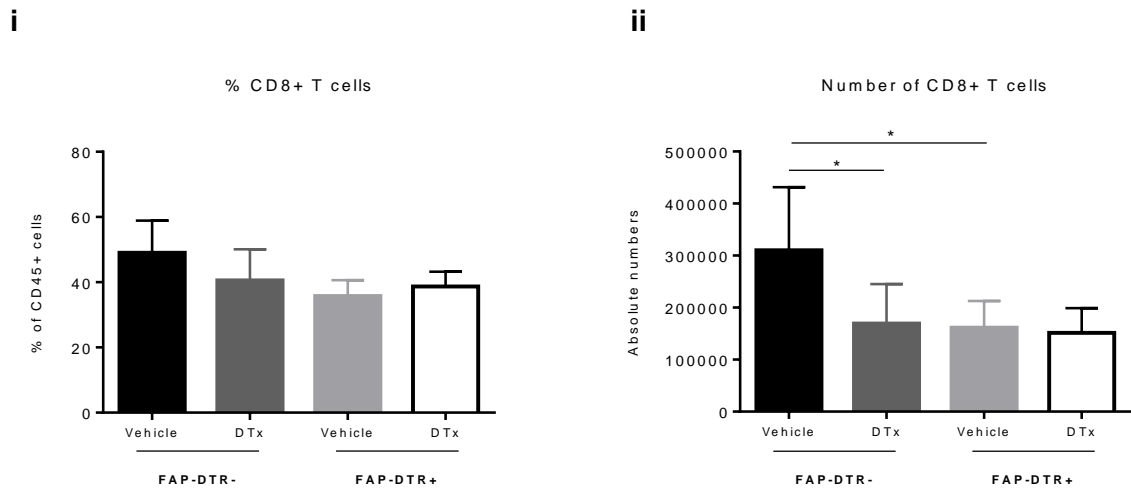
Figure 5.13. Flow cytometry analysis of the leukocyte compartment in FAP-DTR mice at day 23 p.c.. FAP-DTR- mice treated with vehicle (black) and DTx (dark grey) and FAP-DTR+ mice treated with vehicle (light grey) and DTx (white) were cannulated post DTx or vehicle administration and sacrificed at day 23 p.c.. Percentage (i) and absolute numbers (ii) of CD45+ cells (A), CD3ε+ T cells (B), CD19+ B cells (C), CD4+CD3ε+ T cells (D) and CD8+CD3ε+ T cells (E) were determined by flow cytometry staining and presented as mean (SD) of two independent experiments with at least four salivary glands per group. * p < 0.05, unpaired *t* test.

Figure 5.14
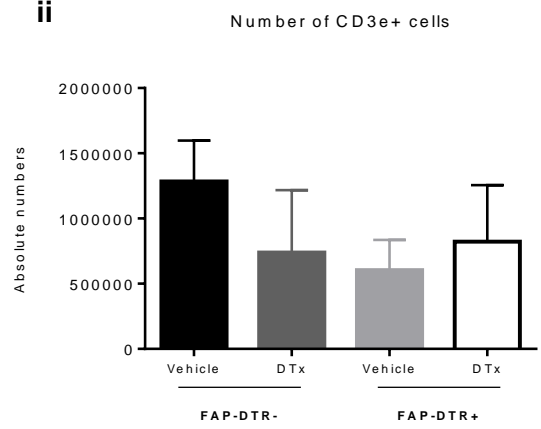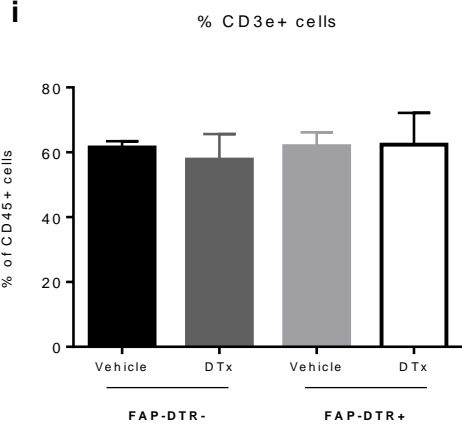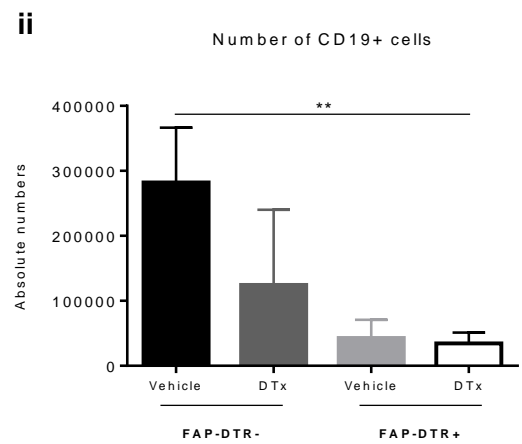
Day 23 p.c.
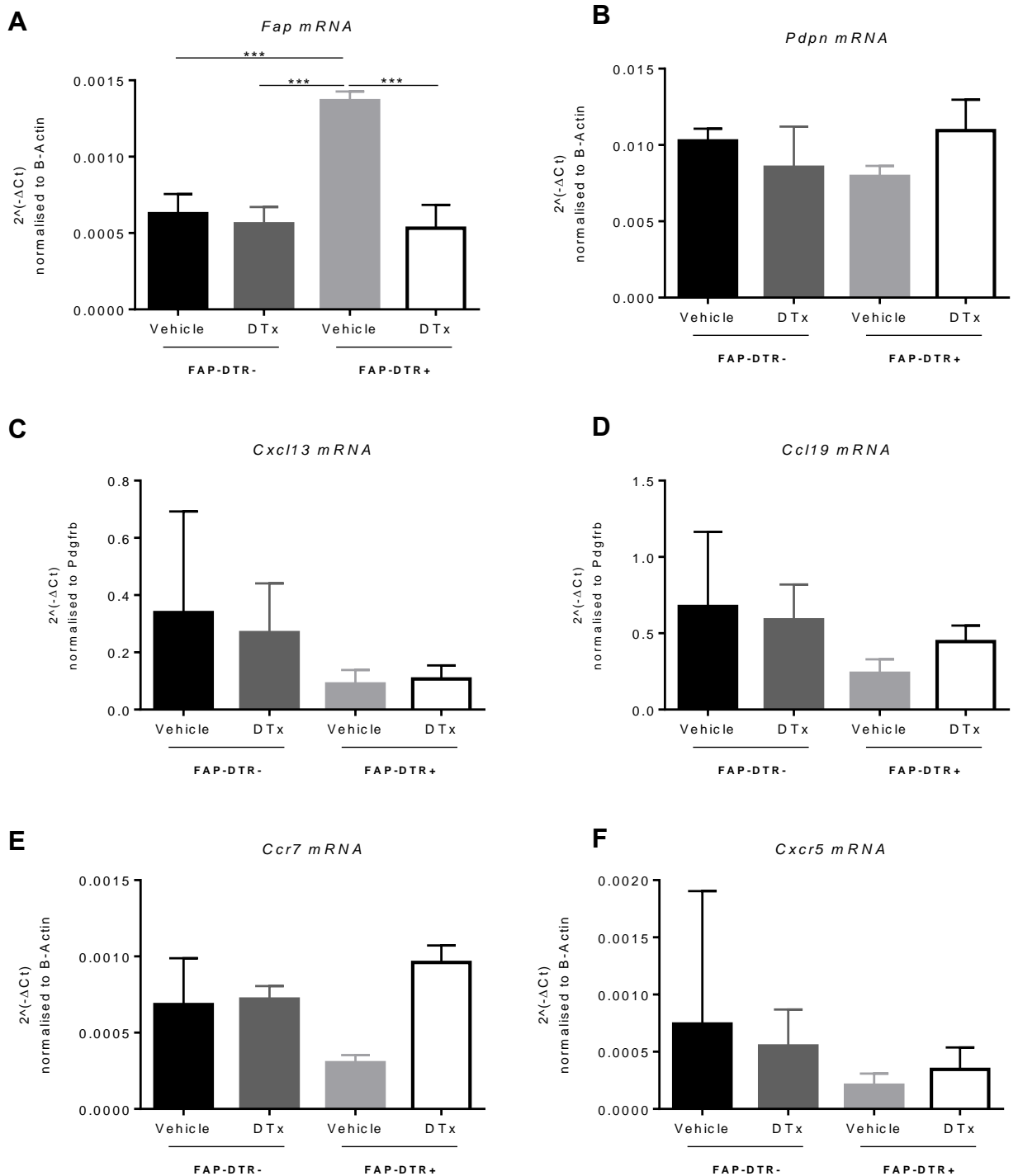
Figure 5.14. DTx treatment in FAP-DTR mice affects expression levels of lymphoid chemokines and recruitment of lymphocytes. qRT-PCR analysis of *Fap* (A), *Pdpn* (B), ccl19 (C), cxcl13 (D), *ccr7* (E) and *cxcr5* (F) mRNA transcripts from FAP-DTR- mice treated with vehicle (black) and DTx (dark grey) and FAP-DTR+ mice treated with vehicle (light grey) and DTx (white) at day 23 p.c.. qRT-PCR results for *Fap, Pdpn, ccr7* and *cxcr5* were normalised to housekeeping gene *β-actin* and *ccl19* and *cxcl13* results normalised to *Pdgfrb*. *** $p < 0.001$, unpaired *t* test, data represented as mean (SD). with two to nine glands analysed per group.

157

5.3. Discussion

In the present study we demonstrate that LLSc characterised by their expression of gp38 and FAP have a functional role in TLO formation during salivary gland inflammation. Using a Tg mouse strain in which FAP expressing cells could be experimentally deleted we demonstrated impaired TLO formation in inflamed salivary glands when FAP expressing cells were deleted prior to the induction of salivary gland inflammation.

Administration of DTx to the FAP-DTR strain enabled the conditional and selective depletion of FAP+gp38+ stromal cells that display f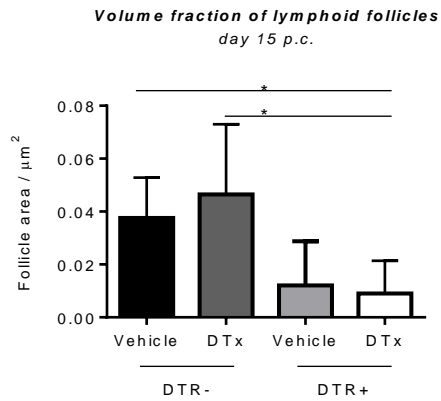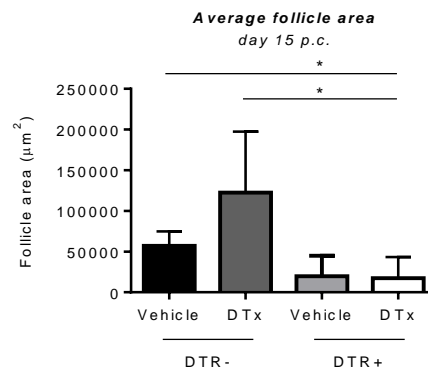eatures of LLSc. This technique allowed us to evaluate the consequences of LLSc cell deletion in a murine model of TLO formation that mimics SS.

In resting tissues, Dolzing et al., 2005 demonstrated that FAP is expressed only at low level, with the exception of the uterus and cervix (Dolznig et al., 2005). In pathology, FAP is selectively expressed by activated stromal cells in areas undergoing tissue remodelling, reactive stroma of epithelial cancers and in chronic inflammatory lesions (Niedermeyer et al., 2000). In agreement with these observations we found that in resting murine salivary glands FAP expression was not detectable by immunofluorescence and detected only at very low levels in sorted gp38+ stromal cells.

The presence of FAP+ stromal cells is common in various types of epithelial cancers, including breast, lung, colorectal and pancreatic (Garin-Chesa et al., 1990b) and these cells have been described to be in close association with tumour capillaries, which allow the recruitment of lymphocytes and facilitate the release of peptide mediators and proteases (Rettig et al., 1993, Scanlan et

al., 1994). Accordingly, a large body of evidence in literature suggests a key role in cancer invasion, angiogenesis, growth and metastases.

In patients with RA, FAP is highly expressed by fibroblast-like synoviocytes, mainly situated in the synovium lining layer and associated with key molecules involved in extracellular matrix degradation in RA joints (Bauer et al., 2006). FAP is also overexpressed in the membrane of stimulated chondrocytes and in the cartilage of osteoarthritis patients (Milner et al., 2006). Experimental arthritis in FAP-deficient mice results in less cartilage degradation whilst inflammation and bone erosion are unaffected (Waldele et al., 2015).

During this project, we detected by flow cytometry, qRT-PCR and immunofluorescence a clear upregulation of FAP in murine salivary glands post cannulation with adenovirus. Moreover, not only was FAP expression increased in whole-tissue sections but also in isolated LLSc, particularly at days 5 and 8 p.c., during active inflammation but also decreased at day 15 p.c. when inflammation within the gland begins to resolve. We demonstrate therefore that FAP is dynamically expressed by activated stromal cells during salivary gland inflammation and is an important biomarker of inflammation. To our knowledge, no literature has been published regarding FAP expression in biopsies of patients with SS, however we believe it would be relevant to screen SS biopsies for FAP expression and possibly correlate it with GC development and incidence of MALT lymphoma.

FAP+ stromal cells have been shown to mediate immune suppression in the tumour microenvironment (Kraman et al., 2010, Feig et al., 2013). FAP+ cell deletion in a model of Lewis lung carcinoma resulted in hypoxic necrosis of

both stroma and cancer cells in tumours that elicit an immune response and in the same study absence of FAP+ stromal cells led to a decrease in tumour growth in a model of pancreatic ductal adenocarcinoma (Kraman et al., 2010).

Denton et al. recently showed that depleting FAP+ FRCs from lymph nodes resulted in naïve T, B and dendritic cells loss, which impaired the immune response mounted against an influenza infection (Denton et al., 2014). Using the same model of conditional ablation of FAP+ cells we have, for the first time, achieved a consistent depletion of gp38+ stromal in murine salivary glands. Therefore, we used this model to test our hypothesis that stromal cells play a role in TLO formation and maintenance.

Prior to salivary gland cannulation with a replication-deficient adenovirus, FAP+ cells were depleted in a prophylactic approach in FAP-DTR+ mice. In our study, the weight loss associated with DTx administration to FAP-DTR+ mice did not cause any obvious distress or reduction in activity and, even though this particular aspect was not investigated in depth and therefore we are unable to rule it out, we do not believe muscle mass loss should affect the immune response in our model of local inflammation. The effects of muscle mass loss would be a rather important question to address in other mouse models of inflammation such as models of rheumatoid arthritis where the inflammatory process in more spread.

Depleting FAP+ LLSc resulted in a clear reduction in infiltrating lymphocytes particularly at day 8 and 15 p.c., associated with unsurprisingly reduced levels of lymphoid chemokines since these are known to be produced by activated stromal cells. Consequently, a defect in TLO formation was observed in mice

lacking FAP+ cells; these mice exhibited less and smaller aggregates of lymphocytes, usually completely absent of B cells. Altogether, these results seem to point towards an important role for FAP+ LLSc in TLO formation within inflamed salivary glands.

In some of the parameters analysed in our study, FAP-DTR+ mice treated with vehicle seemed to show decreased number of infiltrating cells, expression of chemokines and size of lymphoid follicles formed in salivary glands when compared to FAP-DTR- mice. Some preliminary results from recent experiments in our group aimed at investigating these same parameters mentioned above in FAP-DTR- and FAP-DTR+ mice without DTx or vehicle administration. Indeed, cannulated DTR+ mice (without any treatment) have less infiltrating T and B cells, even when the depletion of FAP+ cells does not take place, and therefore further investigation is required to understand the impact of the DTR+ BAC insertion. However this effect in one of the control groups is not as pronounced as the results observed in FAP-DTR+ mice treated with DTx and for this reason and at this moment we believe all controls should be taken in consideration and FAP+ stromal cells play a role in the formation of TLOs in inflamed salivary glands.

Conversely, FRCs have been described as cells with immunosuppressive properties in murine lymph nodes and were recently used as an anti-inflammatory therapy in animal models of sepsis (Fletcher et al., 2014, Fletcher et al., 2015, Siegert et al., 2011, Lukacs-Kornek et al., 2011). Indeed, administration of a single dose of FRCs significantly reduced mortality and local production of inflammatory cytokines (Fletcher et al., 2014).

There are some limitations of our work. Lymph nodes from cannulated FAP-DTR+ mice were not analysed, however we believe this will be a key aspect to further explore in order to understand the role of stromal cells in inflammation. Lymph node immunization experiments are currently taking place in our laboratory to address this question. At the moment, we are not able to comment on the possible immunosuppressive role of these cells, however we believe it would be interesting to isolate FAP+FRCs and FAP+LLSc and deliver them post inflammatory insult.

Similarly, only a prophylactic experimental approach was adopted regarding FAP+ cell ablation and described in this thesis. In the future, it would be highly interesting to deplete FAP+ stromal cells when we know FAP expression peaks after cannulation (day 8 p.c.) or at the peak of TLO organization (day 15 p.c.), since in this model of conditional depletion only cells expressing FAP at the time of depletion are affected.

Altogether, this model has provided us with an extremely powerful tool to study the role of activated stromal cells in the recruitment of lymphocytes into inflamed salivary glands and in the formation of TLOs. Both FAP+ cancer associated fibroblasts and lymph node FRCs have been described as immunosuppressive since they were shown to dampen immune responses (Kraman et al., 2010, Fletcher et al., 2014). In our model of salivary gland inflammation, depletion of FAP+ LLSc resulted in compromised formation of TLO and reduced leucocyte infiltration.

Our work establishes yet another link between salivary gland LLSc and lymph nodes FRCs by showing co-expression of both gp38 and FAP in both

populations of activated stromal cells. Furthermore, these studies suggest that gp38+FAP+ stromal cells are critically required for the organised development of TLOs within inflamed tissues and have a potentially pathogenic function and thus an important therapeutic target.

Chapter 6

GENERAL DISCUSSION AND FUTURE WORK

TLOs are ectopic structures that form at sites of chronic inflammation and are characterized by an organized and compartmentalized infiltration of immune cells within a functional scaffold of stromal cells (Buckley et al., 2015). Despite the importance of TLOs in autoimmune and chronic inflammatory diseases, little is known about the functional role of the stromal compartment in the development and maintenance of these structures. Recently, increased understanding of the role of stromal cells in SLO formation and homeostasis has highlighted the need of better understanding the role of stroma in TLOs.

Several groups, including ours, have attempted to characterise the events and molecular pathways involved in the activation of resident mesenchyme to activated stroma. While the homeostatic role of the stroma in sustaining lymphocyte survival and organization has been largely established (Lindhout et al., 1999, Parsonage et al., 2005, Barone et al., 2015b, Buckley et al., 2015), the ability of stromal cells to influence the dynamic of the autoimmune response is still not fully understood.

Within TLOs, activated stromal cells, that we named LLSc are characterised by the up-regulation of gp38 (Barone et al., 2015b) and FAP, two features shared with the lymphoid stroma within SLOs (Peduto et al., 2009, Denton et al., 2014). Taking advantage of these shared features, we aimed to investigate the functional role of activated stromal cells in the formation of TLOs utilising a mouse model of salivary gland inflammation. In this model of

TLO formation, inflammation was induced by retrograde cannulation of the salivary gland excretory duct with a replication deficient adenovirus, that shared TLO features, such as T/B cell compartmentalization and formation of FDC networks (Bombardieri et al., 2012).

Whilst investigating the function of gp38+ LLSc in inflamed murine salivary glands, we discovered a novel immunological function of the stroma associated with TLOs. We showed that, upon cannulation, LLSc upregulate ICOSL and actively provide costimulatory signals to locally recruited T cells. ICOSL expression by fibroblasts has been previously described *in vitro* (Swallow et al., 1999); however, to our knowledge, our results are the first to describe *in* vivo expression of ICOSL in non-hematopoietic cells. This expression of ICOSL in combination with the expression of ICOSL provided by DCs is required for the release of LTα by T cells that, in turn, influences the early production of lymphoid chemokines necessary for TLO assembly.

This novel function associated with the ability of activated stromal cells in TLOs to secrete lymphoid chemokines and cytokines (Peduto et al., 2009), prompted us to investigate the effects that interfering with the function or the formation of the LLSc network would have on TLO formation and maintenance. LLSc typically upregulate gp38, a mucin-type transmembrane glycoprotein whose expression is shared with SLOs stromal cells but also with cancer associated fibroblasts and inflamed epithelium (Astarita et al., 2012). Recently published work demonstrated that FRCs-derived gp38 engagement with CLEC-2, a type 2 lectin expressed by DCs, is required to support DCs

motility across the FRC network (Acton et al., 2012). Furthermore, FRC contractility is regulated by gp38 expression (Acton et al., 2014). Using a model in which we could selectively and conditionally knockdown *Pdpn,* we aimed to explore the functional role of gp38 expression in the context of inflammation-induced TLO formation. Our experimental setting, in which gp38 deletion was achieved by administration of tamoxifen, did not allow full deletion of gp38 transcription throughout the full duration of the inflammatory response. Indeed, in our setting, downregulation of *Pdpn* did not affect TLO formation as shown by immunofluorescence and qRT-PCR. However, we could observe a defect in maturation of the inflammatory mesenchyme into VCAM^{hi}ICAM^{hi} cells. Upregulation of ICAM and VCAM is critically required in the early phases of lymph node formation to enable cell-cell contact between LTi and LTo. LTi are not required for TLO formation, however upregulation of ICAM and VCAM occurs and might be involved in the clustering of T and B cells required for the production of lymphoid chemokines. Accordingly, in our *in vitro* setting (Chapter 3) we demonstrated that cell-cell contact is required for the production of LTα that, in turn, regulates chemokine production upon binding to TNFR.

Gp38 expression seems therefore able to regulate the upregulation of adhesion molecules required for cell clustering. Whilst limited by the experimental setting, our observation is important and we are currently optimising a methodology of tamoxifen injections combined with tamoxifen-based diet for the duration of the experiment to extend the length of gp38 deletion and better dissect the role of gp38 in the later stages of TLO establishment.

We then sought to delete the gp38+ stromal cell component taking advantage of the FAP-DTR mouse in which deletion of the FAP+ cells in the stroma results in a significant loss of gp38+ cells.

In our hands depletion of FAP+ cells resulted in impaired TLO formation, with diminished expression of lymphoid chemokines and survival factors and decreased lymphocyte aggregation.

Indeed SLO stromal cells exhibit an immune-modulatory activity by influencing the availability of survival factors, inducing clonal deletion and preventing the expansion of auto-reactive T cell clones (Fletcher et al., 2010). This central role in balancing immune stimulation versus peripheral tolerance is achieved by the ability of stromal cells to present a range of peripheral tissue restricted antigens within lymph nodes (e.g. the melanocyte-associated enzyme tyrosinase) and to induce deletion of self-reactive naïve T cell clones (Fletcher et al., 2010, Siegert et al., 2011, Lukacs-Kornek et al., 2011). FRC also limit T cell expansion and priming through a series of mechanisms, for example the release of nitric oxide (Siegert et al., 2011, Lukacs-Kornek et al., 2011). Accordingly, Fletcher et al. recently described FRCs as immunosuppressive cells in the context of murine sepsis (Fletcher et al., 2014).

TLO formation in autoimmune diseases correlates with autoantibody serum levels, local damage and disease severity both in human disease and in animal models (Rangel-Moreno et al., 2011, Salomonsson et al., 2002, Astorri et al., 2010, Bugatti et al., 2012, Bugatti et al., 2005). TLO-associated B cell activation is a recognized mechanism of lymphoma development in the salivary glands of patients with SS and in the gastric mucosa of patients with

Helicobacter Pylori gastritis (Barone et al., 2008, Hallas et al., 1998, Qin et al., 1997, Barone et al., 2012). In SS the identification of ectopic TLOs within the minor salivary glands is currently used as a histological biomarker and prognostic tool for lymphoma development (Theander et al., 2011). However, the role of TLOs in disease pathogenesis and progression remains controversial. Compelling new evidence suggests that, in some cases, TLO formation is protective. TLO formation in the vascular adventitia during atherosclerosis provides an appropriate microenvironment for the generation of T-regulatory cells (Hu et al., 2015). Yet other findings in solid tumours suggest that TLOs are pathogenic through their immunosuppressive role. These contradictory findings suggest a potential dualistic functional role for TLOs that appear to be context, phase and potentially disease-specific. Within TLOs production of IL-7 and BAFF induces maturation into T_H17 cells and survival of B cells, respectively. Is it possible that LLSc within TLOs, alongside providing survival factors and chemokines could provide suppressive signals to counterbalance uncontrolled activation of lymphocytes? Are those functions stable or plastic? Could they change during the different phases of the inflammatory process? Those are questions that yet remain to be addressed.

Recently, our group has discovered that LLSc in the salivary glands post cannulation are characterised by upregulation of another co-stimulatory molecule PD-L1, a protein known to suppress the immune system by inhibiting T cell activation and proliferation and cytokine production (Freeman et al., 2000, Latchman et al., 2001, Carter et al., 2002). Indeed, administration of PD-L1 blocking antibody to NOD mice precipitates the development of diabetes and PD-L1-deficient mice are more susceptible to the development

of more severe EAE compared to wt controls (Ansari et al., 2003, Carter et al., 2007). In contrast, IL-17+ T cells both in psoriatic patients and mice overexpress PD-1 and administration of PD-L1-Fc fusion protein ameliorates inflammation in a mouse model of psoriasis and central nervous system inflammation (Bodhankar et al., 2015, Kim et al., 2016).

This finding is compelling given our previous observation on ICOSL expression by LLSc. Further investigations on PD-L1 expression in the context of TLO formation in inflamed salivary glands and the relative ability of LLSc to provide inhibitory vs. co-stimulatory stimuli are currently taking place in our laboratory.

Despite technical difficulties, in the course of this project I have demonstrated that LLSc display critical immunological functions, among which co-stimulation and potentially immunosuppression, clearly establishing the role of those cells as instrumental players in the establishment and organization of TLOs. These important findings open a series of exciting questions on the broader role of stromal cells in the context of chronic inflammation.

The use of different experimental approaches during the course of this project enabled us to conclude that more than the markers expressed by stromal cells it's the cell population that express FAP, gp38 and co-stimulatory molecules that play a role in the process of TLO formation. In summary, the immunological features of stromal cells reported here support the need to consider these cells as very strong potential therapeutic targets in TLO-associated chronic inflammatory conditions with cell depleting therapies.

References

ABDULKADIR, S. A. 2005. Mechanisms of prostate tumorigenesis: roles for transcription factors Nkx3.1 and Egr1. *Ann N Y Acad Sci,* 1059**,** 33-40.

ACHARYA, P. S., ZUKAS, A., CHANDAN, V., KATZENSTEIN, A. L. & PURE, E. 2006. Fibroblast activation protein: a serine protease expressed at the remodeling interface in idiopathic pulmonary fibrosis. *Hum Pathol,* 37**,** 352-60.

ACTON, S. E., ASTARITA, J. L., MALHOTRA, D., LUKACS-KORNEK, V., FRANZ, B., HESS, P. R., JAKUS, Z., KULIGOWSKI, M., FLETCHER, A. L., ELPEK, K. G., BELLEMARE-PELLETIER, A., SCEATS, L., REYNOSO, E. D., GONZALEZ, S. F., GRAHAM, D. B., CHANG, J., PETERS, A., WOODRUFF, M., KIM, Y. A., SWAT, W., MORITA, T., KUCHROO, V., CARROLL, M. C., KAHN, M. L., WUCHERPFENNIG, K. W. & TURLEY, S. J. 2012. Podoplanin-rich stromal networks induce dendritic cell motility via activation of the C-type lectin receptor CLEC-2. *Immunity,* 37**,** 276-89.

ACTON, S. E., FARRUGIA, A. J., ASTARITA, J. L., MOURAO-SA, D., JENKINS, R. P., NYE, E., HOOPER, S., VAN BLIJSWIJK, J., ROGERS, N. C., SNELGROVE, K. J., ROSEWELL, I., MOITA, L. F., STAMP, G., TURLEY, S. J., SAHAI, E. & REIS E SOUSA, C. 2014. Dendritic cells control fibroblastic reticular network tension and lymph node expansion. *Nature,* 514**,** 498-502.

AGUZZI, A., KRANICH, J. & KRAUTLER, N. J. 2014. Follicular dendritic cells: origin, phenotype, and function in health and disease. *Trends in immunology,* 35**,** 105-13.

AKIBA, H., TAKEDA, K., KOJIMA, Y., USUI, Y., HARADA, N., YAMAZAKI, T., MA, J., TEZUKA, K., YAGITA, H. & OKUMURA, K. 2005. The role of ICOS in the CXCR5+ follicular B helper T cell maintenance in vivo. *J Immunol,* 175**,** 2340-8.

ALLEN, C. D., ANSEL, K. M., LOW, C., LESLEY, R., TAMAMURA, H., FUJII, N. & CYSTER, J. G. 2004. Germinal center dark and light zone organization is mediated by CXCR4 and CXCR5. *Nat Immunol,* 5**,** 943-52.

ALLEN, C. D. & CYSTER, J. G. 2008. Follicular dendritic cell networks of primary follicles and germinal centers: phenotype and function. *Semin Immunol,* 20**,** 14-25.

ALOISI, F. & PUJOL-BORRELL, R. 2006. Lymphoid neogenesis in chronic inflammatory diseases. *Nat Rev Immunol,* 6**,** 205-17.

AMFT, N., CURNOW, S. J., SCHEEL-TOELLNER, D., DEVADAS, A., OATES, J., CROCKER, J., HAMBURGER, J., AINSWORTH, J., MATHEWS, J., SALMON, M., BOWMAN, S. J. & BUCKLEY, C. D. 2001. Ectopic expression of the B cell-attracting chemokine BCA-1 (CXCL13) on endothelial cells and within lymphoid follicles contributes to the establishment of germinal center-like structures in Sjogren's syndrome. *Arthritis Rheum,* 44**,** 2633-41.

ANAYA, J. M., DELGADO-VEGA, A. M. & CASTIBLANCO, J. 2006. Genetic basis of Sjogren's syndrome. How strong is the evidence? *Clinical & developmental immunology,* 13**,** 209-22.

ANDROLEWICZ, M. J., BROWNING, J. L. & WARE, C. F. 1992. Lymphotoxin is expressed as a heteromeric complex with a distinct 33-kDa glycoprotein on the surface of an activated human T cell hybridoma. *J Biol Chem,* 267**,** 2542-7.

ANSARI, M. J., FIORINA, P., DADA, S., GULERIA, I., UENO, T., YUAN, X., TRIKUDANATHAN, S., SMITH, R. N., FREEMAN, G. & SAYEGH, M. H. 2008. Role of ICOS pathway in autoimmune and alloimmune responses in NOD mice. *Clin Immunol,* 126**,** 140-7.

ANSARI, M. J., SALAMA, A. D., CHITNIS, T., SMITH, R. N., YAGITA, H., AKIBA, H., YAMAZAKI, T., AZUMA, M., IWAI, H., KHOURY, S. J., AUCHINCLOSS, H., JR. & SAYEGH, M. H. 2003. The programmed death-1 (PD-1) pathway regulates autoimmune diabetes in nonobese diabetic (NOD) mice. *J Exp Med,* 198**,** 63-9.

ANSEL, K. M., NGO, V. N., HYMAN, P. L., LUTHER, S. A., FORSTER, R., SEDGWICK, J. D., BROWNING, J. L., LIPP, M. & CYSTER, J. G. 2000. A chemokine-driven positive feedback loop organizes lymphoid follicles. *Nature,* 406**,** 309-14.

AOYAMA, A. & CHEN, W. T. 1990. A 170-kDa membrane-bound protease is associated with the expression of invasiveness by human malignant melanoma cells. *Proc Natl Acad Sci U S A,* 87**,** 8296-300.

ARTIS, D. & SPITS, H. 2015. The biology of innate lymphoid cells. *Nature,* 517**,** 293-301.

ASTARITA, J. L., ACTON, S. E. & TURLEY, S. J. 2012. Podoplanin: emerging functions in development, the immune system, and cancer. *Front Immunol,* 3**,** 283.

ASTARITA, J. L., CREMASCO, V., FU, J., DARNELL, M. C., PECK, J. R., NIEVES-BONILLA, J. M., SONG, K., KONDO, Y., WOODRUFF, M. C., GOGINENI, A., ONDER, L., LUDEWIG, B., WEIMER, R. M., CARROLL, M. C., MOONEY, D. J., XIA, L. & TURLEY, S. J. 2015. The CLEC-2-podoplanin axis controls the contractility of fibroblastic reticular cells and lymph node microarchitecture. *Nat Immunol,* 16**,** 75-84.

ASTORRI, E., BOMBARDIERI, M., GABBA, S., PEAKMAN, M., POZZILLI, P. & PITZALIS, C. 2010. Evolution of ectopic lymphoid neogenesis and in situ autoantibody production in autoimmune nonobese diabetic mice: cellular and molecular characterization of tertiary lymphoid structures in pancreatic islets. *J Immunol,* 185**,** 3359-68.

ATKINSON, M. A. & LEITER, E. H. 1999. The NOD mouse model of type 1 diabetes: as good as it gets? *Nat Med,* 5**,** 601-4.

AYOAMA, A. & CHEN, W. T. 1990. A 170-kDa membrane-bound protease is associated with the expression of invasiveness by human malignant melanoma cells. *Proc. Nati. Acad. Sci. USA,* 87**,** 8296-8300.

BACH, J. F. 1994. Insulin-dependent diabetes mellitus as an autoimmune disease. *Endocr Rev,* 15**,** 516-42.

BARON, V., ADAMSON, E. D., CALOGERO, A., RAGONA, G. & MERCOLA, D. 2006. The transcription factor Egr1 is a direct regulator of multiple tumor suppressors including TGFbeta1, PTEN, p53, and fibronectin. *Cancer Gene Ther,* 13**,** 115-24.

BARONE, F., BOMBARDIERI, M., MANZO, A., BLADES, M. C., MORGAN, P. R., CHALLACOMBE, S. J., VALESINI, G. & PITZALIS, C. 2005. Association of CXCL13 and CCL21 expression with the progressive organization of lymphoid-like structures in Sjogren's syndrome. *Arthritis and rheumatism,* 52**,** 1773-84.

BARONE, F., BOMBARDIERI, M., ROSADO, M. M., MORGAN, P. R., CHALLACOMBE, S. J., DE VITA, S., CARSETTI, R., SPENCER, J., VALESINI, G. & PITZALIS, C. 2008. CXCL13, CCL21, and CXCL12 expression in salivary glands of patients with Sjogren's syndrome and MALT lymphoma: association with reactive and malignant areas of lymphoid organization. *Journal of immunology,* 180**,** 5130-40.

BARONE, F., CAMPOS, J., BOWMAN, S. & FISHER, B. A. 2015a. The value of histopathological examination of salivary gland biopsies in diagnosis, prognosis and treatment of Sjogren's Syndrome. *Swiss Med Wkly,* 145**,** w14168.

BARONE, F., NAYAR, S. & BUCKLEY, C. D. 2012. The role of non-hematopoietic stromal cells in the persistence of inflammation. *Front Immunol,* 3**,** 416.

BARONE, F., NAYAR, S., CAMPOS, J., CLOAKE, T., WITHERS, D. R., TOELLNER, K. M., ZHANG, Y., FOUSER, L., FISHER, B., BOWMAN, S., RANGEL-MORENO, J., GARCIA-HERNANDEZ MDE, L., RANDALL, T. D., LUCCHESI, D., BOMBARDIERI, M., PITZALIS, C., LUTHER, S. A. & BUCKLEY, C. D. 2015b. IL-22 regulates lymphoid chemokine production and assembly of tertiary lymphoid organs. *Proc Natl Acad Sci U S A,* 112**,** 11024-9.

BAUER, S., JENDRO, M. C., WADLE, A., KLEBER, S., STENNER, F., DINSER, R., REICH, A., FACCIN, E., GODDE, S., DINGES, H., MULLER-LADNER, U. & RENNER, C. 2006. Fibroblast activation protein is expressed by rheumatoid myofibroblast-like synoviocytes. *Arthritis Res Ther,* 8**,** R171.

BAUQUET, A. T., JIN, H., PATERSON, A. M., MITSDOERFFER, M., HO, I. C., SHARPE, A. H. & KUCHROO, V. K. 2009. The costimulatory molecule ICOS regulates the expression of c-Maf and IL-21 in the development of follicular T helper cells and TH-17 cells. *Nat Immunol,* 10**,** 167-75.

BEKIARIS, V., WITHERS, D., GLANVILLE, S. H., MCCONNELL, F. M., PARNELL, S. M., KIM, M. Y., GASPAL, F. M., JENKINSON, E., SWEET, C., ANDERSON, G. & LANE, P. J. 2007. Role of CD30 in B/T segregation in the spleen. *J Immunol,* 179**,** 7535-43.

BENEZECH, C., WHITE, A., MADER, E., SERRE, K., PARNELL, S., PFEFFER, K., WARE, C. F., ANDERSON, G. & CAAMANO, J. H. 2010. Ontogeny of stromal organizer cells during lymph node development. *J Immunol,* 184**,** 4521-30.

BERG, A. R., WEISENBURGER, D. D., LINDER, J. & ARMITAGE, J. O. 1986. Lymphoplasmacytic lymphoma. Report of a case with three monoclonal proteins derived from a single neoplastic clone. *Cancer,* 57**,** 1794-7.

BERTOSSI, A., AICHINGER, M., SANSONETTI, P., LECH, M., NEFF, F., PAL, M., WUNDERLICH, F. T., ANDERS, H. J., KLEIN, L. & SCHMIDT-SUPPRIAN, M. 2011. Loss of Roquin induces early death and immune deregulation but not autoimmunity. *J Exp Med,* 208**,** 1749-56.

BERTOZZI, C. C., SCHMAIER, A. A., MERICKO, P., HESS, P. R., ZOU, Z., CHEN, M., CHEN, C. Y., XU, B., LU, M. M., ZHOU, D., SEBZDA, E., SANTORE, M. T., MERIANOS, D. J., STADTFELD, M., FLAKE, A. W., GRAF, T., SKODA, R., MALTZMAN, J. S., KORETZKY, G. A. & KAHN, M. L. 2010. Platelets regulate lymphatic vascular development through CLEC-2-SLP-76 signaling. *Blood,* 116**,** 661-70.

BODHANKAR, S., CHEN, Y., LAPATO, A., DOTSON, A. L., WANG, J., VANDENBARK, A. A., SAUGSTAD, J. A. & OFFNER, H. 2015. PD-L1

Monoclonal Antibody Treats Ischemic Stroke by Controlling Central Nervous System Inflammation. *Stroke,* 46**,** 2926-34.

BOIRIVANT, M., FUSS, I. J., CHU, A. & STROBER, W. 1998. Oxazolone colitis: A murine model of T helper cell type 2 colitis treatable with antibodies to interleukin 4. *J Exp Med,* 188**,** 1929-39.

BOMBARDIERI, M., BARONE, F., HUMBY, F., KELLY, S., MCGURK, M., MORGAN, P., CHALLACOMBE, S., DE VITA, S., VALESINI, G., SPENCER, J. & PITZALIS, C. 2007. Activation-induced cytidine deaminase expression in follicular dendritic cell networks and interfollicular large B cells supports functionality of ectopic lymphoid neogenesis in autoimmune sialoadenitis and MALT lymphoma in Sjogren's syndrome. *Journal of immunology,* 179**,** 4929-38.

BOMBARDIERI, M., BARONE, F., LUCCHESI, D., NAYAR, S., VAN DEN BERG, W. B., PROCTOR, G., BUCKLEY, C. D. & PITZALIS, C. 2012. Inducible tertiary lymphoid structures, autoimmunity, and exocrine dysfunction in a novel model of salivary gland inflammation in C57BL/6 mice. *J Immunol,* 189**,** 3767-76.

BOSSALLER, L., BURGER, J., DRAEGER, R., GRIMBACHER, B., KNOTH, R., PLEBANI, A., DURANDY, A., BAUMANN, U., SCHLESIER, M., WELCHER, A. A., PETER, H. H. & WARNATZ, K. 2006. ICOS deficiency is associated with a severe reduction of CXCR5+CD4 germinal center Th cells. *J Immunol,* 177**,** 4927-32.

BOULIANNE, B., PORFILIO, E. A., PIKOR, N. & GOMMERMAN, J. L. 2012. Lymphotoxin-sensitive microenvironments in homeostasis and inflammation. *Front Immunol,* 3**,** 243.

BOWMAN, S. J. & FOX, R. I. 2014. Classification criteria for Sjogren's syndrome: nothing ever stands still! *Annals of the rheumatic diseases,* 73**,** 1-2.

BOWMAN, S. J., IBRAHIM, G. H., HOLMES, G., HAMBURGER, J. & AINSWORTH, J. R. 2004. Estimating the prevalence among Caucasian women of primary Sjogren's syndrome in two general practices in Birmingham, UK. *Scandinavian journal of rheumatology,* 33**,** 39-43.

BREITENEDER-GELEFF, S., MATSUI, K., SOLEIMAN, A., MERANER, P., POCZEWSKI, H., KALT, R., SCHAFFNER, G. & KERJASCHKI, D. 1997. Podoplanin, novel 43-kd membrane protein of glomerular epithelial cells, is down-regulated in puromycin nephrosis. *Am J Pathol,* 151**,** 1141-52.

BRKIC, Z., MARIA, N. I., VAN HELDEN-MEEUWSEN, C. G., VAN DE MERWE, J. P., VAN DAELE, P. L., DALM, V. A., WILDENBERG, M. E., BEUMER, W., DREXHAGE, H. A. & VERSNEL, M. A. 2013. Prevalence of interferon type I signature in CD14 monocytes of patients with Sjogren's syndrome and association with disease activity and BAFF gene expression. *Ann Rheum Dis,* 72**,** 728-35.

BROKOPP, C. E., SCHOENAUER, R., RICHARDS, P., BAUER, S., LOHMANN, C., EMMERT, M. Y., WEBER, B., WINNIK, S., AIKAWA, E., GRAVES, K., GENONI, M., VOGT, P., LUSCHER, T. F., RENNER, C., HOERSTRUP, S. P. & MATTER, C. M. 2011. Fibroblast activation protein is induced by inflammation and degrades type I collagen in thin-cap fibroatheromata. *Eur Heart J,* 32**,** 2713-22.

BROWN, D. D., WANG, Z., FURLOW, J. D., KANAMORI, A., SCHWARTZMAN, R. A., REMO, B. F. & PINDER, A. 1996. The thyroid hormone-induced tail resorption program during Xenopus laevis metamorphosis. *Proceedings of*

the National Academy of Sciences of the United States of America, 93**,** 1924-9.

BRUNET, J. F., DENIZOT, F., LUCIANI, M. F., ROUX-DOSSETO, M., SUZAN, M., MATTEI, M. G. & GOLSTEIN, P. 1987. A new member of the immunoglobulin superfamily--CTLA-4. *Nature,* 328**,** 267-70.

BUCALA, R., SPIEGEL, L. A., CHESNEY, J., HOGAN, M. & CERAMI, A. 1994. Circulating fibrocytes define a new leukocyte subpopulation that mediates tissue repair. *Molecular medicine,* 1**,** 71-81.

BUCH, M. H., CONAGHAN, P. G., QUINN, M. A., BINGHAM, S. J., VEALE, D. & EMERY, P. 2004. True infliximab resistance in rheumatoid arthritis: a role for lymphotoxin alpha? *Ann Rheum Dis,* 63**,** 1344-6.

BUCKLEY, C. D. 2011. Why does chronic inflammation persist: An unexpected role for fibroblasts. *Immunol Lett,* 138**,** 12-4.

BUCKLEY, C. D., BARONE, F., NAYAR, S., BENEZECH, C. & CAAMANO, J. 2015. Stromal cells in chronic inflammation and tertiary lymphoid organ formation. *Annu Rev Immunol,* 33**,** 715-45.

BUCKLEY, C. D., FILER, A., HAWORTH, O., PARSONAGE, G. & SALMON, M. 2004. Defining a role for fibroblasts in the persistence of chronic inflammatory joint disease. *Ann Rheum Dis,* 63 Suppl 2**,** ii92-ii95.

BUGATTI, S., CAPORALI, R., MANZO, A., VITOLO, B., PITZALIS, C. & MONTECUCCO, C. 2005. Involvement of subchondral bone marrow in rheumatoid arthritis: lymphoid neogenesis and in situ relationship to subchondral bone marrow osteoclast recruitment. *Arthritis Rheum,* 52**,** 3448-59.

BUGATTI, S., MANZO, A., BENAGLIO, F., KLERSY, C., VITOLO, B., TODOERTI, M., SAKELLARIOU, G., MONTECUCCO, C. & CAPORALI, R. 2012. Serum levels of CXCL13 are associated with ultrasonographic synovitis and predict power Doppler persistence in early rheumatoid arthritis treated with non-biological disease-modifying anti-rheumatic drugs. *Arthritis Res Ther,* 14**,** R34.

BURMEISTER, Y., LISCHKE, T., DAHLER, A. C., MAGES, H. W., LAM, K. P., COYLE, A. J., KROCZEK, R. A. & HUTLOFF, A. 2008. ICOS controls the pool size of effector-memory and regulatory T cells. *J Immunol,* 180**,** 774-82.

CALMON-HAMATY, F., COMBE, B., HAHNE, M. & MOREL, J. 2011. Lymphotoxin alpha revisited: general features and implications in rheumatoid arthritis. *Arthritis Res Ther,* 13**,** 232.

CARBONE, A., GLOGHINI, A. & FERLITO, A. 2000. Pathological features of lymphoid proliferations of the salivary glands: lymphoepithelial sialadenitis versus low-grade B-cell lymphoma of the malt type. *The Annals of otology, rhinology, and laryngology,* 109**,** 1170-5.

CARRAGHER, D. M., RANGEL-MORENO, J. & RANDALL, T. D. 2008. Ectopic lymphoid tissues and local immunity. *Semin Immunol,* 20**,** 26-42.

CARTER, L., FOUSER, L. A., JUSSIF, J., FITZ, L., DENG, B., WOOD, C. R., COLLINS, M., HONJO, T., FREEMAN, G. J. & CARRENO, B. M. 2002. PD-1:PD-L inhibitory pathway affects both CD4(+) and CD8(+) T cells and is overcome by IL-2. *Eur J Immunol,* 32**,** 634-43.

CARTER, L. L., LEACH, M. W., AZOITEI, M. L., CUI, J., PELKER, J. W., JUSSIF, J., BENOIT, S., IRELAND, G., LUXENBERG, D., ASKEW, G. R., MILARSKI, K.

L., GROVES, C., BROWN, T., CARITO, B. A., PERCIVAL, K., CARRENO, B. M., COLLINS, M. & MARUSIC, S. 2007. PD-1/PD-L1, but not PD-1/PD-L2, interactions regulate the severity of experimental autoimmune encephalomyelitis. *J Neuroimmunol,* 182**,** 124-34.

CASH, E., MINTY, A., FERRARA, P., CAPUT, D., FRADELIZI, D. & ROTT, O. 1994. Macrophage-inactivating IL-13 suppresses experimental autoimmune encephalomyelitis in rats. *J Immunol,* 153**,** 4258-67.

CHAI, Q., ONDER, L., SCANDELLA, E., GIL-CRUZ, C., PEREZ-SHIBAYAMA, C., CUPOVIC, J., DANUSER, R., SPARWASSER, T., LUTHER, S. A., THIEL, V., RULICKE, T., STEIN, J. V., HEHLGANS, T. & LUDEWIG, B. 2013. Maturation of lymph node fibroblastic reticular cells from myofibroblastic precursors is critical for antiviral immunity. *Immunity,* 38**,** 1013-24.

CHANG, H. Y., CHI, J. T., DUDOIT, S., BONDRE, C., VAN DE RIJN, M., BOTSTEIN, D. & BROWN, P. O. 2002. Diversity, topographic differentiation, and positional memory in human fibroblasts. *Proc Natl Acad Sci U S A,* 99**,** 12877-82.

CHEN, H., YANG, W. W., WEN, Q. T., XU, L. & CHEN, M. 2009. TGF-beta induces fibroblast activation protein expression; fibroblast activation protein expression increases the proliferation, adhesion, and migration of HO-8910PM [corrected]. *Experimental and molecular pathology,* 87**,** 189-94.

CHEN, S. C., VASSILEVA, G., KINSLEY, D., HOLZMANN, S., MANFRA, D., WIEKOWSKI, M. T., ROMANI, N. & LIRA, S. A. 2002. Ectopic expression of the murine chemokines CCL21a and CCL21b induces the formation of lymph node-like structures in pancreas, but not skin, of transgenic mice. *J Immunol,* 168**,** 1001-8.

CHENG, J. D., DUNBRACK, R. L., JR., VALIANOU, M., ROGATKO, A., ALPAUGH, R. K. & WEINER, L. M. 2002. Promotion of tumor growth by murine fibroblast activation protein, a serine protease, in an animal model. *Cancer Res,* 62**,** 4767-72.

CHESNEY, J. & BUCALA, R. 1997. Peripheral blood fibrocytes: novel fibroblast-like cells that present antigen and mediate tissue repair. *Biochemical Society transactions,* 25**,** 520-4.

CHISHOLM, D. M. & MASON, D. K. 1968. Labial salivary gland biopsy in Sjogren's disease. *Journal of clinical pathology,* 21**,** 656-60.

CHRISTODOULOU, M. I., KAPSOGEORGOU, E. K. & MOUTSOPOULOS, H. M. 2010. Characteristics of the minor salivary gland infiltrates in Sjogren's syndrome. *Journal of autoimmunity,* 34**,** 400-7.

CHRISTODOULOU, M. I., KAPSOGEORGOU, E. K., MOUTSOPOULOS, N. M. & MOUTSOPOULOS, H. M. 2008. Foxp3+ T-regulatory cells in Sjogren's syndrome: correlation with the grade of the autoimmune lesion and certain adverse prognostic factors. *The American journal of pathology,* 173**,** 1389-96.

CLEMENT, M., GUEDJ, K., ANDREATA, F., MORVAN, M., BEY, L., KHALLOU-LASCHET, J., GASTON, A. T., DELBOSC, S., ALSAC, J. M., BRUNEVAL, P., DESCHILDRE, C., LE BORGNE, M., CASTIER, Y., KIM, H. J., CANTOR, H., MICHEL, J. B., CALIGIURI, G. & NICOLETTI, A. 2015. Control of the T follicular helper-germinal center B-cell axis by CD8(+) regulatory T cells limits atherosclerosis and tertiary lymphoid organ development. *Circulation,* 131**,** 560-70.

COLUMBA-CABEZAS, S., GRIGUOLI, M., ROSICARELLI, B., MAGLIOZZI, R., RIA, F., SERAFINI, B. & ALOISI, F. 2006. Suppression of established experimental autoimmune encephalomyelitis and formation of meningeal lymphoid follicles by lymphotoxin beta receptor-Ig fusion protein. *J Neuroimmunol,* 179**,** 76-86.

CONSTANTINOVITS, M., SIPOS, F., MOLNAR, B., TULASSAY, Z. & MUZES, G. 2012. Organizer and regulatory role of colonic isolated lymphoid follicles in inflammation. *Acta Physiol Hung,* 99**,** 344-52.

CUPEDO, T., LUND, F. E., NGO, V. N., RANDALL, T. D., JANSEN, W., GREUTER, M. J., DE WAAL-MALEFYT, R., KRAAL, G., CYSTER, J. G. & MEBIUS, R. E. 2004. Initiation of cellular organization in lymph nodes is regulated by non-B cell-derived signals and is not dependent on CXC chemokine ligand 13. *J Immunol,* 173**,** 4889-96.

CUPEDO, T. & MEBIUS, R. E. 2005. Cellular interactions in lymph node development. *J Immunol,* 174**,** 21-5.

DANIELS, T. E., COX, D., SHIBOSKI, C. H., SCHIODT, M., WU, A., LANFRANCHI, H., UMEHARA, H., ZHAO, Y., CHALLACOMBE, S., LAM, M. Y., DE SOUZA, Y., SCHIODT, J., HOLM, H., BISIO, P. A., GANDOLFO, M. S., SAWAKI, T., LI, M., ZHANG, W., VARGHESE-JACOB, B., IBSEN, P., KESZLER, A., KUROSE, N., NOJIMA, T., ODELL, E., CRISWELL, L. A., JORDAN, R. & GREENSPAN, J. S. 2011. Associations between salivary gland histopathologic diagnoses and phenotypic features of Sjogren's syndrome among 1,726 registry participants. *Arthritis and rheumatism,* 63**,** 2021-30.

DAWES, C., O'MULLANE, D. & ADGAR, M. 2012. *Saliva and oral health*, Stephen Nancocks Ltd.

DAYAN, M., ZINGER, H., KALUSH, F., MOR, G., AMIR-ZALTZMAN, Y., KOHEN, F., STHOEGER, Z. & MOZES, E. 1997. The beneficial effects of treatment with tamoxifen and anti-oestradiol antibody on experimental systemic lupus erythematosus are associated with cytokine modulations. *Immunology,* 90**,** 101-8.

DE TOGNI, P., GOELLNER, J., RUDDLE, N. H., STREETER, P. R., FICK, A., MARIATHASAN, S., SMITH, S. C., CARLSON, R., SHORNICK, L. P., STRAUSS-SCHOENBERGER, J. & ET AL. 1994. Abnormal development of peripheral lymphoid organs in mice deficient in lymphotoxin. *Science,* 264**,** 703-7.

DEL REY, M. J., FARE, R., IZQUIERDO, E., USATEGUI, A., RODRIGUEZ-FERNANDEZ, J. L., SUAREZ-FUEYO, A., CANETE, J. D. & PABLOS, J. L. 2014. Clinicopathological correlations of podoplanin (gp38) expression in rheumatoid synovium and its potential contribution to fibroblast platelet crosstalk. *PLoS One,* 9**,** e99607.

DELOVITCH, T. L. & SINGH, B. 1997. The nonobese diabetic mouse as a model of autoimmune diabetes: immune dysregulation gets the NOD. *Immunity,* 7**,** 727-38.

DENTON, A. E., ROBERTS, E. W., LINTERMAN, M. A. & FEARON, D. T. 2014. Fibroblastic reticular cells of the lymph node are required for retention of resting but not activated CD8+ T cells. *Proc Natl Acad Sci U S A,* 111**,** 12139-44.

DETEIX, C., ATTUIL-AUDENIS, V., DUTHEY, A., PATEY, N., MCGREGOR, B., DUBOIS, V., CALIGIURI, G., GRAFF-DUBOIS, S., MORELON, E. &

THAUNAT, O. 2010. Intragraft Th17 infiltrate promotes lymphoid neogenesis and hastens clinical chronic rejection. *J Immunol,* 184**,** 5344-51.

DIMITRIOU, I. D., KAPSOGEORGOU, E. K., MOUTSOPOULOS, H. M. & MANOUSSAKIS, M. N. 2002. CD40 on salivary gland epithelial cells: high constitutive expression by cultured cells from Sjogren's syndrome patients indicating their intrinsic activation. *Clin Exp Immunol,* 127**,** 386-92.

DOHI, O., OHTANI, H., HATORI, M., SATO, E., HOSAKA, M., NAGURA, H., ITOI, E. & KOKUBUN, S. 2009. Histogenesis-specific expression of fibroblast activation protein and dipeptidylpeptidase-IV in human bone and soft tissue tumours. *Histopathology,* 55**,** 432-40.

DOLZNIG, H., SCHWEIFER, N., PURI, C., KRAUT, N., RETTIG, W. J., KERJASCHKI, D. & GARIN-CHESA, P. 2005. Characterization of cancer stroma markers: *In silico* analysis of an mRNA expression database for fibroblast activation protein and endosialin. *Cancer Immunity,* 5**,** 1-9.

DONG, C., JUEDES, A. E., TEMANN, U. A., SHRESTA, S., ALLISON, J. P., RUDDLE, N. H. & FLAVELL, R. A. 2001a. ICOS co-stimulatory receptor is essential for T-cell activation and function. *Nature,* 409**,** 97-101.

DONG, C., TEMANN, U. A. & FLAVELL, R. A. 2001b. Cutting edge: critical role of inducible costimulator in germinal center reactions. *J Immunol,* 166**,** 3659-62.

DRAYTON, D. L., YING, X., LEE, J., LESSLAUER, W. & RUDDLE, N. H. 2003. Ectopic LT alpha beta directs lymphoid organ neogenesis with concomitant expression of peripheral node addressin and a HEV-restricted sulfotransferase. *J Exp Med,* 197**,** 1153-63.

DRUCKER, D. J. 2003. Therapeutic potential of dipeptidyl peptidase IV inhibitors for the treatment of type 2 diabetes. *Expert Opin Investig Drugs,* 12**,** 87-100.

EBERL, G. & LOCHNER, M. 2009. The development of intestinal lymphoid tissues at the interface of self and microbiota. *Mucosal Immunol,* 2**,** 478-85.

ECKERT, C., KIM, Y. O., JULICH, H., HEIER, E. C., KLEIN, N., KRAUSE, E., TSCHERNIG, T., KORNEK, M., LAMMERT, F., SCHUPPAN, D. & LUKACS-KORNEK, V. 2016. Podoplanin discriminates distinct stromal cell populations and a novel progenitor subset in the liver. *Am J Physiol Gastrointest Liver Physiol,* 310**,** G1-G12.

EKWALL, A. K., EISLER, T., ANDERBERG, C., JIN, C., KARLSSON, N., BRISSLERT, M. & BOKAREWA, M. I. 2011. The tumour-associated glycoprotein podoplanin is expressed in fibroblast-like synoviocytes of the hyperplastic synovial lining layer in rheumatoid arthritis. *Arthritis Res Ther,* 13**,** R40.

ENDRES, R., ALIMZHANOV, M. B., PLITZ, T., FUTTERER, A., KOSCO-VILBOIS, M. H., NEDOSPASOV, S. A., RAJEWSKY, K. & PFEFFER, K. 1999. Mature follicular dendritic cell networks depend on expression of lymphotoxin beta receptor by radioresistant stromal cells and of lymphotoxin beta and tumor necrosis factor by B cells. *J Exp Med,* 189**,** 159-68.

FAN, L., REILLY, C. R., LUO, Y., DORF, M. E. & LO, D. 2000. Cutting edge: ectopic expression of the chemokine TCA4/SLC is sufficient to trigger lymphoid neogenesis. *J Immunol,* 164**,** 3955-9.

FARR, A. G., BERRY, M. L., KIM, A., NELSON, A. J., WELCH, M. P. & ARUFFO, A. 1992. Characterization and cloning of a novel glycoprotein expressed by stromal cells in T-dependent areas of peripheral lymphoid tissues. *The Journal of experimental medicine,* 176**,** 1477-82.

FAZILLEAU, N., MCHEYZER-WILLIAMS, L. J., ROSEN, H. & MCHEYZER-WILLIAMS, M. G. 2009. The function of follicular helper T cells is regulated by the strength of T cell antigen receptor binding. *Nat Immunol,* 10**,** 375-84.

FEIG, C., JONES, J. O., KRAMAN, M., WELLS, R. J., DEONARINE, A., CHAN, D. S., CONNELL, C. M., ROBERTS, E. W., ZHAO, Q., CABALLERO, O. L., TEICHMANN, S. A., JANOWITZ, T., JODRELL, D. I., TUVESON, D. A. & FEARON, D. T. 2013. Targeting CXCL12 from FAP-expressing carcinoma-associated fibroblasts synergizes with anti-PD-L1 immunotherapy in pancreatic cancer. *Proc Natl Acad Sci U S A,* 110**,** 20212-7.

FILER, A., RAZA, K., SALMON, M. & BUCKLEY, C. D. 2007. Targeting stromal cells in chronic inflammation. *Discov Med,* 7**,** 20-6.

FINKE, D., ACHA-ORBEA, H., MATTIS, A., LIPP, M. & KRAEHENBUHL, J. 2002. CD4+CD3- cells induce Peyer's patch development: role of alpha4beta1 integrin activation by CXCR5. *Immunity,* 17**,** 363-73.

FINNEY, B. A., SCHWEIGHOFFER, E., NAVARRO-NUNEZ, L., BENEZECH, C., BARONE, F., HUGHES, C. E., LANGAN, S. A., LOWE, K. L., POLLITT, A. Y., MOURAO-SA, D., SHEARDOWN, S., NASH, G. B., SMITHERS, N., REIS E SOUSA, C., TYBULEWICZ, V. L. & WATSON, S. P. 2012. CLEC-2 and Syk in the megakaryocytic/platelet lineage are essential for development. *Blood,* 119**,** 1747-56.

FITZGERALD-BOCARSLY, P., DAI, J. & SINGH, S. 2008. Plasmacytoid dendritic cells and type I IFN: 50 years of convergent history. *Cytokine Growth Factor Rev,* 19**,** 3-19.

FLEIGE, H., RAVENS, S., MOSCHOVAKIS, G. L., BOLTER, J., WILLENZON, S., SUTTER, G., HAUSSLER, S., KALINKE, U., PRINZ, I. & FORSTER, R. 2014. IL-17-induced CXCL12 recruits B cells and induces follicle formation in BALT in the absence of differentiated FDCs. *J Exp Med,* 211**,** 643-51.

FLETCHER, A. L., ACTON, S. E. & KNOBLICH, K. 2015. Lymph node fibroblastic reticular cells in health and disease. *Nat Rev Immunol,* 15**,** 350-61.

FLETCHER, A. L., ELMAN, J. S., ASTARITA, J., MURRAY, R., SAEIDI, N., D'ROZARIO, J., KNOBLICH, K., BROWN, F. D., SCHILDBERG, F. A., NIEVES, J. M., HENG, T. S., BOYD, R. L., TURLEY, S. J. & PAREKKADAN, B. 2014. Lymph node fibroblastic reticular cell transplants show robust therapeutic efficacy in high-mortality murine sepsis. *Sci Transl Med,* 6**,** 249ra109.

FLETCHER, A. L., LUKACS-KORNEK, V., REYNOSO, E. D., PINNER, S. E., BELLEMARE-PELLETIER, A., CURRY, M. S., COLLIER, A. R., BOYD, R. L. & TURLEY, S. J. 2010. Lymph node fibroblastic reticular cells directly present peripheral tissue antigen under steady-state and inflammatory conditions. *J Exp Med,* 207**,** 689-97.

FORD, M. L., ADAMS, A. B. & PEARSON, T. C. 2014. Targeting co-stimulatory pathways: transplantation and autoimmunity. *Nat Rev Nephrol,* 10**,** 14-24.

FOS, C., SALLES, A., LANG, V., CARRETTE, F., AUDEBERT, S., PASTOR, S., GHIOTTO, M., OLIVE, D., BISMUTH, G. & NUNES, J. A. 2008. ICOS ligation recruits the p50alpha PI3K regulatory subunit to the immunological synapse. *J Immunol,* 181**,** 1969-77.

FOX, R. I. 2005. Sjogren's syndrome. *Lancet,* 366**,** 321-31.

FOX, R. I., TORNWALL, J. & MICHELSON, P. 1999. Current issues in the diagnosis and treatment of Sjogren's syndrome. *Current opinion in rheumatology,* 11**,** 364-71.

FREEMAN, G. J., LONG, A. J., IWAI, Y., BOURQUE, K., CHERNOVA, T., NISHIMURA, H., FITZ, L. J., MALENKOVICH, N., OKAZAKI, T., BYRNE, M. C., HORTON, H. F., FOUSER, L., CARTER, L., LING, V., BOWMAN, M. R., CARRENO, B. M., COLLINS, M., WOOD, C. R. & HONJO, T. 2000. Engagement of the PD-1 immunoinhibitory receptor by a novel B7 family member leads to negative regulation of lymphocyte activation. *J Exp Med,* 192**,** 1027-34.

FRUMAN, D. A. 2004. Phosphoinositide 3-kinase and its targets in B-cell and T-cell signaling. *Curr Opin Immunol,* 16**,** 314-20.

FU, Y. X., HUANG, G., MATSUMOTO, M., MOLINA, H. & CHAPLIN, D. D. 1997a. Independent signals regulate development of primary and secondary follicle structure in spleen and mesenteric lymph node. *Proc Natl Acad Sci U S A,* 94**,** 5739-43.

FU, Y. X., MOLINA, H., MATSUMOTO, M., HUANG, G., MIN, J. & CHAPLIN, D. D. 1997b. Lymphotoxin-alpha (LTalpha) supports development of splenic follicular structure that is required for IgG responses. *J Exp Med,* 185**,** 2111-20.

FURTADO, G. C., MARINKOVIC, T., MARTIN, A. P., GARIN, A., HOCH, B., HUBNER, W., CHEN, B. K., GENDEN, E., SKOBE, M. & LIRA, S. A. 2007. Lymphotoxin beta receptor signaling is required for inflammatory lymphangiogenesis in the thyroid. *Proc Natl Acad Sci U S A,* 104**,** 5026-31.

FURUZAWA-CARBALLEDA, J., SANCHEZ-GUERRERO, J., BETANZOS, J. L., ENRIQUEZ, A. B., AVILA-CASADO, C., LLORENTE, L. & HERNANDEZ-MOLINA, G. 2014. Differential cytokine expression and regulatory cells in patients with primary and secondary Sjogren's syndrome. *Scand J Immunol,* 80**,** 432-40.

GARIN-CHESA, P., BERESFORD, H. R., WALKER, S. & RETTIG, W. J. 1990a. Immunohistochemical analysis of the A4 and AO10 (gp110) cell-surface antigens of human astrocytoma. *Am J Pathol,* 136**,** 797-807.

GARIN-CHESA, P., OLD, L. J. & RETTIG, W. J. 1990b. Cell surface glycoprotein of reactive stromal fibroblasts as a potential antibody target in human epithelial cancers. *Proc Natl Acad Sci U S A,* 87**,** 7235-9.

GATUMU, M. K., SKARSTEIN, K., PAPANDILE, A., BROWNING, J. L., FAVA, R. A. & BOLSTAD, A. I. 2009. Blockade of lymphotoxin-beta receptor signaling reduces aspects of Sjogren's syndrome in salivary glands of non-obese diabetic mice. *Arthritis Res Ther,* 11**,** R24.

GERLI, R., MUSCAT, C., GIANSANTI, M., DANIELI, M. G., SCIUTO, M., GABRIELLI, A., FIANDRA, E. & VITALI, C. 1997. Quantitative assessment of salivary gland inflammatory infiltration in primary Sjogren's syndrome: its relationship to different demographic, clinical and serological features of the disorder. *British journal of rheumatology,* 36**,** 969-75.

GEURTSVANKESSEL, C. H., WILLART, M. A., BERGEN, I. M., VAN RIJT, L. S., MUSKENS, F., ELEWAUT, D., OSTERHAUS, A. D., HENDRIKS, R., RIMMELZWAAN, G. F. & LAMBRECHT, B. N. 2009. Dendritic cells are crucial for maintenance of tertiary lymphoid structures in the lung of influenza virus-infected mice. *J Exp Med,* 206**,** 2339-49.

GHERSI, G., DONG, H., GOLDSTEIN, L. A., YEH, Y., HAKKINEN, L., LARJAVA, H. S. & CHEN, W. T. 2002. Regulation of fibroblast migration on collagenous matrix by a cell surface peptidase complex. *J Biol Chem,* 277**,** 29231-41.

GIGOUX, M., SHANG, J., PAK, Y., XU, M., CHOE, J., MAK, T. W. & SUH, W. K. 2009. Inducible costimulator promotes helper T-cell differentiation through phosphoinositide 3-kinase. *Proc Natl Acad Sci U S A,* 106**,** 20371-6.

GIOVELLI, R. A., SANTOS, M. C., SERRANO, E. V. & VALIM, V. 2015. Clinical characteristics and biopsy accuracy in suspected cases of Sjogren's syndrome referred to labial salivary gland biopsy. *BMC musculoskeletal disorders,* 16**,** 30.

GOLDSTEIN, L. A., GHERSI, G., PINEIRO-SANCHEZ, M. L., SALAMONE, M., YEH, Y., FLESSATE, D. & CHEN, W. T. 1997. Molecular cloning of seprase: a serine integral membrane protease from human melanoma. *Biochim Biophys Acta,* 1361**,** 11-9.

GOMMERMAN, J. L., GIZA, K., PERPER, S., SIZING, I., NGAM-EK, A., NICKERSON-NUTTER, C. & BROWNING, J. L. 2003. A role for surface lymphotoxin in experimental autoimmune encephalomyelitis independent of LIGHT. *J Clin Invest,* 112**,** 755-67.

GONG, Y., ALSALEH, GHADA, SIBILIA, JEAN, GOTTENBERG, JACQUES-ERIC 2012. New Pathogenic Role of Salivary Gland Epithelial Cells in the Costimulation of T Lymphocytes in Primary Sjgren's Syndrome: 040 Ligand Expression, T-Cell Induction of OX40 and Promotion of T-Cell Survival, Proliferation and Activation. [abstract]. *Arthritis Rheum* 64.

GONZALEZ, S., AGUILERA, S., ALLIENDE, C., URZUA, U., QUEST, A. F., HERRERA, L., MOLINA, C., HERMOSO, M., EWERT, P., BRITO, M., ROMO, R., LEYTON, C., PEREZ, P. & GONZALEZ, M. J. 2011. Alterations in type I hemidesmosome components suggestive of epigenetic control in the salivary glands of patients with Sjogren's syndrome. *Arthritis and rheumatism,* 63**,** 1106-15.

GOODMAN, J. D., ROZYPAL, T. L. & KELLY, T. 2003. Seprase, a membrane-bound protease, alleviates the serum growth requirement of human breast cancer cells. *Clin Exp Metastasis,* 20**,** 459-70.

GOTTENBERG, J. E., CAGNARD, N., LUCCHESI, C., LETOURNEUR, F., MISTOU, S., LAZURE, T., JACQUES, S., BA, N., ITTAH, M., LEPAJOLEC, C., LABETOULLE, M., ARDIZZONE, M., SIBILIA, J., FOURNIER, C., CHIOCCHIA, G. & MARIETTE, X. 2006. Activation of IFN pathways and plasmacytoid dendritic cell recruitment in target organs of primary Sjogren's syndrome. *Proc Natl Acad Sci U S A,* 103**,** 2770-5.

GRABNER, R., LOTZER, K., DOPPING, S., HILDNER, M., RADKE, D., BEER, M., SPANBROEK, R., LIPPERT, B., REARDON, C. A., GETZ, G. S., FU, Y. X., HEHLGANS, T., MEBIUS, R. E., VAN DER WALL, M., KRUSPE, D., ENGLERT, C., LOVAS, A., HU, D., RANDOLPH, G. J., WEIH, F. & HABENICHT, A. J. 2009. Lymphotoxin beta receptor signaling promotes tertiary lymphoid organogenesis in the aorta adventitia of aged ApoE-/- mice. *J Exp Med,* 206**,** 233-48.

GREAVES, W. O. & WANG, S. A. 2011. Selected topics on lymphoid lesions in the head and neck regions. *Head and neck pathology,* 5**,** 41-50.

GREENSPAN, J. S., DANIELS, T. E., TALAL, N. & SYLVESTER, R. A. 1974. The histopathology of Sjogren's syndrome in labial salivary gland biopsies. *Oral surgery, oral medicine, and oral pathology,* 37**,** 217-29.

GREETHAM, D., ELLIS, C. D., MEWAR, D., FEARON, U., AN ULTAIGH, S. N., VEALE, D. J., GUESDON, F. & WILSON, A. G. 2007. Functional characterization of NF-kappaB inhibitor-like protein 1 (NFkappaBIL1), a candidate susceptibility gene for rheumatoid arthritis. *Hum Mol Genet,* 16**,** 3027-36.

GRIMBACHER, B., HUTLOFF, A., SCHLESIER, M., GLOCKER, E., WARNATZ, K., DRAGER, R., EIBEL, H., FISCHER, B., SCHAFFER, A. A., MAGES, H. W., KROCZEK, R. A. & PETER, H. H. 2003. Homozygous loss of ICOS is associated with adult-onset common variable immunodeficiency. *Nature immunology,* 4**,** 261-8.

GROGER, M., LOEWE, R., HOLNTHONER, W., EMBACHER, R., PILLINGER, M., HERRON, G. S., WOLFF, K. & PETZELBAUER, P. 2004. IL-3 induces expression of lymphatic markers Prox-1 and podoplanin in human endothelial cells. *J Immunol,* 173**,** 7161-9.

HALDORSEN, K., MOEN, K., JACOBSEN, H., JONSSON, R. & BRUN, J. G. 2008. Exocrine function in primary Sjogren syndrome: natural course and prognostic factors. *Annals of the rheumatic diseases,* 67**,** 949-54.

HALLAS, C., GREINER, A., PETERS, K. & MULLER-HERMELINK, H. K. 1998. Immunoglobulin VH genes of high-grade mucosa-associated lymphoid tissue lymphomas show a high load of somatic mutations and evidence of antigen-dependent affinity maturation. *Lab Invest,* 78**,** 277-87.

HAMEL, K. M., CAO, Y., OLALEKAN, S. A. & FINNEGAN, A. 2014. B cell-specific expression of inducible costimulator ligand is necessary for the induction of arthritis in mice. *Arthritis Rheumatol,* 66**,** 60-7.

HARA, T. & FU, S. M. 1985. Human T cell activation. I. Monocyte-independent activation and proliferation induced by anti-T3 monoclonal antibodies in the presence of tumor promoter 12-o-tetradecanoyl phorbol-13 acetate. *J Exp Med,* 161**,** 641-56.

HARRIS, N. L. 1999. Lymphoid proliferations of the salivary glands. *American journal of clinical pathology,* 111**,** S94-103.

HAYNES, N. M., ALLEN, C. D., LESLEY, R., ANSEL, K. M., KILLEEN, N. & CYSTER, J. G. 2007. Role of CXCR5 and CCR7 in follicular Th cell positioning and appearance of a programmed cell death gene-1high germinal center-associated subpopulation. *J Immunol,* 179**,** 5099-108.

HENRY, L. R., LEE, H. O., LEE, J. S., KLEIN-SZANTO, A., WATTS, P., ROSS, E. A., CHEN, W. T. & CHENG, J. D. 2007. Clinical implications of fibroblast activation protein in patients with colon cancer. *Clin Cancer Res,* 13**,** 1736-41.

HERZOG, B. H., FU, J., WILSON, S. J., HESS, P. R., SEN, A., MCDANIEL, J. M., PAN, Y., SHENG, M., YAGO, T., SILASI-MANSAT, R., MCGEE, S., MAY, F., NIESWANDT, B., MORRIS, A. J., LUPU, F., COUGHLIN, S. R., MCEVER, R. P., CHEN, H., KAHN, M. L. & XIA, L. 2013. Podoplanin maintains high endothelial venule integrity by interacting with platelet CLEC-2. *Nature,* 502**,** 105-9.

HJELMSTROM, P. 2001. Lymphoid neogenesis: de novo formation of lymphoid tissue in chronic inflammation through expression of homing chemokines. *J Leukoc Biol,* 69**,** 331-9.

HOLSINGER, F. & BUI, D. 2007. *Salivary Gland Disorders - Anatomy, Function, and Evaluation of the Salivary Glands*, Springer Berlin Heidelberg.

HONDA, K., NAKANO, H., YOSHIDA, H., NISHIKAWA, S., RENNERT, P., IKUTA, K., TAMECHIKA, M., YAMAGUCHI, K., FUKUMOTO, T., CHIBA, T. & NISHIKAWA, S. I. 2001. Molecular basis for hematopoietic/mesenchymal interaction during initiation of Peyer's patch organogenesis. *J Exp Med,* 193**,** 621-30.

HONDOWICZ, B. D., BATHEJA, A. O., METZGAR, M. H., CATON, A. J. & ERIKSON, J. 2010. ICOS expression by effector T cells influences the ability of regulatory T cells to inhibit anti-chromatin B cell responses in recipient mice. *J Autoimmun,* 34**,** 460-8.

HONG, Y. K., HARVEY, N., NOH, Y. H., SCHACHT, V., HIRAKAWA, S., DETMAR, M. & OLIVER, G. 2002. Prox1 is a master control gene in the program specifying lymphatic endothelial cell fate. *Developmental dynamics : an official publication of the American Association of Anatomists,* 225**,** 351-7.

HOU, T. Z., BYSTROM, J., SHERLOCK, J. P., QURESHI, O., PARNELL, S. M., ANDERSON, G., GILROY, D. W. & BUCKLEY, C. D. 2010. A distinct subset of podoplanin (gp38) expressing F4/80+ macrophages mediate phagocytosis and are induced following zymosan peritonitis. *FEBS Lett,* 584**,** 3955-61.

HU, D., MOHANTA, S. K., YIN, C., PENG, L., MA, Z., SRIKAKULAPU, P., GRASSIA, G., MACRITCHIE, N., DEVER, G., GORDON, P., BURTON, F. L., IALENTI, A., SABIR, S. R., MCINNES, I. B., BREWER, J. M., GARSIDE, P., WEBER, C., LEHMANN, T., TEUPSER, D., HABENICHT, L., BEER, M., GRABNER, R., MAFFIA, P., WEIH, F. & HABENICHT, A. J. 2015. Artery Tertiary Lymphoid Organs Control Aorta Immunity and Protect against Atherosclerosis via Vascular Smooth Muscle Cell Lymphotoxin beta Receptors. *Immunity,* 42**,** 1100-15.

HU, Y. L., METZ, D. P., CHUNG, J., SIU, G. & ZHANG, M. 2009. B7RP-1 blockade ameliorates autoimmunity through regulation of follicular helper T cells. *J Immunol,* 182**,** 1421-8.

HUTLOFF, A., BUCHNER, K., REITER, K., BAELDE, H. J., ODENDAHL, M., JACOBI, A., DORNER, T. & KROCZEK, R. A. 2004. Involvement of inducible costimulator in the exaggerated memory B cell and plasma cell generation in systemic lupus erythematosus. *Arthritis Rheum,* 50**,** 3211-20.

HUTLOFF, A., DITTRICH, A. M., BEIER, K. C., ELJASCHEWITSCH, B., KRAFT, R., ANAGNOSTOPOULOS, I. & KROCZEK, R. A. 1999. ICOS is an inducible T-cell co-stimulator structurally and functionally related to CD28. *Nature,* 397**,** 263-6.

IIYAMA, R., KANAI, T., URAUSHIHARA, K., TOTSUKA, T., NAKAMURA, T., MIYATA, T., YAGITA, H., KUSHI, A., SUZUKI, K., TEZUKA, K. & WATANABE, M. 2003. The role of inducible co-stimulator (ICOS)/B7-related protein-1 (B7RP-1) interaction in the functional development of Peyer's patches. *Immunol Lett,* 88**,** 63-70.

IWAI, H., KOZONO, Y., HIROSE, S., AKIBA, H., YAGITA, H., OKUMURA, K., KOHSAKA, H., MIYASAKA, N. & AZUMA, M. 2002. Amelioration of collagen-induced arthritis by blockade of inducible costimulator-B7 homologous protein costimulation. *J Immunol,* 169**,** 4332-9.

IWANO, M., PLIETH, D., DANOFF, T. M., XUE, C., OKADA, H. & NEILSON, E. G. 2002. Evidence that fibroblasts derive from epithelium during tissue fibrosis. *The Journal of clinical investigation,* 110**,** 341-50.

IWASA, S., OKADA, K., CHEN, W. T., JIN, X., YAMANE, T., OOI, A. & MITSUMATA, M. 2005. 'Increased expression of seprase, a membrane-type serine protease, is associated with lymph node metastasis in human colorectal cancer'. *Cancer Lett,* 227**,** 229-36.

JIN, L., YU, D., LI, X., YU, N., LI, X., WANG, Y. & WANG, Y. 2014. CD4+CXCR5+ follicular helper T cells in salivary gland promote B cells maturation in patients with primary Sjogren's syndrome. *Int J Clin Exp Pathol,* 7**,** 1988-96.

JONES, G. W., BOMBARDIERI, M., GREENHILL, C. J., MCLEOD, L., NERVIANI, A., ROCHER-ROS, V., CARDUS, A., WILLIAMS, A. S., PITZALIS, C., JENKINS, B. J. & JONES, S. A. 2015. Interleukin-27 inhibits ectopic lymphoid-like structure development in early inflammatory arthritis. *J Exp Med,* 212**,** 1793-802.

JONSSON, M. V., SALOMONSSON, S., OIJORDSBAKKEN, G. & SKARSTEIN, K. 2005. Elevated serum levels of soluble E-cadherin in patients with primary Sjogren's syndrome. *Scand J Immunol,* 62**,** 552-9.

KALLURI, R. & NEILSON, E. G. 2003. Epithelial-mesenchymal transition and its implications for fibrosis. *The Journal of clinical investigation,* 112**,** 1776-84.

KATSIFIS, G. E., REKKA, S., MOUTSOPOULOS, N. M., PILLEMER, S. & WAHL, S. M. 2009. Systemic and local interleukin-17 and linked cytokines associated with Sjogren's syndrome immunopathogenesis. *Am J Pathol,* 175**,** 1167-77.

KAWAMOTO, M., HARIGAI, M., HARA, M., KAWAGUCHI, Y., TEZUKA, K., TANAKA, M., SUGIURA, T., KATSUMATA, Y., FUKASAWA, C., ICHIDA, H., HIGAMI, S. & KAMATANI, N. 2006. Expression and function of inducible co-stimulator in patients with systemic lupus erythematosus: possible involvement in excessive interferon-gamma and anti-double-stranded DNA antibody production. *Arthritis Res Ther,* 8**,** R62.

KELLY, T., KECHELAVA, S., ROZYPAL, T. L., WEST, K. W. & KOROURIAN, S. 1998. Seprase, a membrane-bound protease, is overexpressed by invasive ductal carcinoma cells of human breast cancers. *Mod Pathol,* 11**,** 855-63.

KELLY, T., MUELLER, S. C., YEH, Y. & CHEN, W. T. 1994. Invadopodia promote proteolysis of a wide variety of extracellular matrix proteins. *J Cell Physiol,* 158**,** 299-308.

KHACHIGIAN, L. M. 2006. Early growth response-1 in cardiovascular pathobiology. *Circ Res,* 98**,** 186-91.

KHAN, O., HEADLEY, M., GERARD, A., WEI, W., LIU, L. & KRUMMEL, M. F. 2011. Regulation of T cell priming by lymphoid stroma. *PLoS One,* 6**,** e26138.

KIM, J. H., CHOI, Y. J., LEE, B. H., SONG, M. Y., BAN, C. Y., KIM, J., PARK, J., KIM, S. E., KIM, T. G., PARK, S. H., KIM, H. P., SUNG, Y. C., KIM, S. C. & SHIN, E. C. 2016. Programmed cell death ligand 1 alleviates psoriatic inflammation by suppressing IL-17A production from programmed cell death 1-high T cells. *J Allergy Clin Immunol*.

KIM, J. R., LIM, H. W., KANG, S. G., HILLSAMER, P. & KIM, C. H. 2005. Human CD57+ germinal center-T cells are the major helpers for GC-B cells and induce class switch recombination. *BMC Immunol,* 6**,** 3.

KLIMIUK, P. A., GORONZY, J. J., BJOR NSSON, J., BECKENBAUGH, R. D. & WEYAND, C. M. 1997. Tissue cytokine patterns distinguish variants of rheumatoid synovitis. *Am J Pathol,* 151**,** 1311-9.

KRAMAN, M., BAMBROUGH, P. J., ARNOLD, J. N., ROBERTS, E. W., MAGIERA, L., JONES, J. O., GOPINATHAN, A., TUVESON, D. A. & FEARON, D. T. 2010. Suppression of antitumor immunity by stromal cells expressing fibroblast activation protein-alpha. *Science,* 330**,** 827-30.

KRAMER, J. M., KLIMATCHEVA, E. & ROTHSTEIN, T. L. 2013. CXCL13 is elevated in Sjogren's syndrome in mice and humans and is implicated in disease pathogenesis. *Journal of leukocyte biology,* 94**,** 1079-89.

KRATZ, A., CAMPOS-NETO, A., HANSON, M. S. & RUDDLE, N. H. 1996. Chronic inflammation caused by lymphotoxin is lymphoid neogenesis. *J Exp Med,* 183**,** 1461-72.

KROCZEK, R. A., GRAF, D., BRUGNONI, D., GILIANI, S., KORTHUER, U., UGAZIO, A., SENGER, G., MAGES, H. W., VILLA, A. & NOTARANGELO, L. D. 1994. Defective expression of CD40 ligand on T cells causes "X-linked immunodeficiency with hyper-IgM (HIGM1)". *Immunol Rev,* 138**,** 39-59.

LATCHMAN, Y., WOOD, C. R., CHERNOVA, T., CHAUDHARY, D., BORDE, M., CHERNOVA, I., IWAI, Y., LONG, A. J., BROWN, J. A., NUNES, R., GREENFIELD, E. A., BOURQUE, K., BOUSSIOTIS, V. A., CARTER, L. L., CARRENO, B. M., MALENKOVICH, N., NISHIMURA, H., OKAZAKI, T., HONJO, T., SHARPE, A. H. & FREEMAN, G. J. 2001. PD-L2 is a second ligand for PD-1 and inhibits T cell activation. *Nat Immunol,* 2**,** 261-8.

LEE, H. O., MULLINS, S. R., FRANCO-BARRAZA, J., VALIANOU, M., CUKIERMAN, E. & CHENG, J. D. 2011. FAP-overexpressing fibroblasts produce an extracellular matrix that enhances invasive velocity and directionality of pancreatic cancer cells. *BMC Cancer,* 11**,** 245.

LEE, Y., CHIN, R. K., CHRISTIANSEN, P., SUN, Y., TUMANOV, A. V., WANG, J., CHERVONSKY, A. V. & FU, Y. X. 2006. Recruitment and activation of naive T cells in the islets by lymphotoxin beta receptor-dependent tertiary lymphoid structure. *Immunity,* 25**,** 499-509.

LENSCHOW, D. J., WALUNAS, T. L. & BLUESTONE, J. A. 1996. CD28/B7 system of T cell costimulation. *Annu Rev Immunol,* 14**,** 233-58.

LEVY, M. T., MCCAUGHAN, G. W., ABBOTT, C. A., PARK, J. E., CUNNINGHAM, A. M., MULLER, E., RETTIG, W. J. & GORRELL, M. D. 1999. Fibroblast activation protein: a cell surface dipeptidyl peptidase and gelatinase expressed by stellate cells at the tissue remodelling interface in human cirrhosis. *Hepatology,* 29**,** 1768-78.

LI, X. Y., WU, Z. B., DING, J., ZHENG, Z. H., LI, X. Y., CHEN, L. N. & ZHU, P. 2012. Role of the frequency of blood CD4(+) CXCR5(+) CCR6(+) T cells in autoimmunity in patients with Sjogren's syndrome. *Biochem Biophys Res Commun,* 422**,** 238-44.

LIANG, L., PORTER, E. M. & SHA, W. C. 2002. Constitutive expression of the B7h ligand for inducible costimulator on naive B cells is extinguished after activation by distinct B cell receptor and interleukin 4 receptor-mediated pathways and can be rescued by CD40 signaling. *J Exp Med,* 196**,** 97-108.

LINDHOUT, E., VAN EIJK, M., VAN PEL, M., LINDEMAN, J., DINANT, H. J. & DE GROOT, C. 1999. Fibroblast-like synoviocytes from rheumatoid arthritis

patients have intrinsic properties of follicular dendritic cells. *J Immunol,* 162**,** 5949-56.

LINK, A., HARDIE, D. L., FAVRE, S., BRITSCHGI, M. R., ADAMS, D. H., SIXT, M., CYSTER, J. G., BUCKLEY, C. D. & LUTHER, S. A. 2011. Association of T-zone reticular networks and conduits with ectopic lymphoid tissues in mice and humans. *Am J Pathol,* 178**,** 1662-75.

LINK, A., VOGT, T. K., FAVRE, S., BRITSCHGI, M. R., ACHA-ORBEA, H., HINZ, B., CYSTER, J. G. & LUTHER, S. A. 2007. Fibroblastic reticular cells in lymph nodes regulate the homeostasis of naive T cells. *Nat Immunol,* 8**,** 1255-65.

LIRA, S. A. 2005. A passport into the lymph node. *Nat Immunol,* 6**,** 866-8.

LOCHNER, M., OHNMACHT, C., PRESLEY, L., BRUHNS, P., SI-TAHAR, M., SAWA, S. & EBERL, G. 2011. Microbiota-induced tertiary lymphoid tissues aggravate inflammatory disease in the absence of RORgamma t and LTi cells. *J Exp Med,* 208**,** 125-34.

LUCAS, P. J., NEGISHI, I., NAKAYAMA, K., FIELDS, L. E. & LOH, D. Y. 1995. Naive CD28-deficient T cells can initiate but not sustain an in vitro antigen-specific immune response. *J Immunol,* 154**,** 5757-68.

LUKACS-KORNEK, V., MALHOTRA, D., FLETCHER, A. L., ACTON, S. E., ELPEK, K. G., TAYALIA, P., COLLIER, A. R. & TURLEY, S. J. 2011. Regulated release of nitric oxide by nonhematopoietic stroma controls expansion of the activated T cell pool in lymph nodes. *Nat Immunol,* 12**,** 1096-104.

LUTHER, S. A., BIDGOL, A., HARGREAVES, D. C., SCHMIDT, A., XU, Y., PANIYADI, J., MATLOUBIAN, M. & CYSTER, J. G. 2002. Differing activities of homeostatic chemokines CCL19, CCL21, and CXCL12 in lymphocyte and dendritic cell recruitment and lymphoid neogenesis. *Journal of immunology,* 169**,** 424-33.

LUTHER, S. A., TANG, H. L., HYMAN, P. L., FARR, A. G. & CYSTER, J. G. 2000. Coexpression of the chemokines ELC and SLC by T zone stromal cells and deletion of the ELC gene in the plt/plt mouse. *Proceedings of the National Academy of Sciences of the United States of America,* 97**,** 12694-9.

MA, J., ZHU, C., MA, B., TIAN, J., BAIDOO, S. E., MAO, C., WU, W., CHEN, J., TONG, J., YANG, M., JIAO, Z., XU, H., LU, L. & WANG, S. 2012. Increased frequency of circulating follicular helper T cells in patients with rheumatoid arthritis. *Clin Dev Immunol,* 2012**,** 827480.

MACLENNAN, I. C. 1994. Germinal centers. *Annu Rev Immunol,* 12**,** 117-39.

MAGLIONE, P. J., XU, J. & CHAN, J. 2007. B cells moderate inflammatory progression and enhance bacterial containment upon pulmonary challenge with Mycobacterium tuberculosis. *J Immunol,* 178**,** 7222-34.

MAK, T. W., SHAHINIAN, A., YOSHINAGA, S. K., WAKEHAM, A., BOUCHER, L. M., PINTILIE, M., DUNCAN, G., GAJEWSKA, B. U., GRONSKI, M., ERIKSSON, U., ODERMATT, B., HO, A., BOUCHARD, D., WHORISKY, J. S., JORDANA, M., OHASHI, P. S., PAWSON, T., BLADT, F. & TAFURI, A. 2003. Costimulation through the inducible costimulator ligand is essential for both T helper and B cell functions in T cell-dependent B cell responses. *Nature immunology,* 4**,** 765-72.

MALLADI, A. S., SACK, K. E., SHIBOSKI, S. C., SHIBOSKI, C. H., BAER, A. N., BANUSHREE, R., DONG, Y., HELIN, P., KIRKHAM, B. W., LI, M., SUGAI, S., UMEHARA, H., VIVINO, F. B., VOLLENWEIDER, C. F., ZHANG, W., ZHAO, Y., GREENSPAN, J. S., DANIELS, T. E. & CRISWELL, L. A. 2012. Primary

Sjogren's syndrome as a systemic disease: a study of participants enrolled in an international Sjogren's syndrome registry. *Arthritis care & research,* 64**,** 911-8.

MANZO, A., BUGATTI, S., CAPORALI, R., PREVO, R., JACKSON, D. G., UGUCCIONI, M., BUCKLEY, C. D., MONTECUCCO, C. & PITZALIS, C. 2007. CCL21 expression pattern of human secondary lymphoid organ stroma is conserved in inflammatory lesions with lymphoid neogenesis. *Am J Pathol,* 171**,** 1549-62.

MANZO, A., PAOLETTI, S., CARULLI, M., BLADES, M. C., BARONE, F., YANNI, G., FITZGERALD, O., BRESNIHAN, B., CAPORALI, R., MONTECUCCO, C., UGUCCIONI, M. & PITZALIS, C. 2005. Systematic microanatomical analysis of CXCL13 and CCL21 in situ production and progressive lymphoid organization in rheumatoid synovitis. *Eur J Immunol,* 35**,** 1347-59.

MARINKOVIC, T., GARIN, A., YOKOTA, Y., FU, Y. X., RUDDLE, N. H., FURTADO, G. C. & LIRA, S. A. 2006. Interaction of mature CD3+CD4+ T cells with dendritic cells triggers the development of tertiary lymphoid structures in the thyroid. *J Clin Invest,* 116**,** 2622-32.

MARINKOVICH, M. P., KEENE, D. R., RIMBERG, C. S. & BURGESON, R. E. 1993. Cellular origin of the dermal-epidermal basement membrane. *Developmental dynamics : an official publication of the American Association of Anatomists,* 197**,** 255-67.

MATHEW, S., SCANLAN, M. J., MOHAN RAJ, B. K., MURTY, V. V. V. S., GARIN-CHESA, P., OLD, L. J., RETTIG, W. J. & CHAGANTI, R. S. K. 1995. The Gene for Fibroblast Activation Protein (FAP), a Putative Cell Surface-Bound Serine Protease Expressed in Cancer Stroma and Wound Healing, Maps to Chromosome Band 2q23. *Genomics,* 25**,** 335-337.

MCADAM, A. J., GREENWALD, R. J., LEVIN, M. A., CHERNOVA, T., MALENKOVICH, N., LING, V., FREEMAN, G. J. & SHARPE, A. H. 2001. ICOS is critical for CD40-mediated antibody class switching. *Nature,* 409**,** 102-5.

MCINDOE, R. A., BOHLMAN, B., CHI, E., SCHUSTER, E., LINDHARDT, M. & HOOD, L. 1999. Localization of non-Mhc collagen-induced arthritis susceptibility loci in DBA/1j mice. *Proceedings of the National Academy of Sciences of the United States of America,* 96**,** 2210-4.

MEBIUS, R. E. 2003. Organogenesis of lymphoid tissues. *Nature reviews. Immunology,* 3**,** 292-303.

MEBIUS, R. E. 2007. Lymphoid organogenesis: Educating stroma. *Immunol Cell Biol,* 85**,** 79-80.

MEBIUS, R. E., RENNERT, P. & WEISSMAN, I. L. 1997. Developing lymph nodes collect CD4+CD3- LTbeta+ cells that can differentiate to APC, NK cells, and follicular cells but not T or B cells. *Immunity,* 7**,** 493-504.

MEIER, D., BORNMANN, C., CHAPPAZ, S., SCHMUTZ, S., OTTEN, L. A., CEREDIG, R., ACHA-ORBEA, H. & FINKE, D. 2007. Ectopic lymphoid-organ development occurs through interleukin 7-mediated enhanced survival of lymphoid-tissue-inducer cells. *Immunity,* 26**,** 643-54.

MERKENSCHLAGER, M. & BEVERLEY, P. C. 1989. Evidence for differential expression of CD45 isoforms by precursors for memory-dependent and independent cytotoxic responses: human CD8 memory CTLp selectively express CD45RO (UCHL1). *Int Immunol,* 1**,** 450-9.

MILNER, J. M., KEVORKIAN, L., YOUNG, D. A., JONES, D., WAIT, R., DONELL, S. T., BARKSBY, E., PATTERSON, A. M., MIDDLETON, J., CRAVATT, B. F., CLARK, I. M., ROWAN, A. D. & CAWSTON, T. E. 2006. Fibroblast activation protein alpha is expressed by chondrocytes following a pro-inflammatory stimulus and is elevated in osteoarthritis. *Arthritis Res Ther,* 8**,** R23.

MITTAL, S., REVELL, M., BARONE, F., HARDIE, D. L., MATHARU, G. S., DAVENPORT, A. J., MARTIN, R. A., GRANT, M., MOSSELMANS, F., PYNSENT, P., SUMATHI, V. P., ADDISON, O., REVELL, P. A. & BUCKLEY, C. D. 2013. Lymphoid aggregates that resemble tertiary lymphoid organs define a specific pathological subset in metal-on-metal hip replacements. *PLoS One,* 8**,** e63470.

MONSKY, W. L., LIN, C. Y., AOYAMA, A., KELLY, T., AKIYAMA, S. K., MUELLER, S. C. & CHEN, W. T. 1994. A potential marker protease of invasiveness, seprase, is localized on invadopodia of human malignant melanoma cells. *Cancer Res,* 54**,** 5702-10.

MORI, Y., KONO, K., MATSUMOTO, Y., FUJII, H., YAMANE, T., MITSUMATA, M. & CHEN, W. T. 2004. The expression of a type II transmembrane serine protease (Seprase) in human gastric carcinoma. *Oncology,* 67**,** 411-9.

MOUTSOPOULOS, H. M. 1994. Sjogren's syndrome: autoimmune epithelitis. *Clinical immunology and immunopathology,* 72**,** 162-5.

MOUTSOPOULOS, H. M. & MANOUSSAKIS, M. N. 1998. Lumping or splitting autoimmune rheumatic disorders? Lessons from Sjogren's syndrome. *British journal of rheumatology,* 37**,** 1263-4.

MOYRON-QUIROZ, J. E., RANGEL-MORENO, J., KUSSER, K., HARTSON, L., SPRAGUE, F., GOODRICH, S., WOODLAND, D. L., LUND, F. E. & RANDALL, T. D. 2004. Role of inducible bronchus associated lymphoid tissue (iBALT) in respiratory immunity. *Nat Med,* 10**,** 927-34.

MUELLER, S. N. & GERMAIN, R. N. 2009. Stromal cell contributions to the homeostasis and functionality of the immune system. *Nature reviews. Immunology,* 9**,** 618-29.

NAKAE, S., IWAKURA, Y., SUTO, H. & GALLI, S. J. 2007. Phenotypic differences between Th1 and Th17 cells and negative regulation of Th1 cell differentiation by IL-17. *J Leukoc Biol,* 81**,** 1258-68.

NANJI, S. A., HANCOCK, W. W., LUO, B., SCHUR, C. D., PAWLICK, R. L., ZHU, L. F., ANDERSON, C. C. & SHAPIRO, A. M. 2006. Costimulation blockade of both inducible costimulator and CD40 ligand induces dominant tolerance to islet allografts and prevents spontaneous autoimmune diabetes in the NOD mouse. *Diabetes,* 55**,** 27-33.

NAYLOR, A. J., FILER, A. & BUCKLEY, C. D. 2013. The role of stromal cells in the persistence of chronic inflammation. *Clin Exp Immunol,* 171**,** 30-5.

NEYT, K., PERROS, F., GEURTSVANKESSEL, C. H., HAMMAD, H. & LAMBRECHT, B. N. 2012. Tertiary lymphoid organs in infection and autoimmunity. *Trends Immunol,* 33**,** 297-305.

NGO, V. N., CORNALL, R. J. & CYSTER, J. G. 2001. Splenic T zone development is B cell dependent. *J Exp Med,* 194**,** 1649-60.

NIEDERMEYER, J., ENENKEL, B., PARK, J. E., LENTER, M. C., RETTIG, W. J., DAMM, K. & SCHNAPP, A. 1998. Mouse fibroblast-activation protein - Conserved *Fap* gene organization and biochemical function as a serine protease. *Eur. J. Biochem.,* 254**,** 650-654.

NIEDERMEYER, J., GARIN-CHESA, P., KRIZ, M., HILBERG, F., MUELLER, E., BAMBERGER, U., RETTIG, W. J. & SCHNAPP, A. 2001. Expression of the fibroblast activation protein during mouse embryo development. *Int. J. Dev. Biol.,* 45.

NIEDERMEYER, J., KRIZ, M., HILBERG, F., GARIN-CHESA, P., BAMBERGER, U., LENTER, M. C., PARK, J., VIERTEL, B., PÜSCHNER, H., MAUZ, M., RETTIG, W. J. & SCHNAPP, A. 2000. Targeted Disruption of Mouse Fibroblast Activation Protein. *Mol. Cell. Biol.,* 20**,** 1089-1094.

NIEDERMEYER, J., SCANLAN, M. J., GARIN-CHESA, P., DAIBER, C., FIEBIG, H. H., OLD, L. J., RETTIG, W. J. & SCHNAPP, A. 1997. Mouse Fibroblast Activation Protein: Molecular Cloning, Alternative Splicing and Expression in the Reactive Stroma of Epithelial Cancers. *Int. J. Cancer,* 71**,** 383-389.

NISHIKAWA, S. I., HASHI, H., HONDA, K., FRASER, S. & YOSHIDA, H. 2000. Inflammation, a prototype for organogenesis of the lymphopoietic/hematopoietic system. *Curr Opin Immunol,* 12**,** 342-5.

NURIEVA, R. I. 2005. Regulation of immune and autoimmune responses by ICOS-B7h interaction. *Clin Immunol,* 115**,** 19-25.

O'ROURKE, K. P., O'DONOGHUE, G., ADAMS, C., MULCAHY, H., MOLLOY, C., SILKE, C., MOLLOY, M., SHANAHAN, F. & O'GARA, F. 2008. High levels of Lymphotoxin-Beta (LT-Beta) gene expression in rheumatoid arthritis synovium: clinical and cytokine correlations. *Rheumatol Int,* 28**,** 979-86.

OIKONOMIDOU, O., VLACHOYIANNOPOULOS, P. G., KOMINAKIS, A., KALOFOUTIS, A., MOUTSOPOULOS, H. M. & MOUTSATSOU, P. 2006. Glucocorticoid receptor, nuclear factor kappaB, activator protein-1 and C-jun N-terminal kinase in systemic lupus erythematosus patients. *Neuroimmunomodulation,* 13**,** 194-204.

OKAMOTO, T., SAITO, S., YAMANAKA, H., TOMATSU, T., KAMATANI, N., OGIUCHI, H., UCHIYAMA, T. & YAGI, J. 2003. Expression and function of the co-stimulator H4/ICOS on activated T cells of patients with rheumatoid arthritis. *J Rheumatol,* 30**,** 1157-63.

PARK, J. E., LENTER, M. C., ZIMMERMANN, R. N., GARIN-CHESA, P., OLD, L. J. & RETTIG, W. J. 1999. Fibroblast activation protein, a dual specificity serine protease expressed in reactive human tumor stromal fibroblasts. *J Biol Chem,* 274**,** 36505-12.

PARRY, R. V., RUMBLEY, C. A., VANDENBERGHE, L. H., JUNE, C. H. & RILEY, J. L. 2003. CD28 and inducible costimulatory protein Src homology 2 binding domains show distinct regulation of phosphatidylinositol 3-kinase, Bcl-xL, and IL-2 expression in primary human CD4 T lymphocytes. *J Immunol,* 171**,** 166-74.

PARSONAGE, G., FILER, A. D., HAWORTH, O., NASH, G. B., RAINGER, G. E., SALMON, M. & BUCKLEY, C. D. 2005. A stromal address code defined by fibroblasts. *Trends Immunol,* 26**,** 150-6.

PEACH, R. J., BAJORATH, J., BRADY, W., LEYTZE, G., GREENE, J., NAEMURA, J. & LINSLEY, P. S. 1994. Complementarity determining region 1 (CDR1)- and CDR3-analogous regions in CTLA-4 and CD28 determine the binding to B7-1. *J Exp Med,* 180**,** 2049-58.

PEDUTO, L., DULAUROY, S., LOCHNER, M., SPATH, G. F., MORALES, M. A., CUMANO, A. & EBERL, G. 2009. Inflammation recapitulates the ontogeny of lymphoid stromal cells. *J Immunol,* 182**,** 5789-99.

PENA, A. S. & PENATE, M. 2002. Genetic susceptibility and regulation of inflammation in Crohn's disease. Relationship with the innate immune system. *Rev Esp Enferm Dig,* 94**,** 351-60.

PETERS, A., PITCHER, L. A., SULLIVAN, J. M., MITSDOERFFER, M., ACTON, S. E., FRANZ, B., WUCHERPFENNIG, K., TURLEY, S., CARROLL, M. C., SOBEL, R. A., BETTELLI, E. & KUCHROO, V. K. 2011. Th17 cells induce ectopic lymphoid follicles in central nervous system tissue inflammation. *Immunity,* 35**,** 986-96.

PICARELLA, D. E., KRATZ, A., LI, C. B., RUDDLE, N. H. & FLAVELL, R. A. 1993. Transgenic tumor necrosis factor (TNF)-alpha production in pancreatic islets leads to insulitis, not diabetes. Distinct patterns of inflammation in TNF-alpha and TNF-beta transgenic mice. *J Immunol,* 150**,** 4136-50.

PIKOR, N. B., ASTARITA, J. L., SUMMERS-DELUCA, L., GALICIA, G., QU, J., WARD, L. A., ARMSTRONG, S., DOMINGUEZ, C. X., MALHOTRA, D., HEIDEN, B., KAY, R., CASTANOV, V., TOUIL, H., BOON, L., O'CONNOR, P., BAR-OR, A., PRAT, A., RAMAGLIA, V., LUDWIN, S., TURLEY, S. J. & GOMMERMAN, J. L. 2015. Integration of Th17- and Lymphotoxin-Derived Signals Initiates Meningeal-Resident Stromal Cell Remodeling to Propagate Neuroinflammation. *Immunity,* 43**,** 1160-73.

PILLEMER, S. R., MATTESON, E. L., JACOBSSON, L. T., MARTENS, P. B., MELTON, L. J., 3RD, O'FALLON, W. M. & FOX, P. C. 2001. Incidence of physician-diagnosed primary Sjogren syndrome in residents of Olmsted County, Minnesota. *Mayo Clinic proceedings,* 76**,** 593-9.

PINEIRO-SANCHEZ, M. L., GOLDSTEIN, L. A., DODT, J., HOWARD, L., YEH, Y., TRAN, H., ARGRAVES, W. S. & CHEN, W. T. 1997. Identification of the 170-kDa melanoma membrane-bound gelatinase (seprase) as a serine integral membrane protease. *The Journal of biological chemistry,* 272**,** 7595-601.

PITT, J. M., STAVROPOULOS, E., REDFORD, P. S., BEEBE, A. M., BANCROFT, G. J., YOUNG, D. B. & O'GARRA, A. 2012. Blockade of IL-10 signaling during bacillus Calmette-Guerin vaccination enhances and sustains Th1, Th17, and innate lymphoid IFN-gamma and IL-17 responses and increases protection to Mycobacterium tuberculosis infection. *J Immunol,* 189**,** 4079-87.

PITZALIS, C., JONES, G. W., BOMBARDIERI, M. & JONES, S. A. 2014. Ectopic lymphoid-like structures in infection, cancer and autoimmunity. *Nat Rev Immunol,* 14**,** 447-62.

POWELL, N., WALKER, A. W., STOLARCZYK, E., CANAVAN, J. B., GOKMEN, M. R., MARKS, E., JACKSON, I., HASHIM, A., CURTIS, M. A., JENNER, R. G., HOWARD, J. K., PARKHILL, J., MACDONALD, T. T. & LORD, G. M. 2012. The transcription factor T-bet regulates intestinal inflammation mediated by interleukin-7 receptor+ innate lymphoid cells. *Immunity,* 37**,** 674-84.

QIN, Y., GREINER, A., HALLAS, C., HAEDICKE, W. & MULLER-HERMELINK, H. K. 1997. Intraclonal offspring expansion of gastric low-grade MALT-type lymphoma: evidence for the role of antigen-driven high-affinity mutation in lymphomagenesis. *Lab Invest,* 76**,** 477-85.

RAMIREZ, M. I., MILLIEN, G., HINDS, A., CAO, Y., SELDIN, D. C. & WILLIAMS, M. C. 2003. T1alpha, a lung type I cell differentiation gene, is required for normal lung cell proliferation and alveolus formation at birth. *Dev Biol,* 256**,** 61-72.

RAMOS-CASALS, M., SOLANS, R., ROSAS, J., CAMPS, M. T., GIL, A., DEL PINO-MONTES, J., CALVO-ALEN, J., JIMENEZ-ALONSO, J., MICO, M. L.,

BELTRAN, J., BELENGUER, R. & PALLARES, L. 2008. Primary Sjogren syndrome in Spain: clinical and immunologic expression in 1010 patients. *Medicine,* 87**,** 210-9.

RANDALL, T. D., CARRAGHER, D. M. & RANGEL-MORENO, J. 2008. Development of secondary lymphoid organs. *Annu Rev Immunol,* 26**,** 627-50.

RANGEL-MORENO, J., CARRAGHER, D. M., DE LA LUZ GARCIA-HERNANDEZ, M., HWANG, J. Y., KUSSER, K., HARTSON, L., KOLLS, J. K., KHADER, S. A. & RANDALL, T. D. 2011. The development of inducible bronchus-associated lymphoid tissue depends on IL-17. *Nat Immunol,* 12**,** 639-46.

RANGEL-MORENO, J., MOYRON-QUIROZ, J. E., HARTSON, L., KUSSER, K. & RANDALL, T. D. 2007. Pulmonary expression of CXC chemokine ligand 13, CC chemokine ligand 19, and CC chemokine ligand 21 is essential for local immunity to influenza. *Proc Natl Acad Sci U S A,* 104**,** 10577-82.

RASMUSSEN, A., ICE, J. A., LI, H., GRUNDAHL, K., KELLY, J. A., RADFAR, L., STONE, D. U., HEFNER, K. S., ANAYA, J. M., ROHRER, M., GOPALAKRISHNAN, R., HOUSTON, G. D., LEWIS, D. M., CHODOSH, J., HARLEY, J. B., HUGHES, P., MAIER-MOORE, J. S., MONTGOMERY, C. G., RHODUS, N. L., FARRIS, A. D., SEGAL, B. M., JONSSON, R., LESSARD, C. J., SCOFIELD, R. H. & SIVILS, K. L. 2014. Comparison of the American-European Consensus Group Sjogren's syndrome classification criteria to newly proposed American College of Rheumatology criteria in a large, carefully characterised sicca cohort. *Annals of the rheumatic diseases,* 73**,** 31-8.

RETTIG, W. J., GARIN-CHESA, P., BERESFORD, H. R., FEICKERT, H., JENNINGS, M. T., COHEN, J., OETTGEN, H. F. & OLD, L. J. 1986. Differential Expression of Cell Surface Antigens and Glial Fibrillary Acidic Protein in Human Astrocytoma Subsets. *Cancer Research,* 46**,** 6406-6412.

RETTIG, W. J., GARIN-CHESA, P., BERESFORD, H. R., OETTGEN, H. F., MELAMED, M. R. & OLD, L. J. 1988. Cell-surface glycoproteins of human sarcomas: differential expression in normal and malignant tissues and cultured cells. *Proc Natl Acad Sci U S A,* 85**,** 3110-4.

RETTIG, W. J., GARIN-CHESA, P., HEALEY, J. H., SU, S. L., OZER, H. L., SCHWAB, M., ALBINO, A. P. & OLD, L. J. 1993. Regulation and heteromeric structure of the fibroblast activation protein in normal and transformed cells of mesenchymal and neuroectodermal origin. *Cancer Res,* 53**,** 3327-35.

RISHI, A. K., JOYCE-BRADY, M., FISHER, J., DOBBS, L. G., FLOROS, J., VANDERSPEK, J., BRODY, J. S. & WILLIAMS, M. C. 1995. Cloning, characterization, and development expression of a rat lung alveolar type I cell gene in embryonic endodermal and neural derivatives. *Dev Biol,* 167**,** 294-306.

RISSELADA, A. P., KRUIZE, A. A. & BIJLSMA, J. W. 2013a. Clinical features distinguishing lymphoma development in primary Sjogren's Syndrome--a retrospective cohort study. *Seminars in arthritis and rheumatism,* 43, 171-7.

RISSELADA, A. P., LOOIJE, M. F., KRUIZE, A. A., BIJLSMA, J. W. & VAN ROON, J. A. 2013b. The role of ectopic germinal centers in the immunopathology of primary Sjogren's syndrome: a systematic review. *Seminars in arthritis and rheumatism,* 42**,** 368-76.

ROBAK, T., GLADALSKA, A. & STEPIEN, H. 1998. The tumour necrosis factor family of receptors/ligands in the serum of patients with rheumatoid arthritis. *Eur Cytokine Netw,* 9**,** 145-54.

ROBERTS, E. W., DEONARINE, A., JONES, J. O., DENTON, A. E., FEIG, C., LYONS, S. K., ESPELI, M., KRAMAN, M., MCKENNA, B., WELLS, R. J., ZHAO, Q., CABALLERO, O. L., LARDER, R., COLL, A. P., O'RAHILLY, S., BRINDLE, K. M., TEICHMANN, S. A., TUVESON, D. A. & FEARON, D. T. 2013. Depletion of stromal cells expressing fibroblast activation protein-alpha from skeletal muscle and bone marrow results in cachexia and anemia. *J Exp Med,* 210**,** 1137-51.

SABATELLI, P., BONALDO, P., LATTANZI, G., BRAGHETTA, P., BERGAMIN, N., CAPANNI, C., MATTIOLI, E., COLUMBARO, M., OGNIBENE, A., PEPE, G., BERTINI, E., MERLINI, L., MARALDI, N. M. & SQUARZONI, S. 2001. Collagen VI deficiency affects the organization of fibronectin in the extracellular matrix of cultured fibroblasts. *Matrix biology : journal of the International Society for Matrix Biology,* 20**,** 475-86.

SACCA, R., KRATZ, A., CAMPOS-NETO, A., HANSON, M. S. & RUDDLE, N. H. 1995. Lymphotoxin: from chronic inflammation to lymphoid organs. *J Inflamm,* 47**,** 81-4.

SALOMONSSON, S., JONSSON, M. V., SKARSTEIN, K., BROKSTAD, K. A., HJELMSTROM, P., WAHREN-HERLENIUS, M. & JONSSON, R. 2003. Cellular basis of ectopic germinal center formation and autoantibody production in the target organ of patients with Sjogren's syndrome. *Arthritis and rheumatism,* 48**,** 3187-201.

SALOMONSSON, S., LARSSON, P., TENGNER, P., MELLQUIST, E., HJELMSTROM, P. & WAHREN-HERLENIUS, M. 2002. Expression of the B cell-attracting chemokine CXCL13 in the target organ and autoantibody production in ectopic lymphoid tissue in the chronic inflammatory disease Sjogren's syndrome. *Scand J Immunol,* 55**,** 336-42.

SANTOS, A. M., JUNG, J., AZIZ, N., KISSIL, J. L. & PURE, E. 2009. Targeting fibroblast activation protein inhibits tumor stromagenesis and growth in mice. *J Clin Invest,* 119**,** 3613-25.

SARIGUL, M., YAZISIZ, V., BASSORGUN, C. I., ULKER, M., AVCI, A. B., ERBASAN, F., GELEN, T., GORCZYNSKI, R. M. & TERZIOGLU, E. 2010. The numbers of Foxp3 + Treg cells are positively correlated with higher grade of infiltration at the salivary glands in primary Sjogren's syndrome. *Lupus,* 19**,** 138-45.

SATO, M., HIRAYAMA, S., MATSUDA, Y., WAGNETZ, D., HWANG, D. M., GUAN, Z., LIU, M. & KESHAVJEE, S. 2011. Stromal activation and formation of lymphoid-like stroma in chronic lung allograft dysfunction. *Transplantation,* 91**,** 1398-405.

SATOH, J., ILLES, Z., PETERFALVI, A., TABUNOKI, H., ROZSA, C. & YAMAMURA, T. 2007. Aberrant transcriptional regulatory network in T cells of multiple sclerosis. *Neurosci Lett,* 422**,** 30-3.

SCANLAN, M. J., RAJ, B. K., CALVO, B., GARIN-CHESA, P., SANZ-MONCASI, M. P., HEALEY, J. H., OLD, L. J. & RETTIG, W. J. 1994. Molecular cloning of fibroblast activation protein alpha, a member of the serine protease family selectively expressed in stromal fibroblasts of epithelial cancers. *Proc Natl Acad Sci U S A,* 91**,** 5657-61.

SCHACHT, V., RAMIREZ, M. I., HONG, Y. K., HIRAKAWA, S., FENG, D., HARVEY, N., WILLIAMS, M., DVORAK, A. M., DVORAK, H. F., OLIVER, G. & DETMAR, M. 2003. T1alpha/podoplanin deficiency disrupts normal lymphatic vasculature formation and causes lymphedema. *EMBO J,* 22**,** 3546-56.

SCHAERLI, P., WILLIMANN, K., LANG, A. B., LIPP, M., LOETSCHER, P. & MOSER, B. 2000. CXC chemokine receptor 5 expression defines follicular homing T cells with B cell helper function. *J Exp Med,* 192**,** 1553-62.

SCHMUTZ, S., BOSCO, N., CHAPPAZ, S., BOYMAN, O., ACHA-ORBEA, H., CEREDIG, R., ROLINK, A. G. & FINKE, D. 2009. Cutting edge: IL-7 regulates the peripheral pool of adult ROR gamma+ lymphoid tissue inducer cells. *J Immunol,* 183**,** 2217-21.

SCHOLL, F. G., GAMALLO, C., VILARO, S. & QUINTANILLA, M. 1999. Identification of PA2.26 antigen as a novel cell-surface mucin-type glycoprotein that induces plasma membrane extensions and increased motility in keratinocytes. *J Cell Sci,* 112 (Pt 24)**,** 4601-13.

SCHREIBER, H. & ROWLEY, D. A. 2010. Cancer. Awakening immunity. *Science,* 330**,** 761-2.

SHARPE, A. H. & FREEMAN, G. J. 2002. The B7-CD28 superfamily. *Nat Rev Immunol,* 2**,** 116-26.

SHEN, L., SURESH, L., WU, J., XUAN, J., LI, H., ZHANG, C., PANKEWYCZ, O. & AMBRUS, J. L., JR. 2010. A role for lymphotoxin in primary Sjogren's disease. *J Immunol,* 185**,** 6355-63.

SHI, M., YU, D. H., CHEN, Y., ZHAO, C. Y., ZHANG, J., LIU, Q. H., NI, C. R. & ZHU, M. H. 2012. Expression of fibroblast activation protein in human pancreatic adenocarcinoma and its clinicopathological significance. *World J Gastroenterol,* 18**,** 840-6.

SHIBOSKI, S. C., SHIBOSKI, C. H., CRISWELL, L., BAER, A., CHALLACOMBE, S., LANFRANCHI, H., SCHIODT, M., UMEHARA, H., VIVINO, F., ZHAO, Y., DONG, Y., GREENSPAN, D., HEIDENREICH, A. M., HELIN, P., KIRKHAM, B., KITAGAWA, K., LARKIN, G., LI, M., LIETMAN, T., LINDEGAARD, J., MCNAMARA, N., SACK, K., SHIRLAW, P., SUGAI, S., VOLLENWEIDER, C., WHITCHER, J., WU, A., ZHANG, S., ZHANG, W., GREENSPAN, J. & DANIELS, T. 2012. American College of Rheumatology classification criteria for Sjogren's syndrome: a data-driven, expert consensus approach in the Sjogren's International Collaborative Clinical Alliance cohort. *Arthritis care & research,* 64**,** 475-87.

SIEGERT, S., HUANG, H. Y., YANG, C. Y., SCARPELLINO, L., CARRIE, L., ESSEX, S., NELSON, P. J., HEIKENWALDER, M., ACHA-ORBEA, H., BUCKLEY, C. D., MARSLAND, B. J., ZEHN, D. & LUTHER, S. A. 2011. Fibroblastic reticular cells from lymph nodes attenuate T cell expansion by producing nitric oxide. *PLoS One,* 6**,** e27618.

SIMPSON, T. R., QUEZADA, S. A. & ALLISON, J. P. 2010. Regulation of CD4 T cell activation and effector function by inducible costimulator (ICOS). *Curr Opin Immunol,* 22**,** 326-32.

SONG, G., OUYANG, G. & BAO, S. 2005. The activation of Akt/PKB signaling pathway and cell survival. *J Cell Mol Med,* 9**,** 59-71.

SPORICI, R. A., BESWICK, R. L., VON ALLMEN, C., RUMBLEY, C. A., HAYDEN-LEDBETTER, M., LEDBETTER, J. A. & PERRIN, P. J. 2001. ICOS ligand

costimulation is required for T-cell encephalitogenicity. *Clinical immunology,* 100**,** 277-88.

STUART, R. W. & RACKE, M. K. 2002. Targeting T cell costimulation in autoimmune disease. *Expert Opin Ther Targets,* 6**,** 275-89.

SUEMATSU, S. & WATANABE, T. 2004. Generation of a synthetic lymphoid tissue-like organoid in mice. *Nat Biotechnol,* 22**,** 1539-45.

SUN, S., ALBRIGHT, C. F., FISH, B. H., GEORGE, H. J., SELLING, B. H., HOLLIS, G. F. & WYNN, R. 2002. Expression, purification, and kinetic characterization of full-length human fibroblast activation protein. *Protein Expr Purif,* 24**,** 274-81.

SUZUKI-INOUE, K., INOUE, O., DING, G., NISHIMURA, S., HOKAMURA, K., ETO, K., KASHIWAGI, H., TOMIYAMA, Y., YATOMI, Y., UMEMURA, K., SHIN, Y., HIRASHIMA, M. & OZAKI, Y. 2010. Essential in vivo roles of the C-type lectin receptor CLEC-2: embryonic/neonatal lethality of CLEC-2-deficient mice by blood/lymphatic misconnections and impaired thrombus formation of CLEC-2-deficient platelets. *The Journal of biological chemistry,* 285**,** 24494-507.

SWALLOW, M. M., WALLIN, J. J. & SHA, W. C. 1999. B7h, a novel costimulatory homolog of B7.1 and B7.2, is induced by TNFalpha. *Immunity,* 11**,** 423-32.

SZABO, K., PAPP, G., DEZSO, B. & ZEHER, M. 2014. The histopathology of labial salivary glands in primary Sjogren's syndrome: focusing on follicular helper T cells in the inflammatory infiltrates. *Mediators Inflamm,* 2014**,** 631787.

SZODORAY, P., ALEX, P., JONSSON, M. V., KNOWLTON, N., DOZMOROV, I., NAKKEN, B., DELALEU, N., JONSSON, R. & CENTOLA, M. 2005. Distinct profiles of Sjogren's syndrome patients with ectopic salivary gland germinal centers revealed by serum cytokines and BAFF. *Clinical immunology,* 117**,** 168-76.

TAKAHASHI, N., MATSUMOTO, K., SAITO, H., NANKI, T., MIYASAKA, N., KOBATA, T., AZUMA, M., LEE, S. K., MIZUTANI, S. & MORIO, T. 2009. Impaired CD4 and CD8 effector function and decreased memory T cell populations in ICOS-deficient patients. *J Immunol,* 182**,** 5515-27.

TAKEMURA, S., BRAUN, A., CROWSON, C., KURTIN, P. J., COFIELD, R. H., O'FALLON, W. M., GORONZY, J. J. & WEYAND, C. M. 2001. Lymphoid neogenesis in rheumatoid synovitis. *J Immunol,* 167**,** 1072-80.

TAN, A. H., GOH, S. Y., WONG, S. C. & LAM, K. P. 2008. T helper cell-specific regulation of inducible costimulator expression via distinct mechanisms mediated by T-bet and GATA-3. *J Biol Chem,* 283**,** 128-36.

TAN, A. H., WONG, S. C. & LAM, K. P. 2006. Regulation of mouse inducible costimulator (ICOS) expression by Fyn-NFATc2 and ERK signaling in T cells. *J Biol Chem,* 281**,** 28666-78.

TANGYE, S. G., MA, C. S., BRINK, R. & DEENICK, E. K. 2013. The good, the bad and the ugly - TFH cells in human health and disease. *Nat Rev Immunol,* 13**,** 412-26.

TARIN, D. & CROFT, C. B. 1969. Ultrastructural features of wound healing in mouse skin. *J Anat,* 105**,** 189-90.

THEANDER, E., HENRIKSSON, G., LJUNGBERG, O., MANDL, T., MANTHORPE, R. & JACOBSSON, L. T. 2006. Lymphoma and other malignancies in primary Sjogren's syndrome: a cohort study on cancer incidence and lymphoma predictors. *Annals of the rheumatic diseases,* 65**,** 796-803.

THEANDER, E., VASAITIS, L., BAECKLUND, E., NORDMARK, G., WARFVINGE, G., LIEDHOLM, R., BROKSTAD, K., JONSSON, R. & JONSSON, M. V. 2011. Lymphoid organisation in labial salivary gland biopsies is a possible predictor for the development of malignant lymphoma in primary Sjogren's syndrome. *Annals of the rheumatic diseases,* 70**,** 1363-8.

THOMPSON, C. B., LINDSTEN, T., LEDBETTER, J. A., KUNKEL, S. L., YOUNG, H. A., EMERSON, S. G., LEIDEN, J. M. & JUNE, C. H. 1989. CD28 activation pathway regulates the production of multiple T-cell-derived lymphokines/cytokines. *Proc Natl Acad Sci U S A,* 86**,** 1333-7.

TOMITA, T., NAKASE, T., KANEKO, M., SHI, K., TAKAHI, K., OCHI, T. & YOSHIKAWA, H. 2002. Expression of extracellular matrix metalloproteinase inducer and enhancement of the production of matrix metalloproteinases in rheumatoid arthritis. *Arthritis and rheumatism,* 46**,** 373-8.

TRUNEH, A., REDDY, M., RYAN, P., LYN, S. D., EICHMAN, C., COUEZ, D., HURLE, M. R., SEKALY, R. P., OLIVE, D. & SWEET, R. 1996. Differential recognition by CD28 of its cognate counter receptors CD80 (B7.1) and B70 (B7.2): analysis by site directed mutagenesis. *Mol Immunol,* 33**,** 321-34.

TUMANOV, A., KUPRASH, D., LAGARKOVA, M., GRIVENNIKOV, S., ABE, K., SHAKHOV, A., DRUTSKAYA, L., STEWART, C., CHERVONSKY, A. & NEDOSPASOV, S. 2002. Distinct role of surface lymphotoxin expressed by B cells in the organization of secondary lymphoid tissues. *Immunity,* 17**,** 239-50.

TUMANOV, A. V., KUPRASH, D. V., MACH, J. A., NEDOSPASOV, S. A. & CHERVONSKY, A. V. 2004. Lymphotoxin and TNF produced by B cells are dispensable for maintenance of the follicle-associated epithelium but are required for development of lymphoid follicles in the Peyer's patches. *Journal of immunology,* 173**,** 86-91.

UHRIN, P., ZAUJEC, J., BREUSS, J. M., OLCAYDU, D., CHRENEK, P., STOCKINGER, H., FUERTBAUER, E., MOSER, M., HAIKO, P., FASSLER, R., ALITALO, K., BINDER, B. R. & KERJASCHKI, D. 2010. Novel function for blood platelets and podoplanin in developmental separation of blood and lymphatic circulation. *Blood,* 115**,** 3997-4005.

VAN BERKEL, M. E. & OOSTERWEGEL, M. A. 2006. CD28 and ICOS: similar or separate costimulators of T cells? *Immunology letters,* 105**,** 115-22.

VAN DAMME, J., STRUYF, S., WUYTS, A., VAN COILLIE, E., MENTEN, P., SCHOLS, D., SOZZANI, S., DE MEESTER, I. & PROOST, P. 1999. The role of CD26/DPP IV in chemokine processing. *Chem Immunol,* 72**,** 42-56.

VINUESA, C. G., COOK, M. C., ANGELUCCI, C., ATHANASOPOULOS, V., RUI, L., HILL, K. M., YU, D., DOMASCHENZ, H., WHITTLE, B., LAMBE, T., ROBERTS, I. S., COPLEY, R. R., BELL, J. I., CORNALL, R. J. & GOODNOW, C. C. 2005. A RING-type ubiquitin ligase family member required to repress follicular helper T cells and autoimmunity. *Nature,* 435**,** 452-8.

VINUESA, C. G., SANZ, I. & COOK, M. C. 2009. Dysregulation of germinal centres in autoimmune disease. *Nature reviews. Immunology,* 9**,** 845-57.

VITALI, C., BOMBARDIERI, S., JONSSON, R., MOUTSOPOULOS, H. M., ALEXANDER, E. L., CARSONS, S. E., DANIELS, T. E., FOX, P. C., FOX, R. I., KASSAN, S. S., PILLEMER, S. R., TALAL, N. & WEISMAN, M. H. 2002. Classification criteria for Sjogren's syndrome: a revised version of the

European criteria proposed by the American-European Consensus Group. *Annals of the rheumatic diseases,* 61**,** 554-8.

VITALI, C., BOMBARDIERI, S., MOUTSOPOULOS, H. M., COLL, J., GERLI, R., HATRON, P. Y., KATER, L., KONTTINEN, Y. T., MANTHORPE, R., MEYER, O., MOSCA, M., OSTUNI, P., PELLERITO, R. A., PENNEC, Y., PORTER, S. R., RICHARDS, A., SAUVEZIE, B., SCHIODT, M., SCIUTO, M., SHOENFELD, Y., SKOPOULI, F. N., SMOLEN, J. S., SOROMENHO, F., TISHLER, M., WATTIAUX, M. J. & ET AL. 1996. Assessment of the European classification criteria for Sjogren's syndrome in a series of clinically defined cases: results of a prospective multicentre study. The European Study Group on Diagnostic Criteria for Sjogren's Syndrome. *Annals of the rheumatic diseases,* 55**,** 116-21.

VON FREEDEN-JEFFRY, U., VIEIRA, P., LUCIAN, L. A., MCNEIL, T., BURDACH, S. E. & MURRAY, R. 1995. Lymphopenia in interleukin (IL)-7 gene-deleted mice identifies IL-7 as a nonredundant cytokine. *J Exp Med,* 181**,** 1519-26.

VOULGARELIS, M., DAFNI, U. G., ISENBERG, D. A. & MOUTSOPOULOS, H. M. 1999. Malignant lymphoma in primary Sjogren's syndrome: a multicenter, retrospective, clinical study by the European Concerted Action on Sjogren's Syndrome. *Arthritis and rheumatism,* 42**,** 1765-72.

VU, F., DIANZANI, U., WARE, C. F., MAK, T. & GOMMERMAN, J. L. 2008. ICOS, CD40, and lymphotoxin beta receptors signal sequentially and interdependently to initiate a germinal center reaction. *J Immunol,* 180**,** 2284-93.

WALDELE, S., KOERS-WUNRAU, C., BECKMANN, D., KORB-PAP, A., WEHMEYER, C., PAP, T. & DANKBAR, B. 2015. Deficiency of fibroblast activation protein alpha ameliorates cartilage destruction in inflammatory destructive arthritis. *Arthritis Res Ther,* 17**,** 12.

WANG, X. M., YU, D. M., MCCAUGHAN, G. W. & GORRELL, M. D. 2005. Fibroblast activation protein increases apoptosis, cell adhesion, and migration by the LX-2 human stellate cell line. *Hepatology,* 42**,** 935-45.

WARE, C. F., CROWE, P. D., GRAYSON, M. H., ANDROLEWICZ, M. J. & BROWNING, J. L. 1992. Expression of surface lymphotoxin and tumor necrosis factor on activated T, B, and natural killer cells. *J Immunol,* 149**,** 3881-8.

WARNATZ, K., BOSSALLER, L., SALZER, U., SKRABL-BAUMGARTNER, A., SCHWINGER, W., VAN DER BURG, M., VAN DONGEN, J. J., ORLOWSKA-VOLK, M., KNOTH, R., DURANDY, A., DRAEGER, R., SCHLESIER, M., PETER, H. H. & GRIMBACHER, B. 2006. Human ICOS deficiency abrogates the germinal center reaction and provides a monogenic model for common variable immunodeficiency. *Blood,* 107**,** 3045-52.

WATSON, S. P., HERBERT, J. M. & POLLITT, A. Y. 2010. GPVI and CLEC-2 in hemostasis and vascular integrity. *Journal of thrombosis and haemostasis : JTH,* 8**,** 1456-67.

WELT, S., DIVGI, C. R., SCOTT, A. M., GARIN-CHESA, P., FINN, R. D., GRAHAM, M., CARSWELL, E. A., COHEN, A., LARSON, S. M., OLD, L. J. & ET AL. 1994. Antibody targeting in metastatic colon cancer: a phase I study of monoclonal antibody F19 against a cell-surface protein of reactive tumor stromal fibroblasts. *J Clin Oncol,* 12**,** 1193-203.

WENGNER, A. M., HOPKEN, U. E., PETROW, P. K., HARTMANN, S., SCHURIGT, U., BRAUER, R. & LIPP, M. 2007. CXCR5- and CCR7-dependent lymphoid neogenesis in a murine model of chronic antigen-induced arthritis. *Arthritis Rheum,* 56**,** 3271-83.

WETTERWALD, A., HOFFSTETTER, W., CECCHINI, M. G., LANSKE, B., WAGNER, C., FLEISCH, H. & ATKINSON, M. 1996. Characterization and cloning of the E11 antigen, a marker expressed by rat osteoblasts and osteocytes. *Bone,* 18**,** 125-32.

WEYAND, C. M. & GORONZY, J. J. 2003. Ectopic germinal center formation in rheumatoid synovitis. *Ann N Y Acad Sci,* 987**,** 140-9.

WEYAND, C. M., KLIMIUK, P. A. & GORONZY, J. J. 1998. Heterogeneity of rheumatoid arthritis: from phenotypes to genotypes. *Springer Semin Immunopathol,* 20**,** 5-22.

WHITE, A., CARRAGHER, D., PARNELL, S., MSAKI, A., PERKINS, N., LANE, P., JENKINSON, E., ANDERSON, G. & CAAMANO, J. H. 2007. Lymphotoxin a-dependent and -independent signals regulate stromal organizer cell homeostasis during lymph node organogenesis. *Blood,* 110**,** 1950-9.

WILDENBERG, M. E., VAN HELDEN-MEEUWSEN, C. G., VAN DE MERWE, J. P., DREXHAGE, H. A. & VERSNEL, M. A. 2008. Systemic increase in type I interferon activity in Sjogren's syndrome: a putative role for plasmacytoid dendritic cells. *Eur J Immunol,* 38**,** 2024-33.

WILLIAMS, M. C., CAO, Y., HINDS, A., RISHI, A. K. & WETTERWALD, A. 1996. T1 alpha protein is developmentally regulated and expressed by alveolar type I cells, choroid plexus, and ciliary epithelia of adult rats. *Am J Respir Cell Mol Biol,* 14**,** 577-85.

WINTER, S., LODDENKEMPER, C., AEBISCHER, A., RABEL, K., HOFFMANN, K., MEYER, T. F., LIPP, M. & HOPKEN, U. E. 2010. The chemokine receptor CXCR5 is pivotal for ectopic mucosa-associated lymphoid tissue neogenesis in chronic Helicobacter pylori-induced inflammation. *J Mol Med (Berl),* 88**,** 1169-80.

WONG, S. C., OH, E., NG, C. H. & LAM, K. P. 2003. Impaired germinal center formation and recall T-cell-dependent immune responses in mice lacking the costimulatory ligand B7-H2. *Blood,* 102**,** 1381-8.

WU, W. M., SUEN, J. L., LIN, B. F. & CHIANG, B. L. 2000. Tamoxifen alleviates disease severity and decreases double negative T cells in autoimmune MRL-lpr/lpr mice. *Immunology,* 100**,** 110-8.

YANG, C. Y., VOGT, T. K., FAVRE, S., SCARPELLINO, L., HUANG, H. Y., TACCHINI-COTTIER, F. & LUTHER, S. A. 2014. Trapping of naive lymphocytes triggers rapid growth and remodeling of the fibroblast network in reactive murine lymph nodes. *Proc Natl Acad Sci U S A,* 111**,** E109-18.

YAZISIZ, V., BEHLUL, A., BASAK, S. T. & BORLU, F. 2013. Expression of podoplanin in minor salivary glands increases in primary Sjogren syndrome. *J Rheumatol,* 40**,** 2100-2.

YOSHIDA, H., HONDA, K., SHINKURA, R., ADACHI, S., NISHIKAWA, S., MAKI, K., IKUTA, K. & NISHIKAWA, S. I. 1999. IL-7 receptor alpha+ CD3(-) cells in the embryonic intestine induces the organizing center of Peyer's patches. *Int Immunol,* 11**,** 643-55.

YOSHINAGA, S. K., WHORISKEY, J. S., KHARE, S. D., SARMIENTO, U., GUO, J., HORAN, T., SHIH, G., ZHANG, M., COCCIA, M. A., KOHNO, T., TAFURI-

BLADT, A., BRANKOW, D., CAMPBELL, P., CHANG, D., CHIU, L., DAI, T., DUNCAN, G., ELLIOTT, G. S., HUI, A., MCCABE, S. M., SCULLY, S., SHAHINIAN, A., SHAKLEE, C. L., VAN, G., MAK, T. W. & SENALDI, G. 1999. T-cell co-stimulation through B7RP-1 and ICOS. *Nature,* 402**,** 827-32.

YOSHINAGA, S. K., ZHANG, M., PISTILLO, J., HORAN, T., KHARE, S. D., MINER, K., SONNENBERG, M., BOONE, T., BRANKOW, D., DAI, T., DELANEY, J., HAN, H., HUI, A., KOHNO, T., MANOUKIAN, R., WHORISKEY, J. S. & COCCIA, M. A. 2000. Characterization of a new human B7-related protein: B7RP-1 is the ligand to the co-stimulatory protein ICOS. *Int Immunol,* 12**,** 1439-47.

YU, D., TAN, A. H., HU, X., ATHANASOPOULOS, V., SIMPSON, N., SILVA, D. G., HUTLOFF, A., GILES, K. M., LEEDMAN, P. J., LAM, K. P., GOODNOW, C. C. & VINUESA, C. G. 2007. Roquin represses autoimmunity by limiting inducible T-cell co-stimulator messenger RNA. *Nature,* 450**,** 299-303.

YUSUF, I., STERN, J., MCCAUGHTRY, T. M., GALLAGHER, S., SUN, H., GAO, C., TEDDER, T., CARLESSO, G., CARTER, L., HERBST, R. & WANG, Y. 2014. Germinal center B cell depletion diminishes CD4+ follicular T helper cells in autoimmune mice. *PLoS One,* 9**,** e102791.

ZAMOYSKA, R., BASSON, A., FILBY, A., LEGNAME, G., LOVATT, M. & SEDDON, B. 2003. The influence of the src-family kinases, Lck and Fyn, on T cell differentiation, survival and activation. *Immunol Rev,* 191**,** 107-18.

ZHANG, J., VALIANOU, M. & CHENG, J. D. 2010. Identification and characterization of the promoter of fibroblast activation protein. *Front Biosci (Elite Ed),* 2**,** 1154-63.

ZHENG, Y., CHAUDHRY, A., KAS, A., DEROOS, P., KIM, J. M., CHU, T. T., CORCORAN, L., TREUTING, P., KLEIN, U. & RUDENSKY, A. Y. 2009. Regulatory T-cell suppressor program co-opts transcription factor IRF4 to control T(H)2 responses. *Nature,* 458**,** 351-6.